CUADERNOS de INVESTIGACIÓN GEOGRÁFICA

GEOGRAPHICAL RESEARCH LETTERS

Tomo 50 (2) **2024** **ISSN: 1697-9540**

UNIVERSIDAD DE LA RIOJA
LOGROÑO (ESPAÑA)

CUADERNOS DE INVESTIGACIÓN GEOGRÁFICA
GEOGRAPHICAL RESEARCH LETTERS

Cuadernos de Investigación Geográfica = Geographical Research Letters (ISSN: 0211-6820) is a scientific journal that publishes two issues per year. It includes papers on Physical Geography and other related environmental sciences (Hydrology, Ecology, Climatology). Interdisciplinary studies with Human Geography are also welcome. The peer review and publication of articles in *Cuadernos de Investigación Geográfica* is free of charge, in agreement with the policy of the journal of making accessible the advances in Physical Geography to the scientific community. All papers are subject to full peer review.

Since 2015 **Cuadernos de Investigación Geográfica = Geographical Research Letters** has been included in the Emerging Sources Citation Index (ESCI) of Clarivate Analytics, a new edition of the Web of Science, within the subject category of *Geography (Physical)*. The journal is also indexed in SCOPUS and SCIMAGO Journal & Country Rank within the subject categories of Geography, Planning and Development, Environmental Sciences, and Earth and Planetary Sciences.

Fotografía de portada / Cover photo: Montes Obarenes, La Rioja (España) / Obarenes Mountains, La Rioja (Spain). Autor / Author: J. Arnáez

CUADERNOS DE INVESTIGACIÓN GEOGRÁFICA
GEOGRAPHICAL RESEARCH LETTERS

ISSN 1697-9540

Tomo 50 (2) 2024

CONTENIDO / CONTENT

Cuadernos de Investigación Geográfica *Geographical Research Letters*	2024	Nº 50 (2)	pp. 3-28	EISSN 1697-9540

http://doi.org/10.18172/cig.6453

WATER PLANNING AND MANAGEMENT IN SPAIN IN A CLIMATE CHANGE CONTEXT: FACTS AND PROPOSALS

JORGE OLCINA CANTOS*

Departamento de Análisis Geográfico Regional y Geografía Física. Universidad de Alicante, Campus de San Vicente del Raspeig s/n.03690 Alicante. Spain.

ABSTRACT. Water planning and management in Spain is being affected by the recorded effects of the current climate change process. The traditional paradigm based on a policy of continuous water supply no longer fits with the forecasts of decreasing water flows identified by climate and hydrological modelling. The guarantee of water security, a guiding principle of planning, as indicated by Spanish Climate Change Law (2021), requires the incorporation of new water resources that allow water management to be less dependent on rainfall. Effective demand management, the incorporation of regenerated water with a high level of purification, the inclusion of rainwater for urban and leisure uses and the use of desalinated water in coastal areas to be used mainly for urban water supply are presented as viable alternatives to the development of large public hydraulic works that prove ineffective in drought conditions. This paper presents an updated balance of water resources and demands and analyses the increasing difficulty of hydrological planning in our country within a complex political context that requires cooperation and governance actions in water matters. A series of recommendations are proposed, from a geographical perspective, for the necessary adaptation of hydrological planning to the effects of climate change in Spain.

Planificación y gestión del agua en España en el contexto del cambio climático. Realidades y propuestas

RESUMEN. La planificación y gestión del agua en España se está viendo afectada por los efectos registrados del proceso actual de cambio climático. El paradigma tradicional basado en una política de continua oferta de agua ya no se ajusta a las previsiones de disminución de caudales que señalan la modelización climática e hidrológica. La garantía de la seguridad hídrica, principio rector de la planificación, como señala la Ley de Cambio Climático de 2021, requiere de la incorporación de nuevos recursos hídricos que permitan hacer menos dependiente la propia gestión del agua de las precipitaciones. La eficaz gestión de la demanda, la incorporación de aguas regeneradas con alto nivel de depuración, la inclusión de las aguas pluviales para usos urbanos y de ocio y el uso de aguas desaladas en zonas de litoral con finalidad principal de abastecimiento se presentan como alternativas viables frente al desarrollo de grandes obras públicas hidráulicas que se demuestran ineficaces en condiciones de sequía. El trabajo muestra un balance actualizado de recursos y demandas de agua y analiza la creciente dificultad de la planificación hidrológica en nuestro país en un contexto político complejo que requiere acciones de cooperación y gobernanza en materia hídrica. Se presentan una serie de recomendaciones, desde la geografía, para la necesaria adaptación de la planificación hidrológica a los efectos del cambio climático en España.

Keywords: hydrological planning, climate change, water security, governance, demand management.

Palabras clave: Planificación hidrológica, cambio climático, seguridad hídrica, gobernanza, gestión de la demanda.

Received: 18 November 2024

Accepted: 9 December 2024

***Corresponding author**: Jorge Olcina Cantos. Departamento de Análisis Geográfico Regional y Geografía Física. University of Alicante. Campus de San Vicente del Raspeig s/n. 03690 Alicante, Spain. Email: jorge.olcina@ua.es

1. Introduction

Water is one of the elements of the natural environment that is most sensitive to the effects of the current global warming process. The changes in rainfall patterns recorded over the last few decades in many regions of the world (including Spain) are conditioning the future of the planning and management of this resource, which should adapt to the alterations in the climate elements indicated by modelling (Caretta *et al.,* 2022).

Water is an essential element for the development of societies. If water is not controlled, civilising work cannot take place. This has been the case throughout the history of humankind to the present day. Water is the cause of development but it also gives rise to conflicts between societies. The pressure on water resources has been increasing in recent decades (Karamidehkordi *et al.,* 2024). Populated countries and regions around the world with growing economic activity require an increasing supply of water. Sometimes, these resources do not exist and generate disputes between territories (Fernández-Jáuregui *et al.,* 2017; Angelakis *et al.,* 2021). The future perspectives in terms of water resource management on a global level indicate a greater complexity in the planning of water uses. Fortunately, in Spain there are no intense conflicts related to water resources, although there is territorial tension with regard to the use of water. This situation requires decisions to be made in order to guarantee a water supply in a difficult climate context (Martínez-Fernández *et al.* 2020).

There are many studies that analyse the impact of the current climate changes on precipitations, the volume of water available on the Earth's surface and the differences in each climate region. On a global level, we can observe an increase in precipitations in the inter-equatorial region, a decrease in the areas affected by subtropical subsidence, due to the polar expansion of the Hadley cells, and an increase in mid and high latitudes, due to the greater intensity of the atmospheric readjustment processes with an increase in meridian circulations. (Muñoz *et al.,* 2020; Cresswell-Clay *et al.,* 2022)

Climate change affects four principal plans in modern society. That is, it obliges specific mitigation and adaptation actions to be designed to guarantee well-being. The measures to implement affect the planning processes of economic activities, particularly those most exposed to the consequences of the change in the climate elements (temperatures and precipitations), such as agriculture and tourism. Furthermore, the guidelines for territorial planning also need to be adapted. In other words, the assignment of new uses to the land has, until now, been carried out within a context in which the climate was unalterable but this is no longer the case. Water planning requires special attention and should be focused on the management of demand and not so much on a resource supply policy in view of the irregularity in precipitations. Finally, emergency planning should be adapted due to the increase in extreme weather events, the increasing prominence of certain climate hazards and the emergence of new risks within the framework of climate modelling. In short, fundamental planning changes are required to guarantee the future functioning of a society, driven by the modifications recorded in climate conditions (Olcina Cantos, 2024).

The twenty-first century is, or should be, the century of the commitment to sustainability in territorial and economic processes and of the adaptation to climate change. It should be the guiding principle steering the actions of governments and individuals. The definition of sustainable development is complex, hence it is preferable to sideline theoretical aspects and address its practical embodiment, which should be governed by rationality, common sense, ethics, prudence and the acknowledgement of its transversal and multidisciplinary nature. Sustainable development, understood in this way as a guideline for action, is a development that is implemented according to the features of the natural environment in which it takes place; a process that does not seek to surpass the limits imposed by nature

or, in any case, which contemplates actions that contribute, where possible, to overcoming these limits (Elorrieta-Sanz and Olcina-Campos, 2021).

In the European context, these principles are set out in two documents that have helped to guide policies over the last two decades. The European Territorial Strategy (1999) and the Water Framework Directive (2000). Both of them contain the objectives that territorial planning and water planning should fulfil, which should be oriented towards the respect for the territory, the reduction of risks and the search for a social well-being that does not irreversibly alter the features of the environment (Farinós-Dasí, 2021; Navarro-Sousa, 2022). The incorporation of the effects of climate change in territorial and water policies is a principal action for the European Union (EEA, 2024 a). Moreover, addressing hydrological extremes is the main focus of policies and promotes the research in the territory of the Union in the search for adaptation strategies (EEA, 2024 b).

In Spain, we have struggled to incorporate these action guidelines in the sustainable planning of territories and water; but the evident effects of the current global warming process have fuelled the implementation of initiatives consisting in public actions aimed at managing natural resources (land, air, water, coasts) under the principles of protecting them against the unstoppable human desire for a transforming and continuous economic growth of the environment (Solorzano-Chamorro *et al.,* 2022). This concept of development based on the continued use of resources, including water, has begun to experience changes in Spanish society and even in economic sectors, which are perceiving an exhaustion of these resources and their shortage due to a global climate change process whose effects are visible in Iberian latitudes (Fundación BBVA, 2022; CEOE, 2023).

In Spain, traditional water planning has been governed by supply policy (Figure 1). That is, in response to an existing demand, the State, responsible for large-scale water planning, should cover this use with its own resources from the river basin or from other basins when its own resources are insufficient. It is a planning model that is based on the principle that the water existing in Spain is abundant and sufficient to supply all of the existing demand. And this is true, although with an important geographical nuance: the unequal regional distribution of precipitations and the uneven distribution of water resources in the country as a whole. Therefore, the concepts of surpluses and deficits of water resources arise in the territories (Morote Seguido, 2014; Sotelo Pérez *et al.* 2021).

Law 7/2021 on climate change proposes an interesting concept as a guiding principle for water planning within the current context of climate change: water security (art.19). We must understand this expression from science not politics, given that it runs the risk of being interpreted as the objective that should be fulfilled with some kind of action, that is, reinforcing the continued water supply policy. Water security refers to the guarantee of the supply of the demands existing in a territory (prioritised according to the Water Law). A supply designed from a demand management perspective that respects the environmental values of the water resources (surface and ground) and avoids conflicts between territories to achieve this security. This process should be under constant review in relation to climate evolution at all times (López Gum and Vargas Amelín, 2020).

This study analyses the state of the question of water planning in Spain. It presents an updated balance of resources and uses and proposes measures for the efficient management of situations of circumstantial water deficit (droughts) and structural water deficit (aridity) that have an impact that differs in terms of its diversity and intensity across the Spain territory. It addresses the relationship between natural limits and political-administrative limits in water planning and management in Spain which makes this task even more complex, sometimes generating territorial disputes and conflicts. It calls for a necessary change in the paradigm of water planning in Spain to adapt it to the European policy determinations on water and, particularly, the effects of current climate change that are generating a greater irregularity in precipitations, with evident decreasing trends in some of its territories.

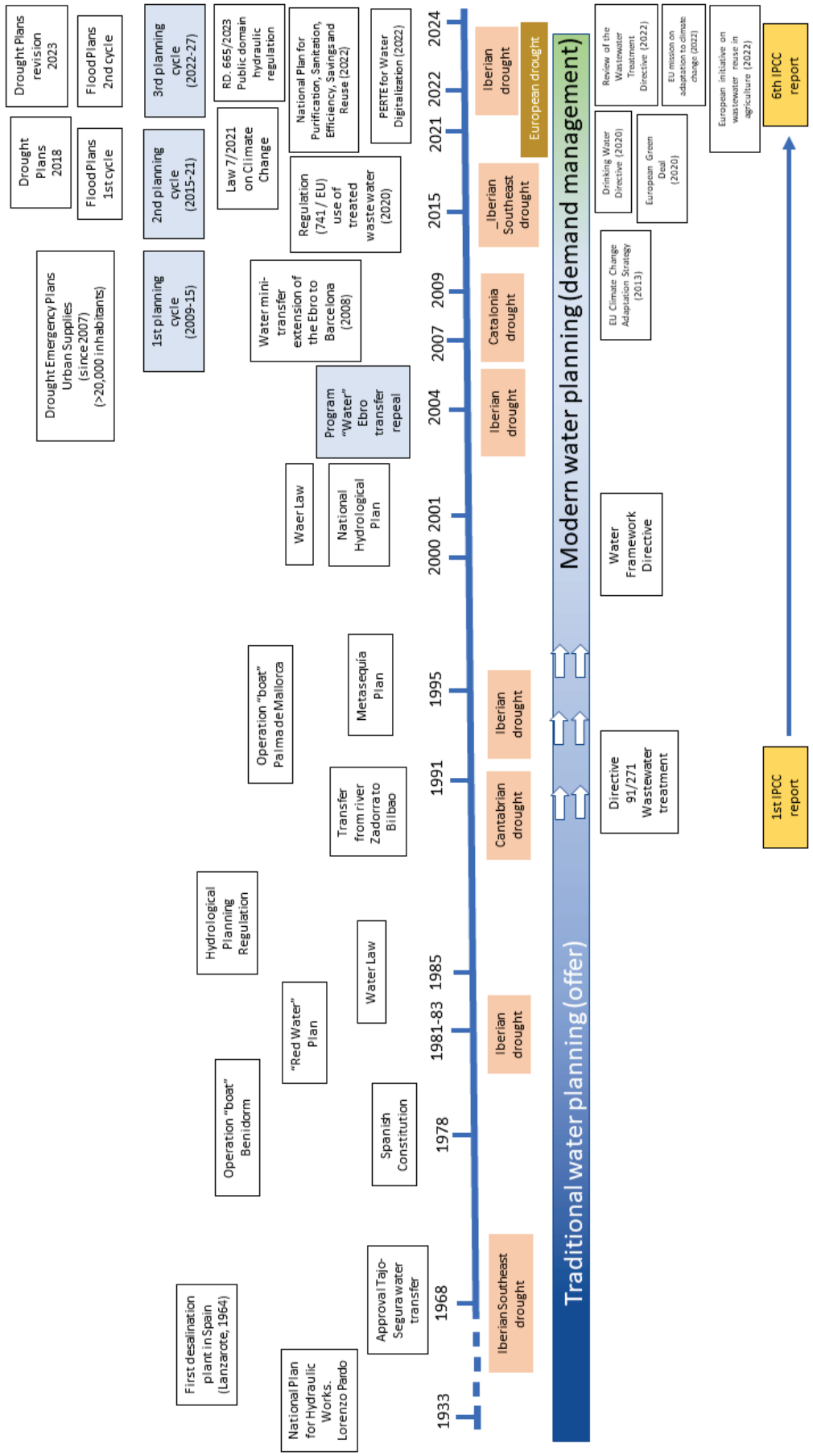

Figure 1. Evolution of the water policy in Spain 1933-2024.

2. Method and sources

This study uses data, reports and official documents of government departments (state and regional) related to water management and planning. Furthermore, in order to analyse local cases, company reports on the distribution of drinking water and reports of the Spanish Association of Water Supply and Wastewater (AEAS) have been consulted. Moreover, it also uses the projects applying for European economic subsidies (Next Generation Funds) processed by the Spanish Government and projects related to water management, particularly with the promotion of the reuse of treated water.

For references of a climate nature, the most recent publications on the relationship between rain, climate change and the effects on water resources in Spain published by Spanish research groups have been used. All of the sources consulted are free to access online, except the local scale projects, which have been obtained by the author (Table 1).

Table 1. Sources used relating to the planning and management of water in Spain (2024).

Scale of study	Sources consulted
Europe	- European Water Framework Directive - European Directive on urban wastewater treatment. Reports on the status of the compliance with the Directive (European Commission). - European Floods Directive - European Drought Observatory (EDO) - Reports on the status of water in Europe (European Environment Agency, 2024)
Spain	- River Basin Plans (1st, 2nd and 3rd planning cycle) - Drought Management Plans - Law of the National Hydrological Plan 2001 - Water Law of 2001 - Water Programme 2005 - Portal of the Spanish National Recovery, Transformation and Resilience Plan (Next Generation Funds). Water Section. - Meteorological drought monitor - Reports on the State of the Climate in Spain (AEMET) - Reports and research articles - Reports of AEAS, FEDEA, AEDyR, CEOE, Instituto Elcano.
Autonomous regions	-Wastewater treatment plans -Plans for the reuse of treated water
Local scale	- Annual reports on drinking water management - Local experiences in the management of droughts and floods (Barcelona, Alicante, Madrid, Seville)

One of the most noteworthy aspects in the study of water is the lack of transparency in the information related to water data; in some cases because no precise calculations are made (agricultural uses) as there are no water measurement systems on the plots of land; in others because there is no record of the unregistered resources in the urban environment (losses in the supply network); and, in general, because, traditionally, the consultation of these data has not been facilitated for professionals and experts of official bodies or private companies in the sector (PWC, 2018). The European Directive on the right to information on the environment (2003/4/EC) has not been effective in the public dissemination of water data (Razquín Lizárraga, 2018). The implementation of the so-called PERTE for the digitalisation of the water cycle in 2022 as part of the Spain's National Recovery, Transformation and Resilience Plan (Government of Spain, 2022), which includes, among other actions, the creation of a Water Management Observatory in order to improve the governance and management of the digital infrastructure, could become the great public water databank.

The work method used is the hypothetical-deductive method. It responds to the objectives stated in the research through the analysis of the data consulted and readings. It is based on the precept that the

guiding principle of water planning in Spain (continuous supply of water) is incorrect within the current context of climate change and proposals are presented to implement a change in this paradigm within the principles of sustainability and adaptation. All of this is backed with data and own analyses and those of researchers who have studied this topic in recent years.

3. Results

3.1. A climate context of uncertainty: Effects on dry sequences

Water planning based on long-term climate scenarios no longer makes sense in Spain. The current climate context, which clearly reveals the effects of global warming in the principal climate elements (temperatures and precipitations), obliges us to periodically review the forecasts and their effects on the available water resources. In Iberian latitudes, the current climate change is manifested in an increase in temperatures and an overall loss of thermal comfort, with a more irregular behaviour of precipitations and the alteration of seasonal rainfall patterns (Cramer *et al.,* 2018; Meseguer-Ruiz and Olcina Cantos, 2023). In addition, there is a greater intensity and frequency of extreme weather events, related to temperature and precipitation. The latter is related to the intensification of the global energy readjustment processes and the warming of the seas that surround the mainland territory, particularly the Mediterranean sea basin (Olcina Cantos*,* 2024).

Different studies have analysed the change in the seasonal precipitation patterns in Spain (Ruiz-Sinoga *et al.,* 2011; Acero *et al.,* 2012; Serrano-Notivoli, 2017; CEDEX, 2021; Senent-Aparicio *et al.,* 2023), highlighting the "Mediterraneanisation" process of the maximum precipitations towards the west of the peninsula (Cordillera Ibérica sector) with a main peak in autumn (González-Hidalgo *et al.,* 2010). Recently, González-Hidalgo *et al.* (2023, 2024) have shown the recent trend in rainfall in the Iberian peninsula with an increase in the amounts in autumn and a reduction in spring (Paredes *et al.,* 2006). This is particularly important for the planning and management of water resources, given that the volumes of water that can accumulate in spring are fundamental for guaranteeing the demands of the summer season, which increase considerably due to the increase in agricultural and tourist uses and the increase in the real evaporation due to the higher temperature. This trend of a reduction in spring rains is significant in the southern sector of the Cordillera Ibérica, where the sources of two important rivers are located (Júcar and Tajo), which serve demand systems (agricultural and urban-tourist) that are highly valuable to the Spanish economy (Miró *et al.,* 2021, 2023).

Drought has become an important study topic for water planning in Spain (Vicente-Serrano, 2021). There is uncertainty as to the duration of droughts which have been occurring since the beginning of the current century. Contrary to the long sequences that occurred in the second half of the twentieth century that generated droughts in the Iberian Peninsula (Iberian droughts), with a duration of between 3 and 5 years (calendar year), the droughts occurring in the twenty-first century are more intense, but with a shorter duration (one or two calendar years) (González *et al.,* 2020; Torelló-Sentelles *et al.,* 2022; Trullenque-Blanco *et al.,* 2024). Similarly, the drought sequences display diverse regional manifestations (droughts in the north-east of the peninsula, south-eastern droughts, Cantabrian droughts) (Olcina, 2001; Lana *et al.,* 2021), with their own calendars of development and repercussion on the percentage reduction in precipitation recorded with respect to the annual averages.

The occurrence of shorter and more intense droughts would correspond to the changes in the overall atmospheric circulation in mid latitudes, with an expansion of the Hadley cell towards the pole (Xian *et al.,* 2021; Cresswell-Clay *et al.,* 2022), which generates a greater probability of anticyclonic days each year, with energy readjustment days with the installation of cold air masses in mid and hight layers of the troposphere, which generate unstable configurations (cold drops) and the possibility of the occurrence of occasional intense rain events, which, in general, cannot be used to satisfy agricultural demand (Olcina Cantos, 2024).

In any case, the shortage of water for agricultural and particularly urban use generated by a drought situation reveals a failure in water planning and management on a water basin, regional or local scale. In the dry sequence recorded in Spain during the hydrological years 2021/22 and 2022/23, it is interesting to observe that the population nuclei that suffered from a shortage of supply and in which emergency measures had to be applied are small areas in the interior or north of the peninsula, with no alternative supply sources and which have not optimised their drinking water systems so as to guarantee the storage of volumes of water for a supply of three months (Fig. 2 a and b).

a)

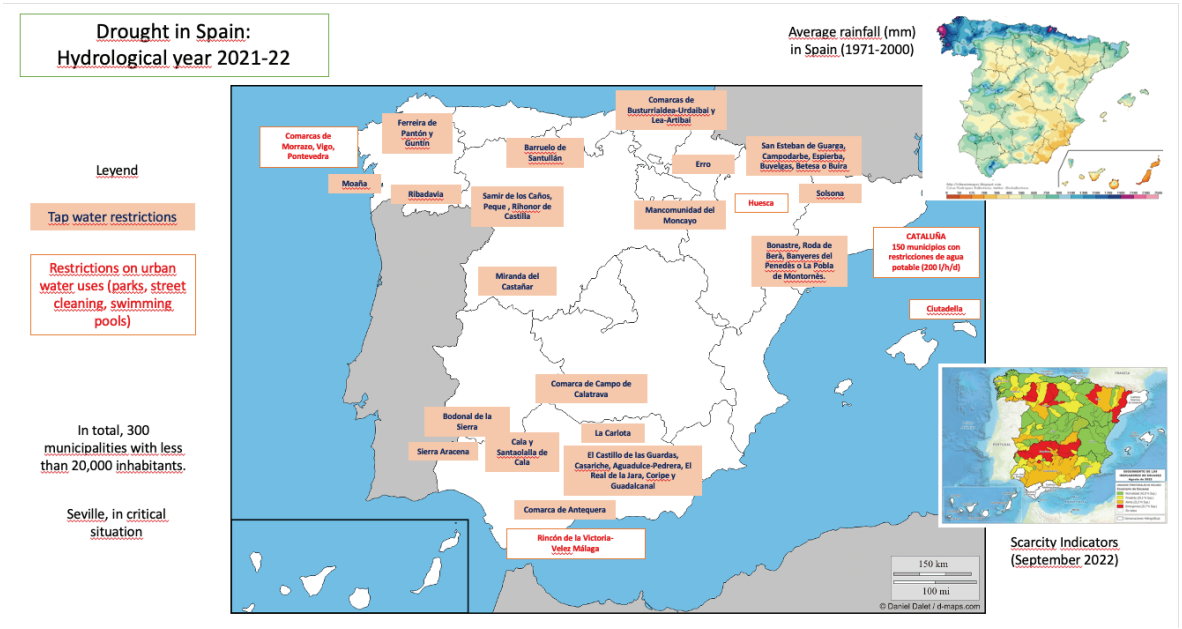

b)

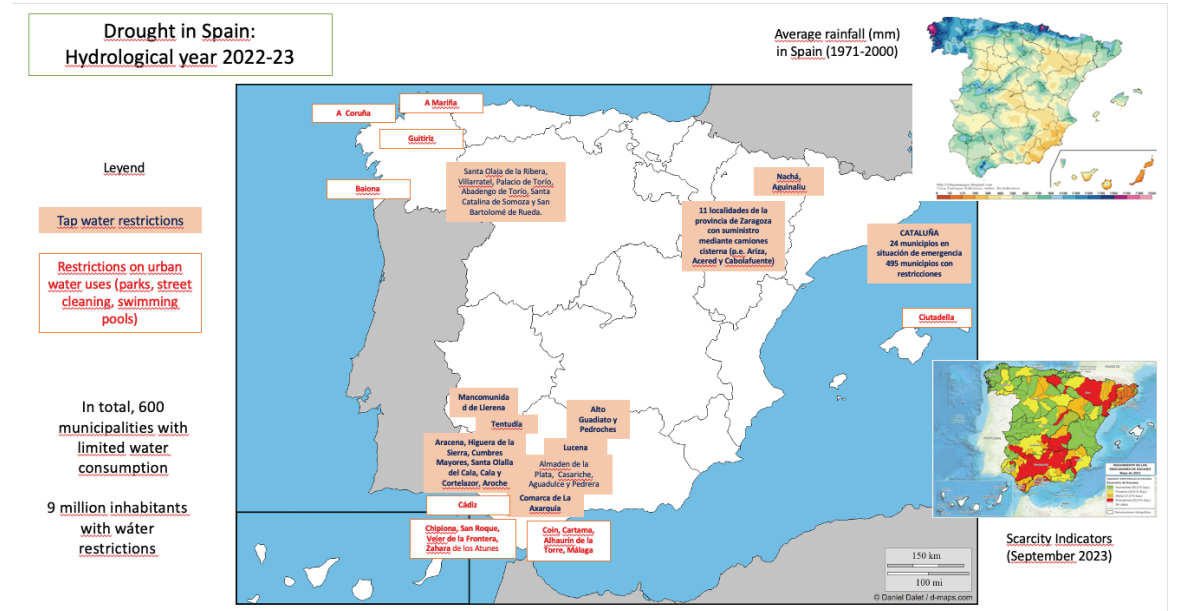

Figure 2. Map of towns affected by an urban water supply shortage. Hydrological year 2021/22(a) of towns affected by an urban water supply shortage. Hydrological year 2022/23(b). Source: Own elaboration based on monthly drought reports (Spanish Ministry of Ecological transition and Demographic Challenge) and regional press news reports.

In Spain, the risk map, with its integral components (hazard, vulnerability and exposure) reveals significant regional differences (Fig. 3). Based on the analysis of the effects of the latest droughts recorded in Spain over the last three decades on water security, it is possible to represent a map of the hazard, vulnerability and exposure to drought, which shows the need to activate water management mechanisms for supplying areas with a greater volume of annual precipitation, given that their excessive dependence on this climate element generates conditions of shortages in supply at times of less rainfall.

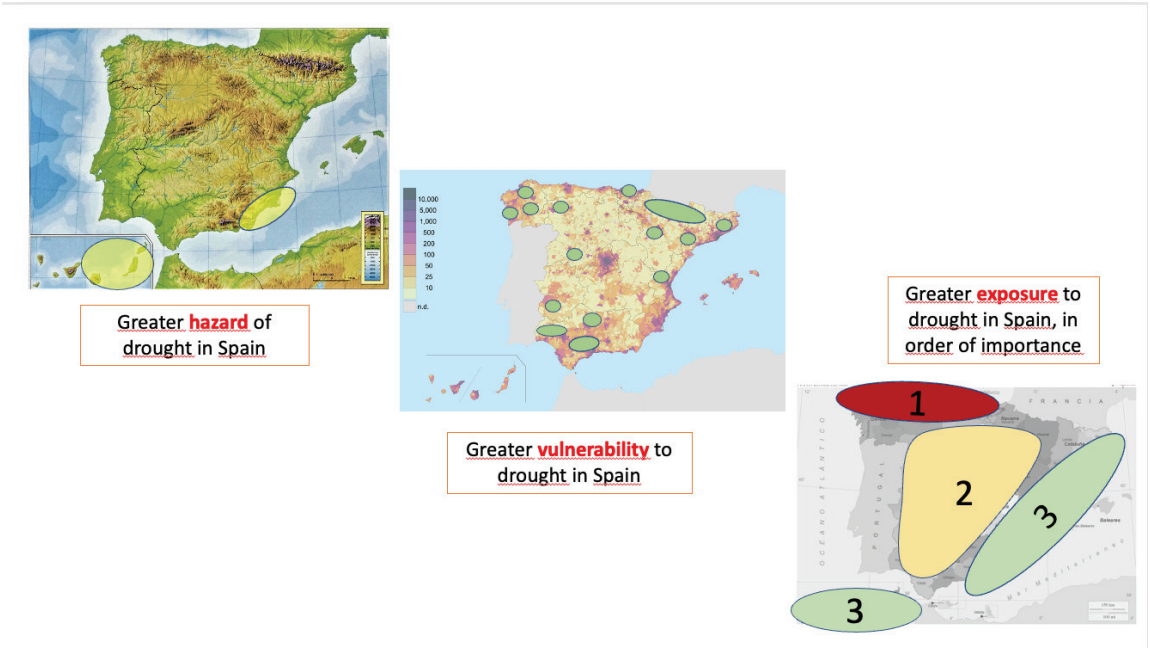

Figure 3. Drought in Spain in terms of risk analysis.

3.2. In a complex political context: Water, State and Autonomous Regions

As a general rule, the local scale of the planning and management of natural resources is the work unit closest to the citizens. However, the general interests can (usually) clash with individual (local) interests. Hence, there is a need to establish a hierarchy for the planning and management of natural resources. The hierarchy of natural resource planning and management in Spain integrates the global sustainable development goals (SDGs) established by the international bodies to which the Spanish government belongs; the European scale, which is decisive due to the obligation of member countries of the European Union to comply with the environmental directive; the State scale, which, in terms of the environment, is limited to the enactment of general regulations (water, coasts, natural and protected spaces, climate change) and fundamentally planning and managing the public domain (water, coast); and the Regional Governments, which are the key actors in environmental management because this competence has been transferred to them by constitutional mandate.

In recent years, legal disputes have arisen between the regional and state levels due to the interest of the autonomous regions to control the planning and, most of all, the management of two basic resources whose public domain belongs to the state (water and coast). Finally, land uses are planned on a local scale, including the natural environment and its resources; some autonomous regions have been given the power to establish and manage natural spaces that are protected on a local or supralocal level with the final approval by the regional government.

The conflicts between administrations, depending on their working scale are resolved by higher legal entities: regional, state or European. This is because the resources found in the natural environment are a potential source of revenue, which is desired by the management level closest to the resource (local

and regional). In Spain, the planning and management of the natural environment and its resources is regulated in Articles 148 and 149 of the Constitution, which refer to the competencies assumed by the autonomous regions and those that are the exclusive competence of the State (Romero, 2009, 2017). The autonomous regions are responsible for territorial and urban planning, housing, the mountains and forest uses, the management and protection of the environment and construction and exploitation projects related to water use. The State has the exclusive competence for the legislation, the planning and concession of resources and water uses and the basic legislation regarding the protection of the environment (mountains, forest uses and livestock trails), together with the management of the coast with respect to the Public Domain (Fig. 4).

On paper, the competences of the state and regional governments regarding the environment and its resources are clear. However, there are misalignments in their planning and management, particularly when the political party in power is different in the regional and state governments and when there is no willingness to compromise because a resource is considered as being strategic for a state or a region. On the contrary, in general, there are no misalignments when the political party in power in the state and regional governments is the same (or there is a similar ideology) and when the willingness to compromise of the governments involved is clear (Romero, 2017). In the first scenario, there is a political utilisation of the natural environment, with actions taken that lead to legal disputes and, in short, an inefficient planning and management of the natural environment. In the second scenario, planning is ordered, the governance is effective and the benefit of the government action is collective.

The elements of the natural environment that generate the most conflicts between territories and between different levels of governments are coasts and water. Article 132.3 of the Spanish Constitution indicates that they are elements of the state public domain by law, but it states that "the maritime-land area, beaches, territorial sea and natural resources of the economic area and continental platform" belong to the state. Therefore, the coast is a public domain because it is indicated as such in the constitutional text. The waters also belong to the State, but in this case this is determined by a state law. In this case (water), the State also has the power to elaborate a national hydrological plan and manages the river basin districts, which are the territorial representation of the state in a water basin. Meanwhile, one of the competences of the autonomous regions is becoming increasing more prominent in the current context of climate change: the treatment and reuse of wastewaters. Finally, the local governments are obliged to guarantee the supply of water in the municipality.

In terms of planning and management, water is a matter of the State. However, there are different interpretations of this precept. It may be understood that water, as a public domain asset is the property of all Spaniards. In a situation of conjunctural or structural shortage, it becomes a liquid element able to be displaced form its natural territory in order to satisfy human demands; in short, water is basically understood as a resource at the service of economic development and the maintenance of the well-being of a population. On the other hand, the public domain can understand water as a resource owned by the territory, as a liquid element that favours the creation of ecosystems, therefore, as a resource that should first satisfy the needs of the natural environment before the demands of human beings. From this perspective, water is a resource at the service of the environment. In Spain, the "economic" discourse has prevailed over the "environmental" discourse when contemplating water planning and management proposals. It has only been since the enactment of the Water Framework Directive (60/2000) that the environmental view of water has gained prominence in water planning actions in Spain.

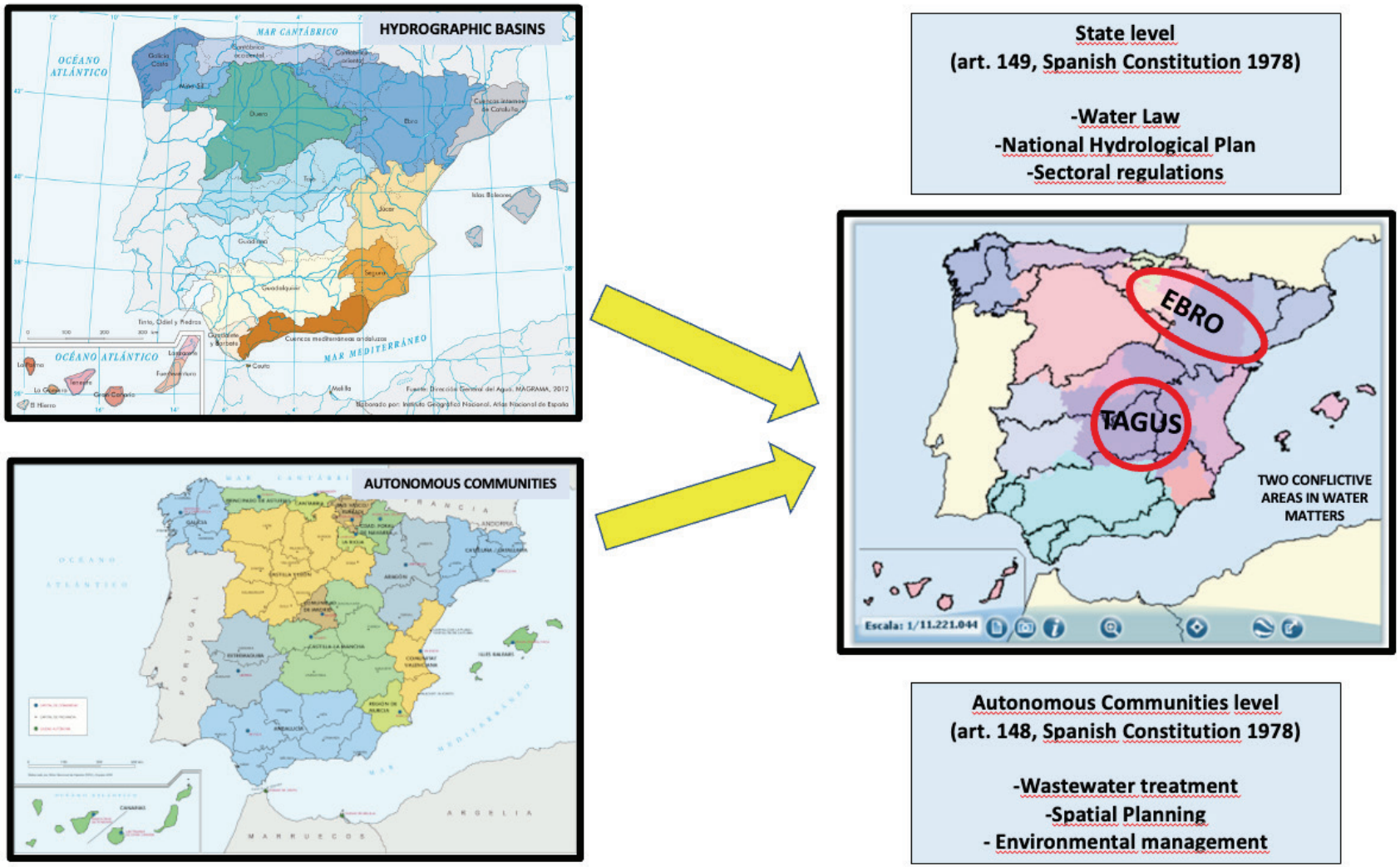

Figure 4. Natural limits (river basins) and political limits (autonomous regions) in the planning and management of water in Spain. Source: Own elaboration. Cartographic base. IGN. España en mapas. https://www.ign.es/resources/acercaDe/libDigPub/EspanaenMapas.pdf

In Spain, there are two river basins whose water planning and management, for different reasons, are the focus of territorial disputes over water: The Ebro and the Tajo. The Ebro river basin is a large Iberian river whose whole length runs through Spanish territory. This water basin has been strongly altered by the needs of urban supply and, particularly, that of agriculture and the defence against situations of the extraordinary swelling of the river. The prominence given to the River Ebro in the water transfer proposal to the Mediterranean coast included in the Hydrological Plan of 2001 has generated debate and controversy from the beginning. First, due to its approval and, on paper, the start of the works; then, due to the repeal of Article 13 of the Law of the National Hydrological Plan, which rendered this proposal for an annual macro-transfer of water ineffective. And, since then, due to the repeated attempts to restart the project by the autonomous regions of Valencia and Murcia under right-wing governments. The last link, resulting from the drought situation suffered in Catalonia between 2022 and the spring of 2024, has been the attempt to restart the project to extend the transfer from Tarragona to Barcelona, which was attempted during the previous drought of 2008. Both then and now, this proposal was strongly rejected by the population of Les Terres del Ebre.

The Tajo basin has a unique feature in its current water planning and management process. It has a water transfer infrastructure (Tajo-Segura Transfer) which was built during the final years of the Franco dictatorship and began operating in 1979 when the first waters arrived in the Segura basin. It has an international regulation agreement (Albufeira Agreement, 1998), in the review phase in 2024, which establishes the amount of water that should circulate in Portuguese territory (De Stefano and Hernández Mora, 2019). The first has been a cause of conflict between territories since its implementation, because the territories of Castilla-La Mancha have demanded water resources from the upper Tajo basin in order to satisfy different demands (agriculture, urban and environmental). These demands have been met unsatisfactorily according to the users, who demand more resources for the territories belonging to the Tajo basin. These demands imply the rejection of the water transfer to the south-east of the peninsula established by law, although the transfer amounts stipulated in the regulation have never been covered, nor the annual petitions of the farmers benefiting from the Tajo waters. The main problem in the management of the resources of the upper Tajo basin is, therefore, related to the existence of this infrastructure approved in 1968 and in the democratic period, with the delimitation of the regional limits, whose interests do not coincide with the territory of the river basin. The effects of climate change on the precipitations in the headwaters of the Tajo have given rise to an uncertain future for this water transfer, as in recent decades there has been a decreasing trend in the volumes of potentially transferable water. Furthermore, political decisions have led to the establishment of minimums in the headwater reservoirs below which transfers are not permitted (Escudero Gómez and Martin Trigo, 2020; Olcina Cantos, 2024).

3.3. Water data in Spain

The real data corresponding to water resources and demands in Spain are unknown. In order to estimate the resources, annual average precipitation is analysed, together with the calculation of groundwater volumes with the purpose of calculate the total available resources for hydrological planning. In Spain, total resources are estimated at 112,000 hm^3/year, of which 82,000 are surface waters and 30,000 groundwaters. The reservoir capacity, in work project conditions, is calculated at 56,069 hm^3, although different studies indicate that this theoretical capacity would be lower, in fact 15-20% lower due to the accumulation of sediments dragged by the regulated rivers since their implementation. This aspect has had particular attention in the Ebro river, due to the expectations created for using "excess" water retained in its reservoirs for the development of water transfers (Ibáñez *et al.,* 1996; Vericat and Batalla, 2006; Horacio *et al.,* 2018; Vázquez-Tarrío *et al.,* 2023; Goroztiza *et al.,* 2023).

These natural resources are not directly usable by humans, given that the rivers have to fulfil their ecological function and, most of all, due to the evaporation recorded in Spain, with its regional differences, and which is very intense in the summer months. This means that the balance between

precipitation and the evapotranspiration of water in Spain only generates positive values in the Cantabrian regions, while from the Duero basin to the south of the peninsula the deficit of this indicator increases until it reaches values of over -600 mm/year in a large part of the south of the peninsula and -900 mm/year in the south-east of the Iberian peninsula (Martí Ezpeleta *et al,* 2019). For the economic uses of water, Spain has 27,400 hm^3/year in conventional resources (20,600 of surface water + 6,800 of groundwater) to which "non-conventional" resources are added (treated water + desalinated water + rainwater), representing around 1,000 hm^3/year more (between 350-500 hm^3/year of reused water + 600 hm^3/year of desalinated water + 10 hm^3/year of rainwater collected in urban nuclei).

Meanwhile, the demands are also estimates, due to the lack of a real calculation of agriculture consumption. It is estimated that agriculture consumes around 22,500 hm^3/year. This figure is basically obtained from calculating the water needs of the different irrigated crops grown in Spain, given that there is no effective control of the water used or recording systems (meters), except in certain forms of irrigation with a high degree of technification (crops grown under plastic, crops with a high commercial value), which represent only 20% of the volume of water used for irrigation in Spain (Gómez Espín, 2019; Albiac Murillo *et al.,* 2023). Sixty-eight per cent of crops are irrigated with surface water; the rest with groundwater. And 902,163 use gravity irrigation (24% of the total). The belief that localised irrigation reduces the cost of water used in irrigation is incorrect. Irrigation with localised irrigation systems (53% of the total in Spain) is more efficient and favours the productivity of the plant, but it does not lead to a reduction in the volume of water used (Sanchis-Ibor *et al.,* 2016; Berbel and Espinosa-Tasón, 2020).

Urban demand is calculated at 4,236 hm^3/year, of which 3,180 hm^3/year is water that has been invoiced and the rest is an estimate. Meanwhile, industrial water is estimated at 1,264 hm^3/year. Urban and industrial water is the volume of water in Spain whose calculation is the closest to reality. Although the percentage of losses in the supply network recorded for all Spanish cities should be taken into account and calculated at 15% (AEAS, 2022) (Table 2).

Table 2. Water resources and demands in Spain (2024).

RESOURCES	TOTAL RESOURCES	**112,000 hm^3/year** (82,000 surface water+ 30,000 groundwater)
	Reservoir capacity	**56,069hm^3/year**
DEMANDS	AGRICULTURA USE	**22,500 hm^3/year**
	URBAN USE	**4,236 hm^3/year** (3,180 invoiced+1048 estimated)
	INDUSTRIAL USE	**1,264 hm^3/year**
CONVENTIONAL RESOURCES	SURFACE AND GROUND RESOURCES	**27,400 hm^3/year** (20,600 surface water +6,800 groundwater)
NON-CONVENTIONAL RESOURCES	TREATED WATER	**4,200 hm^3/year**
	REUSED WATER	**350-350 hm^3/year**
	DESALINATED WATER	**600 hm^3/year**

Therefore, a priori, in the general accounting of water in Spain, the demands can be met by the existing resources (conventional and non-conventional) under normal climate conditions. The problem is the uneven territorial distribution of resources and demands throughout the territory of Spain, which includes river basins with sufficient resources to guarantee water security (North, Duero, Ebro) and others where the level of demand notably exceeds that of the conventional resources (Segura, Júcar, Andalusian Mediterranean, Canarias, Ibiza).

However, the guarantee of supply is questioned at times of drought, which constitute a defining feature of the climate conditions in all Spanish climate regions. As previously indicated, up to five types of drought can be distinguished according to the territory affected in Spain (Olcina Cantos, 2001), being more frequent in the south-east of the peninsula (south-eastern droughts), which have a structural nature in the climate features of this geographical space.

The development of a dry sequence leads to the gradual reduction in the volumes of surface and groundwater due to the insufficient replenishment of the supply systems by rainfall (Fig. 5). In these cases, the sequence of effects of a drought cause the reduction in water resources, effects on rain-fed crops and non-stabled livestock farming, the reduction in resources for irrigation and in the most intense periods, there are effects on the urban supply systems, which can lead to the supply being cut off at extreme moments of a drought. Long-lasting and intense droughts call into question, therefore, the management of water if it is exclusively designed for moments of normality or rainfall abundance and if the supply system does not have non-conventional resources to make up the deficit of rainfall-based resources.

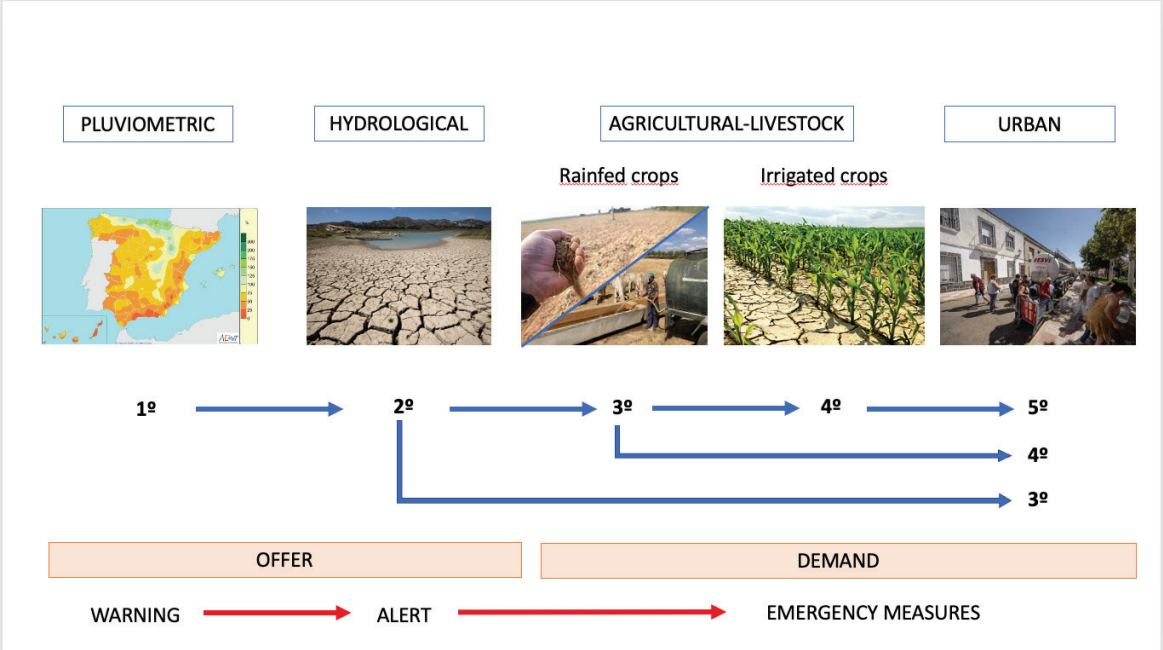

Figure 5. Phases of a drought sequence and sectors affected.

Within the context of climate change, with more irregular precipitations, the solution of the water transfers as a mechanism for supplying water in territories affected by conjunctural drought or structural shortage is not ideal due to environmental, economic and political reasons. We should remember that in Spain there are forty water transfer pipes for agricultural use and urban supply; of these, sixteen are large-scale transfers including those of the Tajo-Segura, Tajo-Guadiana, Pas-Besaya, Alto de Tornos, Zadorra-Arratia, Cerneja-Ordunte, Carol-Ariége, Alzania-Oria, Siurana-Riudecañas, Ebro-Tarragona, Guadiario-Majaceite, Negratín-Almanzora, Del Condado, Júcar-Turia, Júcar-Vinalopó and Ter-Llobregat transfers (Molina Giménez, 2010). Together, these large water transfers move an annual volume (variable depending on rainfall) of 800 hm^3/year.

Traditionally, Spain's water policy has promoted the development of these water transfers from areas of the country acting as "assignors" as they had volumes of water above their demands and could transfer their surplus towards "recipients" with conjunctural or structural water deficits. In addition to the Tajo-Segura transfer, which was considered during the Franco dictatorship, during the democratic era several interconnections have been developed between nearby river basins or with the same basin.

Furthermore, hydrological planning has considered water transfers as the principal solution to the water shortage in territories mainly in the east and south of Spain. Therefore, the proposal of the Hydrological Plan of 1993 (Plan Borrell, never approved) proposed the interconnection of basins through annual transfers of 4,000 hm^3; meanwhile, the National Hydrological Plan of 2001 considered a single large transfer from the Ebro of 1,000 hm^3 to the internal basins of Catalonia, Júcar, Segura and Mediterranean Andalusia (Almería). The transfer was abolished in 2004 and the volume of water that would have theoretically been transferred from the final section of the Ebro to the afore-mentioned territories on the Mediterranean coast were replaced with non-conventional resources (basically desalination) within the so-called "AGUA Programme" (Rico Amorós, 2010; Morote Seguido, 2014; Albiac Murillo *et al.,* 2023).

Water transfers are not useful for resolving Iberian drought sequences, given that at times of scarce rainfall the volumes of water reduce considerably in all of the river basins, so surpluses that could be moved between river basins are not recorded. The Tajo-Segura transfer has mainly been used to resolve situations of structural scarcity, however, the decrease in precipitations and available volumes of water recorded in the headwaters of the Tajo have led to a gradual decrease in the flows transferred since 2000 to the present. In fact, the average flow transferred since 1979 to the present is 330 hm^3. We should remember that this transfer considered a first phase with an annual transferred volume from the Tajo to the Segura of 600 hm^3/year, extendible to 1,000 hm^3/year in a second phase. Over the last two decades, there has been a significant reduction in precipitations in the southern sector of the Cordillera Ibérica, where the sources of the Tajo and Júcar are located. If we compare the contributions in the headwaters of the Tajo between 1940-79 and 1980-2018, the reduction is 275 hm^3/year (Miró *et al.,* 2021). This reduction could also have been affected by the increase in the forest area in this mountainous sector, which would generate a greater natural demand for water by the vegetation. For all practical purposes, the reality is that the headwaters of the Tajo have less available water to transfer than when the transfer began to operate (Olcina Cantos, 2024).

3.4. The need to incorporate non-conventional resources into the system

Guaranteeing water security in Spain within the context of climate change should involve increasing the prominence of non-conventional resources. In order of prominence, these are treated water, rainwater and desalinated water. This requires the provision and improvement of the necessary infrastructures for generating water resources that would allow a supply that would guarantee the satisfaction of the existing demands in terms of quantity and quality. In the case of treated water, a modernisation plan should be elaborated that includes the connection of the treatment stations with the potential reuse areas; and, for the use of rainwater, the installation of large-capacity tanks that harvest the waters of the river valley derived from intense rains with the dual objective of reducing the flood risk and using the collected waters for urban uses. In the case of the desalinated water, the cost of the water produced will decrease in the coming years if changes are made in the energy supply required by the desalination plants with the installation of solar energy.

The widespread treatment of water in Spain began after the passing of European Directive 91/271, at the beginning of the 1990s (Rico Amorós et al., 1998). Since then, and in compliance with the determinations of the afore-mentioned directive, which was subsequently modified, a large number of treatment stations (EDARs) began to operate in the Spanish regions, although with very diverse paces: with a more accelerated rhythm in the eastern regions of the peninsula and a very slow pace in the Cantabrian regions. This directive represented a significant change in urban water management, given that it made it compulsory to treat the flows used in the city and by industry and to potentially reuse them. It is true that the objectives of the Directive of 1991 did not include the direct reuse of purified water for economic uses. The water treatment technology installed in the majority of the EDARs implemented in Spain over the last three decades limit the potential use of the treated flows as their level of purification is not high (basically, secondary treatment). The reuse possibilities increase in relation to the type of treatment. The European Union has recently made a new commitment to wastewater

treatment and, as a novelty, the reuse of treated waters (Directive 2024 of the European Parliament and Council on the treatment of urban wastewater, recast version; González, 2024). In 2021, the Ministry of Ecological Transition approved the National Sanitation and Treatment, Efficiency, Savings and Reuse Plan - the DSEAR Plan - to promote this water resource in different uses, particularly agriculture (Miterd, 2021). Meanwhile, the Spanish Ministry of Agriculture has launched a sustainable water management in Spanish irrigation that contemplates the increase in the volume of treated water as an important resource for agriculture after the updating of the regulations on the reuse of treated water (Royal Decree 1085/2024).

The reality of water treatment and reuse in Spain provides an important lesson for future water planning. In Spain, the level of treatment is very high compared to other European countries, particularly those in the Mediterranean region. But the level of reuse with economic ends (agricultural, urban-tourist uses) could be vastly improved. Barely 10% of the total volume of treated water is used in urban and industrial environments in Spain (Fig. 6).

This means that there is a wide margin of water reuse that can mitigate occasional severe droughts or enable "first use" waters (rivers or aquifers) to be replaced with treated waters in order to reduce the final consumption of water of urban and agricultural uses. In this way, water management adapts to the circular economy model, sharing the principles established by Raworth (2012, 2017) in a proposal for the sustainable management of resources and activities to constitute a principle of action of the economy.

The promotion of water reuse should include the improvement of wastewater treatment stations to extend and enhance the purification systems and the development of treated water piping infrastructures so that it is possible to use these flows in the urban environment and the fields. In this respect, and within the framework of the European economic recovery policies after the Covid-19 pandemic, Spain is the country that has presented the most projects for treated water reuse in recent years (Bluefield Research, 2023) (Fig. 7).

There are examples of good practices in the promotion of the use of treated waters in Spain, such as the implementation of a wastewater network in the city of Alicante for the irrigation of gardens (public and private) that distributes 1.5 hm^3 per year for this use. This has involved the installation of a specific treated water distribution network through the urban fabric that enables the treated flows to reach the parks or private gardened areas (Aguas de Alicante, 2023). Meanwhile, the government of the Region of Valencia is developing a project for transferring treated wastewater for agricultural use from the municipality of Alicante (28 hm^3/year of treated waters in its two treatment stations) to the Bajo Vinalopó (Campo de Elche). This frees up other resources from the River Segura and the wells that can be used for irrigating the fields of the Bajo Segura. The "Vertido Cero" (Zero Waste) project will be the first treated water transfer within the same large scale river basin in Spain (Fig. 8).

However, it is necessary to indicate that the reuse of treated waters should be planned in detail. Direct reuse (agricultural use, urban-tourism use) should be compulsory in those territories with a natural shortage of water and with mostly dry rivers that do not require an ecological status based on the existence of a continuous run-of river in its courses. However, in river environments with a continuous circulation and rich aquatic ecosystems, the treated waters with a high level of treatment should be used primarily for environmental use to maintain these environments. In the case of the River Tajo, a high percentage of the flow circulating through Toledo is derived from the treated wastewater of Madrid (Martin *et al.,* 2024). Therefore, the promotion of reuse should be a principal objective of the water policy in Spain, but taking into account the needs that these waters could cover in each territory.

URBAN WATER CONSUMPTION IN SPAIN(2022)→**4.237 hm³**

VOLUME OF WATER PURIFIED IN SPAIN (2022)→**4.200 hm³**

VOLUME OF WATER REUSED IN SPAIN (2022)→**350-500 hm³. (343 hm³, según AEAS)**

10% OF TREATED WATER

→Valencia is the spanish region that reuses the greatest amount of water (123 hm³ in 2022) and Murcia is the one that does so in a higher percentage, reaching 90% of the treated wastewater.

→Valencian Community and Murcia region produce more than half of the reclaimed water used for irrigation throughout Spain, which is the main use of this resource.

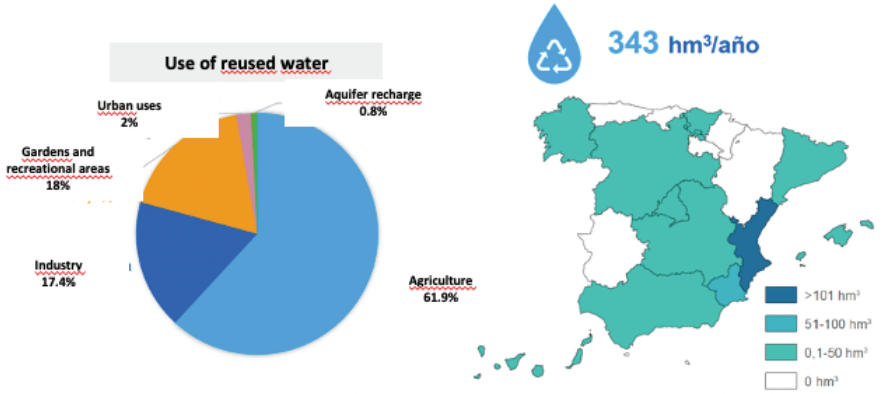

Fuente: AEAS, 2022

Figure 6. State of wastewater treatment in Spain (2023). Source: Own elaboration based on the reports of regional urban wastewater treatment bodies.

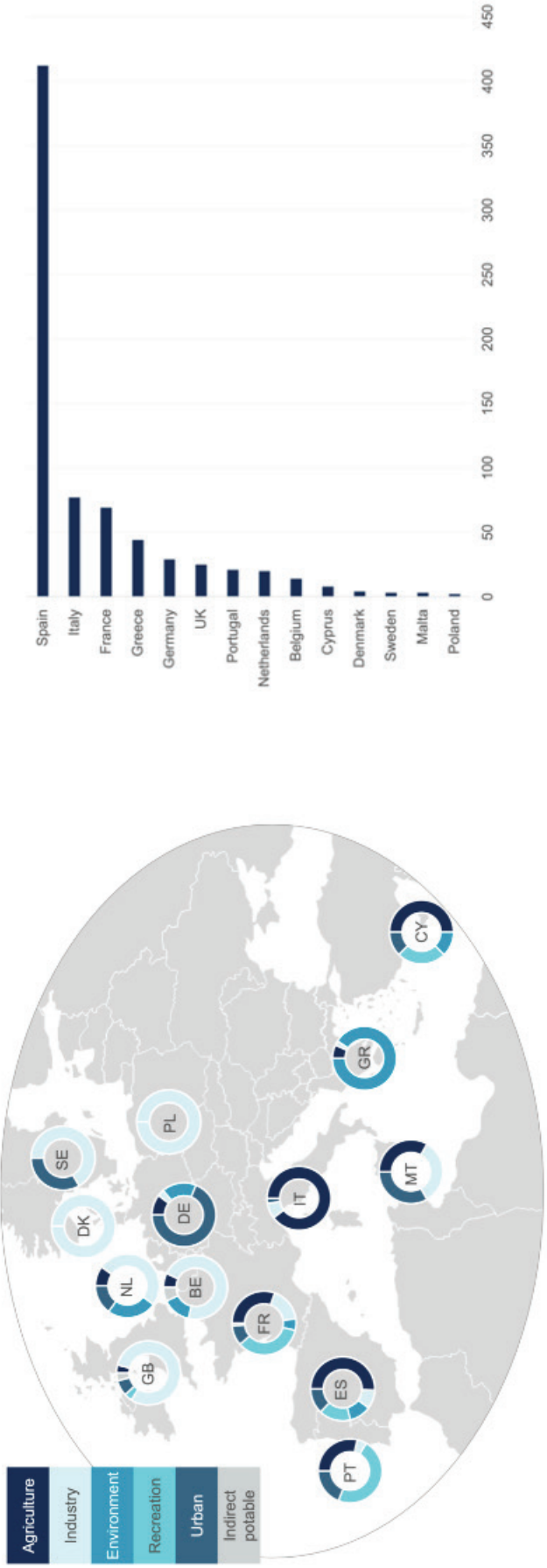

Figure 7. New projects for the reuse of treated water in Europe, financed with Next Generation funds. a) Share of reuse projects in Europe by sector; b) Number of reuse projects by country. Source: Water Reuse Europe. Bluefield Research.

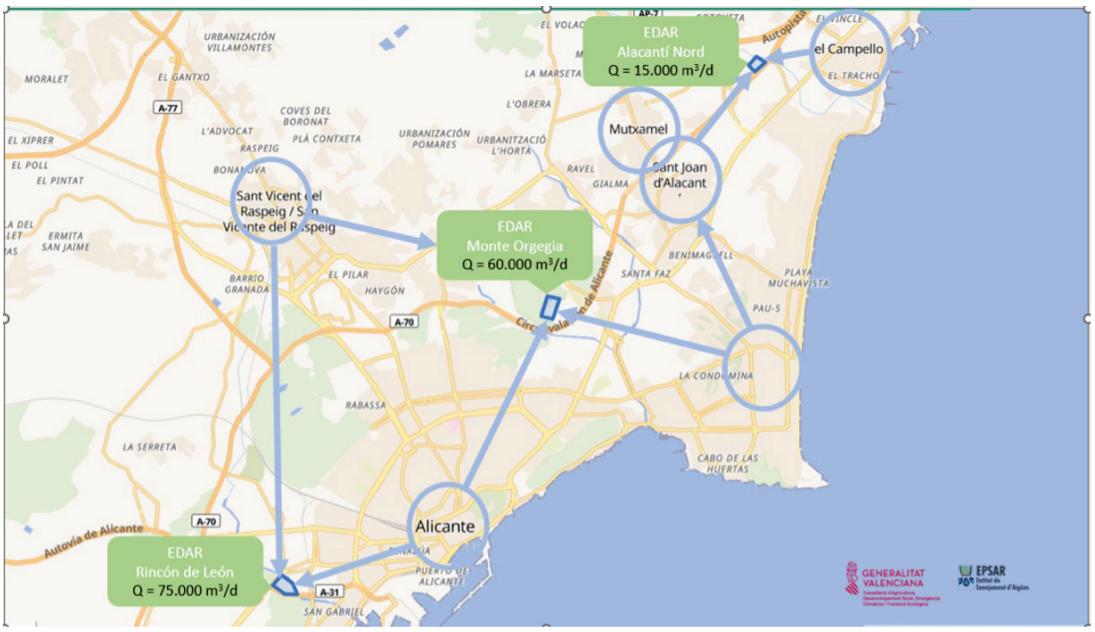

Figure 8. "Vertido Cero" water project for the comprehensive reuse of treated waters of the city of Alicante for agricultural purposes. Its development will give rise to the implementation of the first "transfer" of wastewater between districts of the same province in Spain. Source: Generalitat Valenciana. EPSAR.

Desalination provides an "inexhaustible" source of water in coastal areas and large volumes in the areas far from the coast with saline groundwater resources. Desalinised water enables the state of emergency to be modified in situations of drought as it provides water that does not depend on the rain and guarantees supply, particularly in urban nuclei. Spain is the European leader and one of the global powers in terms of the production capacity of desalinated water (5.6 hm^3/day). Since the first desalination plant was opened in Lanzarote in 1964 until the present day, the desalination capacity, the type of plants and the production costs have improved continuously. In 2024, the volume of water from the desalination of marine water and continental brackish water is 600 hm^3/year. The principal use of desalinated water is urban. The cost of the water produced (€0.70/m^3) is high for its use in irrigation, except in the avant-garde agricultural crops. This is the case even though the cost has decreased considerably over the last three decades due to the improvement in the productivity of the membranes (inverse osmosis) and the lower energy cost (Swyngedouw and Williams, 2016). Voutchkov (2016) indicates that the cost of desalinated seawater will continue to decrease over the coming years from €1.1/m^3 at the end of the 2020s to €0.3-0.8 €/m^3 at the end of the 2030s. However, currently, the public administrations (state and regional) are required to promote support measures in order to reinforce the use of desalinated water in agriculture. In recent years, within the framework of the Iberian drought 2021-23 and applicable until 2026, the Ministry of Ecological Transition issued a series of economic grants to subsidise the cost of desalinated water production in the provinces of Alicante, Murcia and Almería, establishing a maximum price of €0.40/m^3 for the waters produced in the desalination plants in these territories. These subsides were extended with regional funds in the Region of Valencia, resulting in a final price of desalinated water (Torrevieja plant) of € 0.24/m^3 (plus VAT), an amount that is highly competitive with the price established for the use of the water of the Tajo-Segura transfer (€ 0.18/m^3, exempt from VAT).

To the treated wastewater resources we should add the rainwater collected in the urban environment. This volume of water is small but the implementation of rainwater harvest systems represents a commitment of the cities to the recovery of a resource that would otherwise cause damage (intense rains) in the urban fabric and would be lost if a direct human use were not made of them through the sewer network or collectors in the urban nuclei. Rainwater harvesting recovers the historical tradition dating back to Roman times, widely disseminated throughout urban nuclei and rural dwellings in the south-east of the peninsula, which used the rainwater for their drinking water supply in daily life. These systems fell into

disuse with the implementation of a widespread domestic water supply with the mapping and consolidation of the suburbs and the contemporary evolution of Spanish cities. At the end of the last century, some cities on the Mediterranean coast designed modern rainwater harvesting systems in order to reduce the risk of floods in urban environments. They are municipally managed sustainable urban drainage systems (SUDS), designed to harvest torrential rainwater and the principal aim is to reduce the risk generated by the circulation of water in the streets and floods. Barcelona was the first city (1999) to develop a harvesting system in the suburbs seeking to reduce the water circulating in the streets. This reduces the risk to human life in the city during intense rain episodes, which are becoming more frequent in Spain, particularly in the territories of the Mediterranean coast (Arahuetes and Olcina Cantos, 2019). In addition to tanks, floodable parks have also been designed that capture water in a gardened area and with a recreational everyday use, while acting as a rainwater storage facility on days of abundant rainfall. The water remains in this tank for a few days and can be returned to the natural environment (river) or sent to a nearby treatment station to be reused after treatment. In this respect, we can refer to the floodable parks of Alicante (La Marjal) (Morote Seguido and Hernández Hernández, 2017) and those constructed since 2021 in the Vega Baja del Segura as an effect of the development of the Vega Renhace Plan after the flood of September 2019 (Generalitat Valenciana, 2020).

As a whole, the rainwater harvesting systems installed in different Spanish cities with a capacity to be incorporated into the municipal water supply network represent 1% of the volume of urban water resources. However, it is important to promote their implementation as an example of good practices for the management of flood risk and the urban commitment to the circular economy of water. The rainwater tanks or floodable parks do not resolve the problem of a large impact flood; but they enable the risk in intense rain episodes of between 50 and 100 mm/h to be reduced.

All of these "non-conventional" resources, together with the traditional water sources, should be managed efficiently; that is, a precise accounting of the expenditure should be made in both the agricultural and urban environments and water should be supplied avoiding as much as possible losses associated with the distribution of a liquid in continuous use. In the agricultural environment, the PERTE of water, approved in 2022, considers the installation of meters on the plots of land in order to practice a real accounting of the agricultural expenditure. In the cities, 650 hm^3/year are lost in the distribution networks, which indicates an inadequate accounting of the urban consumption of water (approx. 4,000 hm^3/year) (Fig. 9). To this volume we must add the losses to obtain the real figure of water distributed in the municipal supply networks and that did not reach the meters in the homes (due to direct losses in the network or non-invoiced water in the households). The existence of a transparency portal in water management in Spain is one of the most important tasks that should be undertaken by the State in the coming years. Its development constitutes a basic piece of water planning in the current context of climate change.

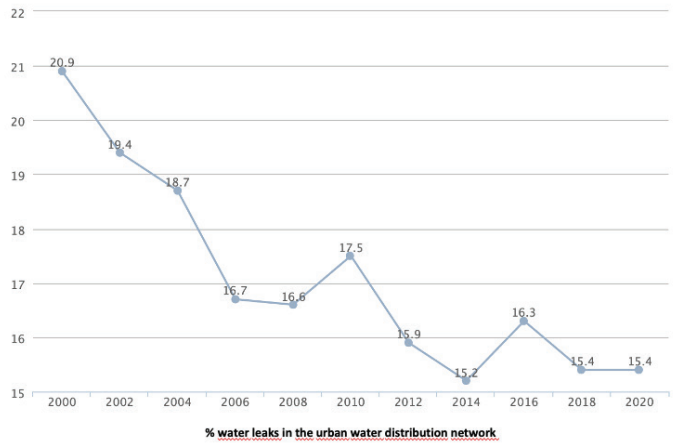

Figure 9. Losses of water distributed in the drinking water network in Spanish municipalities Source: AEAS.

4. Discussion and conclusions: water planning in Spain, future agenda

The planning and management of water in Spain within the context of climate change should be based on clear principles of action: quality instead of quantity, the improvement of the management of demand as opposed to a continued resource supply policy and the circular management of water with the incorporation of all the available resources in a territory in water planning. Hence, according to scientific-technical criteria, Spain needs a medium-term planning scheme that should be approved in the next hydrological cycle (4th cycle 2028-33) to be able to integrate a precise modelling of the effects of climate change on the temperatures and precipitations of our country and, in short, on the volumes of water available until 2050, updating the report elaborated in 2017 by the Cedex (Cedex, 2017).

The firm commitment to the mobilisation of new water resources that guarantees Spain's water security should be based on the reuse of treated waters, which should have a percentage share in the water resources mix of over 50% for the whole of the country and 80% in the regions and areas with a higher precariousness of conventional resources (Murcia, Region of Valencia, Balearic Islands, Canary Islands, Eastern Andalusia). Large population nuclei (>100,000 inhabit.) should become spaces for the production of regenerated water for its use in nearby agricultural areas and for urban supply (irrigation of parks and gardens, street cleaning and the irrigation of private green spaces) (Bernabé-Crespo *et al.,* 2023). Within this urban context, rainwater should be incorporated into the circular water cycle of the city.

Desalination will become a commonly used source of water resources on the Mediterranean coast. The volumes contributed should replace flows of conventional resources used in the urban nuclei that can be partly or wholly used for the agricultural activity. The use of desalinated water by agriculture for irrigation should receive public subsidies to adjust the final price to the income statement of the agricultural production in each case. The technological improvements will enable the price of desalinated water to be reduced over the next two decades.

The existing water transfers in Spain will be able to continue operating, although in some cases they will experience the alterations forecast in precipitations within the context of climate change. The contemplation of new transfers between water basins does not seem to be feasible due to climate and political reasons. However, transfers within the same river basin would be possible, particularly when they are located within the borders of the same autonomous region, provided that there is an agreement between the users (assignors and recipients). On the contrary, the future is uncertain for the transfers between different river basins that have their origin in rivers whose headwaters are currently experiencing a decrease in rainfall contributions and available volumes (Tajo-Segura). In this case, it is necessary to plan alternative solutions to the volumes transferred each year through other non-conventional resources if we wish to maintain the current level of agricultural and urban-tourism development in the receiving territories (Oliva *et al.,* 2022). There is no unanimity with respect to this option in the scientific-technical community. The continuity of the hydraulic engineering works for the retention and transfer of water is still a focus of economic (Melgarejo and López Ortiz, 2015) and engineering (Cabezas, 2002, 2013) studies. Although other studies defend an integrated management of the basins, in which the structural works (dams, canals) should constitute just one more piece in an overall plan for a river basin (Grindlay *et al.*, 2007, Magdaleno Mas, 2020).

It will be necessary to activate economic "compensation" systems in terms of water between the city and the countryside for the use of treated waters in the rural environment; and also between the coast and the inland territory for the use of desalinated waters in conditions of economic profitability for agriculture. The agricultural activity should begin to work on adapting to climate change, with the installation of meters on farms that enable us to determine the real cost of water. Over the coming decades, there will be improvements in irrigation systems, in crop varieties and changes in cropping calendars, which will facilitate the adaptation to the new climate conditions being recorded, with higher temperatures and a greater irregularity of precipitations. Agronomic research will play a prominent role in restraining the agricultural use of water in Spain. And the hydrological plans of the basin should

constitute an element of containment and reduction in the aspirations of new agricultural changes, particularly in regions with a natural shortage of conventional resources.

In any case, water planning, with its different figures (river basin plans, drought plans, flood risk plans) should take into account regular review calendars in their estimates in accordance with the improvements that are taking place in climate modelling.

Water planning in Spain should harmonise water resources and demands with territorial planning, both for agriculture and urban uses of water. From the next hydrological cycle plan (2027), the implementation of new irrigation techniques should adapt to the rainfall reality in the river basins. Future hydrological plans for river basins should only approve new irrigation techniques if they use treated waters or groundwater from aquifers that are not at risk of overexploitation in the medium term (horizon 2050). An identical procedure should be applied for golf course projects, which, from now on should only be permitted if they can be maintained with regenerated water. The example of the golf course law of the Balearic Islands should serve as an example for the rest of the Spanish territories with these kinds of project, particularly in the Mediterranean coast regions. Urban planning should establish growth indicators in the housing stock that ensures its future supply with the currently existing resources; and compact city models should be imposed on dispersed cities that incur a greater urban consumption of water (150 litres/inhabitant/day in the former as opposed to 350-400 litres/inhabitant/day in the latter) and greater losses in the distribution network. The case of Benidorm, with a drinking water network efficiency of 95% (one of the greatest in Europe) can serve as an example for the whole of Spain (Rico *et al.,* 2019).

In short, the planning and management of water in Spain should seek to become more transparent in terms of the data for research purposes. This planning should be based exclusively on scientific-technical criteria, which means the exclusion of ideological interferences in the elaboration of water-related action programmes in Spain. In this respect, the geography discipline will play a prominent role in the future of water in this country due to its comprehensive knowledge in physical and human aspects in the territory. Hence the importance of the training of geography professionals in order to prepare them for participating in water planning and management.

Author's note

This paper is a compilation of ideas presented in the closing conference given by the author at the XVIII Congress of the AGE at the University of La Rioja between 12 and 14 September 2023. The author expresses his gratitude to the editors of the journal for their professionalism in the editing process of this paper.

References

Acero, F.J., Gallego, M.C., García, J.A., 2012. Multi-day rainfall trends over the Iberian Peninsula. *Theor Appl Climatol* 108, 411–423. https://doi.org/10.1007/s00704-011-0534-5

AEAS, 2022. Datos del sector del agua urbana, 2022. *XVII Estudio Nacional de Suministro de Agua potable y saneamiento en España 2022*. https://www.aeas.es/component/content/article/52-estudios/estudios-suministro/301-xvii-estudio-nacional-aeas-aga?Itemid=101

Aguas de Alicante, 2023. *Informe de Sostenibilidad*. Alicante, 117 pp. https://www.aguasdealicante.es/documents/231378/2543694/IDS-AMAEM-2024.pdf/52be7c48-98aa-11e8-0dda-774e0cac575b?t=1718282853887

Albiac Murillo, J., Esteban Gracia, E., Baccour, S., 2023. La situación y perspectiva de los recursos hídricos en España. *Estudios sobre Economía Española* 2023/29. Fedea, 34 pp., Madrid.

Angelakis, A. N., Valipour, M., Ahmed, A.T., Tzanakakis, V., Paranychianakis, N.V., Krasilnikoff, J., Drusiani, R., Mays, L., El Gohary, F., Koutsoyiannis, D., Khan, S., Del Giacco, L.J., 2021. Water Conflicts: From

Ancient to Modern Times and in the Future. *Sustainability* 13, 8: 4237. https://doi.org/10.3390/su13084237

Arahuetes, A., Olcina Cantos, J., 2019. The potential of sustainable urban drainage systems (SuDS) as an adaptive strategy to climate change in the Spanish Mediterranean. *International Journal of Environmental Studies* 76(5), 764–779. https://doi.org/10.1080/00207233.2019.1634927

Berbel, J., Espinosa-Tasón, J., 2020. La gestión del regadío ante la escasez del agua. *Presupuesto y gasto público* 101 (Ejemplar dedicado a: El agua en España: economía y gobernanza), 137-152.

Bernabé-Crespo M.B., Olcina Cantos J., Oliva, Cañizares A., 2023. Proposal of the "Wastewater Use Basin" Concept as an Integrated Sewage and Rainwater Management Unit in Semiarid Regions—A Case Study in the Southeast of the Iberian Peninsula. Water 15(12): 2181. https://doi.org/10.3390/w15122181

Bluefield Research, 2023. *Europe municipal wastewater reuse: market trends and forecast, 2023-2030*. https://www.bluefieldresearch.com/research/europe-municipal-wastewater-reuse-market-trends-and-forecasts-2023-2030/

Cabezas, F., 2002. El Plan Hidrológico Nacional. En *Insuficiencias Hídricas y Plan Hidrológico Nacional*. Ed. Universidad de Alicante, p. 45-55.

Cabezas, F., 2013. *El sistema de cabecera del Tajo y el trasvase Tajo-Segura*. https://paisajesdelagua.wordpress.com/wp-content/uploads/2021/04/sitemacabeceratajomemorandum.pdf

Caretta, M.A., Mukherji, A., Arfanuzzaman, M., Betts, R.A., Gelfan, A., Hirabayashi, Y., Lissner, T.K., Liu, J., Lopez Gunn, E., Morgan, R., Mwanga, S., Supratid, S., 2022. Water. In: *Climate Change 2022: Impacts, Adaptation and Vulnerability.* Contribution of Working Group II to the Sixth Assessment Report of the Intergovernmental Panel on Climate Change (H.O. Pörtner, D.C. Roberts, M. Tignor, E.S. Poloczanska, K. Mintenbeck, A. Alegría, M. Craig, S. Langsdorf, S. Löschke, V. Möller, A. Okem, B. Rama (eds.). Cambridge University Press, pp. 551–712, Cambridge, UK and New York, NY, USA,

CEDEX, 2021. *Impacto del cambio climático en las precipitaciones máximas en España*, Centro de Estudios Hidrográficos, 404 pp., Madrid

CEOE, 2023. *Informe sobre el agua en España: situación actual, retos y oportunidades*. 28 pp., Madrid, resumen ejecutivo. https://www.cen.es/wp-content/uploads/2023/11/OT01NV23_1.pdf

Cramer, W., Guiot, J., Fader, M., Garrabou, J., Gattuso, J.P., Iglesias, A., Lange, M.A., Lionello, P., Llasat, M. C., Paz, S., Peñuelas, J., Snoussi, M., Toreti, A., Tsimplis, M.N., Xoplaki, E., 2018. Climate change and interconnected risks to sustainable development in the Mediterranean. *Nature Climate Change* 8, 972-980. https://doi.org/10.1038/ s41558-018-0299-2

Cresswell-Clay, N., Ummenhofer C.C., Thatcher D.L., Wanamaker A.D., Denniston R.F., Asmerom Y., Polyak V.J., 2022. Twenthieth Century Azores High expansion unprecedented in the last 1200 years. *Nature Geoscience* 15, 548-553. https://doi.org/10.1038/s41561-022-00971-w

De Stefano, L., Hernández-Mora, N., 2019. Gestión de los recursos naturales en España: cooperación interadministrativa en un contexto descentralizado. *Fundación Ramón Areces* 21. pp. 106-119, Madrid. https://www.fundacionareces.es/recursos/doc/portal/2019/07/17/revista-fra-num-21-gestion-de-los-recursos-naturales.pdf

Elorrieta-Sanz, B., Olcina-Cantos, J., 2021. Infraestructura verde y Ordenación del Territorio en España. *Ciudad y Territorio Estudios Territoriales* 53(207), 23–46.

Escudero Gómez, L. A., Martín Trigo, A., 2020. La gestión pública de una obra hidráulica compleja, entre el marco internacional y los intereses regionales privados: el caso del trasvase Tajo-Segura (España). *Relaciones Internacionales* 45, 327-344.

European Environment Agency, 2024. *Europe´s state of water, 2024*. European Environment Agency, 108 pp., Copenhagen. https://www.eea.europa.eu/en/analysis/publications/europes-state-of-water-2024

European Environment Agency, 2024. *European Climate Risk Assessment*. European Environment Agency, 488 pp., Copenhagen. https://www.eea.europa.eu/publications/european-climate-risk-assessment

Farinós-Dasí, J., 2021. Agenda Territorial Europea 2030: un marco político orientado a la acción para el objetivo de la cohesión territorial. *Ciudad y Territorio Estudios Territoriales* 53 (208), 583–594. https://doi.org/10.37230/CyTET.2021.208.17.2

Fernández-Jáuregui, C., coord., 2017. El agua ¿fuente de conflicto o de cooperación?, *Cuadernos de Estrategia* 186, Instituto Español de Estudios Estratégicos. Ministerio de Defensa, 268 pp., Madrid

Fundación BBVA, 2022. *Valores, actitudes y conducta medioambiental de los españoles*. Departamento de Estudios sociales y opinión pública. https://www.biophilia-fbbva.es/wp-content/uploads/sites/3/2022/06/estudio-cultura-medioambiental.pdf

Generalitat Valenciana, 2020. *Plan Vega Rehace. Una estrategia integral para la resiliencia de la comarca de la Vega Baja del Segura*. Dirección General de Análisis y Políticas Publicas, Valencia. http://www.presidencia.gva.es/es/web/vega-renhace

Gómez Espín, J.M., 2019. Modernización de regadíos en España: experiencias de control, ahorro y eficacia en el uso del agua para riego. *Agua y Territorio* 69-76. https://doi.org/10.17561/at.13.3972

González, A., Santos, M., Hernández, J.C., Acosta, B., Montalvo, J., 2020. *Aumenta la frecuencia e intensidad de las sequías por el cambio climático en España*. Fundación Matrix. Proyecto Climvac. https://fundacionmatrix.es/aumenta-la-frecuencia-e-intensidad-de-la-sequia-por-el-cambio-climatico-en-espana/

González, M.J., 2024. El impacto en España de la nueva directiva europea de aguas residuales. Iagua, Madrid. https://www.iagua.es/blogs/manuel-j-gonzalez/impacto-espana-nueva-directiva-europea-aguas-residuales

González-Hidalgo, J.C., Brunetti, M., de Luis, M., 2010. Preicipation trends in Spanish hydrological divisions, 1946-2005. *Climate Research* 43(3), 215-228. https://doi.org/10.3354/cr00937

González-Hidalgo, J. C., Beguería, S., Peña-Angulo, D., Trullenque-Blanco, V., 2023. MOPREDAS_century database and precipitation trends in mainland Spain, 1916–2020. *International Journal of Climatology* 43(8), 3828–3840. https://doi.org/10.1002/joc.8060

Gonzalez-Hidalgo, J.C., Trullenque Blanco, V., Beguería, S., Peña-Angulo, D., 2024. Seasonal precipitation changes in the western Mediterranean Basin: The case of the Spanish mainland, 1916–2015, *International Journal of Climatology* 44(5). https://doi.org/10.1002/joc.8412

Gorostiza, S., Parrinello, G., Aguettaz, D., Saurí, D., 2023. Where have all the sediments gone? Reservoir silting and sedimentary justice in the lower Ebro River. *Political Geogr.* 107, 102975. https://doi.org/10.1016/j.polgeo.2023.102975

Grindlay, A., Molero, E., Rodríguez-Rojas, M., 2007. Desarrollo Infraestructural Hidráulico, Planificación Hídrica y Territorial en la cuenca del Segura: hacia una Planificación Integrada. *V Congreso Internacional de Ordenación del Territorio*, Volume: Agua, Territorio y Paisaje. De los instrumentos programados a la planificación aplicada. Málaga (Spain)

Horacio, J., Ibisate, A., Sánchez Pinto, I., Beltrán de Lubiano, J., Ollero, A., 2018. Seguimiento del transporte de sedimentos mediante trazadores en el río Leitzaran. In C. Garcia, L. Gómez-Pujol, E. Morán-Tejeda, R.J., Batalla (Eds.). *Geomorfología del "Antropoceno": Efectos del Cambio Global Sobre los Procesos Geomorfológicos* Universitat de les Illes Balears, pp. 53-56, Mallorca, Spain.

Ibáñez, C., Prat, N., Canicio, A., 1996. Changes in the hydrology and sediment transport produced by large dams on the lower Ebro river and its estuary. *Regul. Rivers Res. Manag.* 12, 51–62. https://doi.org/10.1002/(SICI)1099-1646(199601)12:1<51::AID-RRR376>3.0.CO;2-I

Karamidehkordi, E., Karimi, V., Singh, G., Naderi, L., 2024.Water conflicts and sustainable development: concepts, impacts, and management approaches. In S. A. Bandh, F. A. Malla (eds.) *Current Directions in Water Scarcity Research*, Elsevier, Volume 8. https://doi.org/10.1016/B978-0-443-23631-0.00016-9

Lana, X., Casas-Castillo, M.C., Rodríguez-Solà, R., Serra, C., Martínez, M.D., Kirchner, R., 2021. Rainfall regime trends at annual and monthly scales in Catalonia (NE Spain) and indications of CO_2 emissions effects. *Theoretical and Applied Clim*atology 14, 981-996. https://doi.org/10.1007/s00704-021-03773-z

López Gum, E., Vargas Amelín, E., 2020. La gobernanza del agua subterránea y la seguridad hídrica en España. *Estudios sobre la Economía Española* - 2020/40. Fedea, 26 pp.

Magdaleno Mas, F., 2020. La política hídrica en España: hacia una integración avanzada de agua, *Territorio y Sociedad*. Fedea, 23 pp., Madrid,

Martí Ezpeleta, A., Cuadrat Prats, J.M., Marzol Jaén, M.V., Royé, D., Serrano, R., 2019. Clima y Agua. En: *España en Mapas. Una síntesis geográfica*, IGN. Madrid. https://atlasnacional.ign.es/wane/Clima

Martín, B., Urquiaga, R., Larraz, B., Bernal, I., 2024. *Estudio sobre la contaminación de las aguas del río Tajo a su paso por Toledo y posibles causas de la generación de espumas*. Catedra del Tajo, 77 pp., Toledo. https://catedradeltajo.es/wp-content/uploads/2024/06/Informe-Contaminacion-y-Espumas-rio-Tajo-en-Toledo_compressed.pdf

Martínez-Fernández, J., Roca, S., Hernández-Mora, N., Del Moral, L., La Roca, F., 2020. The role of the Water Framework Directive in the controversial transition of water policy paradigms in Spain and Portugal. *Water Alternatives* 13(3), 556-581

Melgarejo, J., López Ortiz, M., 2015. Evolución de la Planificación Hidrológica en la España democrática, 1978-2014. En: *Agua y Derecho. Retos para el sigo XXI* (Reflexiones y estudios a partir del WATER LAW, Congreso Internacional de Derecho de Agua). Alicante, octubre 2014.

Meseguer-Ruiz, O., Olcina Cantos, J., 2023. Climate change in two Mediterranean climate areas (Spain and Chile): Evidences and projections. *Investigaciones Geográficas* 79, 9-31.

Ministerio de Transición Ecológica y Reto Demográfico, 2021. *Plan Nacional de Depuración, Saneamiento, Eficiencia, Ahorro y Reutilización*, 189 pp., Madrid. https://www.miteco.gob.es/content/dam/miteco/es/agua/temas/planificacion-hidrologica/plan_dsear_final_tcm30-529674.pdf

Miró, J.J., Estrela, M.J., Olcina-Cantos, J., Martin-Vide, J., 2021. Future Projection of Precipitation Changes in the Júcar and Segura River Basins (Iberian Peninsula) by CMIP5 GCMs Local Downscaling. *Atmosphere* 12(7), 879. https://doi.org/10.3390/atmos12070879

Miró, J.J., Estrela, M.J., Corell, D., Gómez, I., Luna, M. Y., 2023. Precipitation and drought trends (1952–2021) in a key hydrological recharge area of the eastern Iberian Peninsula. *Atmospheric Research* 286, 106695. https://doi.org/10.1016/j.atmosres.2023.106695

Molina Giménez, A., 2010. Derecho de los trasvases en España. *Diario La Ley*, Nº 7366, Sección Tribuna, 22 de marzo de 2010, Año XXXI.

Morote Seguido, A. F., 2014. La planificación y gestión de los recursos hídricos en España: aproximación a los principales grupos y líneas de investigación, *Investigaciones Geográficas* 62, 113-125.

Morote Seguido, A. F., Hernández Hernández, M., 2017. El uso de aguas pluviales en la ciudad de Alicante. De viejas ideas a nuevos enfoques. *Papeles de Geografía* 1, 7–25. https://doi.org/10.6018/geografia/2017/279451

Muñoz, C., Schultz, D., Vaughan, G., 2020. A Midlatitude Climatology and Interannual Variability of 200- and 500-hPa Cut-Off Lows. *Journal of Climate* 33 (6), 2201-2222. https://doi.org/10.1175/JCLI-D-19-0497.1

Navarro-Sousa, S., Estruch-Guitart, V., 2022. Implementación de la Directiva Marco del Agua en España: perspectivas futuras. Revisión bibliográfica. *ITEA-Informacion Tecnica Economica Agraria* 118(2), 318-338. https://doi.org/10.12706/itea.2021.029

Olcina Cantos, J. 2001. Tipología de sequías en España. *Ería* 56, 201-227

Olcina Cantos, J., 2024. El cambio climático y la gestión del riesgo: algunas experiencias en el litoral mediterráneo español. En: I. Alkorta, Y. Hernández, U. Etxeberria (dir.). *Mugarteko ingurumena: aldaketa klimatikoa, hezkuntza-testuinguruak eta erronka digital berriak / Environnements transfrontaliers : changements climatique, contextes éducatifs et nouveaux défis numériques / Entornos transfronterizos: cambio climático, contextos educativos y nuevos retos digitales*, Pessac, PUPPA, collection Schol@ 4, 33-56, https://una-editions.fr/el-cambio-climatico-y-la-gestion-del-riesgo

Olcina Cantos, J. 2024. Trasvase Tajo-Segura: futuro incierto. En J. Martínez Valderranma, S. Soliveres Codina, F.T. Maestre Gil (Edits.). *Arida Cutis. Ecología y retos de las zonas áridas en un mundo cambiante*. Publicaciones de la Universidad de Alicante, pp. 137-145, Alicante

Oliva Cañizares, A., Olcina Cantos, J., Baños Castiñeira, C.J., 2022. The Effects of Climate Change on the Tagus–Segura Transfer: Diagnosis of the Water Balance in the Vega Baja del Segura (Alicante, Spain), *Water* 14(13), 2023. https://doi.org/10.3390/w14132023

Paredes, D., Trigo, R.M., Garcia-Herrera, R., Trigo, I.F., 2006. Understanding precipitation changes in iberia in early spring: weather typing and storm-tracking approaches *J. Hydrometeorol*. 7, 101-113, https://doi.org/10.1175/JHM472.1

PWC, 2018. *La gestión del agua en España. Análisis y retos del ciclo urbano del agua*. 128 pp., Madrid, 128 pp., https://www.pwc.es/es/publicaciones/energia/assets/gestion-agua-2018-espana.pdf

Raworth, K., 2012. A safe an just space por humanity. Can we live within the doughnut? *Oxfam Discussion Papers*, February. https://www-cdn.oxfam.org/s3fs-public/file_attachments/dp-a-safe-and-just-space-for-humanity-130212-en_5.pdf

Raworth, K., 2017. A Doughnut for the Anthropocene: humanity's compass in the 21st century. *The Lancet Planetary Health* 1 (2), e48-e49. https://www.thelancet.com/journals/lanplh/article/PIIS2542-51961730028-1/fulltext

Razquín Lizárraga, J.A., 2018. El acceso a la información en materia de medio ambiente en España: balance y retos de futuro. *Revista Catalana de Dret Ambiental* 9, 1. https://doi.org/10.17345/rcda2409

Rico Amorós, A. M., 2010. Plan Hidrológico Nacional y Programa A.G.U.A.: Repercusión en las regiones de Murcia y Valencia. *Investigaciones Geográficas* 51, 235-267

Rico Amorós, A., Olcina Cantos, J., Paños Callado, V., Baños Castiñeira, C., 1998. *Depuración, desalación y reutilización de aguas en España*. Vilassar de Mar. Ed. Oikos-Tau.

Rico, A., Olcina, J., Baños, C., García, X., Sauri, D., 2019. Declining water consumption in the hotel industry of mass tourism resorts: contrasting evidence for Benidorm, Spain. *Current Issues in Tourism 23*(6), 770–783. https://doi.org/10.1080/13683500.2019.1589431

Romero, J. 2009. *Geopolítica y gobierno del territorio en España*, Tirant Lo Blanch, Valencia

Romero, J. 2017. El gobierno del territorio en España. Organización territorial del Estado y políticas públicas con impacto territorial. *Naturaleza, territorio y ciudad en un mundo global*. Asociación de Geógrafos Españoles, 2379-2393 pp., Madrid.

Ruiz-Sinoga, J., García-Marín, R., Martínez Murillo, J., Gabarrón-Galeote, M., 2011. Precipitation dynamics in southern Spain: Trends and cycles. *International Journal of Climatology* 31, 2281 - 2289. https://doi.org/10.1002/joc.2235

Sanchis-Ibor, C., Mollá, M., Reus, L., 2016. Las políticas de implantación del riego localizado. Efectos en las entidades de riego de la Comunidad Valenciana. *Boletín de la Asociación de Geógrafos Españoles* 72, 9. https://doi.org/10.21138/bage.2330

Senent-Aparicio, J., López-Ballesteros, A., Jimeno-Sáez, P., Pérez-Sánchez, J., 2023. Recent precipitation trends in Peninsular Spain and implications for water infrastructure design. *Journal of Hydrology: Regional Studies* 45, 101308. https://doi.org/10.1016/j.ejrh.2022.101308

Serrano Notivoli, R., 2017. *Reconstrucción climática instrumental de la precipitación diaria en España: Ensayo metodológico y aplicaciones*. Tesis doctoral, Universidad de Zaragoza.

Solorzano Chamorro, J. J., Vera Basurto, J. S., Buñay Cantos, J. P., 2022. Crecimiento económico y medio ambiente. *RECIAMUC* 6(1), 203-212. https://doi.org/10.26820/reciamuc/6.(1).enero.2022.203-212

Sotelo Pérez, M., Sotelo Pérez, I., Galvani, A., 2021. Una aproximación a las Políticas del Agua en España: gestión y planificación de los recursos hídricos. *Anales de Geografía de la Universidad Complutense* 41(1), 217-264. https://doi.org/10.5209/aguc.76730

Swyngedouw, E., Williams, J., 2016. From Spain's hydro-deadlock to the desalination fix. *Water International* 41, 54-73. https://doi.org/10.1080/02508060.2016.1107705

Torelló-Sentelles, H., Franzke, C. L. E., 2022. Drought impact links to meteorological drought indicators and predictability in Spain. *Hydrol. Earth Syst. Sci*. 26, 1821–1844, https://doi.org/10.5194/hess-26-1821-2022

Trullenque-Blanco, V., Beguería, S., Vicente-Serrano, S.M., Peña Ángulo, D., González-Hidalgo, C., 2024. Catalogue of drought events in peninsular Spanish along 1916–2020 period. *Scientific Data* 11, 703. https://doi.org/10.1038/s41597-024-03484-w

Vázquez-Tarrío, D., Ruiz-Villanueva, V., Garrote, J., Benito, G., Calle, M., Lucía, A., Díez-Herrero, A., 2023. Effects of sediment transport on flood hazards: Lessons learned and remaining challenges. *Geomorphology* 446, 108976. https://doi.org/10.1016/j.geomorph.2023.108976

Vericat, D., Batalla, R.J., 2006. Sediment transport in a large impounded river: The lower Ebro, NE Iberian Peninsula. *Geomorphology* 79, 72–92. https://doi.org/10.1016/j.geomorph.2005.09.017

Vicente-Serrano, S., 2021. The evolution of climatic drought studies in Spain over the last few decades. *Geographicalia* 7-34. https://doi.org/10.26754/ojs_geoph/geoph.2021734640

Voutchkov, N., 2016. Desalination: Past, Present and Future. *International Water Association* 17/08/2016. https://iwa-network.org/Desalination,-past-present-future

Xian, T., Xia, J., Wei, W., Zhang, Z., Wang, R., Wang, L. P., Ma, Y. F., 2021. Is Hadley cell expanding? *Atmosphere* 12(12), 1699. https://doi.org/10.3390/atmos12121699

Cuadernos de Investigación Geográfica *Geographical Research Letters*	2024	Nº 50 (2)	pp. 29-44	EISSN 1697-9540

http://doi.org/10.18172/cig.5847

THE INFLUENCE OF CLIMATE VARIABILITY ON RISK ASSESSMENT OF TROPICAL CYCLOGENESIS IN THE GULF OF MEXICO

ERNESTO VILLATE GARCÍA[1], GUILLERMO GUTIÉRREZ DE VELASCO SANROMÁN[2], LEMAY ENTENZA TILMAN[3], IRINA TERESHCHENKO[2], JULIO CÉSAR MORALES HERNÁNDEZ[4]*, FAUSTINO O. GARCÍA CONCEPCIÓN[2]

[1]*PhD Student, University of Guadalajara, Guadalajara, 44840, Jalisco, México.*

[2]*Department of Basic Sciences, University Centre for Exact Sciences and Engineering, University of Guadalajara, 44840, Jalisco, México.*

[3]*PhD Student, National Autonomous University of Mexico, Coyoacán, 04510 Ciudad de México, CDMX, México.*

[4]*Department of Exact Sciences, University Center of the Coast, University of Guadalajara, Guadalajara, 48280, Jalisco, México.*

ABSTRACT. Climate change and climate variability risk assessments are usually focus on tropical cyclones due to the potential hazard for human society, especially in urban coastal areas such as those along the Gulf of México. The frequency of this natural phenomenon depends on the confluence of different dynamic (wind divergence and relative vorticity) and thermodynamic (atmospheric water content and sea surface temperature) factors. Large scale atmospheric oscillations modulate these factors and influence tropical cyclone (TC) formation and development, producing important social and economic impacts. This work explores the Maden-Julian Oscillation (MJO) and El Niño-South ern Oscillation (ENSO) relationship in regard to the Gulf of México tropical cyclogenesis, using time series and synoptic case study analyses, in order to contribute to future risk assessments in these coastal zones. Results indicate MJO and ENSO frequencies are present in wind divergence and relative vorticity, atmospheric water vapor content, and sea surface temperature. Concurring cold phase ENSO and convective phase MJO conditions benefit TC formation, while warm phase ENSO conditions inhibit TC formation and affect the MJO cycle. Synoptic case study analyses show wind divergence and atmospheric water content anomalies dominate TC behavior.

Influencia de la variabilidad climática en la evaluación del riesgo de ciclogénesis tropical en el Golfo de México

RESUMEN. Las evaluaciones de riesgos del cambio climático y la variabilidad climática generalmente se centran en ciclones tropicales debido al peligro potencial para la sociedad humana, especialmente en áreas costeras urbanas como las que se encuentran a lo largo del Golfo de México. La frecuencia de este fenómeno natural depende de la confluencia de diferentes factores dinámicos (divergencia del viento y vorticidad relativa) y termodinámicos (contenido de agua atmosférica y temperatura de la superficie del mar). Las oscilaciones atmosféricas a gran escala modulan estos factores e influyen en la formación y el desarrollo de ciclones tropicales (TC), produciendo importantes impactos sociales y económicos. Este trabajo explora la relación entre la Oscilación Maden-Julian (MJO) y El Niño-Oscilación del Sur (ENSO) con respecto a la ciclogénesis tropical del Golfo de México, utilizando series temporales y análisis de estudios de casos sinópticos, con el fin de contribuir a futuras evaluaciones de riesgos en estas zonas costeras. Los resultados indican que las frecuencias de OMJ y ENSO están presentes en la divergencia del viento y la vorticidad relativa, el contenido de vapor de agua atmosférico y la

temperatura de la superficie del mar. Las condiciones concurrentes de ENOS de fase fría y OMJ de fase convectiva benefician la formación de TC, mientras que las condiciones de ENOS de fase cálida inhiben la formación de TC y afectan el ciclo de OMJ. Los análisis sinópticos de los estudios de caso muestran que la divergencia del viento y las anomalías en el contenido de agua atmosférica dominan el comportamiento de los TC.

Key words: Tropical cyclogenesis, natural hazard, risk assessment, Madden-Julian Oscillation, El Niño-Southern Oscillation, Gulf of México.

Palabras clave: Ciclogénesis tropical, peligro natural, evaluación de riesgos, Oscilación Madden-Julian, El Niño-Oscilación del Sur, Golfo de México.

Received: 13 October 2023

Accepted: 2 May 2024

***Corresponding author:** Julio César Morales Hernández, Department of Basic Sciences, University Centre for Exact Sciences and Engineering, University of Guadalajara, Mexico. Email: julio.morales@academicos.udg.mx

1. Introduction

Tropical cyclogenesis involves several ambient factors acting at multiple time-space scales. Previous studies evidence the importance of the environmental dynamic and thermodynamic state: low-level wind vorticity, low and high-level wind divergence, atmospheric water content, sea surface temperature; for tropical cyclone formation and development (Emanuel, 1986). Large scale atmospheric and oceanic phenomena, such as the Madden-Julian Oscillation (MJO) and El Niño-Southern Oscillation (ENSO), also play an important role in tropical cyclogenesis, modulating these dynamic and thermodynamic factors and tropical weather patterns.

MJO's first reports date from the early 1970s (Madden and Julian, 1971) evidencing a 30-60 day period atmospheric pressure oscillation at Cantón Island, propagating East from the Indian Ocean. MJO represents the tropical weather, dominant variability mode at intra-seasonal time scales; having high impact influences on weather patterns around the world, such as monsoon circulations, tornadoes, cold waves, flooding, forest fires, tropospheric zonal wind anomalies (Kiladis, 2005; Lafleur *et al.,* 2015). Positive and negative wind divergence regions defined from the 200 hPa wind potential, and outgoing long-wave radiation, indicating high and low cloud coverage regions are used as main indexes to monitor MJO.

MJO's influence on North Atlantic and North Pacific TC activity has been documented by Barret and Leslie (2009). MJO modulation of the tropical cyclogenesis on the northeast Pacific and Gulf of México during August and September 1995 was studied by Aiyyer and Molinari (2008); Rao *et al.* (2017) also studied this modulation in the Indian Ocean.

ENSO represents a coupled large-scale ocean-atmosphere phenomena originating in the Equatorial Pacific Ocean, impacting global climate variability. During its warm phase (El Niño) East Pacific Sea surface temperature (SST) increase above normal along the coast of America north and south from the Equator, and trade winds weaken; during its cold phase (La Niña) East Pacific SST decrease below normal north and south from the Equator, and trade winds strengthen (Capel, 1999). ENSO is considered as the most singular and significant teleconnection event (Magaña, 1997) worldwide. Has been shown that ENSO and TC interactions in the North Atlantic and North Pacific basins are strong at every TC formation and development stage (Reyes and Troncoso, 1993; Xu and Huang, 2015).

Tropical cyclogenesis changes position in the North Pacific, eastern, and western, during both cold and warm ENSO stages, shifting to the northwest (Irwin and Davis, 1999). El Niño events are

associated with a cyclogenesis decrease west of 160°E; a corresponding cyclogenesis increase from 160°E to the dateline; a tendency for cyclogenesis to increase near the Equator (Pan, 1981; Chan, 1985; Lander, 1994); an increment of TC activity for the northeastern Pacific towards México, due to higher SST, without an increase in cyclogenesis (Bell, 2006); and higher TC intensity and duration, with no changes in TC formation frequency. La Niña events have, in general, opposite effects (Gray and Sheaffer, 1991; Whitney and Hobgood, 1997).

During warm-phase ENSO events, TCs in the North Atlantic are less frequent, less intense, and short-lived, due to the increase vertical wind shear produced by the westerly winds at 200 hPa height (Gray, 1984; Knaff, 1997; Goldenberg and Shapiro, 1996; Landsea *et al.,* 1999).

Since the discovery of these large-scale oscillations, many results have pointed out their impact on tropical cyclogenesis. Nevertheless, there still questions to answer regarding their own interactions and the resulting effects on tropical cyclogenesis, as MJO's main footprint lies in dynamic, while ENSO's main footprint lies in thermodynamic aspects of atmospheric physics. Furthermore, most studies focus on large oceanic basins like the North Atlantic and North Pacific oceans, not in regional basins such as the Gulf of México. A basin with distinct physiographic, atmospheric, and oceanic conditions, having densely populated human settlements along its coasts, and continuous high-impact economic activities taking place at its coastal and marine environments.

Tropical cyclones represent one of the major natural hazards on human life and infrastructure in the Gulf of México region, due to high-intensity winds, storm surges, large volume rainfall, and flooding. Risk assessment for proper urban development and emergency response highly depends on accurate TC prognostic models incorporating, as possible, all ambient factors involved. This work aims to further our understanding of how MJO and ENSO oscillations relate to tropical cyclogenesis in the Gulf of México. We use correlation and Fourier analyses to study these oscillations inter-relationships and their signature on dynamic and thermodynamic variables; classify tropical cyclogenesis occurrence in relation to possible MJO and ENSO state combinations, and review the synoptic ambient conditions present for two TC sample cases associated to the combination of MJO and ENSO states related to higher cyclogenesis.

2. Materials and Methods

To monitor MJO convection activity location and intensity we use the RMM (Real-time Multivariate index described by Wheeler and Halton, 2004), published by the Australian Government's Bureau of Meteorology (www.bom.gov.au/climate/mjo). RMM index definition uses the two leading modes resulting from an empirical orthogonal function analysis (EOF). The EOF covariance matrix is constructed with intra-seasonal anomalies time series in the tropical region of outgoing long wave radiation, 850hPa zonal wind, and 250hPa zonal wind; normalized respectively by their standard deviation. RMM index values [<0, 0, >0] indicate no-convective activity, inactivity, and convective activity respectively. MJO convection intensity is defined, according to RMM index magnitude range as (Lafleur et al., 2015): inactive [0 - 1], active [1 – 1.5], highly active [1.5 – 2.5], and strongly active [> 2.5].

ENSO description and analysis is done with the Oceanic El Niño Index (ONI); used by United States National Oceanic and Atmospheric Administration (NOAA) as the standard to identify warm (El Niño) and cold (La Niña) events in the tropical Pacific (http://ggweather.com/enso/oni.htm). ONI values are calculated as the 3 months running mean of ERSST.v5 SST anomalies in El Niño 3.4 region (5°N-5°S, 120°-170°W), based on 30-year base-periods updated every 5 years. A threshold of ± 0.5°C for the ONI values define warm (+) and cold (-) periods. Events (El Niño/La Niña) are defined by 5 consecutive months of ONI values above the threshold; classified as weak, moderated, strong, and very strong for ONI values in the respective absolute ranges: 0.5 to 0.9, 1.0 to 1.4, 1.5 to 1.9, ≥ 2.0.

TC data corresponds to NOAA IbTraCs v03r10 database (https://www.ncdc.noaa.gov/ibtracs) which gathers tropical cyclone best track, distribution, frequency, and intensity worldwide from all US Regional Specialized Meteorological Centers and other international centers and individuals. In this work, TC genesis is counted at the time an organism is named, i.e. when it reaches Tropical Storm status.

Atmospheric parameter time series used are from NOAA's NCEP/NCAR reanalysis database (Kalnay et al., 1996); while SST time series are from NOAA High-resolution Blended Analysis of Daily SST and ICE with a 0.25° latitude/longitude resolution.

ENSO and MJO state will be noted further as: -ENSO (no presence); ENSO- (cold pahse); ENSO+ (warm phase); -MJO (no presence); MJO- (no convective); MJO+ (convective).

The following data analysis was carried out for the time period 1981 to 2019: time series power spectra of SST, 700hPa relative humidity, 200hPa divergence, and 850hPa vorticity where calculated to identify their frequency distribution and variability at MJO and ENSO frequencies; daily tropical cyclogenesis was classified according to 9 different ENSO and MJO state combinations (1 = ENSO+, -MJO; 2 = ENSO+, MJO-; 3 = ENSO+, MJO+; 4 = ENSO-, -MJO; 5 = ENSO-, MJO-; 6 = ENSO-, MJO+; 7 = -ENSO, -MJO; 8 = -ENSO, MJO-; 9 = -ENSO, MJO+).

The power spectrum is a mathematical representation illustrating how the power of a signal is distributed across different frequencies, providing a description of the relative contribution of each frequency to the energy content of that signal. To conduct the research, the initial numerical series was decomposed into a series of frequencies in order to identify those with the highest energy, as these would optimally represent the oscillations present in the time series. Subsequently, these dominant frequencies were compared to the oscillation periods associated with the climatic phenomena ENSO and MJO.

The software utilized to compute the power spectrum is MATrix LABoratory (MATLAB), a widely recognized tool for signal processing and data analysis. MATLAB provides various functions and tools specifically designed to calculate power spectra of signals, both in the time domain and in the frequency domain.

Covariance function was used to determine ENSO, MJO, and tropical cyclogenesis daily time series relationships; and synoptic conditions anomalies where calculated for two TC case, developed under the ENSO and MJO state combination with higher cyclogenesis presence. The covariance function is not directly related to wavelet coherence or cross-wavelet analysis. While these concepts may be related in time series analysis, the covariance function is a more general measure of the relationship between two random variables, whereas wavelet coherence and cross-wavelet analysis are specific techniques used in signal and time series analysis.

3. Results

3.1 Power Spectra

Tropical cyclones, like any natural phenomena, have a multi-factor character were different-scale variables converge. Predicting tropical cyclogenesis, by analyzing and weighting its different influence factors behavior, is an undergoing challenge for the scientific community. Large-scale weather oscillations as MJO and ENSO, whose impact around the globe on several environmental variables are well known, represent influence factors still open for discussion in some TC formation regions such as the GOM.

To explore MJO and ENSO influence on tropical cyclogenesis, normalized power spectra were calculated for: daily TC formation, MJO, ONI, SST, 700 hPa relative humidity, 200 hPa wind divergence, and 850 hPa wind vorticity time series. TC formation time series includes only those organisms with name, formed within the GOM; SST and 700 hPa relative humidity time series correspond to averages over the entire GOM region; for 200 hPa divergence and 850 hPa vorticity the

GOM was divided in four regions (I - northwest, II - southwest, III - northeast, and IV - southeast; Fig. 1), constructing time series for each region's spatial average.

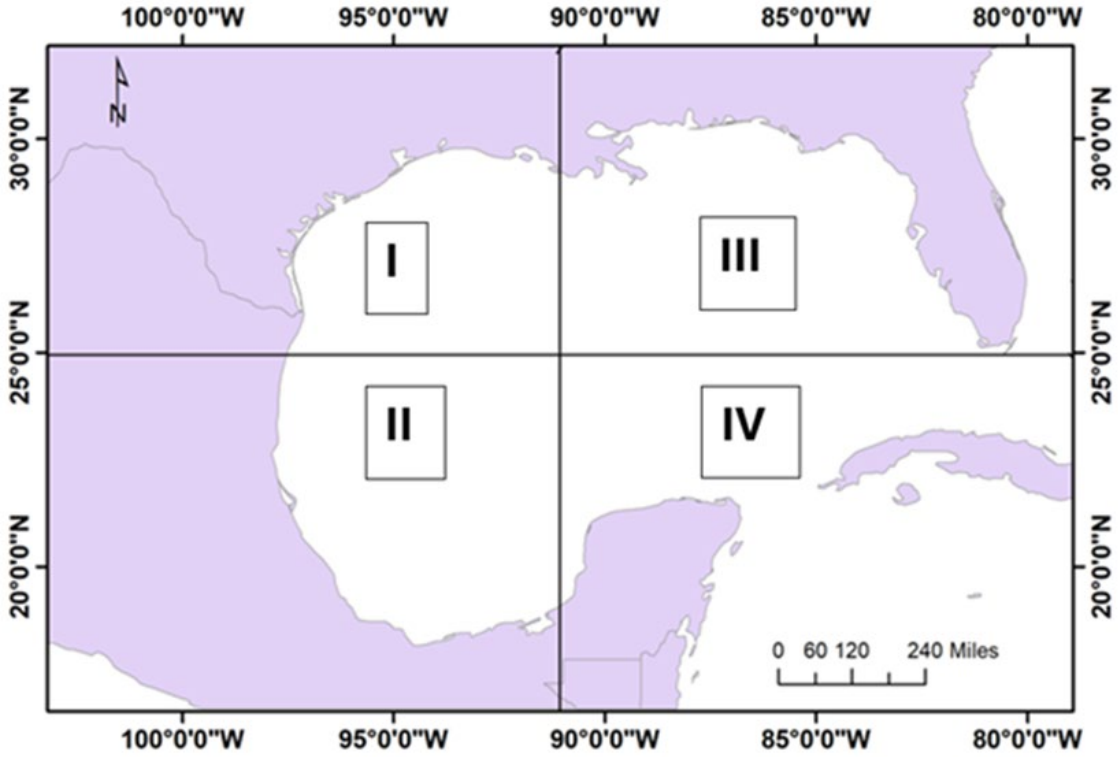

Figure 1. Study Area.

In Figure 2, the spectra of low frequency are shown Low (< 1 cycle/year) and high (> 1 cycle/year) frequency spectra for the time series. Shaded areas represent 95% confidence intervals; for reference, spectral peaks are marked with vertical color lines throughout the plots for, TC formation (red), MJO (green), and ONI (blue); TC formation spectral peaks corresponding period values are shown on top the plots.

700 hPa relative humidity and SST spectra show significant variability at 5.6 and 4.2-year periods respectively indicating ENSO modulation; an expected result, considering SST is the principal oceanic index to trace ENSO activity. MJO modulation is also evident in 700 hPa relative humidity, represented by 60 to 40 days period variability; but it is not so clear for SST, showing 70.5 and 62.8 day periods, out of the Madden and Julian (1971) period range.

200 hPa wind divergence shows the MJO signal presence in all four GOM regions as expected since it reflects vertical convection, and it is used to monitor MJO activity. GOM regions I, II, and III present 200 hPa wind divergence variability within the period range 66 to 34 days in which, periods 62, 52, 41, and 34 days are present in all three regions. GOM region IV only has significant 200 hPa wind divergence variability at periods of 63 and 38 days. Variability within the MJO period range is less intense on region II, possibly influenced for the continental high relief on the southwest GOM coast. At low frequencies, 200 hPa wind divergence in GOM regions I and II show significant variability at 6.5 years period while the significant period within the ENSO range in region IV is at 4.5 years. These results reflect the ENSO atmospheric component modifying circulations like Walker's and the trade wind strength, with a consequent high troposphere response.

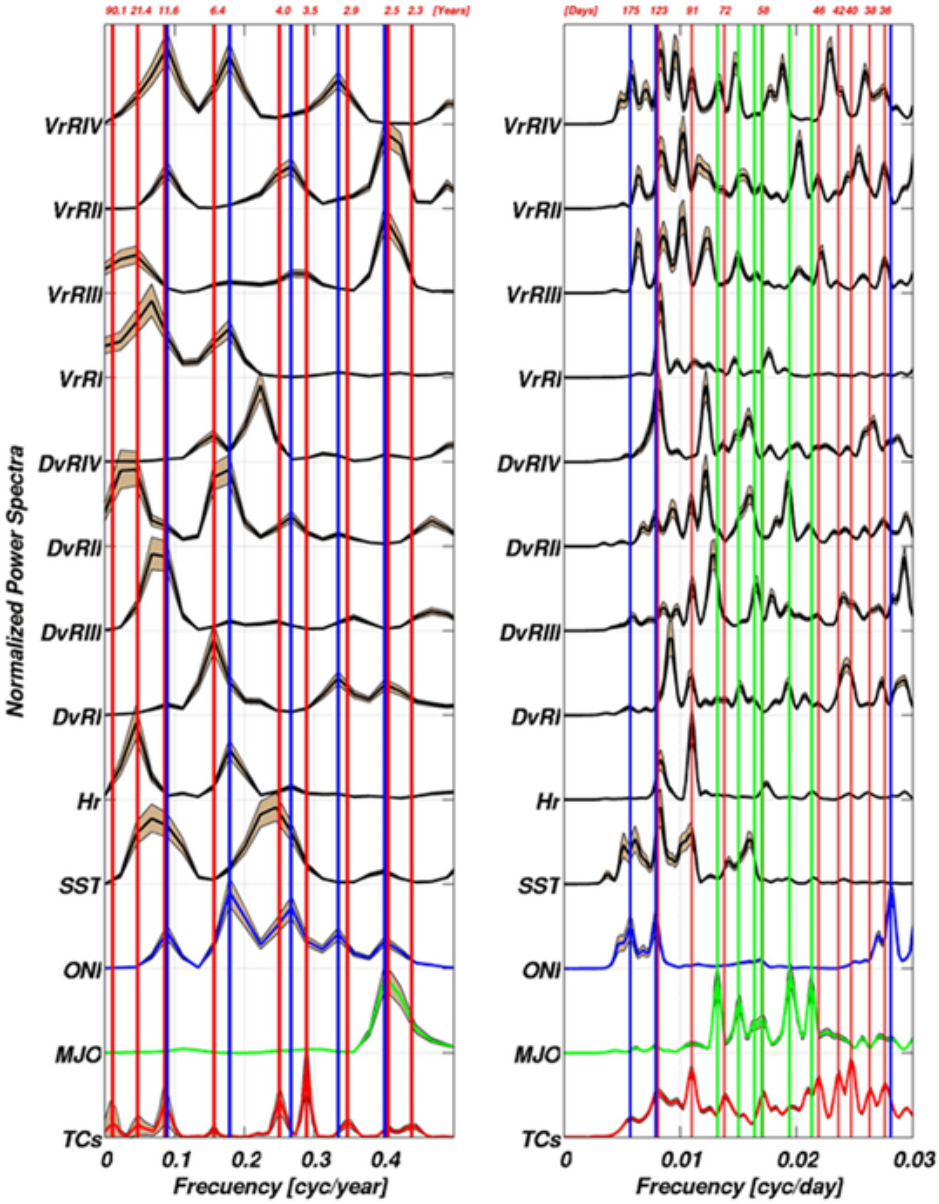

Figure 2. Frequency spectra of vorticity (VrR), divergence (DvR), relative humidity (Hr), sea surface temperature (SST), ONI, MJO and tropical cyclones (TCs) time series.

3.2 Phase Configurations

TC formation individual events are associated in this section according to ENSO and MJO phase configurations at formation time (configurations defined in Section 2 and listed in Table 1). There were 72 TC formation events within the GOM for the period 1981 to 2019.

Table 1. Phase Configurations at TC formation time. -ENSO (no presence); ENSO- (cold phase); ENSO+ (warm phase); -MJO (no presence); MJO- (no convective); MJO+ (convective).

Phase Configurations		
1 ENSO+, -MJO	4 ENSO-, -MJO	7 -ENSO, -MJO
2 ENSO+, MJO-	5 ENSO-, MJO-	8 -ENSO, MJO-
3 ENSO+, MJO+	6 ENSO-, MJO+	9 -ENSO, MJO+

Phase configuration relative frequency, during TC formation, is shown in Figure 3a. Configuration 7 represents 42% of total cases being the most frequent. This is expected since this is the most common circumstance during the TC season (ENSO is only present about once every five years and the MJO convective phase is seldom present during TC season).

Leaving out configurations 7 to 9, representing ENSO absence, the highest relative frequency, 59%, corresponds to Configuration 4 (Fig. 3b), i.e. cold phase ENSO, and no MJO presence. An extra 16% corresponds to cold phase ENSO and MJO presence: 11% with (Case 6), and 5% without active convection (Case 5). Only 12% correspond to ENOS configuration, lower than the other two states of ENSO (-ENSO and ENSO-) that were presented before.

To further evaluate these results the number of days corresponding to each configuration, for the period 1981-2019, are presented in Figure 4. ENSO absence accounts 5663 days; of which 5003 days are also MJO free. Cold and warm ENSO phases are present 3680 and 3806 days respectively. There is a noteworthy difference of more than 1000 fewer days with MJO presence with configurations having ENSO cold than with ENSO warm phase, indicating a negative influence on MJO behavior.

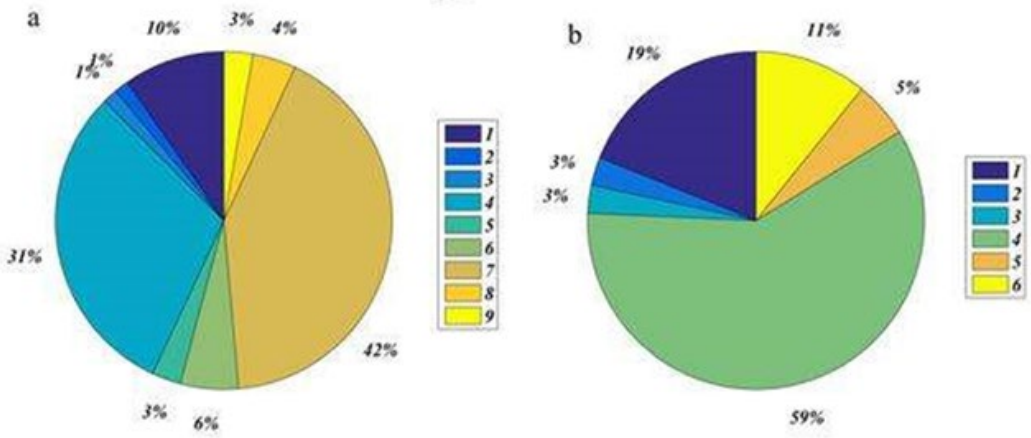

Figure 3. Phase Configuration Relative frequency. a) values taking all configurations into account; b) values taking only configurations 1 to 6 into account.

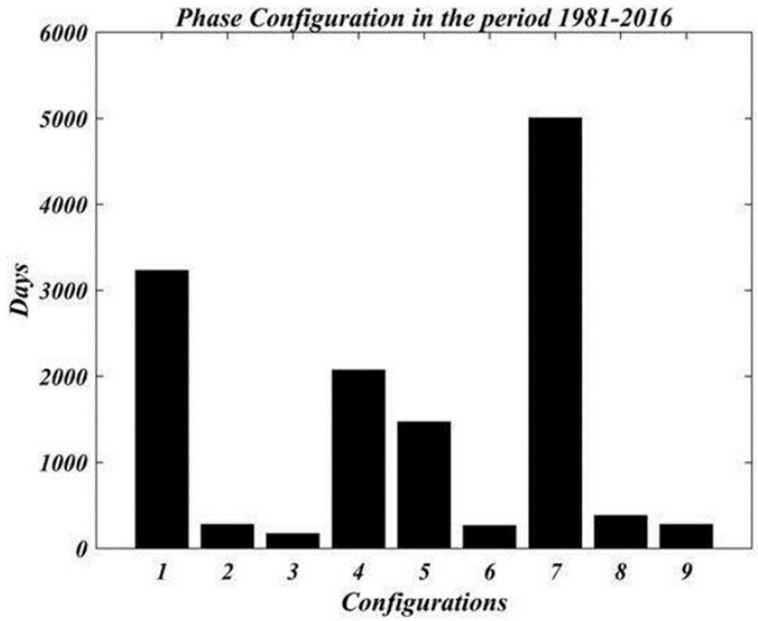

Figure 4. Number of days corresponding to each Phase Configuration for the time period 1981-2016.

Percentages of TC formation for each configuration (Fig. 5) indicate Configuration 6 (ENSO-, MJO+) is the most frequent, followed by Configuration 4 (ENSO, -MJO). Configuration 7 (-ENSO, -MJO), is no longer the dominant one as was for absolute frequency; it falls to the fifth position in relative frequency, behind configurations 8 and 9.

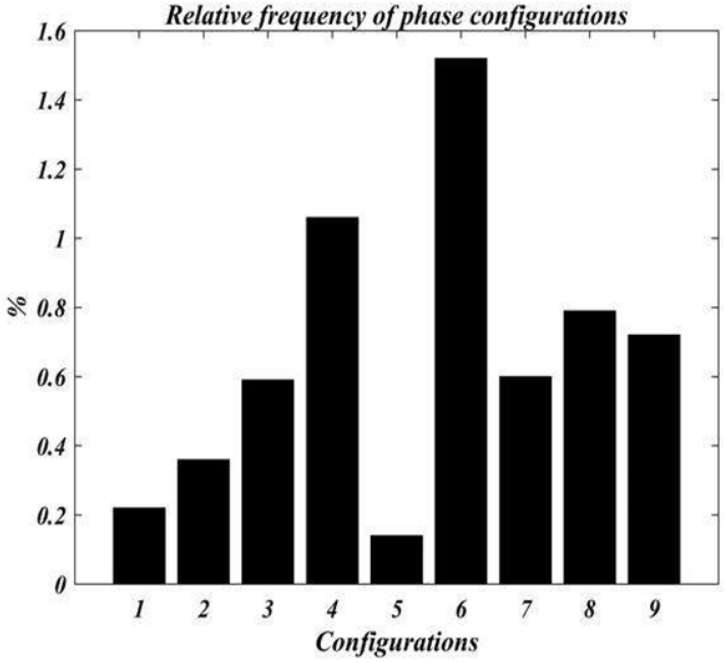

Figure 5. Relative frequency of TC formation related to each Phase Configuration and the number of days in which each configuration is present during the time period 1981-2019.

3.3 ENSO-MJO-TC Correlations

We used the covariance function to explore the statistical relationship between ENSO, MJO, and TC formation time series. Yearly time series for the period 1981-2019 are formed as follows for this task: number of TC formed during each season (June 1 to November 30); ENSO phase for the season (-1, 0, +1); and the number of days of MJO presence during the season.

The normalized time-series covariance matrix is presented in Table 2. There is a significant negative covariance (-0.55) between TC formation and ENSO phase, confirming a decrease in TC formation during its warm phase and an increase during its cold phase.

Covariance values also show an inverse relation between TC formation and MJO presence (- 0.001) but its value is below the 95% confidence threshold. This result may not represent accurately their interaction; different to ENSO, that establishes an environmental pattern lasting for months, MJO convective phase travels throughout the region in short periods, so its contribution is limited to a short time perturbation that could trigger a TC formation event.

ENSO and MJO have a negative but less energetic covariance (-0.25), which indicates that ENSO alters the periodicity and persistence of MJO along with a decrease in TC formation.

Table 2. ENSO, MJO, TC formation covariance matrix.

	TC	**ENSO**	**MJO**
TC	1	-0.5522	-0.0014
ENSO	-0.5522	1	-0.2488
MJO	-0.0014	-0.2488	1

3.4 Synoptic Environment

In the previous section, it was established which state combinations of ENSO and MJO oscillations favor TC formation: ENSO presence in both its warm and cold phase, along with MJO convection. This section discusses, based on two particular TC cases, the synoptic environmental footprint of the cold phase ENSO and MJO convective phase combination.

On August 31, 1998, Hurricane Earl was named in the southwest GOM as shown in Figure 6a. On that date, the ONI value (-1.1) indicated the presence of a moderate La Niña event, while the RRM index value (1.6) indicating a very active MJO convection. On September 8, 1998, Tropical Storm Frances was named in the west GOM as shown in Figure 6b. ONI value (-1.3) corresponds to a moderate La Niña event and RMM value (2.0) to a very active MJO convection.

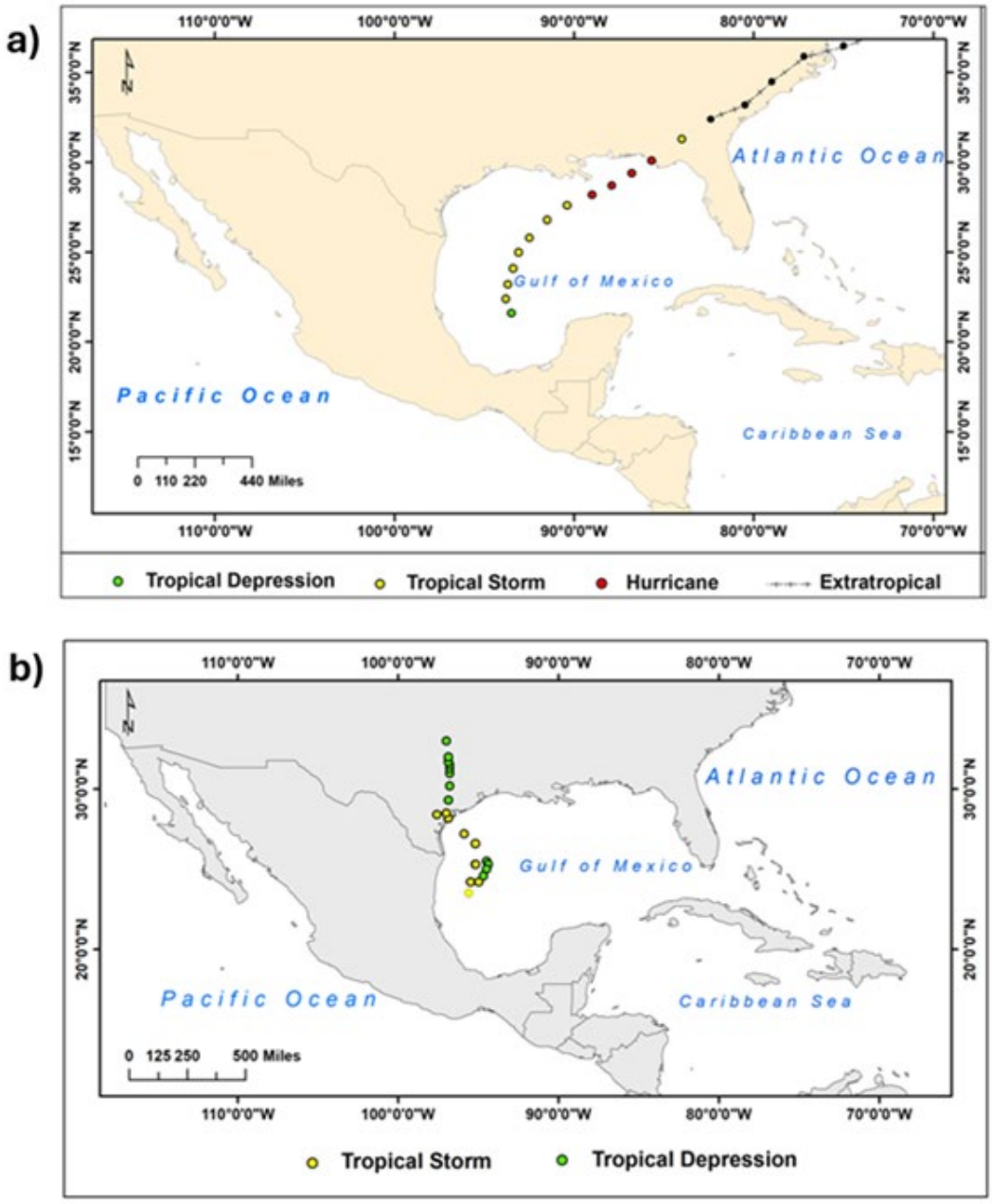

Figure 6. Origin and track of: a) Hurricane Earl, and b) Tropical Storm Frances. National Hurricane Center, NOAA.

Synoptic changes will be described using anomalies from the 1981-2019 means of the SST, 700 hPa Relative Humidity, 200 hPa Wind Divergence, and 850 hPa Wind Relative Vorticity fields.

The first field to discuss is SST, a source of energy for tropical cyclogenesis and development. High temperatures (>26°C as most researchers agree on), as well as a deep mixed ocean layer of at least 50 m, are needed for TC formation. Figure 7 shows the SST anomalies for the two TC formation cases. August 31, 1998, anomalies (Fig. 7a, case 1) have mainly positive values up to 2°C, even for this summer date. Nevertheless, there are two negative anomaly centers north of the Yucatan Peninsula with values less than -1°C.

On September 8, 1998, negative anomalies (Fig. 7b, case 2) have a higher spatial coverage extending to the south GOM coast, north of Tehuantepec Isthmus, suggesting cold Pacific waters influence produced by the cold phase ENSO.

SST anomaly time averages for the period June 1 to November 30, 1998, covering the TC season (Fig. 8a), and for the period August 28 to September 10, 1998, covering the MJO transit over GOM (Fig. 8b), allow for a different analysis. Average anomalies for the 1998 TC season, under moderate La Niña conditions, are positive or close to zero throughout GOM reflecting strengthen in trade winds flow and westward warm water transport as expected. Average anomalies for the transit period of the MJO convective phase (August 28 to September 10, 1998) show distinct negative anomaly regions up to -1°C. These distributions shear light to the fact of why SST anomaly's spatial patterns can be unique for each TC formation case.

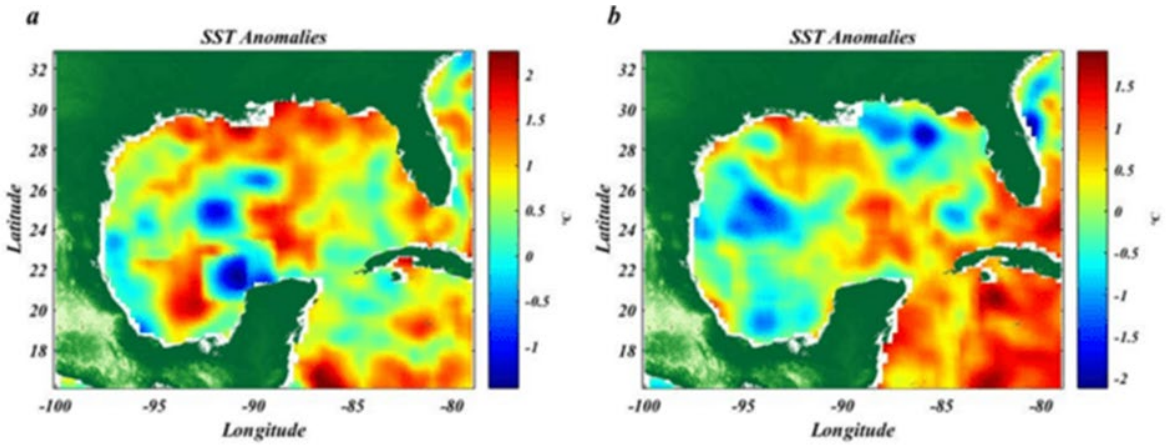

Figure 7. SST anomalies. a) August 31,1998; b) September 8, 1998.

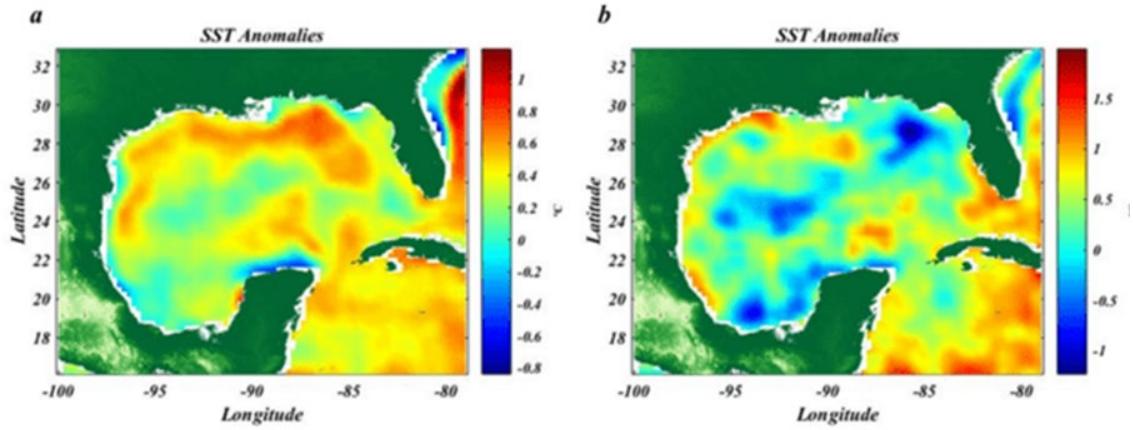

Figure 8. Time average SST anomalies over the GOM. a) Period June1 to September 30, 1998 (TC season); b) Period August 28 to September 10, 1998 (MJO transit over GOM).

The mid-level relative humidity is another key factor for tropical cyclogenesis and subsequent TC development. High mid-level water vapor content means high condensation as air rises releasing latent heat, increasing air temperature, and developing deep convection, ultimately fueling these meteorological organisms.

On August 31, 1998, 700 hPa relative humidity anomalies are high and positive (up to 40%) in the central GOM, with small absolute values near the coasts (Fig. 9a). On the second case, corresponding to September 8, 1998, positive anomalies, with values exceeding 30%, shift towards the western GOM, and a region of negative anomalies develops centered over the Florida Strait with -10% to -20% values (Fig. 9b). As shown, relative humidity values in GOM increase above average under de combined effect of ENSO and MJO oscillations.

200 hPa wind divergence anomalies for August 31, 1998, are positive (above 15x10-6 s-1) over the central GOM and the Mexican coast (Fig. 10a) and have negative, less intense, values (below -5x10-6 s-1) over the Yucatan and Florida straits, and Florida east coast. September 8, 1998, positive anomalies cover the entire GOM (Fig. 10b), having maximum values up to 2x10-6 s-1 over the Campeche Gulf on the south GOM coast. In both TC cases, Earl and Frances, these maximum positive regions correspond to their cyclogenesis positions. 200 hPa wind divergence, used also to monitor MJO and influenced by ENSO atmospheric component, shows changes under the combined presence of these two oscillations, favorable to tropical cyclogenesis.

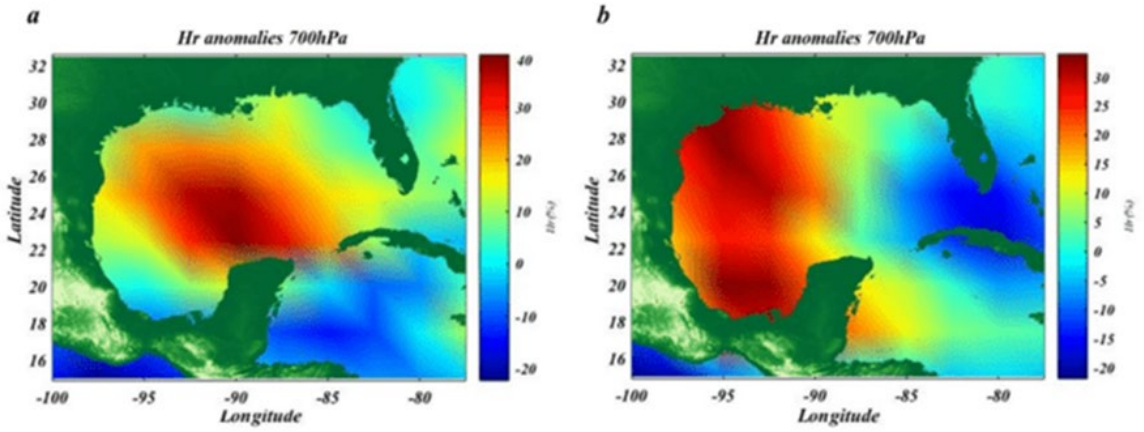

Figure 9. 700hPa relative humidity anomalies. a) August 31, 1998; b) September 8, 1998.

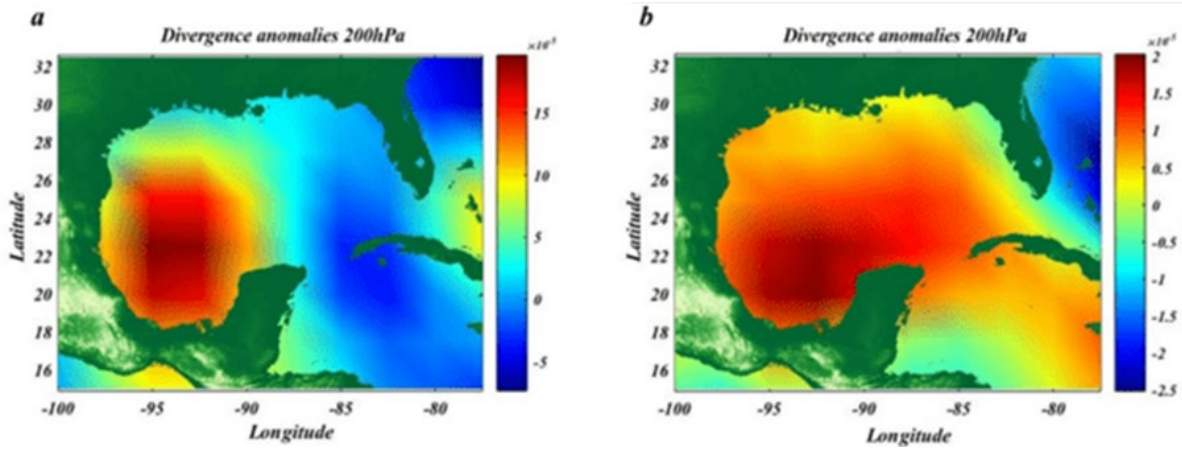

Figure 10. 200hPa wind divergence anomalies. a) August 31, 1998; b) September 8 1998.

850 hPa wind relative vorticity anomaly patterns are similar over the GOM during both dates presented, August 31, and September 8, 1998 (Fig. 11). East GOM anomalies are negative, while West GOM values are positive. Positive anomalies (~ 1.5x10-5 s-1) are present over the Campeche Gulf and Louisiana-Texas coast on August 31; with negative values up to -2x10-5 s-1 occupying the northeast GOM region down to the northwest coast of Cuba. September 8 positive anomalies cover the west GOM region with values around 1x10-5 s-1 from the south coast, up to the USA-Mexico border, and maximum values over the Campeche Gulf (2x10-5 s-1); negative anomalies are present along the north coast from Texas to Florida and the East GOM, with minimum values below -3x10-5 s-1 off the Mississippi-Alabama coast.

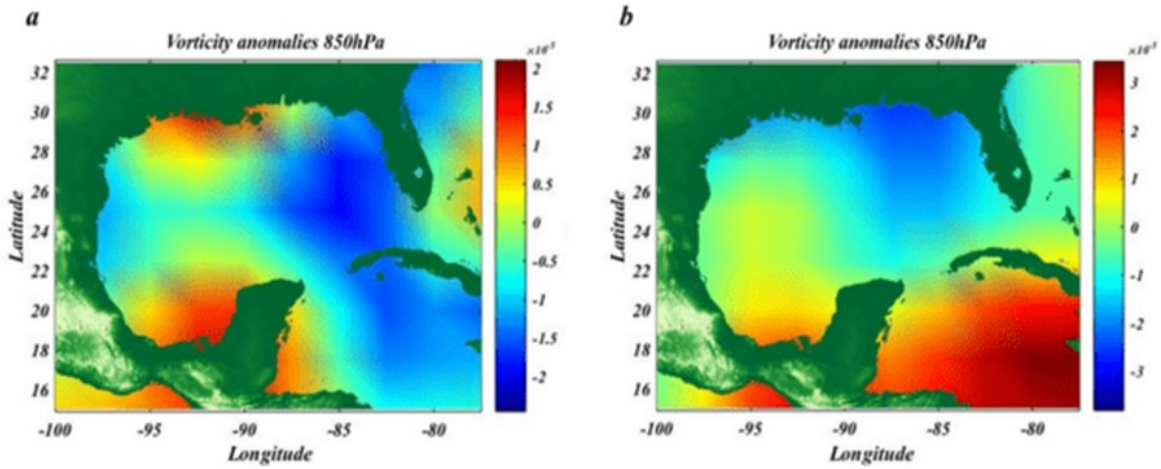

Figure 11. 850hPa wind relative vorticity anomalies. a) August 31, 1998; b) September 8 1998.

4. Discussion

The inherent complexity of climate systems, coupled with the challenges associated with long-term prediction, uncertainty in climate models, and interannual and seasonal variability, underscore the continued need to improve our understanding of climate variability and its effects on the occurrence of tropical cyclogenesis in the Gulf of Mexico region. The scope ranges from tropical cyclone prediction and monitoring to disaster preparedness and policy development for climate change adaptation.

TC formation power spectra show the modulating effect of large-scale phenomena such as MJO and ENSO. At low frequencies, TC formation power spectra show significant variability over 11-year periods, corresponding to a multi-decadal oscillation; 6, 4 and 3.5 years, within the limits of the ENSO periods; and 2.5 years, around the Quasi-Biennial Oscillation. For high frequencies, TC formation shows significant variability in annual and semi-annual periods; and at different periods within the MJO period range (70, 60, 45, 40 days).

The origins of MJO and ENSO can be traced back to a variety of oceanic and atmospheric factors: from changes in the Walker circulation to alterations in equatorial warming; However, they have a particular imprint on environmental variables such as sea surface temperature, relative humidity, wind divergence, and vorticity.

A period of 11.6 years in wind vorticity of 850 hPa is present in the southern portion of GOM (regions II and IV), while in the northern regions (I and III) the decadal to multidecadal periods are centered on 15.5 and 28 years, respectively. The variability of the ENSO period range is represented in regions I and IV by a cycle of 5.6 years, and in regions II and III by a cycle of 3.7 years. The quasi-two-year cycle of 2.5 years is present in Regions II and III, but is not evident in Regions I and IV.

Other studies such as those by Philip and Willian, 2008 have analyzed the multidecadal variability in tropical cyclone activity in the North Atlantic, including the Gulf of Mexico, and its relationship with climatic factors such as El Niño and La Niña.

The response of various variables related to tropical cyclones, including activity in the Gulf of Mexico, to changes in sea surface temperatures, and other global and local climate forcings, such as ENSO and ENSO- are referenced by (Emanuel & Sobel, 2013).

Variability from 46 to 75 days (related to MJO) is present in the southern and northeast regions (II, IV and III) with periods equal to or close to the time series of the MJO index; but being practically absent in region I (northwest), as in the divergence of 200 hPa.

Periods of intraannual variability (90 to 180 days) are present in all the variables analyzed, except for the MJO index. The high-frequency variability of MJO time series is limited to the range of 46 to 75 days.

As shown, ENSO and MJO oscillations play an important role in modulating TC formation within GOM. The ENSO signal dominates for the low frequencies and the MJO signal plays a secondary role in the high frequencies.

The discussion is related to studies by Emanuel (2005) where he examines the increase in the intensity and destructiveness of tropical cyclones during the last decades. It discusses how factors such as El Niño and La Niña may be related to this increase in cyclone activity.

These results indicate that cold-phase favors the formation of TCs in the GOM, unlike the Pacific region where it is warm-phase ENSO that favors it. The influence of MJO is weak in the presence of ENSO, with only two cases. As warming decreases in the ENSO 3.4 region and negative SST anomalies increase, the role of MJO becomes important, presenting 5 TC formation events during the neutral ENSO condition and 6 events during the La Niña condition.

The results indicate the importance of MJO in favoring TC formation conditions when ENSO is absent; configurations with warm-phase ENSO are the least favorable for TC formation; CT formation during the presence of MJO is greater than CT formation without ENSO and MJO.

Maloney and Hartmann (2001) have also examined the relationship between the Madden-Julian Oscillation and tropical cyclone formation in several regions, including the Gulf of Mexico, and provide insights into how MJO may influence tropical cyclone genesis.

Tropical cyclone dynamics is a complex topic, even with some aspects lacking definition, which presents many obstacles to the prediction of tropical cyclogenesis. In this regard, the divergence of high-level winds plays a crucial role; It provides an escape route at altitude for the excess mass provided by vertical convection, allowing the ascent of free air with the consequent increase in heat available by true condensation.

The influence of climate variability on the assessment of tropical cyclogenesis risk in the Gulf of Mexico is closely related to phenomena such as ENSO, ENSO- and the Madden-Julian Oscillation (MJO). During ENSO events, oceanic and atmospheric conditions change significantly, which can increase the likelihood of tropical cyclone formation in the Gulf of Mexico. The presence of warm waters in the equatorial Pacific during ENSO may create conditions conducive to the intensification of tropical storms and hurricanes in this region.

On the other hand, during La Niña events, warm waters are concentrated in the western Pacific, which can reduce the likelihood of tropical cyclone formation in the Gulf of Mexico. During these periods, atmospheric conditions may be less favorable for the development of storms and hurricanes in this area.

As for the Madden-Julian Oscillation (MJO), this large-scale weather pattern may have a significant impact on tropical cyclogenesis activity in the Gulf of Mexico. During the active phases of

the MJO, conditions conducive to the formation and strengthening of tropical systems in this region may be generated, while during the inactive phases, tropical cyclogenesis activity may decrease.

Taken together, the interplay between climate variability, represented by ENSO, ENSO- and MJO, plays an important role in assessing the risk of tropical cyclogenesis in the Gulf of Mexico. Understanding how these phenomena influence atmospheric and oceanic conditions in this region is critical to improving the ability to forecast and manage the risk associated with tropical cyclones.

5. Conclusions

In this work, we explored the ENSO and MJO oscillations influence on tropical cyclogenesis within the Gulf of Mexico.

ENSO and MJO oscillation periods are present in different environmental parameters variability, like sea surface temperature, mid-level relative humidity, high-level wind divergence, and low-level wind relative vorticity, as well as tropical cyclone activity, within the Gulf of Mexico. ENSO low-frequency signal dominates TC activity variability, with MJO low-frequency signal playing a secondary role.

Cold phase ENSO (La Niña) in combination with the MJO convective phase constituted the best conditions for tropical cyclogenesis within the GOM. Warm phase ENSO (El Niño) is associated with low tropical cyclogenesis. MJO convective phase is associated with increased tropical cyclogenesis in presence of ENSO (cold or warm phase).

Results indicate combined effects on SST spatial distribution of, positive ENSO, negative MJO, and negative cold Pacific water influence at the Tehuantepec Isthmus limit the usefulness of this variable to determine or predict tropical cyclogenesis. Low-level relative vorticity anomalies spatial distribution depicts no clear evidence of the combined effect of ENSO and MJO oscillations; nevertheless, positive values present over the Campeche Gulf during both dates, along with high-level wind divergence values, constitute favorable conditions for deep convection and tropical cyclogenesis. Mid-level relative humidity and high-level divergence spatial distribution proved the best indicators of combined ENSO-MJO conditions favorable to tropical cyclogenesis.

References

Aiyyer, A., Molinari, J., 2008. MJO and Tropical Cyclogenesis in the Gulf of Mexico and Eastern Pacific: Case Study and Idealized Numerical Modeling. *American Meteorological Society* 65, 2691-2703. https://doi.org/10.1175/2007JAS2348.1

Barret, B., Leslie, L., 2009. Links between Tropical Cyclone Activity and Madden–Julian Oscillation Phase in the North Atlantic and Northeast Pacific Basins. *American Meteorological Society* 137, 727-743. ,https://doi.org/10.1175/2008MWR2602.1

Bell, G.D., Chelliah M., 2006. Leading tropical modes associated with interannual and multi-decadal fluctuations in North Atlantic hurricane activity. *J. Climate* 19, 590-612. https://doi.org/10.1175/JCLI3659.1

Capel, J., 1999. El Niño and the Earth's climate system. Nimbus 4, 157-161. http://hdl.handle.net/10835/1484

Chan, J.C.L., 1985. Tropical cyclone activity in the Northwest Pacific in relation to the El Nino/Southern Oscillation phenomenon. *Monthly Weather Review* 113, 599-606. https://doi.org/10.1175/1520-0493(1985)113<0599:TCAITN>2.0.CO;2

Emanuel, K., 1986. An air–sea interaction theory for tropical cyclones. *Journal of the Atmospheric Sciences* 45, 585–604 https://doi.org/10.1175/1520-0469(1986)043<0585:AASITF>2.0.CO;2

Emanuel, K., 2005. Increasing destructiveness of tropical cyclones over the past 30 years. *Nature* 436, 686-688. https://doi.org/10.1038/nature03906

Emanuel, K., Sobel, A., 2013. Response of tropical sea surface temperature , precipitation , and tropical cyclone-related variables to changes in global and local forcing. *Journal of Advances in Modeling Earth Systems* 5(2), 447–458. https://doi.org/10.1002/jame.20032

Goldenberg, S.B., Shapiro, L.J., 1996. Physical mechanisms for the association of El Niño and West Africa rainfall with Atlantic major hurricanes. *J. Climate* 9, 1169–1187. https://doi.org/10.1175/1520-0442(1996)009<1169:PMFTAO>2.0.CO;2

Gray, W.M., Sheaffer, J.D., 1991. El Niño and QBO influences on tropical cyclone activity. In: M. H. Glantz, R. W. Katz, and N. Nicholls (Eds). *Teleconnections Linking Worldwide Anomalies,* Cambridge University Press, 257–284.

Gray, W.M., 1984. Atlantic seasonal hurricane frequency. Part I: El Niño and 30 mb Quasi-Biennial Oscillation influences. *Monthly Weather Review* 112, 1649–1668. https://doi.org/10.1175/1520-0493(1984)112<1649:ASHFPI>2.0.CO;2

Irwin, R., Davis, R., 1999. The relationship between the Southern Oscillation Index and tropical cyclone tracks in the eastern North Pacific. *Geophysical Research Letters* 26, 2251-2254. https://doi.org/10.1029/1999GL900533

Kalnay, E., Kanamitsu, M., Kistler, R., Collins, W., Deaven, D., Gandin, L., Iredell, M., Saha, S., White, S., Woollen, J., Zhu, Y., Chelliah, M., Ebisuzaki, W., Higgins, W., Janowiak, J., Mo, K.C., Ropelewski, C., Wang, J., Leetmaa, A., Reynolds, R., Jenne, R., Joseph, D., 1996. The NCEP/NCAR 40-Year Reanalysis Project. *Bulletin of the American Meteorological Society* 77(3), 437-472. https://doi.org/10.1175/15200477(1996)077<0437: TNYRP>2.0.CO;2

Kiladis, G.N., Straub, K.H., Haertel, P.T. 2005. Zonal and vertical structure of the Madden–Julian oscillation. *Journal of the Atmospheric Sciences* 62, 2790–2809. https://doi.org/10.1175/JAS3520.1

Knaff, J.A., 1997. Implications of summertime sea level pressure anomalies in the tropical Atlantic region. *J. Climate* 10, 789–804. https://doi.org/10.1175/1520-0442(1997)010<0789:IOSSLP>2.0.CO;2

Lafleur, D., Barret, B., Henderson, G., 2015. Some Climatological Aspects of the Madden–Julian Oscillation (MJO). *J. Climate* 28, 6039-6053. https://doi.org/10.1175/JCLI-D-14-00744.1

Lander, M., 1994. An exploratory analysis of the relationship between tropical storm formation in the Western North Pacific and ENSO. *Monthly Weather Review* 122, 636-651. https://doi.org/10.1175/1520-0493(1994)122<0636:AEAOTR>2.0.CO;2

Landsea, C.W., Pielke, R.A., Mestas, A.M., Knaff, J.A., 1999. Atlantic Basin hurricanes: Indices of climatic changes. *Climatic Change* 42, 89–129. https://doi.org/10.1023/A:1005416332322

Madden, R., Julian, P., 1971. Detection of 40-50 day oscillation in the zonal wind in the tropical Pacific. *Journal of the Atmospheric Sciences* 12, 702-708. https://doi.org/10.1175/1520-0469(1971)028<0702:DOADOI>2.0.CO;2

Magaña, V., Pérez, J., Conde, C., 1997. The phenomenon of El Niño and the Southern Oscillation (ENSO) and its impacts in Mexico. *Ciencias* 51, 14-18.

Maloney, E. D., Hartmann, D. L., 2001. The Madden-Julian Oscillation , Barotropic Dynamics, and North Pacific Tropical Cyclone Formation. Part I : Observations. *Journal of the Atmospheric Sciences* 58(17), 2545-2558. https://doi.org/10.1175/1520-0469(2001)058%3C2545:TMJOBD%3E2.0.CO;2

Pan, Y., 1981. The effect of the thermal state of eastern equatorial Pacific on the frequency typhoons over western Pacific. *Acta Meteorologica Sinica* 40, 24-32. https://doi.org/10.11676/qxxb1982.003

Klotzbach, P.J., Gray, W.M., 2008. Multidecadal Variability in North Atlantic Tropical Cyclone Activity. *Journal of Climate* 21(15), 3929–3935. https://doi.org/10.1175/2008JCLI2162.1

Rao, P.C.S., Nair, S.A., Khole, M., 2017. The Influence of Madden-Julian Oscillation on the Bay of Bengal Tropical Cyclogenesis During the Year 2013. In: M. Mohapatra, B.K. Bandyopadhyay, L.S. Rathore (Eds.). *Tropical Cyclone Activity over the North Indian Ocean.* Springer, pp. 227-232, Cham. https://doi.org/10.1007/978-3-319-40576-6_15

Reyes, S., Troncoso, R., 1993. The impact of the El Niño-Southern Oscillation phenomenon on the generation of tropical cyclones around Mexico. *Ciencia y Mar* 5, 3-21.

Wheeler, M., Helton, H., 2004. An all-season real-time multivariate MJO index: Development of an index for monitoring and prediction. *Monthly Weather Review* 132 (8), 1917–1932. https://doi.org/10.1175/1520-0493(2004)132<1917:AARMMI>2.0.CO;2

Whitney, L. D., Hobgood, J., 1997. The relationship between sea surface temperatures and maximum intensities of tropical cyclones in the eastern North Pacific Ocean. *J. Climate* 10, 2921–2930.https://doi.org/10.1175/1520-0442(1997)010%3C2921:TRBSST%3E2.0.CO;2

Xu, S., Huang, F.J., 2015. Impacts of the two types of El Niño on Pacific tropical cyclone activity. *Journal of Ocean University of China* 14, 191-198. https://doi.org/10.1175/JCLI-D-17-0298.1

Cuadernos de Investigación Geográfica *Geographical Research Letters*	2024	Nº 50 (2)	pp.45-67	EISSN 1697-9540

http://doi.org/10.18172/cig.5977

CHANGES IN THE CLIMATE COMFORT OF THE COAST OF SPAIN (1940-2022)

DAVID ESPÍN SÁNCHEZ [1]*, **JORGE OLCINA CANTOS [2]**

[1]*Geography Department, University of Murcia, 30001 Murcia, Spain.*

[2] *Regional Geographic Analysis and Physical Geography Department, University of Alicante, 03690 San Vicente del Raspeig, Alicante, Spain.*

ABSTRACT. The Spanish coastal regions register specific climatic conditions due to the combination of mild temperatures with little variation throughout the year, high relative humidity and the influence of maritime storms. In summer, the climatic comfort conditions are excessively hot, especially on the Mediterranean coast of Spain. Understanding these conditions and analysing the temporal evolution of recent decades, as well as regional differences, is fundamental for future summer tourism planning in the coming decades. This study analyses the principal 37 coastal tourist hubs of Spain grouped into 10 large regions (the Atlantic, Cantabrian, Mediterranean coasts, and the two archipelagos of the Balearic and Canary Islands). Daily data drawn from the ERA-5 (Copernicus) atmospheric reanalysis from 1940 to 2022 have been used (mean air temperature, mean relative humidity, and mean wind speed), with which the Climate Comfort Index has been calculated (CCI) by González (1998). The results show a significant reduction of the CCI in all the coastal areas analyzed, being more relevant in winter (-0.10 decade). The decrease in the index implies a decrease in cold thresholds and an expansion of comfort throughout the study area, especially in the central Mediterranean and Cantabrian Sea. For its part, in summer, the most important decreases (-0.07 and -0.08 / decade) show an increase in the most important climatic discomfort on the Cantabrian Coast – Euskal Kostaldea and on the Costa Brava-El Garraf, with a significant intensification and expansion temporary thermal sensation of heat. In other coastal sectors, in recent years, the climatic thresholds of heat and extreme heat have been reached for the first time.

Cambios en el confort climático del litoral de España (1940-2022)

RESUMEN. Las regiones costeras españolas registran condiciones climáticas específicas por la combinación de temperaturas suaves y poco contrastadas durante todo el año, humedad relativa elevada, e influencia de temporales marítimos. En verano, las condiciones de confort climático son de calor excesivo, especialmente en el litoral mediterráneo de España. Comprender estas condiciones y analizar la evolución temporal de las últimas décadas, así como las diferencias regionales, es clave para la futura planificación turística estival en las próximas décadas. Este estudio analiza los principales 37 ejes turísticos litorales de España agrupados en 10 grandes regiones costeras (litoral atlántico, cantábrico, mediterráneo, así como los dos archipiélagos de las Islas Baleares y Canarias). Se han utilizado datos diarios de reanálisis atmosférico ERA-5 (Copernicus) de 1940 a 2022 (temperatura media del aire, humedad relativa media del aire, y velocidad media del viento), con los que se ha calculado el índice Climate Comfort Index (CCI) de González (1998). Los resultados muestran una importante reducción del CCI en todos los ámbitos costeros analizados, siendo más relevantes en invierno (-0.10 década). El descenso del índice implica una disminución de umbrales fríos y una expansión del confort en la totalidad del área de estudio, especialmente en el Mediterráneo central y Cantábrico. Por su parte, en verano, los descensos más importantes (-0.07 y -0.08 / década) muestran un aumento del disconfort climático más importante en la Costa Cántabra – Euskal Kostaldea y en la Costa Brava – El Garraf, con una importante intensificación y expansión temporal de la sensación térmica de calor. En otros sectores litorales durante los últimos años se alcanzan por primera vez los umbrales climáticos de calor y mucho calor.

Key words: climatic comfort, coastline, tourism, reanalysis, ranks.

Palabras clave: confort climático, litoral, turismo, reanálisis, umbrales.

Received: 9 March 2024

Accepted: 15 July 2024

***Corresponding author:** David Espín Sánchez, Geography Department, University of Murcia, 30001 Murcia, Spain. Email: david.espin1@um.es

1. Introduction

The analysis of thermal comfort (TC) has gained great scientific significance in recent years due to the close relationships existing between climate, health and certain economic activities related to the human enjoyment of the outdoors, such as tourism. TC is the condition of mind that expresses satisfaction with the thermal environment, as defined by the ASHRAE (1996) or Persons (2014). In recent years, many model indices have been designed that incorporate climate variables such as air temperature, relative humidity, wind speed and direction or solar radiation, which has given rise to climate comfort indices, such as Effective Temperature Comfort (ET) proposed by Missenard (1937); the Discomfort Index (DI) by Thom (1959), the Heat Index (Steadman, 1984), the Tourism Climatic Index (ICTI) by Mieczkowski (1985), the Comfort Index (IC) by González (1998), the Equivalent Temperature Index (Quayle and Steadman, 1998), the Universal Thermal Climate Index (UTCI) (Bröde *et al*. 2011), or more recently the Actual Sensation Vote (ASV) thermal comfort index proposed by Nikolopoulou and Steemers (2003).

The coastal regions are home to an increasing percentage of the global population, with approximately half of the planet's inhabitants (3.6 billion people) living within a radius of 200 km from the coast (Crossland, 2006). Furthermore, they continue to constitute spaces with a significant tourism impact, particularly in the summer season. Since its beginnings in the 1990s, the field of study of Tourism Climatology has evolved from addressing the climate-tourism bionomial to analysing the limiting factors for the practice of tourism today (Besancenot, 1991; Millán López, 2016; de Freitas, 2017; Tanana *et al*., 2021). The majority of studies on this topic identify it as being a priority in future ecological planning (Cetin and Sevik 2016a, 2016b).

Studies have been conducted that apply comfort indices to the tourism activity, due to its high degree of exposure to climate conditions and the high impact that it has on the GDP of the regions and destinations engaged in this economic activity. Hence, the effect that the current climate change process could have on the future evolution of the tourism activity, particularly the sun and beach model, is concerning. Therefore, in recent years, the comfort conditions in different parts of the planet with a clear tourism vocation or significant tourism potential have been analysed so as to be used in planning and decision-making at different scales.

According to Arabadzhyan *et al*., (2020), the priority given to the analysis of climate comfort in coastal areas is due to two reasons: the tourism activity is mainly based on the 3Ss (sea, sun and sand), possibly the largest tourism segment on a global level and second, due to the environmental fragility of the ecosystems, particularly on islands. For example, more frequent and severe heatwaves or the reduction in the availability of beaches due to the rising sea level influence the value of the recreational experience in the destination, affecting the demand and tourist expenditure. In this respect, different studies have confirmed the loss of thermal comfort recorded due to the considerable increase in “tropical nights” over the last few decades in different regions of the world, with a notable incidence in the coastal

areas of the Mediterranean basin, related to the warming of the seawater (Olcina *et al*, 2019). The current context of change and global warming forebodes a greater frequency of hot days throughout the year, giving rise to increasingly severe summers in tropical and sub-tropical countries, leading to a loss of thermal comfort for visitors (de Freitas, 2003). This aspect could be particularly relevant in the city climate, where bioclimatic urbanism attempts to adapt to the new realities (Nikolopoulou, 2004).

In this respect, the impact of Climate Change (CC) on coastal tourism has been extensively analysed, but as it is a multidisciplinary topic, researchers from different fields propose their conceptual models for studying the vulnerability and adaptation of tourism to CC. According to Nilsson and Gössling, (2013), the changes occurring in the climate characteristics of the coastal spaces can give rise to the propagation of invasive marine species, with the resulting danger generated for tourists. To this we should add the future trend in the reduction of the size of the beaches due to the rising sea level and the greater frequency of extreme heat events. These aspects are some of the most important indirect environmental effects generated by climate change. So much so that the reduction in the area of the beach has a negative impact on the destination's image, leading to a decrease in arrivals and tourist revenue (Raybould *et al*., 2013).

The objective of this study is to analyse the evolution and distribution of climatic comfort on the Spanish coast. To do this, previous research on the topic conducted for the selected area of study has been analysed and based on the knowledge of the evidence of climate change, which is being recorded in the Spanish Mediterranean region, the following objectives have been established:

- To conduct a comparative analysis of the characteristics of climate comfort between the different coastal sectors of Spain, with the purpose of identifying regional differences and the changes registered over the last few decades.
- To study the temporal evolution of the Climate Comfort Index (CCI) and the changes experienced by the different climate comfort thresholds in recent decades (1940-2022).
- To identify changes in the seasonal distribution of the different climate comfort thresholds in the coastal regions analysed, with a view to establishing more favourable tourist seasons in the future.

2. Materials and methods

2.1. Study area

The area of study covers 7,905 km of Spain's coast, including the Iberian Peninsula and the Canary Islands and Balearic Islands (Fig. 1). A total of 37 coastal stretches corresponding to the most relevant Spanish coastal municipalities from a tourism point of view have been defined (tourist accommodation places), according to the *Atlas de contribution municipal del turismo en España* (Exceltur, 2023). The coastal stretches have been defined by proximity and geographical similarity (Table 1) and all of the official coastal municipalities of Spain are represented.

The 37 coastal tourist areas have been grouped into 10 regions or clusters, in order to simplify the results obtained. The regionalisation or clusterisation process had been conducted by way of a hierarchical clustering, following the Euclidean distance method, recommendable for this study as it uses homogeneous variables in similar units (Table 2). The regionalisation process determines two large Cantabrian regions (the most westerly of the Rías Gallegas – Costa Verde, and the most easterly of the Cantabrian Coast – Euskal Kostaldea). There are six large regions on the Mediterranean coast, from the northernmost part (Costa Brava - El Garraf) to the southernmost region (Costa del Sol - Tropical). The Costa Cálida in the Region of Murcia has been divided between the eastern part (next to the Costa Blanca) and the southern part (next to the coast of Almería). Then there is the archipelago of the Balearic Islands. Finally, on the Atlantic coast there are the regions of the south-west of the Iberian Peninsula (Costa de la Luz) and the Canary archipelago.

The data analysed for calculating the Climate Comfort Index (CCI) have been obtained through the atmospheric reanalysis of the Copernicus Project, formerly known as Global Monitoring for Environment and Security (GMES) programme of the European Union (EU) for establishing a European capacity for observing the Earth. The data have been downloaded from the ERA-5 reanalysis in the climate change service section. ERA-5 is the reanalysis of the fifth generation of the global meteorological model of the European Centre for Medium-Range Weather Forecasts (ECMWF) for global climate over the last eight decades. The data are available from 1940 to the present day. ERA5 provides hourly estimates of atmospheric variables with a horizontal resolution of 31 km and at 137 levels from the surface to 1 Pa (around 80 km) (Hersbach *et al.,* 2020).

Daily data have been downloaded corresponding to the average air temperature (ºC), the average relative air humidity (%), and average wind speed (m/s) from 01/01/1940 to 31/12/2022 through multidimensional files (NetCDF) for each of the 37 tourist areas.

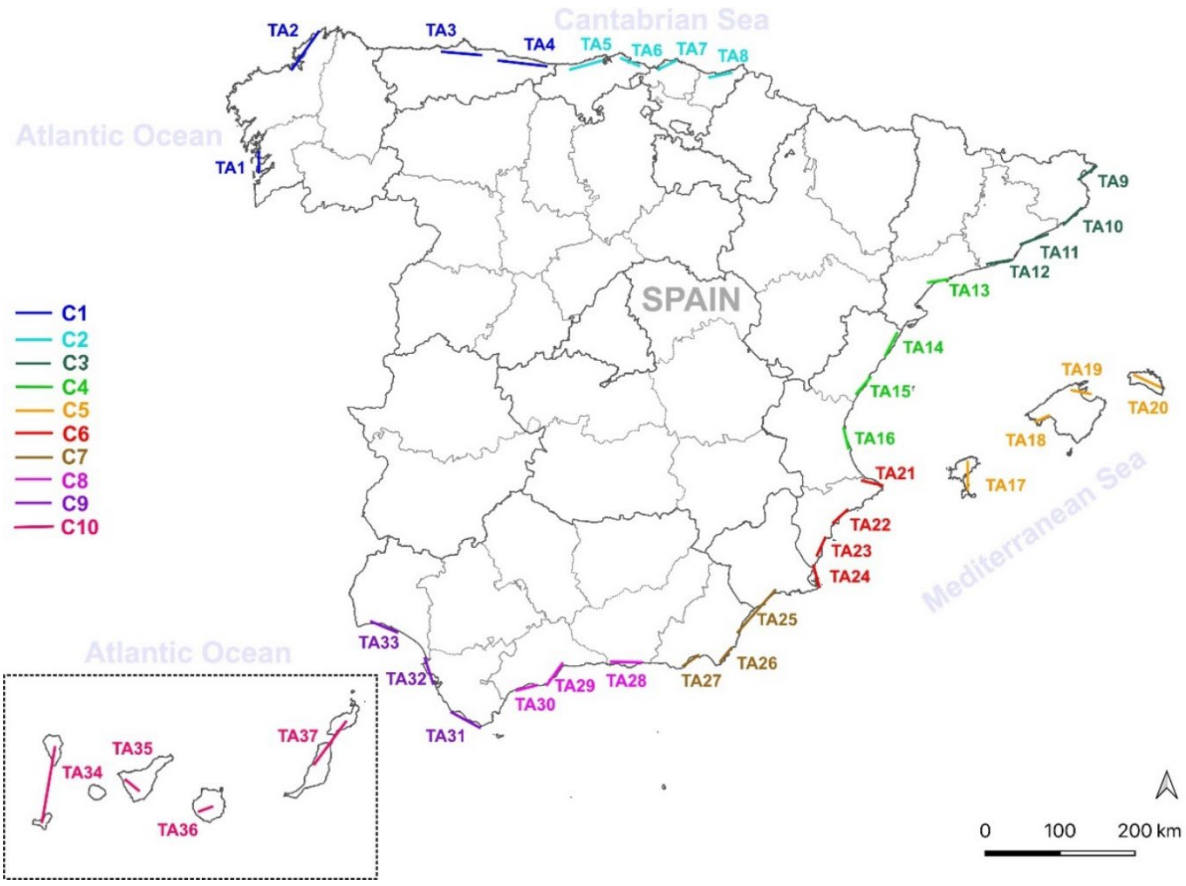

Figure 1. Coastal tourist areas (TA) grouped into clusters (characteristics in Tables 1 and 2)

Table 1. Principal coastal tourist areas in Spain analysed.

ID	NAME / MUNICIPALITIES	ID	NAME / MUNICIPALITIES
TA1	RIAS BAIXAS (Sansenxo, O Grove, Vigo)	TA20	BALEARIC I. – MENORCA (Ciutadella, Mahón)
TA2	RIAS ALTAS (A Coruña – Foz)	TA21	COSTA BLANCA N. (Denia, Jávea, Calpe)
TA3	COSTA VERDE W. (Cudillero, Gijón)	TA22	COSTA BLANCA C. (Benidorm, San Juan, Alicante)
TA4	COSTA VERDE E. (Ribadesella, Llanes, Villaviciosa)	TA23	COSTA BLANCA S. (Santa Pola, Torrevieja)
TA5	CANTABRIAN COAST W. (Santillana, Suances, Santander)	TA24	COSTA BLANCA S. – CÁLIDA E. (Orihuela, San Javier, Cartagena)
TA6	CANTABRIAN COAST E. (Noja, Laredo, Castro Urdiales)	TA25	COSTA CÁLIDA S. – EASTERN COAST OF ALMERIA N. (Mazarrón, Vera, Mojácar)
TA7	EUSKAL KOSTALDEA W. (Bilbao, Bermeo)	TA26	EASTERN COAST OF ALMERIA S. (San José, Las Negras)
TA8	EUSKAL KOSTALDEA E. (Mutriku, Zarautz, San Sebastián)	TA27	WESTERN COAST OF ALMERIA (Almería, Roquetas de Mar)
TA9	COSTA BRAVA N. (Roses, Cadaqués, Port de la Selva)	TA28	COSTA TROPICAL (Almuñécar, Motril, Nerja)
TA10	COSTA BRAVA C. (Platja D´Aro, Calonge)	TA29	COSTA DEL SOL E. (Málaga, Torremolinos, Fuengirola)
TA11	COSTA BRAVA S. (Tossa, Lloret de Mar, Blanes)	TA30	COSTA DEL SOL W. (Marbella, Estepona)
TA12	COSTA EL GARRAF (Barcelona, Sitges)	TA31	COSTA DE LA LUZ SE. (Tarifa, Barbate, Conil)
TA13	COSTA DORADA (Salou, Cambrils, Tarragona)	TA32	COSTA DE LA LUZ C. (Cádiz, Sanlúcar de Barrameda, Doñana).
TA14	COSTA AZAHAR N. (Vinaròs, Benicarló, Peñíscola)	TA33	COSTA DE LA LUZ NW. (Isla Cristina – Punta Umbría)
TA15	COSTA AZAHAR C. (Oropesa, Benicàssim, Castellón)	TA34	CANARY ISLANDS W. (Breña Baja, Llanos de Aridane – Valle Gran Rey)
TA16	COSTA AZAHAR S. (Valencia, Cullera, Gandía)	TA35	CANARY ISLANDS – TENERIFE (Adeje – Arona)
TA17	BALEARIC I. - IBIZA / FORMENTERA (Sant Josep de Sa Talaia - Sta. Eulalia del Río)	TA36	CANARY ISLANDS – GRAN CANARIAS (San Bartolomé de Tirajana – Mogán)
TA18	BALEARIC I. - MALLORCA W. (Calviá, Palma de Mallorca)	TA37	CANARY ISLANDS E. (Tías – Pájara)
TA19	BALEARIC I. - MALLORCA E. (Alcudia – Pollença)		

Table 2. Regionalisation of the different coastal tourist areas analysed.

Cluster	Region Name	ID (TA)
C1	Rías Gallegas – Costa Verde	T1, T2, T3, T4
C2	Cantabrian Coast – Euskal Kostaldea	T5, T6, T7, T8
C3	Costa Brava – Costa El Garraf	T9, TA10, TA11, TA12
C4	Costa Dorada – Costa Azahar	TA13, TA14, TA15, TA16
C5	Balearic Islands	TA17, TA18, TA19, TA20
C6	Costa Blanca – Costa Cálida (east)	TA21, TA22, TA23, TA24
C7	Coast of Almería – Costa Cálida (south)	TA25, TA26, TA27
C8	Costa Tropical – Costa del Sol	TA28, TA29, TA39
C9	Costa de la Luz	TA31, TA32, TA33
C10	Canary Islands	TA34, TA35, TA36, TA37

2.2. Climate Comfort Index (CCI)

This study analyses climate comfort through the use of the CCI. The indices described below have been subjected to a time trend analysis for each of the 37 coastal tourist areas, divided into ten different regions using a clustering process (Table 2).

The CCI proposed by González is adapted and adjusted from the Cooling Power of Leonardo Hill and Morikofer-Davos (IDEAM, 1998) with some modifications: first, a comfort index IC is obtained instead of a cooling power; second, the humidity parameter is included and third, the base values for each of the parameters are modified so that the results are more appropriate for our conditions, taking into account the change in temperature with altitude, as the relief in the country is an important factor (Table 3).

Table 3. Classification of thermal comfort according to climate comfort indices (CCIs).

Comfort Thermal Classification	CCI Ranks
Cold	13 -14
Cool-Cold	12 -13
Cool	11 -12
Cool-Comfort	10 -11
Comfort	8 -10
Comfort-Warm	7 -8
Warm	6 -7
Warm-Heat	5 -6
Heat	4 -5

The CCI is a function of the air temperature, relative humidity and wind speed measured at 10 m. In this case, the geographical coordinates of each weather station influence the results. Therefore, there are three variants of each of the formulas, depending on the altitude of the place: one for those with altitudes of under 1000 metres, another for those at altitudes of between 1000 and 2000 and a final one for those higher than 2000 metres.

All the mean ERA5 grid boxes centroids used in the analysis are located at an altitude of less than 1000 m, as they are coastal areas (Table 1).

$$CCI = (36.5 - TM)\ (0.05 + 0.04\sqrt{WS10} + HR250)$$

TM= Average daily temperature (%); WS10= Average daily wind speed (%); RH250= Average daily relative humidity (%).

The excessive heat (<4) and excessive cold (>14) thresholds have been omitted as they have not been recorded in any of the areas analysed (Table 3).

2.3. Trend Analysis

The time trend analysis was calculated using the Mann–Kendall test (MKT) (Mann, 1945; Kendall, 1975). In order to quantify the rate of temporal change, a trend line slope and Theil–Sen analysis (TSE) has been used (Theil, 1950; Sen, 1968). All trends were evaluated at a statistical significance of 0.05 (confidence level of 95%).

The MKT statistic S is that which has a mean of zero and a variance computed by Equation (3). It is calculated using Equations (1) and (2) and is asymptotically normal:

$$S = \sum k = 1n - 1 \sum j = k + 1 nsgn\ (xj - xk) \quad (1)$$

$$\text{sgn}(xj - xk) = \{+1 \text{ if } (xj - xk) > 00 \text{ if } (xj - xk) = 0 - 1 \text{ if } (xj - xk) < 0\} \quad (2)$$

$$\text{Var}(S) = [n(n - 1)(2n + 5) - \sum i = 1m\ ti(ti - 1)(2ti + 5)]18 \quad (3)$$

where S is the number of positive differences less the number of negative differences, n is the number of data points, m is the number of tied groups (a tied group is a set of sample data having the same value), and ti is the number of data points in the group. In cases where the sample size n > 10, the standard normal variable Z is computed by using Equation (4).

$$Z = \{S - 1\text{Var}(S) \text{if } S > 00 \text{ if } S = 0S + 1\text{Var}(S) \text{if } S < 0\} \quad (4)$$

Positive values of Z indicate positive trends, while negative values of Z show negative trends. When testing either increasing or decreasing monotonic trends at an α significance level, the null hypothesis was rejected for an absolute value of Z greater than Z1−α/2, obtained from the standard normal cumulative distribution tables.

The TSE model for the trend magnitude is conducted by calculating the slopes of all possible combinations of data pairs (Equation 5).

$$\left(\begin{Bmatrix} n \\ V \\ 2 \end{Bmatrix}\right) = \frac{n\,(n-1)}{2} \quad (5)$$

The final slope is then defined as the median of all slopes (Equation (6)):

$$\beta 1 \ = \ median\,\{\tilde{B}\}, \tilde{}\text{B} = \left\{\frac{\text{bij}}{\text{bij}}\right\} = \frac{yj - yi}{xj - xi}, xi \ \neq \ xj, 1 \ \leq i \ < j \ < n \quad (6)$$

Because the TSE computes the trend line's slope alone, the model intercept can be given by (Equation (7):

$$\beta 0 = \text{Ymedian} - \hat{}\beta 1 \times \text{Xmedian} \quad (7)$$

where Xmedian and Ymedian are the medians of the measurements and of the response variables, correspondingly.

3. Results

3.1. General characteristics of the CCI index

The Spanish coast displays a wide climatic diversity throughout the year, between the northern Atlantic and Cantabrian coasts (C1 and C2) with cool and cold climate thresholds during the winter season and comfortable summers and the Mediterranean coast from the Costa Brava of Gerona (C3) to the Costa de la Luz of Cádiz and Huelva (C9) with cool and comfortable winters and hot summers. With different dynamics due to their subtropical location, the Canary Islands (C10) exhibit lesser annual oscillations, with a comfortable end of winter and spring and a warm CCI threshold at the beginning of autumn (Fig. 2).

Over the last eight decades (1940-2022), significant changes have taken place in the annual evolution of the CCI in the different coastal regions analysed. On the Cantabrian Coast (C1 and C2), a highly significant change is recorded during the coldest period of the year, with cold thresholds from mid-December to the end of February (1941-1970 and 1951-1980) to cool-cold thresholds in the more recent periods of reference. Even during the month of February, the values are close to 12.0 (cool). One of the most remarkable changes has occurred during the first half of March, from values close to 13.0

(cool-cold) to records of average values of 11.3-11.2 (very close to comfort-cool). This is the moment in the year with the greatest reduction in the CCI. The months of December, January and February register the greatest reductions from -0.10 to -0.12 / decade, being statistically significant (Table 4). In general, the largest CCI decreases are concentrated between the second half of December and the first half of January. During the summer, despite the fall in the CCI the value recorded is one of the lowest in the year, with significant changes registered, particularly during the month of August, reaching the warm-comfort threshold in the Rías Gallegas and the Costa Verde (C1) for the first time during the last periods of reference.

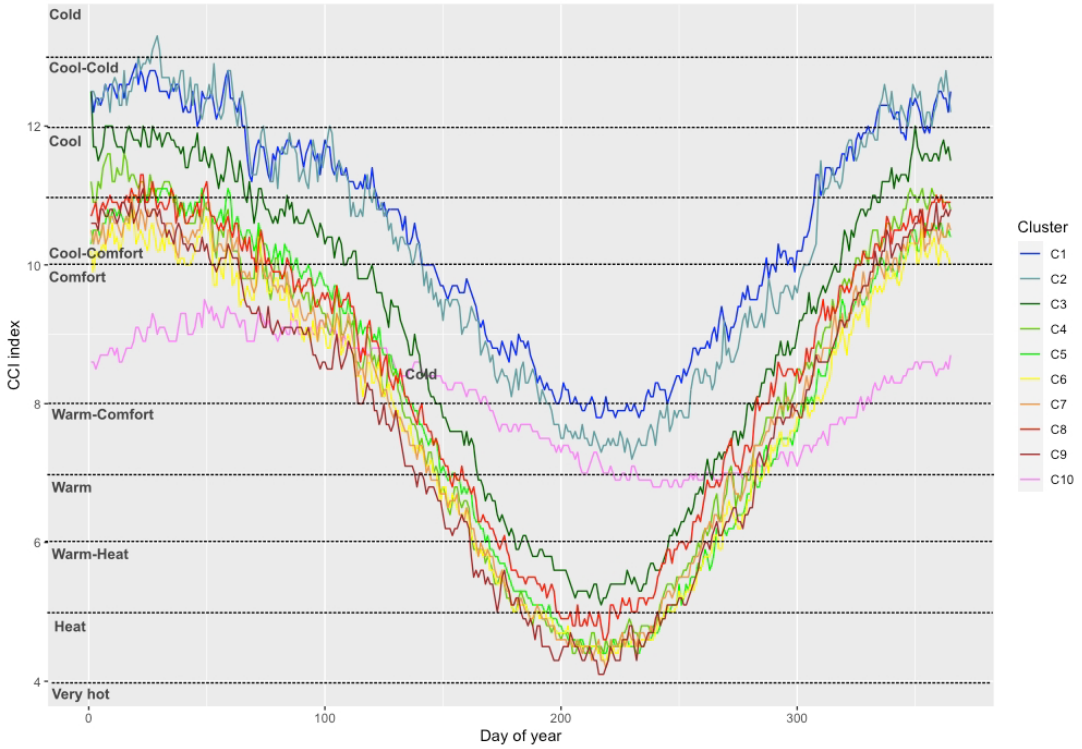

Figure 2. Annual average evolution of the CCI in the different regions of analysis (1991-2020).

Table 4. Monthly and seasonal trends in the CCI in the different regions of analysis (by decade). Values in bold are statistically significant (p value <0.01).

	C1	C2	C3	C4	C5	C6	C7	C8	C9	C10	Spain
Jan	**-0.10**	**-0.11**	**-0.10**	**-0.17**	**-0.10**	**-0.14**	**-0.11**	**-0.09**	**-0.08**	**-0.05**	**-0.11**
Feb	**-0.11**	**-0.09**	**-0.10**	**-0.15**	**-0.08**	**-0.09**	**-0.09**	**-0.07**	**-0.07**	-0.02	-0.09
Mar	**-0.09**	-0.05	**-0.09**	**-0.14**	-0.05	-0.06	**-0.06**	**-0.08**	**-0.10**	0.00	-0.07
Apr	-0.06	-0.07	**-0.06**	**-0.08**	**-0.04**	**-0.05**	-0.04	-0.03	-0.01	-0.02	-0.05
May	**-0.09**	-0.07	-0.07	-0.08	-0.05	-0.05	**-0.07**	-0.07	-0.07	-0.03	-0.06
Jun	-0.05	**-0.06**	-0.08	-0.08	-0.07	-0.07	-0.06	-0.05	-0.03	-0.03	-0.06
Jul	-0.05	**-0.06**	-0.07	-0.05	**-0.06**	-0.05	**-0.04**	-0.02	-0.01	-0.02	-0.04
Aug	-0.06	**-0.08**	**-0.08**	**-0.07**	**-0.06**	**-0.06**	**-0.06**	-0.04	-0.02	-0.03	-0.06
Sept	**-0.06**	**-0.05**	**-0.05**	**-0.06**	**-0.05**	**-0.06**	**-0.04**	-0.02	-0.02	-0.03	-0.05
Oct	-0.07	**-0.10**	**-0.07**	**-0.12**	**-0.08**	**-0.10**	**-0.09**	**-0.07**	**-0.06**	-0.04	**-0.08**
Nov	**-0.06**	-0.05	**-0.06**	**-0.11**	-0.04	**-0.09**	**-0.09**	**-0.06**	**-0.05**	-0.04	**-0.06**
Dec	**-0.13**	**-0.14**	**-0.10**	**-0.13**	**-0.09**	**-0.11**	**-0.10**	**-0.08**	**-0.07**	**-0.04**	**-0.10**
Win	**-0.11**	**-0.12**	**-0.10**	**-0.15**	**-0.09**	**-0.11**	**-0.10**	**-0.08**	**-0.07**	-0.04	**-0.10**
Spr	**-0.08**	-0.06	**-0.07**	**-0.10**	-0.05	-0.05	-0.06	-0.06	-0.06	-0.02	-0.06
Sum	-0.05	**-0.07**	**-0.08**	-0.07	-0.07	-0.06	**-0.05**	-0.03	-0.02	-0.03	-0.05
Aut	-0.06	**-0.07**	**-0.06**	**-0.10**	-0.06	**-0.08**	**-0.07**	-0.05	-0.04	-0.04	**-0.06**
Year	-0.08	**-0.08**	**-0.08**	**-0.10**	**-0.06**	**-0.08**	**-0.07**	-0.06	-0.05	-0.03	-0.07

Again, the most significant changes in the CCI in the C3 and C4 regions (Costa Brava – El Garraf and Costa Dorada – Azahar) were recorded during the winter season, with the difference that they extend to the month of March. In this coldest period of the year, the CCI thresholds have shifted from being cool-cold to cool, even reaching values of 11 (cool-comfort) on the Costa Dorada-Azahar. The summer season records the principal changes during the month of August, with C3 (Dorada-El Garraf) close to the heat threshold. The same is the case for C4 (Costa Dorada – Azahar) with a very hot threshold during the final reference periods. This coastal area is where the greatest decreases in the CCI are recorded for the whole of the Spanish coastline (-0.17 / decade in January and 0.15 / decade in the winter as a whole) (Table 4).

The coastal area C5 (Balearic Islands) registers the greatest decreases in the CCI during the second half of December and the first half of January, with rates that are lower than those of the Cantabrian regions and the northern Mediterranean area. The data corresponding to the winter season shift from cool conditions during the first periods of reference (1941-1970 and 1951-1980) towards the comfort-cool threshold during the later years. This is where the greatest decreases (statistically significant) are recorded, with values of -0.10 / decade in January and -0.09 / decade in December (Table 4). In the summer period (JJA), the second half of August is particularly noteworthy. There is a change in the thresholds from warm-hot in the first decades of the study to the hot threshold during the second half of the time period analysed.

The coastal area of the south-east of the Iberian Peninsula (C6 and C7), comprising the Costa Blanca in the Region of Valencia, the Costa Cálida in the Region of Murcia and the Coast of Almeria also register the highest rates of decreases in the CCI during the winter season. This is particularly the case during the second half of December and the month of January. In the case of the Coast of Almería, the decrease is greater and lasts until the first half of March. One of the most notable cases is on the Costa Blanca-Cálida (east) where the cool conditions prevailing during the first periods of reference change to comfort conditions during the winter months in 1991-2020 (Fig. 3). This is where the greatest statistically significant decrease rates are recorded during the month of January (-0.14 / decade and -0.11 / decade in December). In the summer season, the second half of August in C6 and the first half of August in C7 with a statistically significant decrease of between -0.05 and -0.06 / decade stand out. In the last period of reference (1991-2020), the summer records are close to the very hot threshold (4) on the Almeria coast and the southern part of the Costa Cálida.

The southernmost coast of the Iberian Peninsula, the Mediterranean area of the Costa Tropical and the Costa del Sol (C8) and the Atlantic with the Costa de la Luz (C9) register the most significant changes during the winter and the first half of spring, specifically from the second half of December until the second half of March. In December, January and March statistically significant decreases are recorded of between -0.07 and -0.10 / decade (Table 4). In the case of the thresholds, the change is evident, with a shift from cool characteristics to comfort-cool characteristics (Fig. 3). Meanwhile, the lowest variations in all the coastal areas analysed are recorded in the summer season, with slight reductions of between -0.04 and -0.01 / decade. The thermal thresholds have not changed particularly in the last few decades and, despite a less significant decrease being recorded than in the rest of the Iberian Peninsula, in the last periods of reference (particularly 1991-2020) the hot threshold was reached in the Costa Tropical – Costa del Sol (C8). Furthermore, the Costa de la Luz (9) recorded the hottest summer thresholds and during the last period of reference values very close to the very hot threshold (4).

Finally, the Canary Islands (C10) experienced the greatest changes during the autumn (between the second half of October and the first half of November) and the central part of winter (between the second half of December and the first half of January). With regard to the change in the CCI index, January and December stand out (-0.04 and -0.05 / decade) as the only months with statistically significant reductions (Table 4). During the last periods of reference, the CCI values during the winter remained within the comfort threshold, although increasingly further away from the cool-comfort threshold. Meanwhile, during the summer season, there has also been an increase in temperatures over

the last few decades increasing from a comfort-warm threshold to a hot threshold for the first time during the two last reference periods (1981-2010 and 1991-2020) (Fig. 3).

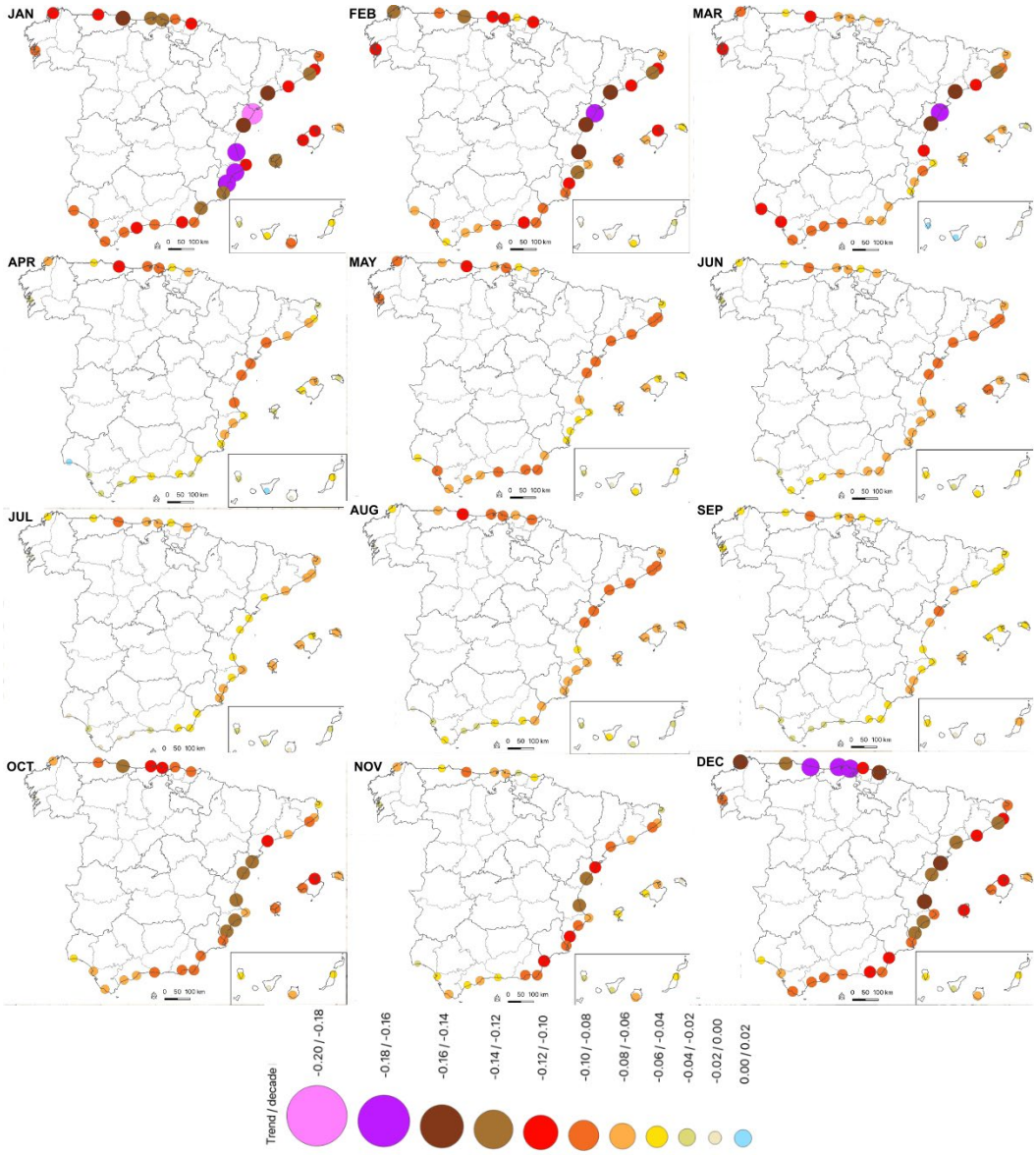

Figure 3. Space-time distribution of the CCI index trend for the different months of the year.

3.2. Seasonal changes in the CCI index (1940-2022)

Figure 4 shows the space-time evolution of the different thresholds of the CCI index, according to the different reference periods used. Combined with Table 5, we can observe the changes at the start, end and the total number of days per threshold. Therefore, Table 5 groups the different thresholds into three large blocks: warm, comfortable and cold conditions. Warm conditions have not been detected on the Cantabrian strip (C1 and C2) during the last few decades, but comfort-warm conditions have been recorded. The cold threshold disappears as from the reference period 1981-2010, with a reduction in the number of days of the cold group from 198 to 179 days in C1 (-29 days) and from 192 to 169 in C2 (- 23 days). Meanwhile, the comfort threshold increased in terms of the number of days from 167 to 186 (19 days) in C1 and from 173 to 196 in C2 (23 days).

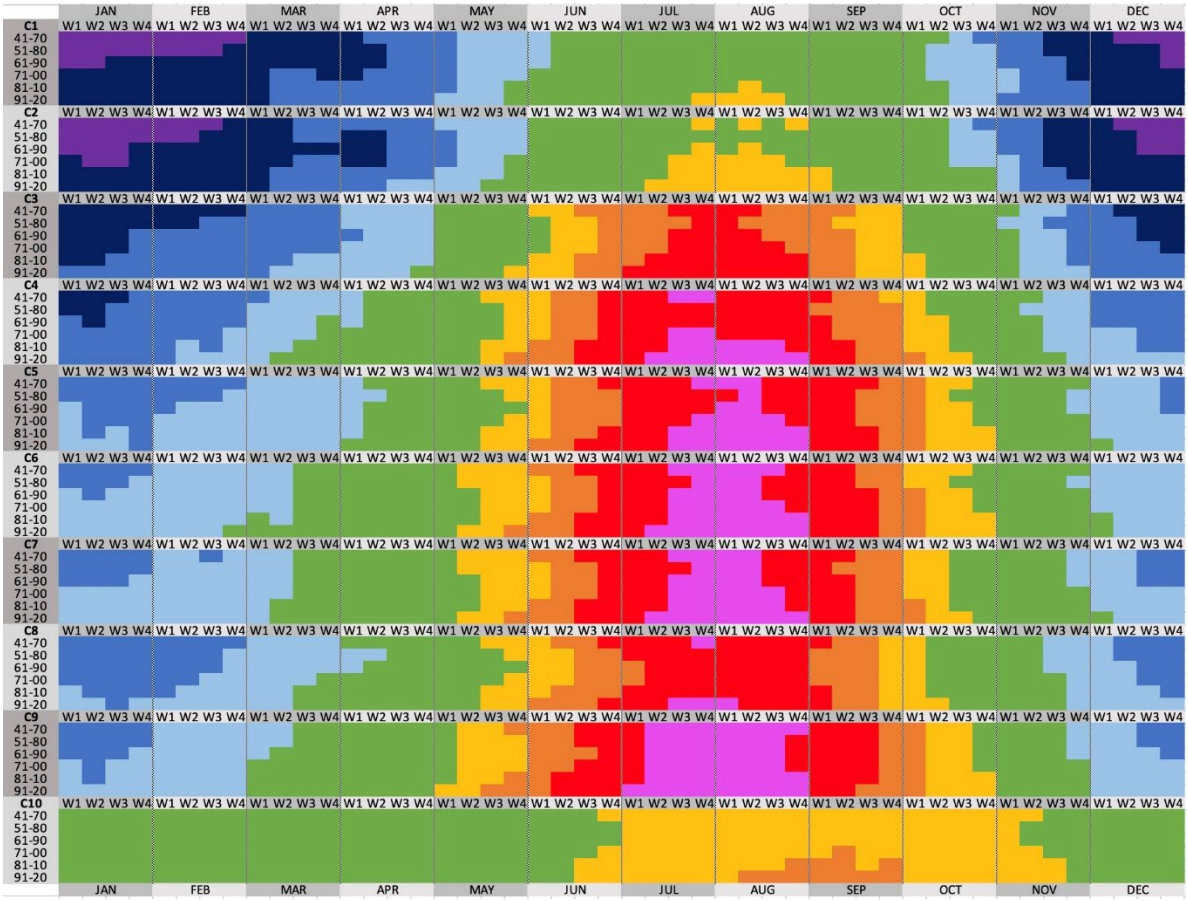

Figure 4. Weekly CCI thresholds during the year in the regions of study (according to periods of reference). Legend: Pink (heat), red (heat-warm), orange (warm), Pink (warm-comfort), green (comfort), light blue (cool-comfort), blue (cool), dark blue (cool-cold) and dark purple (cold).

Table 5. Changes in the number of days of the different climate threshold groups of the CCI for the regions of study and reference periods.

		C1	C2	C3	C4	C5	C6	C7	C8	C9	C10
Warm Heat	41 -70	0	0	89	114	120	121	116	107	138	4
	51 -80	0	0	81	108	115	117	112	101	128	0
	61 -90	0	0	80	110	117	122	115	100	127	1
	71 -00	0	0	79	111	116	123	119	101	132	10
	81 -10	0	0	94	122	123	130	127	109	137	28
	91 -20	0	0	99	130	133	138	134	115	144	54
	Variation	**0**	**0**	**18**	**22**	**18**	**21**	**22**	**15**	**17**	**54**
Comfort	41 -70	169	176	144	151	179	220	195	177	187	361
	51 -80	167	173	150	168	192	230	209	188	194	365
	61 -90	172	182	151	170	206	229	219	201	205	364
	71 -00	175	186	156	190	220	239	237	217	218	355
	81 -10	183	195	155	180	220	235	237	222	222	337
	91 -20	186	196	166	198	222	227	230	237	219	311
	Variation	**19**	**23**	**22**	**47**	**43**	**7**	**35**	**60**	**32**	**-50**
Cool Cold	41 -70	196	189	132	100	66	24	54	81	40	0
	51 -80	198	192	134	89	58	18	44	76	43	0
	61 -90	193	183	134	85	42	14	31	64	33	0
	71 -00	190	179	130	64	29	3	9	47	15	0
	81 -10	182	170	116	63	22	0	1	34	6	0
	91 -20	179	169	100	37	10	0	1	13	2	0
	Variation	**-21**	**-33**	**-34**	**-63**	**-56**	**-24**	**-53**	**-68**	**-41**	**0**

On the Costa Brava – El Garraf (C3) a notable prolongation of the warm-heat threshold can be observed during the months of July and August. In the last reference period (1991-2020), this applies to the whole of both of these months, while in the reference period 1951-1980 it is recorded for the last week of July and the first week of August. The increase in the number of days of the heat grouping is considerable from 79 to 99 days (20 days). The cool-cold threshold disappears as from the reference period 1991-2020, with the number of cold days reducing from 134 to 100 (-34 days). Finally, an increase in the number of comfortable days can be observed, rising from 144 to 166 days (22 days) (Table 5).

The cold CCI thresholds of coastal region C4 (Costa Dorada – Costa Azahar) have decreased notably, with the elimination of the cold-cool characteristic in January as from the reference period 1970-2000 and with a very large decrease in the number of days, from 100 to 37 (-63 days). This decrease has been partly compensated by the comfort threshold with an increase from 151 to 198 days (47 days) and, on the other hand, by the increase from 108 to 130 days of the warm thresholds (22 days). The heat CCI threshold appears during the last reference period 1991-2020 throughout the last three weeks of July and the whole of the month of August (Fig. 4).

The Balearic Islands (C5) follows the same pattern as the rest of the area of study. There is a clear reduction in the cold CCI thresholds; in the last reference period the cool threshold was present only in the last week of January. The number of cold days reduced from 66 to 10 days (-56 days). Similarly to the rest of the regions, an increase in the comfortable days throughout the year may be observed, rising from 179 to 222 (43 days). Finally, during the last few decades, there has been an expansion of the warm thresholds, with an increase from 115 to 133 days (17 days). The heat CCI threshold appears during the last reference period 1991-2020, during the second half of July and the whole of the month of August (Fig. 4).

The cold thresholds have practically disappeared from the Mediterranean regions in the south-east of the peninsula (C6 and C7) represented by the Costa Blanca, the Costa Cálida and the Coast of Almería over the last few decades. Specifically, the cool CCI threshold has disappeared since the reference period 1971-2000 to the present day, from 24 days to 0 days in C6 (-24 days) and from 54 to 1 days in C7 (-53 days). The loss of the cold winter has been replaced with more comfortable conditions. There has been an increase from 195 to 230 days in C7 (35 days). On the other hand, in region C6, a greater change in the increase in the warm thresholds can be observed, with an evolution from 117 to 138 days (21 days). The change is also evident in C7, with an increase from 112 to 134 days over the last few decades (22 days). In both regions, the heat threshold appears during the last reference period 1991-2020, throughout the last three weeks of July and the whole of the month of August (Fig. 4).

The southern coast of Spain, represented by C8 and C9 (Costa Tropical, del Sol and Costa de La Luz) has experienced a drastic reduction in the cold thresholds during the winter, to the point where the decrease is particularly notable in C8 (from 81 to 13 days) and in C9 (from 40 to 2), with reductions of 68 and 38 days, respectively. There has also been a major time extension of the comfort threshold, with the period starting earlier from the third week of March and ending between the second and third week of November. In total, the increase in the number of days reached 60 days in C8 and 32 in C9. Finally, the warm conditions lasted longer during the last decades of the period of study, with an increase from 15 to 17 days, respectively. After several reference periods, the hot threshold appears in C9 during 1991-2020 from the third week of July to the first week of August (Fig. 4).

Finally, the Canary Islands (C10) have experienced the expansion of the warm-comfort threshold and the warm threshold appeared for the first time (reference period 1991-2020) between the second week of August and the whole month of September. The CCI comfort group experienced a notable decrease (-50 days) in detriment to the warm group (54 days).

A greater decrease in the CCI is recorded in the winter trimester (DJF) throughout the whole of Spain (-0.10 / decade). This is a significant reduction. Of the different areas analysed, the Costa Dorada – Azahar (C4) particularly stands out with the greatest recorded decrease (-0.15 / decade) (Fig. 5). In general,

and with the exception of the Costa de la Luz (C9) and the Canary Islands (C10), the decreases have been homogeneous from the 1940s to the present day. In the latter two cases, there was a cooler period during the 1960s and 1970s. Furthermore, in recent years, the reduction of the CCI has accelerated in certain coastal sectors, particularly the Costa Dorada – Azahar (C4) and Costa Blanca – Cálida (C6). During the last winters of the time period, milder CCI values were registered, particularly in 2022. Therefore, there has been a clear increase in winter thermal comfort on the Spanish coast in recent years, except in the Rías Gallegas-Costa Verde (C1), where the CCI has not followed this trend over the last two decades.

No significant changes have been observed in the spring (MAM) during the last few decades, at least in the full-time trend from 1940 to the present day (-0.06 / decade). The decreases on the Costa Dorada – Azahar (C4), in the Rías Bajas of Galicia (C1) and the Costa Brava – El Garraf (C3) are notable, with statistically significant values between -0.10 and -0.07 / decade. On the other hand, the Canary Islands (C10) record the smallest decrease with -0.02 / decade. Figure 7 shows the evolution of the CCI in the different coastal regions, with the coolest values during the 1970s and 1980s particularly standing out (in the Mediterranean regions). After the decrease that occurred mainly in the 1990s and part of the 2000s, without trend can be observed in several coastal regions in recent years, such as the north Atlantic strip and Cantabria (C1 and C2), the Balearic Islands (C5) or the Costa Tropical-Sol (C8). There has even been a slight recovery (cooler springs) in the coastal areas of the south-east of the peninsula (C6 and C7) and the Costa de la Luz (C9).

Summer (JJA) is the season with the lowest decrease of the year in Spain as a whole (-0.05 / decade), mainly due to the fact that the CCI already establishes low values (heat thresholds). Even so, the decrease is evident in all of the regions in the study, but particularly in eastern Cantabria (C2) and the northernmost Mediterranean coast (C3) with statistically significant values between -0.07 and -0.08 / decade, respectively. The sector in the north-east of the peninsula is where the summers are becoming increasingly hotter. Meanwhile, the smallest decreases are recorded in the southern Mediterranean coast (Costa Tropical -Sol) and the south-west Atlantic coast (Costa de la Luz) with -0.02 and -0.03 / decade. In the same way, the Canary Islands register a decrease of -0.03 / decade. The areas between TA10 and TA15 (central and southern Costa Brava, El Garraf, Costa Dorada, and northern and central Costa Azahar) with a decrease of between -0.09 and -0.08 / decade).

Figure 6 shows the time evolution of the CCI during the summer season. We can observe that the 1970s was the least warm decade of the period of study (1940-2022). From then, there has been a constant decrease in all of the regions of study, but with spatial differences. In this respect, during the last years of the study there was an evident decrease in the CCI in the majority of the areas studied (from C3 to C8), that is, the Mediterranean coast of the peninsula from the Costa Brava in Gerona to the Costa del Sol in Málaga. Therefore, it should be pointed out that the summer of 2022 was the hottest since 1940 in C3, C4, C6, C7 and C8, that is, the Mediterranean coast on the peninsula, from the Costa Brava to the Costa del Sol. On the other hand, the east of Cantabria (C2) and the Canary Islands (C10) experienced a slight decrease. Meanwhile, the two Atlantic coastal regions displayed a dynamic that was different to the rest of the regions. The Costa de la Luz (C9) experienced very little changes during the last years of the study period and the Rías Gallegas and the Costa Verde in Asturias even experienced a slight increase in the CCI (less hot) in the last two decades.

Finally, in the analysis of the autumn (SON), there was a national decrease of -0.06 / decade (statistically significant) but more homogeneous than the rest of the seasons. With the exception of the Costa Dorada-Azahar (C4), which recorded a greater decrease of -0.10 / decade, the rest of the Mediterranean coast (C3 to C7) experienced reductions of between -0.06 and -0.08 / decade. In this regard, it is necessary to point out that the southern coast on the peninsula (C8 and C9) and the Canary Islands registered the smallest decreases (-0.04 to -0.05 / decade). Figure 8 shows the evolution of the CCI during the autumn season, which indicates that the coolest CCI rates were recorded during the 1970s. From then until the present day, there has been a homogeneous and generalised decrease in all of the regions of study, with the exception of the Canary Islands, which recorded a trend with a few

changes during the last years. A coastal warming in the autumn season has been manifested in recent years, particularly in 2022. The lowest average values were recorded in C3, C5, C6, C7 and C8, that is, on the majority of the Mediterranean coast of the peninsula from the Costa Brava and the Costa del Sol. In many cases, the figures display a wide margin of difference, constituting, to date, the hottest autumn in the Mediterranean region since 1940.

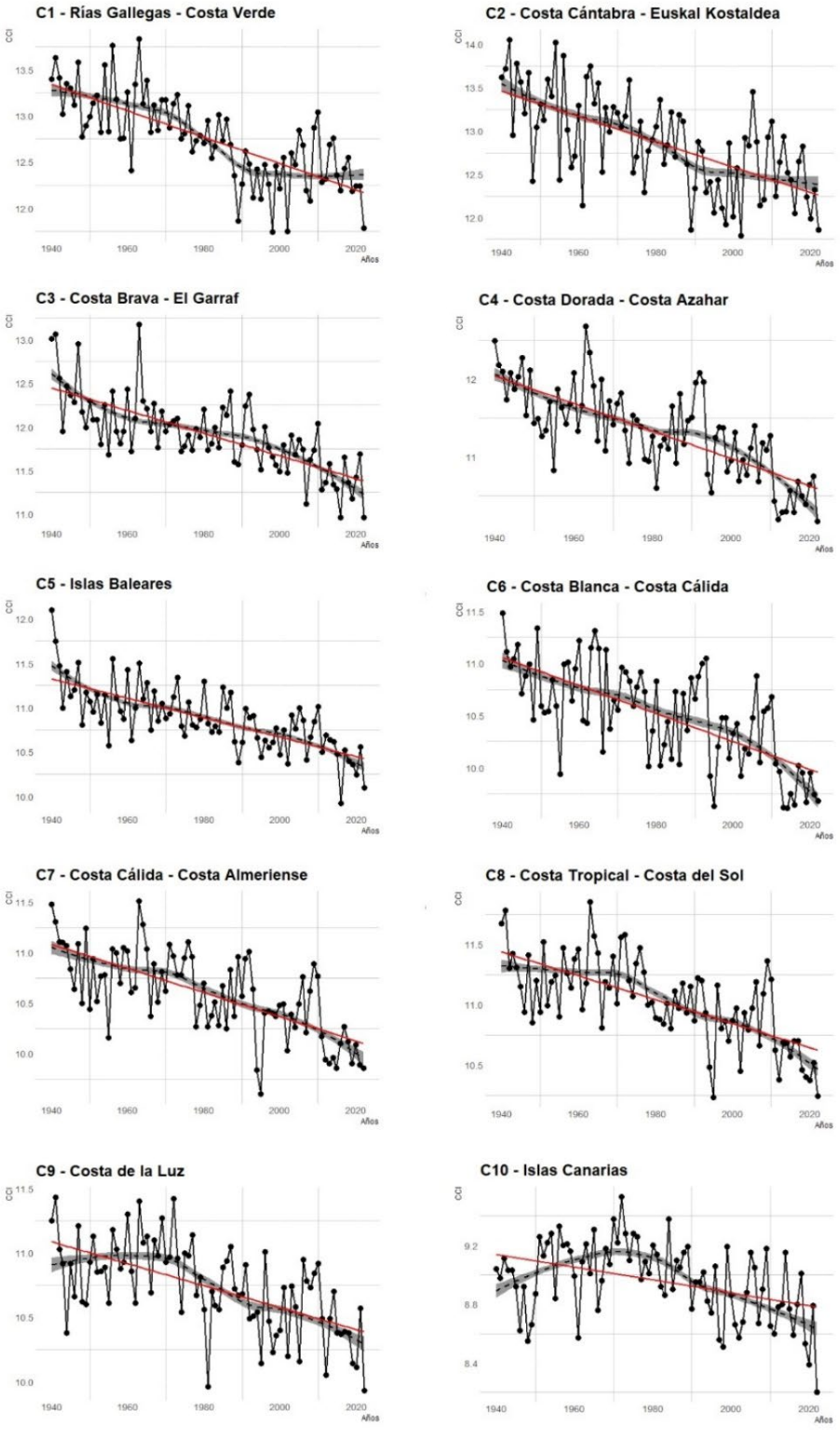

Figure 5. Time evolution of the CCI in the winter season (DJF) in the different regions (1940-2022).

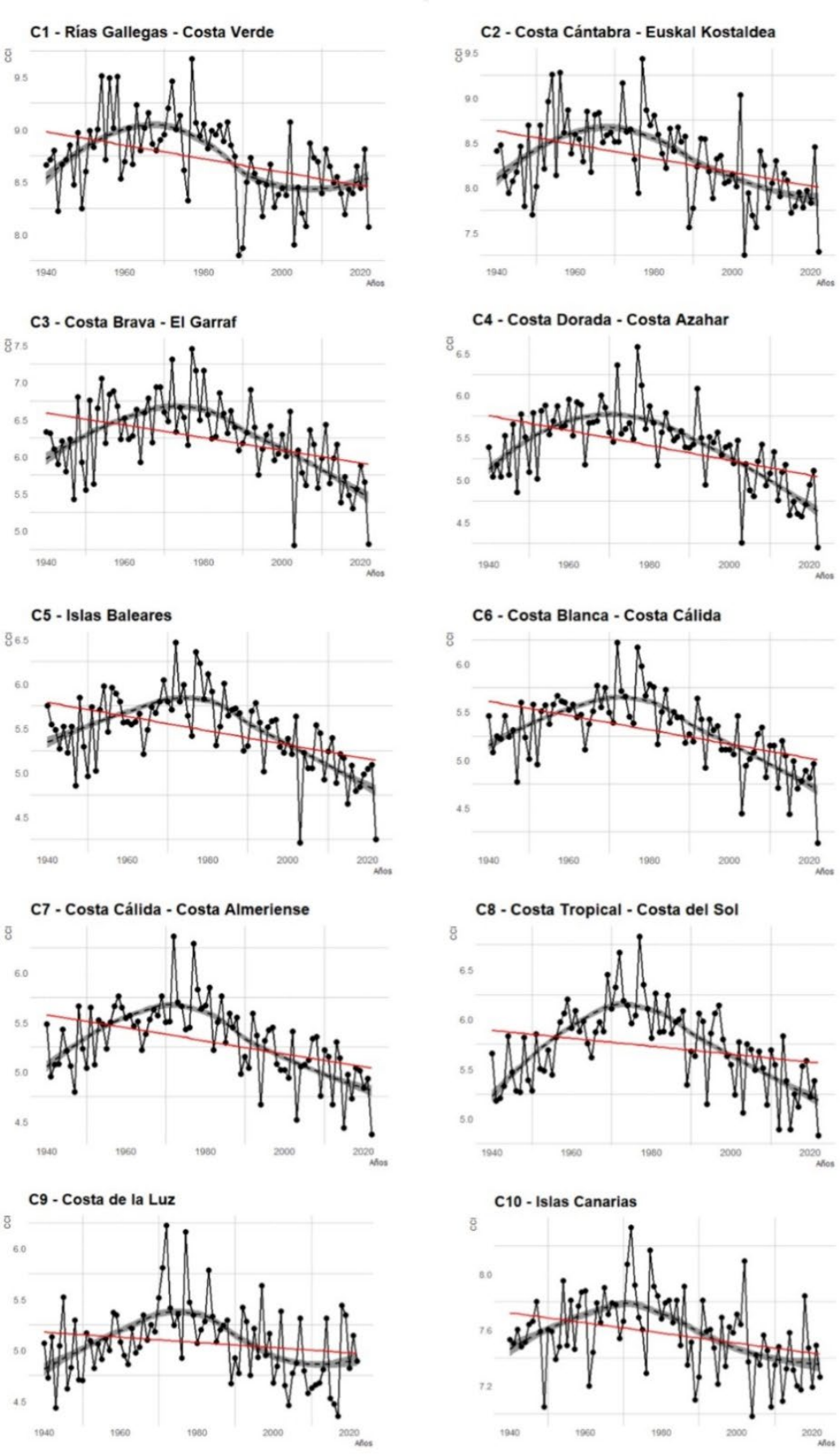

Figure 6. Time evolution of the CCI in the summer season (JJA) in the different regions (1940-2022)

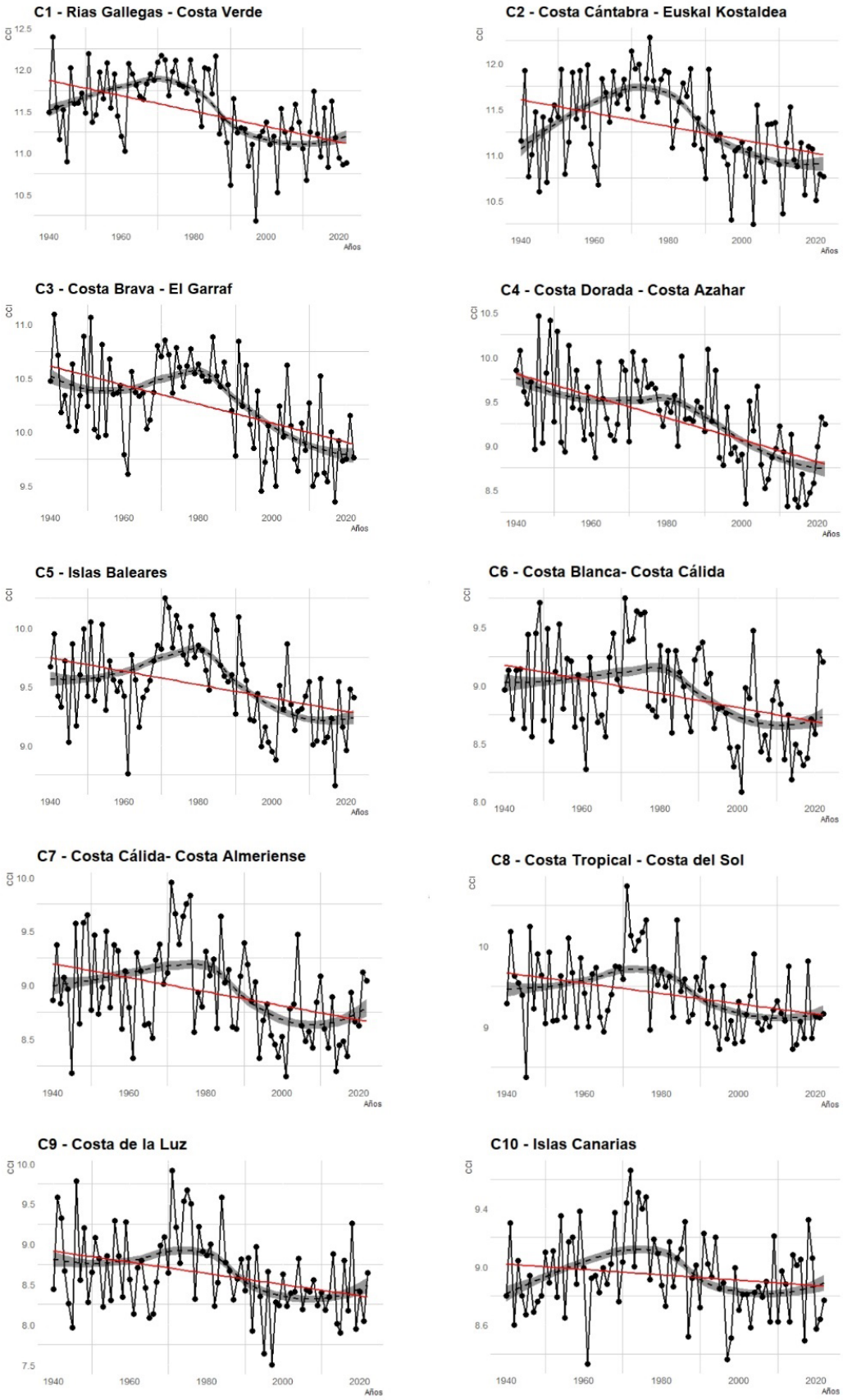

Figure 7. Time evolution of the CCI in the spring season (MAM) in the different regions (1940-2022).

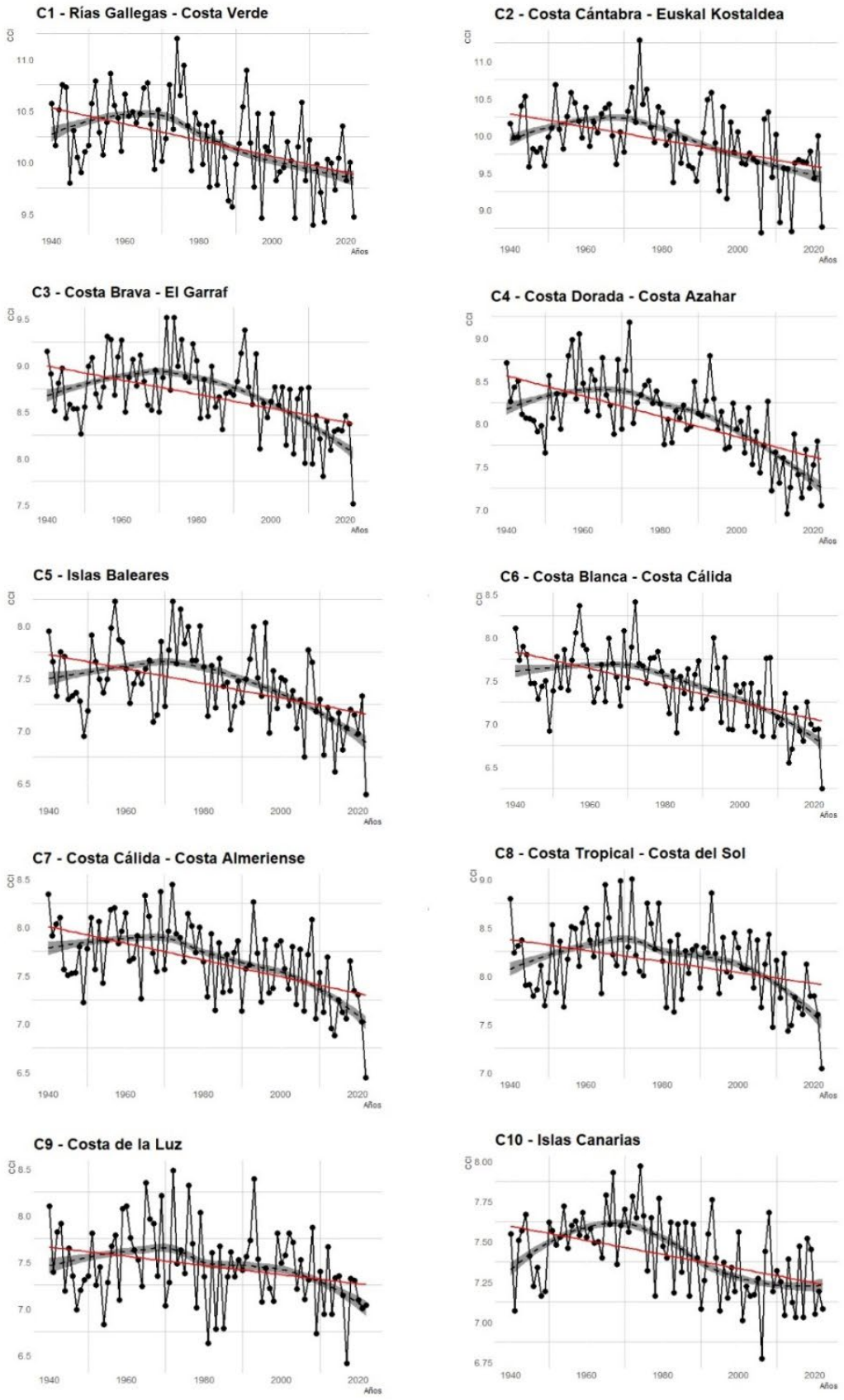

Figure 8. Time evolution of the CCI in the autumn season (SON) in the different regions (1940-2022).

4. Discussion

The Spanish coastline has been facing a new climate reality in recent years, particularly significant during the summer season with the increase in the duration and intensity of climate discomfort. The different coastal regions of Spain, particularly the Costa Blanca (Benidorm), the Costa Dorada (Salou), the coast of the Balearic Islands (Calviá), the Costa del Sol (Marbella) or the Canary Islands (Adeje), are regional leaders in sun and beach holidays in Europe, based on a Ford (mass) tourism model and characterised by high seasonality and environmental pressure. Therefore, analysing the current conditions and the evolution of the last few years is fundamental for evaluating the future tourism potential of the different coastal regions of Spain. According to Bafaluy et al., (2013), the climate conditions will continue to deteriorate during the peak period of tourist visits, while they will improve in spring and autumn. Thus, future efforts to understand tourists' destination decision-making in the context of climate change should consider climate change-induced cognition-affective aspects as part of knowledge-centered models connecting destination choice with perceived risks (Lin and Wang, 2023).

In the final years of the study period, the relationship between climate, tourism and water has been analysed and it has been found that there is a clear relationship between the increase in temperatures and the reduction in rainfall on the Mediterranean coast of the Iberian Peninsula, which has caused severe droughts with major economic losses (Martínez Ibarra, 2015). Moreover, beach tourism requires relatively high temperatures for it to be attractive to tourists, and relatively modest changes have been observed in the tourist flows in recent years. As concluded by March *et al.,* (2014), tourists do not seem to be so worried by climate change on the coast, but more so in winter tourist destinations (ski resorts).

It is likely that the Mediterranean will continue to constitute Europe's leading beach tourist destination in the summer for at least the next 50 years (Moreno and Amelung, 2009), although the extreme climate discomfort values, which have been increasingly recurrent in recent years, could modify the time distribution, with a greater occupancy in the months prior to and after the summer. According to Gómez-Martín (2006), in recent years, the beginning and the end of the summer are the best times for tourism. However, currently the visitor rates at these times are low considering how ideal the conditions are. The repercussions of climate change on the Spanish tourism sector will require an adaptation of the activity to the new calendars, either to create new tourism products or to take advantage of the new climate characteristics (Gómez-Martín, 2017). The studies also show that the loss of attractiveness of coastal tourist destinations can lead to changes in the flow and behaviour of tourists (Perry, 2005), generating a carry-over effect on other elements of the system.

According to the B1 scenario (CGCM2 model) developed by Flato and Boer (2001), the provinces in the south of Spain are those that would experience a greater reduction in the frequency of visits. The study by Bujosa and Rosselló (2013) finds that Málaga and Tarragona would be the provinces with the greatest loss of tourism (-5.4% and -5.1%, respectively), although other provinces with a high tourism weight, such as Almería or Barcelona would lose -3.6% and -3.1%, respectively. The greatest gains, on the other hand, would be seen in Gerona and Valencia (5.6 and 4.6%). The authors conclude that the coastal provinces that will lose most tourists are those located in the south of Spain (particularly Huelva, Cádiz, Málaga and Almería), while the coastal provinces of the north (A Coruña, Cantabria, Guipúzcoa and Girona) will experience a major increase in their probabilities to be chosen as destinations. At the same time, the impact on the eastern provinces of Spain (Murcia, Alicante, Valencia, Castellón, Tarragona and Barcelona) would be lesser but there would be a greater variability from one province to another.

Contrary to the flows and variations in tourists that will occur in the coming years, the data analysed in this study show that the Mediterranean coastal regions with a greater thermal discomfort are those in the north. This analysis reveals a clear gradient in the time trend of the CCI from the northern regions to the southernmost Mediterranean regions. From the summer decrease of -0.08 / decade of the Costa Brava to the -0.02 / decade of the Costa de la Luz.

The practice of mass sun and beach tourism cannot be understood without the conditions of sun and heat, and authors such as Besancenot (1985, 1989), Gómez-Martín (2005), Batista and Matos (2004), and De Freitas *et al.* (2008) coincide in giving greater importance to sunny and hot types of climate. Martínez Ibarra (2011) analysed the influence that thermal comfort, solar radiation, precipitation and wind speed have on the tourists who visit the beach on the east coast (Benidorm, Alicante), one with the greatest occupancy in Spain and with a lower deseasonalisation throughout the year. The results showed that the tourists most visited the beach with a wind speed of less than 8 m/s, with no rain and with thermal sensations or PET values (Physiological equivalent temperature) of between 35 and 41 (heat threshold). When a PET value of 41 (very hot) is reached or exceeded, the percentage of cases reduced considerably (25%).

According to *Hein et al.* (2009), the best conditions for practising sun and beach tourism (excellent) are found in the countries of the Europe Mediterranean Riviera, with large areas in Spain. According to the climate forecasts of the HadCM3-A1 (2051-2080) scenario, Spain would have favourable conditions on the Mediterranean coast and very good conditions on the Cantabrian coast. Excellent conditions would prevail on the French Brittany coast, the coasts of Germany and Denmark and the southern coast of the Baltic Sea. The conditions would be most favourable during the spring and autumn with good, very good and excellent categories. Finally, Jacob et al., (2018) conclude that between June and August, future negative impacts are forecast for the tourism activity in the south and east of Spain, with a potential reduction of between 2% and 8%, although this could be compensated by a probable increase in tourism on the northern coast of Spain. Furthermore, sea-level rise is a long-term, intractable problem during which costly, large-scale inundation could occur in many countries; hence, tourism development should take this matter into account because ecology and biodiversity are the fundamentals underpinning tourism performance (Yong, 2021).

5. Conclusions

The greatest CCI decreases throughout the year are recorded in the winter season (-0.11/decade) and are particularly relevant on the Costa Dorada - Azahar (0.14/decade). Here the reduction experienced by the northern part of the Costa Azahar (TA14) in the municipalities of Vinarós, Benicarló and Peñíscola during January (-0.20/decade) particularly stands out as it is the largest of the tourist areas analysed. This decrease has led to the change of cold conditions between 1941-1990 to cool-cold thresholds between 1971 and 2020 on the Atlantic coast of Galicia and Cantabria (C1 and C2). Currently, cool climate thresholds are registered in C3 and C4 (northern Mediterranean coast) and comfortable-cool on the rest of the Mediterranean coast. The number of days of cold climate thresholds has reduced considerably in recent decades, with decreases of up to 69 days on the Costa del Sol – Tropical (C8) or 63 days on the Costa Dorada – Azahar (C4). The trend of increasingly milder winters would be a very positive aspect for winter tourism, especially in Mediterranean coastal areas.

The changes experienced by the equinoctial seasons are also relevant, with reductions in the CCI of -0.06 in spring and -0.06 in autumn in the country as a whole. Particularly in the Mediterranean coastal sectors there has been a notable prolongation of the comfortable climate threshold, with an increase of up to 60 days on the Costa del Sol (C8) or 47 on the Costa Dorada – Azahar. For example, in the latter region, the comfort climate threshold has evolved from beginning in the second week of April in the time period 1941-1970 to beginning in the second week of March in that of 1991-2020. In other words, it starts one month earlier. This aspect is also tremendously positive for the tourist season outside of summer, with increasingly favourable weather conditions in the equinoctial months.

Summer is the season with the lowest decrease (-0.05), although it is statistically significant on the Cantabrian Coast – Euskal Kostaldea - C2 (-0.07), Costa Brava – El Garraf - C3 (-0.08) and Costa Cálida – Coast of Almería - C7 (-0.05). The greatest decreases (-0.09 to -0.10) are observed on the eastern part of the Costa Verde (TA4) in the municipalities of Ribadesella, Llanes or Villaviciosa). There

is a clear gradient from a greater to lesser decrease from the Costa Brava – El Garraf (C3) to the Costa de la Luz (-0.02). As latitudes decrease along the peninsula Mediterranean coast until the Andalusian Atlantic coast, the CCI reduction becomes lower. Despite this, the changes experienced by the number of days with warm and heat climate thresholds is highly relevant, with increases of up to 54 days in the Canary Islands (C10). The increase in the number of hot days in the Canary Islands should be taken into account in future summer tourism planning for the coming years. The decrease in the CCI is mainly due to the increase in the average temperature in recent decades (0.02ºC / decade) as relative humidity and the average wind speed have hardly changed.

Finally, the analysis of the heat climate threshold shows a considerable expansion in terms of is duration through the year in the different coastal regions analysed (with the exception of the two northern coastal regions (C1 and C2) and the Canary Islands (C10)). In some coastal regions such as the Costa Dorada – Azahar (C4) the period has lengthened by 42.8 days, with the beginning of the heat threshold starting 12 days earlier (from 19 to 7 July) and the end date finishing 31 days later (from 2 August to 2 September). Without a doubt, the expansion of the warmest period of the year is one of the main conclusions of the analysis carried out, which should be taken into account for the coming years, especially with the increase in extreme thermal sensations of heat in the Mediterranean and the progressive comfort summer climate on the Galician and Cantabrian coasts.

References

Moreno, A., Amelung, B., 2009. Climate Change and Tourist Comfort on Europe's Beaches in Summer: A Reassessment. *Coastal Management* 37 (6), 550-568. https://doi.org/10.1080/08920750903054997

Arabadzhyan, A., Figini, P., García Galindo, C., González Hernández, M.M., Lam-González, Y.E., León, C.J., 2020. *Climate change impact chains across the environment and the economy in coastal and marine destinations.* Universitat Politècnica de Catalunya. http://hdl.handle.net/10553/112687

Bafaluy, D., Amengual, A., Romero, R., 2014. Present and future climate resources for various types of tourism in the Bay of Palma, Spain. *Reg Environ Change* 14, 1995-2006. https://doi.org/10.1007/s10113-013-0450-6

Batista Tamayo L.M., Matos Pupo F., 2004. La aptitud climática del destino turístico Jardines del Rey (Cuba). Los tipos de tiempo. In: C. Diego Liaño, J.C. García Codrón, D.F. Rasilla Alvarez, P. Fernández de Arróyabe Hernáez, C. Garmendia Pedraja (Ed). *El clima entre el mar y la montaña. Asociación Española de Climatología*, pp. 561-570, Santander.

Besancenot J.P., 1985. Climat et tourisme estival sur les côtes de la péninsule ibérique. *Geogr Pyren Sud-Ouest* 56(4), 427–451.

Besancenot J.P., 1989. *Clima et turismes*. Masson, París

Besancenot, J.P., 1991. *Clima y Turismo*; Masson, Barcelona.

Bröde, P., Krüger, E., Rossi, F., 2011. Assessment of urban outdoor thermal comfort by the Universal Thermal Climate Index UTCI. In*: Proceedings of the 14th International Conference on Environmental Ergonomics*, Nafplio, Greece.

Bujosa, A., Rosselló, J., 2013. Climate change and summer mass tourism: the case of Spanish domestic tourism. *Climatic Change* 117, 363–375. https://doi.org/10.1007/s10584-012-0554-x

Cetin, M., Sevik, H., 2016a. Measuring the Impact of Selected Plants on Indoor CO_2 Concentrations. *Polish Journal of Environmental Studies* 25(3), 973-979. https://doi.org/10.15244/pjoes/61744

Cetin, M., Sevik, H., 2016b. Evaluating the recreation potential of Ilgaz mountain national park in Turkey. *Environmental monitoring and assessment* 188, 1-10. https://doi.org/10.1007/s10661-015-5064-7

Crossland, D.R., 2006. *Defining a forest reference condition for Kouchibouguac National Park and adjacent landscape in eastern New Brunswick using four reconstructive approaches* (Doctoral dissertation). University of New Brunswick, Faculty of Forestry and Environmental Management.

De Freitas, C.R., 2003. Tourism climatology: evaluating environmental information for decision making and business planning in the recreation and tourism sector. *Int. J. Biometeorol.* 48, 45-54. https://doi.org/10.1007/s00484-003-0177-z

De Freitas C.R., Scott D, McBoyle G., 2008. A second generation climate index for tourism (CIT): specification and verification. *Int. J. Biometeorol.* 5, 399–407. https://doi.org/doi:10.1007/s00484-007-0134-3

De Freitas, C.R. Grigorieva, E.A., 2017. A comparison and appraisal of a comprehensive range of human thermal climate indices. *Int. J. Biometeorol.* 61, 487–512. https://doi.org/10.1007/s00484-016-1228-6

Flato, G.M., Boer, G.J., 2001. Warming asymmetry in climate change simulations. *Geophysical Research Letters* 28(1), 195-198. https://doi.org/10.1029/2000GL012121

Gómez-Martín M.B., 2005. Weather, climate and tourism. A geographical perspective. *Ann. Tour. Res.* 32(3), 571–591. https://doi.org/doi:10.1016/j.annals.2004.08.004

Gómez-Martín, M.B., 2006. Climate potential and tourist demand in Catalonia (Spain) during the summer season. *Climate Research* 32(1), 75-87. https://doi.org/10.3354/cr032075

Gómez Martín, M.B., 2017. Retos del turismo español ante el cambio climático. *Investigaciones Geográficas* 67, 31-47. https://doi.org/10.14198/INGEO2017.67.02

González, O.C., 1998. *Metodología Para el Cálculo del Confort Climático en Colombia*. IDEAM-Instituto de Hidrología, Meteorología y Estudios Ambientales (Santa Fe de Bogotá, Colombia). Available online: http://documentacion.ideam.gov.co/openbiblio/bvirtual/007574/Metodologiaconfort.pdf

Hein, L., Metzger, M. J., Moreno, A., 2009. Potential impacts of climate change on tourism; a case study for Spain. *Current Opinion in Environmental Sustainability* 1(2), 170-178. https://doi.org/10.1016/j.cosust.2009.10.011

Hersbach, H., Bell, B., Berrisford, P., Hirahara, S., Horányi, A., Muñoz-Sabater, J., Nicolas, J., Peubey, C., Radu, R., Schepers, D., Simmons, A., Soci, C., Abdalla, S., Abellan, X., Balsamo, G., Bechtold, P., Biavati, G., Bidlot, J., Bonavita, M., De Chiara, G., Dahlgren, P., Dee, D., Diamantakis, M., Dragani, R., Flemming, J., Forbes, R., Fuentes, M., Geer, A., Haimberger, L., Healy, S., Hogan, R.J., Hólm, E., Janisková, M., Keeley, S., Laloyaux, P., Lopez, P., Lupu, C., Radnoti, G., de Rosnay, P., Rozum, I., Vamborg, F., Villaume, S., Jean-Noël, Thépaut, J.N., 2020. The ERA5 global reanalysis. *Quarterly Journal of the Royal Meteorological Society* 146 (730), 1999-2049. https://doi.org/10.1002/qj.3803

Instituto de Hidrología, Meteorología y Estudios Ambientales (IDEAM) (1998). *Metodología para el Cálculo del Confort Climático en Colombia. Ministerio de Medio Ambiente y Desarrollo Sostenible.* Available online: http://documentacion.ideam.gov.co/openbiblio/bvirtual/007574/Metodologiaconfort.pdf

Jacob, D., Kotova, L., Teichmann, C., Sobolowski, S. P., Vautard, R., Donnelly, C., Koutroulis, A.G., Grillakis, M.G., Tsanis, I.K., Damm, A., Sakalli, A., van Vliet. M.T.H., 2018. Climate impacts in Europe under +1.5ºC global warming. *Earth's Future* 6(2), 264-285. https://doi.org/10.1002/2017EF000710

Kendall, M.G., 1975. *Rank Correlation Methods*, 4th ed.; Charles Griffin: London, UK.

Lin, C.H., Wang, W.C., 2023. Impacts of climate change knowledge on coastal tourists´ destination decision-making and revisit intentions. *Journal of Hospitality and Tourism Management* 56, 322-335. https://doi.org/10.1016/j.jhtm.2023.07.005

Mann, H.B., 1945. Nonparametric tests against trend. *Econometrica* 13, 245–259. https://doi.org/10.2307/1907187

March, H., Saurí, D. Llurdés, J.C., 2014. Perception of the effects of climate change in winter and summer tourist areas: the Pyrenees and the Catalan and Balearic coasts, Spain. *Reg. Environ. Change* 14, 1189–1201. https://doi.org/10.1007/s10113-013-0561-0

Martínez Ibarra, E.M., 2011. The use of webcam images to determine tourist–climate aptitude: favourable weather types for sun and beach tourism on the Alicante coast (Spain). *Int. J. Biometeorol.* 55, 373-385. https://doi.org/10.1007/s00484-010-0347-8

Martínez Ibarra, E.M., 2015. Climate, water and tourism: causes and effects of droughts associated with urban development and tourism in Benidorm (Spain). *Int. J. Biometeorol.* 59, 487–501. https://doi.org/10.1007/s00484-014-0851-3

Mieczkowski, Z., 1985. The tourism climatic index: A method of evaluating world climates for tourism. *Can. Geogr*. 29, 220–233. http://doi.org/10.1111/j.1541-0064.1985.tb00365.x.

Missenard, A., 1937. Warmth and Comfort. *Journal of the Institution of Heating and Ventilating Engineers* 4, 602-606.

Nikolopoulou, M., 2004. *Designing Open Spaces in the Urban Environment: A Bioclimatic Approach*. Centre for Renewable Energy Sources, EESD, FP5: Bath, UK.

Nikolopoulou, M., Steemers, K., 2003. Thermal comfort and psychological adaptation as a guide for designing urban spaces. *Energy and Buildings* 35, 95-101. https://doi.org/10.1016/S0378-7788(02)00084-1

Nilsson, J.H., Gössling, S., 2013. Tourist responses to extreme environmental events: The case of Baltic Sea algal blooms. *Tourism Planning & Development* 10(1), 32-44. https://doi.org/10.1080/21568316.2012.723037

Olcina Cantos, J., Serrano-Notivoli, R., Miró, J., Meseguer-Ruiz, O., 2019. Tropical nights on the Spanish Mediterranean coast, 1950−2014. *Clim. Res*. 78, 225-236. https://doi.org/10.3354/cr01569

Quayle, R.G., Steadman, R.G., 1998. The Steadman wind chill: An improvement over present scale. *Weather. Forecast* 13, 1187–1193. https://doi.org/10.1175/1520-0434(1998)013<1187:TSWCAI>2.0.CO;2

Perry, A., 2005. The Mediterranean: how can the world's most popular and successful tourist destination adapt to a changing climate? In: C. M. Hall, J. Higham (Ed.). *Tourism, recreation and climate change*, pp. 86-96, Channel View Publications.

Raybould, M., Anning, D., Ware, D., Lazarow, N., 2013. *Beach and surf tourism and recreation in Australia: Vulnerability and adaptation*. Robina, QLD, Australia: Bond University.

Sen, P.K., 1968. Estimates of the regression coefficient based on Kendall's tau. *J. Am. Stat. Assoc. 63*, 1379–1389.

Steadman, R.G., 1984. A universal scale of apparent temperature. *J. Appl. Meteorol. Climatol. 23*, 1674–1687. https://doi.org/10.1175/1520-0450(1984)023<1674:AUSOAT>2.0.CO;2

Tanana, A.B., Ramos, M.B., Gil, V., Campo, A.M., 2021. Confort climático y turismo. Estudio aplicado a diferentes niveles de resolución temporal en Puerto Iguazú, Argentina. *Estudios Geográficos* 82, e064. https://doi.org/10.3989/estgeogr.202076.076

Theil, H., 1950. A Rank-Invariant Method of Linear and Polynomial Regression Analysis. *Indag. Math.* 12, 173.

Thom, E.C., 1959. The discomfort index. *Weatherwise 12*, 57–61. https://doi.org/10.1080/00431672.1959.9926960.

Yong, E.L., 2021. Understanding the economic impacts of sea level rise on tourism prosperity: Conceptualization and panel data evidence. *Advances in Climate Change Research* 12(2), 240-253. https://doi.org/10.1016/j.accre.2021.03.009

Annex

Time trend of the tourist areas (TA) analysed in the period 1940-2022. Values in bold are statistically significant (p value <0.01).

	ENE	FEB	MAR	APR	MAY	JUN	JUL	AUG	SEPT	OCT	NOV	DEC
TA1	**-0.08**	**-0.10**	**-0.11**	-0.03	**-0.09**	-0.03	0.00	-0.01	**-0.04**	-0.01	-0.03	**-0.09**
TA2	**-0.10**	**-0.13**	**-0.09**	**-0.07**	**-0.09**	**-0.05**	**-0.04**	**-0.05**	**-0.05**	**-0.07**	**-0.07**	**-0.14**
TA3	**-0.10**	**-0.09**	**-0.05**	**-0.05**	**-0.06**	**-0.05**	**-0.05**	**-0.06**	**-0.05**	**-0.09**	**-0.05**	**-0.12**
TA4	**-0.14**	**-0.13**	**-0.10**	**-0.11**	**-0.10**	-0.09	**-0.09**	**-0.10**	**-0.09**	**-0.12**	**-0.08**	**-0.17**
TA5	**-0.12**	**-0.11**	**-0.06**	**-0.08**	**-0.07**	**-0.06**	**-0.06**	**-0.08**	**-0.05**	**-0.11**	**-0.06**	**-0.16**
TA6	**-0.12**	**-0.11**	**-0.07**	**-0.08**	**-0.08**	**-0.07**	**-0.06**	**-0.09**	**-0.06**	**-0.11**	**-0.06**	**-0.16**
TA7	**-0.08**	**-0.05**	-0.03	-0.05	-0.05	-0.05	**-0.05**	**-0.07**	**-0.05**	**-0.09**	-0.03	**-0.11**
TA8	**-0.11**	**-0.10**	**-0.06**	-0.07	-0.07	**-0.07**	**-0.06**	**-0.08**	-0.05	**-0.09**	-0.05	**-0.14**
TA9	**-0.09**	**-0.06**	**-0.06**	**-0.03**	-0.05	-0.06	-0.06	-0.06	**-0.05**	**-0.05**	-0.03	**-0.09**
TA10	**-0.10**	**-0.10**	**-0.08**	**-0.05**	-0.08	-0.08	-0.07	**-0.08**	**-0.05**	**-0.07**	**-0.06**	**-0.10**
TA11	**-0.12**	**-0.13**	**-0.12**	**-0.07**	**-0.09**	-0.09	-0.07	**-0.09**	-0.05	**-0.09**	**-0.08**	**-0.12**
TA12	**-0.11**	**-0.10**	**-0.10**	**-0.07**	-0.08	**-0.09**	**-0.07**	**-0.08**	**-0.05**	**-0.06**	**-0.07**	**-0.10**
TA13	**-0.15**	**-0.14**	**-0.15**	**-0.08**	**-0.09**	**-0.09**	-0.05	**-0.08**	**-0.06**	**-0.11**	**-0.08**	**-0.13**
TA14	**-0.20**	**-0.16**	**-0.17**	**-0.08**	**-0.09**	**-0.09**	**-0.05**	**-0.08**	**-0.08**	**-0.12**	**-0.10**	**-0.14**
TA15	**-0.15**	**-0.14**	**-0.14**	**-0.09**	**-0.09**	**-0.09**	**-0.05**	**-0.09**	**-0.07**	**-0.12**	**-0.12**	**-0.12**
TA16	**-0.17**	**-0.15**	**-0.11**	**-0.08**	-0.06	-0.06	-0.04	-0.05	**-0.05**	**-0.12**	**-0.12**	**-0.14**
TA17	**-0.12**	**-0.09**	**-0.07**	-0.03	-0.06	-0.07	**-0.07**	**-0.07**	**-0.07**	**-0.09**	**-0.05**	**-0.10**
TA18	**-0.10**	**-0.07**	**-0.06**	**-0.04**	-0.06	**-0.08**	**-0.07**	**-0.07**	**-0.05**	**-0.08**	-0.04	**-0.08**
TA19	**-0.11**	**-0.10**	**-0.07**	**-0.06**	-0.05	-0.06	-0.05	-0.06	**-0.04**	**-0.10**	**-0.06**	**-0.11**
TA20	**-0.06**	**-0.05**	-0.02	**-0.03**	-0.05	**-0.07**	**-0.07**	**-0.06**	-0.04	**-0.06**	-0.01	**-0.07**
TA21	**-0.10**	**-0.07**	-0.05	-0.04	-0.04	-0.06	**-0.06**	**-0.06**	**-0.05**	**-0.07**	**-0.06**	**-0.08**
TA22	**-0.16**	**-0.12**	**-0.09**	**-0.06**	-0.05	-0.07	-0.04	-0.06	**-0.05**	**-0.12**	**-0.09**	**-0.13**
TA23	**-0.17**	**-0.11**	-0.06	**-0.06**	-0.05	-0.07	**-0.06**	**-0.07**	**-0.07**	**-0.12**	**-0.10**	**-0.12**
TA24	**-0.13**	**-0.08**	-0.04	-0.04	-0.05	**-0.06**	**-0.06**	**-0.07**	**-0.06**	**-0.08**	**-0.09**	**-0.09**
TA25	**-0.12**	**-0.08**	-0.06	-0.05	**-0.06**	-0.06	**-0.05**	**-0.06**	**-0.05**	**-0.09**	**-0.10**	**-0.10**
TA26	**-0.09**	**-0.09**	**-0.06**	-0.03	**-0.08**	-0.06	**-0.04**	**-0.06**	**-0.05**	**-0.09**	**-0.08**	**-0.09**
TA27	**-0.11**	**-0.11**	**-0.07**	-0.04	**-0.08**	-0.07	-0.04	-0.05	**-0.04**	**-0.09**	**-0.08**	**-0.10**
TA28	**-0.09**	**-0.08**	**-0.08**	-0.04	**-0.08**	-0.06	-0.02	-0.05	-0.02	**-0.08**	**-0.05**	**-0.08**
TA29	**-0.10**	**-0.07**	**-0.09**	**-0.04**	-0.06	-0.05	-0.01	-0.03	-0.02	**-0.07**	**-0.07**	**-0.09**
TA30	**-0.09**	**-0.06**	**-0.08**	-0.02	-0.06	-0.05	-0.01	-0.03	-0.02	**-0.07**	**-0.05**	**-0.08**
TA31	**-0.09**	**-0.05**	**-0.08**	-0.02	**-0.07**	-0.05	-0.01	**-0.04**	**-0.03**	**-0.06**	**-0.06**	**-0.08**
TA32	**-0.08**	**-0.08**	**-0.11**	-0.02	**-0.08**	-0.03	-0.02	-0.02	-0.03	**-0.07**	**-0.05**	**-0.07**
TA33	**-0.10**	**-0.07**	-0.05	-0.04	-0.04	-0.06	**-0.06**	**-0.06**	**-0.05**	**-0.07**	**-0.06**	**-0.08**
TA34	**-0.04**	-0.02	0.00	**-0.04**	**-0.05**	**-0.04**	-0.02	**-0.03**	**-0.06**	**-0.04**	**-0.05**	**-0.05**
TA35	**-0.08**	-0.04	-0.03	-0.01	**-0.04**	-0.04	-0.01	-0.02	-0.01	-0.06	**-0.07**	**-0.06**
TA36	**-0.04**	0.00	0.01	0.01	-0.01	-0.02	**-0.03**	**-0.04**	-0.01	-0.01	-0.02	-0.03
TA37	-0.03	-0.01	0.01	**-0.03**	-0.02	**-0.04**	**-0.02**	**-0.03**	**-0.05**	**-0.04**	**-0.03**	**-0.04**

Cuadernos de Investigación Geográfica *Geographical Research Letters*	2024	Nº 50 (2)	pp. 69-91	EISSN 1697-9540

http://doi.org/10.18172/cig.6023

HOW DOES CLIMATIC VARIABILITY AFFECT THE HIGHLAND LAGOONS OF THE VENEZUELAN ANDES?

JOEL MEJÍA BARAZARTE[1], JOSÉ GONZÁLEZ RAMÍREZ[2], ANDERSON ALBARRÁN TORRES [3]

[1] *Instituto de Geografía y Conservación de Recursos Naturales, Universidad de Los Andes, 5101 Mérida, Venezuela / Department of Integrative Environmental Geography, University of Hamburg, D-20146, Hamburg, Germany..*

[2]*Geógrafo.*

[3]*Escuela de Geografía, Universidad de Los Andes, 5101 Mérida, Venezuela.*

ABSTRACT. The influence of climate variability in the highland headwater lagoons of the Miguaguó watershed - Venezuela was evaluated from an initially defined time series of 46 years, climatologically classified by the Oceanic Niño Index (ONI). 18 climatologically different sample years were selected with the availability of Landsat imagery to evaluate the degree of surface water extent fluctuation using the Normalized Water Index (NDWI). The NDWI values were then statistically compared with the ONI and with local climate parameters, and the percentage deviations of the anomalies from the averaged neutral years were estimated. The results showed that the surface water extent of the lagoons is affected by the combination of ENSO, anti-ENSO anomalies and neutral years, although the effect is different depending on the location of the lagoons in the landscape, biophysical conditions and the intensity of the anomalies. Mapire, La Burra and Masiegal lagoons showed "severe" impact, with deviations from the surface water extent in neutral years ranging from 20 to 70%. On the other hand, the impact on the Miguaguo lagoon was mostly "slight", with deviations ranging from 0 to 10%. Positive deviations derived from anti-ENSO events and neutral conditions were generally dominant, except for La Burra lagoon, where the opposite trend was observed. Although the results were clear and conclusive, they have a limited spatial and temporal scope due to the complexity of the processes involved. Therefore, additional research is needed to complete the understanding of the climatic and atmospheric relationships in the processes governing the highlands of the tropics.

¿Cómo afecta la variabilidad climática a las lagunas altoandinas de los Andes venezolanos?

RESUMEN. Se evaluó la influencia de la variabilidad climática en las lagunas altoandinas de la microcuenca Miguaguó – Venezuela, para lo cual se definió una serie de tiempo inicial de 46 años, que fue climatológicamente tipificada a partir del Índice del Niño Oceánico (ONI). Se seleccionaron 18 años muestrales climatológicamente distintos con disponibilidad de imágenes Landsat, para evaluar el grado de fluctuación del espejo de agua de las lagunas a través del Índice Diferencial de Agua Normalizado (NDWI). Los valores de NDWI fueron estadísticamente comparados con el ONI y con indicadores climáticos locales, y se estimaron las desviaciones porcentuales de las anomalías respecto al promedio de los años neutrales. Los resultados mostraron que la extensión superficial del espejo de agua de las lagunas está influenciada por la combinación de anomalías ENOS, anti-ENOS y años neutrales, aunque la afectación es diferencial, dependiendo de la localización de las lagunas en el paisaje, de las condiciones biofísicas del entorno y de la intensidad de las anomalías. Las lagunas: Mapire, La Burra y Masiegal mostraron un impacto "severo", con desviaciones en la extensión del espejo de agua que oscilaron entre el 20 y el 70% respecto a los años neutrales. Por otro lado, el impacto en la laguna de Miguaguo fue mayoritariamente "leve", con desviaciones que oscilaron entre el 0 y el 10%. Las desviaciones positivas

derivadas de eventos anti-ENOS y condiciones neutrales fueron en general dominantes, excepto en la laguna de La Burra, donde se observó la tendencia opuesta. Se concluye que, si bien los resultados fueron claros y contundentes, tienen un alcance espacial y temporal limitado, y los procesos estudiados son extremadamente complejos, por lo que se requieren investigaciones adicionales que complementen la comprensión objetiva de las relaciones climáticas y atmosféricas en los procesos hídricos de la alta montaña tropical.

Keywords: Andean lagoons, climate variability, ENSO and anti-ENSO, Normalized Difference Water Index (NDWI), headwaters watershed.

Palabras clave: lagunas andinas, variabilidad climática, ENOS y anti-ENOS, Índice Diferencial de Agua Normalizado (NDWI), cuenca de cabecera.

Received: 2 April 2024

Accepted: 9 December 2024

***Corresponding author:** Joel Francisco Mejía Barazarte, Institut für Geographie, Universität Hamburg. Bundestrasse 55, D-20146, Hamburg. E-mail: jmejia@ula.ve; joel.francisco.mejia.barazarte@uni-hamburg.de

1. Introduction

The Andean highland wetlands are a specific type of ecosystem located above 3000 m.a.s.l. along the Andes in the bioregions of Páramo, Jalca and Puna Plateau; they form a diversity of aquatic and semi-aquatic environments that have been classified by the International Convention on RAMSAR Wetlands (2005) into the following categories: Andean high lagoons, swamps, marshes, peatlands, marshlands and wet grasses or meadows.

Both the topography and morphology of the Andean highlands above this altitude are largely dominated by the inherited glacial landforms (Franco *et al.,* 2013), creating the conditions for the formation of commonly interconnected aquatic ecosystems, usually forming a wetland complex (Ortiz, 2016) (Quintero, 2019); this complex represents the headwaters of the Andean River systems. According to Hofstede *et al.* (2014), highland ecosystems are the leading suppliers of freshwater in the northern Andes due to their capacity to regulate water, which is due to glacial and periglacial geomorphology that facilitates the accumulation of flow, the high regulatory capability of the páramo as an ecosystem, the particular soil conditions of the highlands, and favourable climatic regimes (abundant rainfall, high relative humidity, and low evapotranspiration rates).

Water regulation is the leading ecosystem service that provides value to high Andean wetlands and plays an essential role in the fluvial dynamics of river basins (Franco *et al.,* 2013; Valencia and Figueroa, 2015; Ortiz, 2016; Quesada-Román and Mora-Vega, 2017; Cáceres, 2019; Quintero, 2019; Lopez-Moreno *et al.*, 2022). Its functionality goes even further, providing humans with other environmental services that have direct and indirect use value: habitat for endemic flora and fauna, carbon storage, source of fresh water for consumption, and local traditional productive activities, mainly agriculture and livestock (Hernández, 2005). Similarly, wetlands provide other environmental services such as fisheries, aquaculture, wood production, fodder, and energy resources such as peat, as well as opportunities for tourism and recreation (Stolk *et al.,* 2006; Franco *et al.,* 2013; Valencia and Figueroa, 2015; Uribe *et al.,* 2017; Quintero, 2019).

There is no doubt about the biophysical, economic and cultural value of the high Andean wetlands to local and regional populations. Paradoxically, some anthropogenic activities have caused changes in the structure and functionality of the wetlands, increasing their vulnerability to climate

variability and change, two processes that can produce various positive and negative effects and feedbacks at different scales in the Earth system.

According to Quesada-Román and Mora-Vega (2017), wetlands tend to have low ecological resilience to anthropogenic actions such as drainage, agricultural expansion, or changes in land use/land cover in their surroundings, which can lead to drastic changes in the ecosystem given the complex and intricate level of hydrological connectivity already aforementioned. In fact, Andean highland wetlands have been identified by the International Convention on RAMSAR Wetlands (2005) as fragile ecosystems, vulnerable to modification by external factors such as climate change and landscape alteration due to land use/land cover change, with negative impact on the intrinsic environmental status. They are among the most threatened ecosystems worldwide in the last 50 years (Betancur-Vargas *et al.,* 2017).

Andean highland ecosystems are highly vulnerable to climate change, especially climate variability, as argued by various authors (Franco *et al.,* 2013; De la Torre, 2014; Valencia and Figueroa, 2015; Cáceres, 2019). Wetlands are particularly sensitive to climate-induced hydrological changes: changes in precipitation significantly affect soil moisture, affecting vegetation growth and health, while increasing temperatures accelerate evaporation and ETP, affecting biodiversity and altering oxygen levels in water (Hangnan *et al.,* 2018).

The main source of climate variability in the northern Andes is the El Niño-Southern Oscillation (ENSO) phenomenon, which is characterized by the occurrence of warm (El Niño) and cold (La Niña, also referred to as anti-ENSO (Holden, 2017) phases. Both anomalies affect the temporal and spatial distribution of precipitation in South America and are the cause of extreme droughts and heavy rainfall in different geographical regions of the planet. In the northern Andes, El Niño events are associated with below-normal precipitation, while the opposite occurs during La Niña events (Herzog *et al.,* 2010).

However, the processes that dynamize the changes that occur in wetlands are usually complex, highly dynamic, stochastic, following a nonlinear path. This makes it difficult to set predictions about the transitions that can occur in wetlands after the occurrence of disturbances (Alibakhshi *et al.,* 2017). Quintero (2019) considers it very difficult to delineate the real influence of climate change in the Andean region, because it is accelerated by different anthropogenic activities, so it is difficult to separate the real influence of both processes.

The incidence of climate in any biophysical environment is limited to demonstrate and difficult to verify because it requires observations of high frequency and spatial density on the variables involved, as well as field data with high spatial and temporal resolution (Alibakhshi *et al.,* 2017). In the Andes, the scarcity of observations and monitoring add uncertainty when assessing the impact of land use change and climate change on ecosystem condition and health (Hofstede *et al.,* 2014; Uribe *et al.,* 2017).

In this sense, remote sensing has gained relevance and usefulness in recent years as a viable long-term spatial and temporal alternative for deriving indicators that allow the detection and monitoring of the status or condition of hydro-ecosystems, allowing the analysis of remote areas (Adam *et al.,* 2010; Middleton and Souter, 2016; Dos Santos *et al.,* 2019). As vegetation stress is a primary indicator of the degree of alteration of a wetland, it can be easily estimated and monitored with a reasonable degree of accuracy through the derivation and interpretation of vegetation indices, which are dimensionless radiometric metrics that serve as indicators of the relative abundance and activity of green vegetation and moisture condition (Dos Santos *et al.,* 2019). Indices such as the Normalized Difference Water Index (NDWI) allow for efficient indirect estimation of soil and vegetation moisture available and open water features.

Such methods are potentially relevant in our region. De la Torre (2012) claimed for rigorous scientific research on the issue of water resources and climate change in south American mountain ecosystems, as a basis for making relevant decisions in land planning and management. To date, research has been carried out in the local context, analysing the impact or occurrence of climate change in high Andean ecosystems and wetlands: Colombia (Franco *et al.,* 2013; Valencia and Figueroa, 2015; Ortiz,

2016; Cáceres, 2019; and Quintero, 2019); Ecuador (Guerra, 2018); Chile (Uribe *et al.,* 2017); and in Venezuela (Moncada *et al.,* 2010; Paredes *et al.,* 2020). Research on the effects of climate variability on wetland integrity and behaviour is more recent, with few examples to date: Mexico (Castro, 2019), Costa Rica (Quesada-Román and Mora-Vega, 2017; Esquivel, 2018), Colombia (Pinilla *et al.,* 2012), Ecuador (Ramírez and Vallejo, 2018), Chile (Meza and Diaz, 2014), and Venezuela (González, 2018). However, research evaluating the effects of climate variability in the headwater systems in which the wetlands are located is remarkable scarce, and the existing experiences like: Vergara *et al.* (2010), Mejía (2012), González-Zeas *et al.* (2019) and Escanilla-Minchel *et al.* (2020), were developed on the basis of GCM (Global Circulation Models) and IPCC scenarios. Only Mejía *et al.* (2022) and Carilla *et al.* (2023) have directly included the effect of the ENSO and A-ENSO events in the hydro ecological conditions of the highlands in Venezuela and Chile, respectively. Certainly, even more research in this topic is needed.

The relevance of this issue deserves greater attention, more research and monitoring processes on the incidence of climate change and climate variability in the increasing vulnerability of high Andean ecosystems, which facilitates the design of effective strategies to guarantee its conservation.

In this context, the main goal of this paper was to analyse the occurrence of climate variability through the combination of ENSO and anti-ENSO anomalies in the degree of surface water extent fluctuation of high Andean lagoons in a watershed of the Venezuelan Andes, through the interpretation of a moisture available index derived from Landsat images, calibrated with a reliable indicator of ENSO anomalies. The results provide a first approach to the problem in the local context, which will serve as a basis for further research about this topic.

2. Methods

2.1. The study Area

A headwater watershed located in the central section of the Cordillera de Mérida was selected as a case of study. The Miguaguó watershed is located northeast of Mérida state, between the coordinates: 8º42'20.59”- 8º42'20.90” N, and 70º52'41.33”- 70º53'44.80” W. It has a surface area of 375.07 ha, with a length of 3.5 km and an average width between 0.9 and 1.5 km (Fig. 1). The watershed is located in the high Andean Mountain range, whose altitude gradient ranges from 3460 to 4060 m.a.s.l. The relief is mountainous and dissected, with a morphology dominated by periglacial and fluvioglacial dynamics during the Quaternary; therefore, periglacial landforms are the most important, representing about 90% of the surface area; this is evidenced by forms such as glacial cirques, glacial steps, muddy rocks, lateral and terminal moraines, and large rock outcrops (González, 2018).

The lithology is largely dominated by Sierra Nevada Association (Iglesias Group) materials, mainly: schists, gneisses, and highly metamorphosed feldspathic quartz (Sandoval, 2015). The gradient is highly variable (from 0% to more than 60%), with a spatial predominance of the 30-60% range in 41.2% of the area (Fig. 1).

The area is characterized by a predominantly high-mountain humid climate, with an average annual rainfall of 1170 mm and average annual temperatures ranging from 9°C in the lower part to 2°C in the upper part (Córdoba, 2014). Solar radiation is intense (1200 w m^{-2}), especially during the dry season; consequently, the contrasts between minimum night temperatures and maximum day temperatures are quite marked.

The lagoons in the Miguaguó headwaters watershed form an interconnected wetland system that is the hydrological structural source for the Miguaguó stream. Figure 2 shows an individual view of each lagoon in its local environment. La Burra Lagoon (Fig. 2a) is located in the upper part or head of the watershed, being the source and starting point of the drainage network (Fig. 1). Masiegal and Miguaguó are intra network lagoons (Fig. 2b and 2c) located in the middle sector of the watershed, completely connected by the main vector of the Miguaguó stream. On the other hand, Mapire Lagoon

(Fig. 2d) is a semi-independent entity located at the beginning of a secondary drainage in the middle part of the watershed that, after a short distance, joins the main stream vector (Fig. 1).

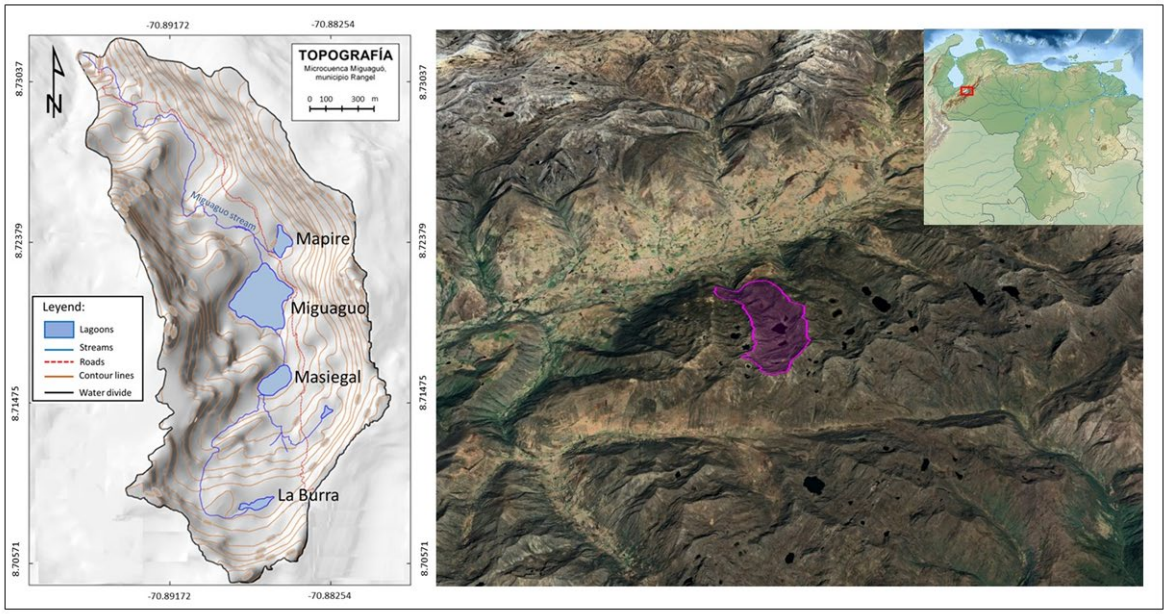

Figure 1. Location of the Miguaguo watershed. (Image: Landsat 8- Copernicus, Google Earth Pro).

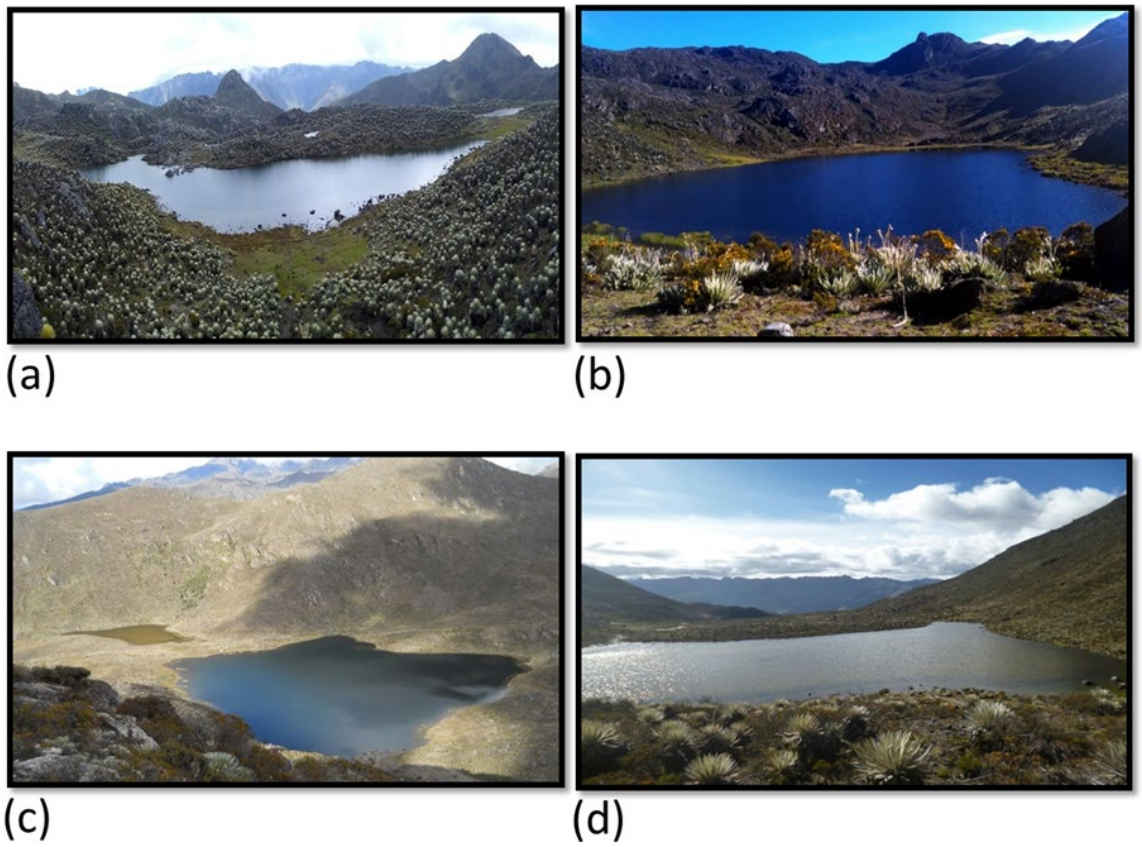

Figure 2. Watershed Lagoons: (a) La Burra; (b) Masiegal; (c) Miguaguó; (d) Mapire. (Pics. taken by Gonzalez, 2021)

2.2. Data Acquisition

The base map layer was created from a 1:25000 analog topographic map produced by Cartografía Nacional (1974), which had been previously digitized. It was rasterized using GIS software and the watershed was then delineated. The topological information was updated using aerial photographs corresponding to the flight mission 10408 (1989).

Climate data (precipitation and temperature) were collected from six rain gauges and climatic stations adjacent to the watershed, summarized in Table 1. The raw data were obtained from the Ministry of Environment and Water (MINEA) and the Institute of Agricultural Research (INIA). Since INIA-Mucuchíes has the longest and most complete historical record, it was selected as the reference station.

The data had to be preprocessed to estimate surrogate daily and monthly data (pseudo data), data distortion, and correction of anomalous records using the normal ratio and linear regression methods (Kashani and Dinpashoh, 2012; Guevara, 2013). Once the time series was completed, a common time series was defined for the comparative analysis: 1971 - 2022, considering the historical record of aerial photographs and satellite images available.

Table 1. Rain gauges and climatic stations used in the research.

Gauging station	Gauging number	Type	Coordinates		Elevation (m a.s.l.)	Distance to the watershed (km)	Serie lenght
			Latitude	Longitude			
INIA-Mucuchíes	7901	C1	084600	705400	3100	4	1971-2015
Mucubají	3072	PR	084810	704922	3560	11	1971-2003
Mucurubá	3029	C3	084222	705933	2320	12	1971-1983
Los Plantíos	3161	PR	084911	704705	3878	15	1971-2003
Páramo Pico El Águila	3112	PR	085100	704937	4126	15	1971-1998
Páramo Mucuchíes	3111	PR	085105	705019	3685	14	1971-1993

2.3. Climatological classification of the data series according to Oceanic Niño Index - ONI

The climatological classification of the years was done based on the criteria of climate variability, due to the remarkable influence of ENSO and anti-ENSO events on the convective processes and climate dynamics of Venezuela (Pulwarty *et al.,* 1998); (Andressen *et al.,* 2000). One of the most commonly used indicators for monitoring ENSO and anti-ENSO anomalies is the Oceanic Niño Index – ONI, which is defined as the three-month moving average of the sea surface temperature anomalies that occur in the Niño 3.4 region (Bedoya *et al.,* 2010). Therefore, a review of the historical behaviour of the ONI on the National Oceanic and Atmospheric Administration (NOAA) website was made to identify the years affected by the ENSO phenomenon, anti-ENSO years, and neutral or no event years. Using this index, it was possible to define the occurrence of ENSO from a 0.5 °C anomaly in surface sea temperature (SST) with respect to the historical average according to NOAA, with a positive sign indicating the occurrence of the warm phase (El Niño) and a negative sign indicating the occurrence of the cold phase (La Niña). Those years with anomalies between 0 and 0.4 °C, both negative and positive, were considered as no event or neutral years in this study.

Using this index, it was also possible to classify the anomalies according to the intensity of their occurrence: weak (between 0.5 and 0.9 °C); moderate (between 1 and 1.4 °C); strong (between 1.5 and 2°C) and very strong (greater than 2 °C), as shown in Table 2. In this sense, all the years corresponding to the selected historical series were climatologically classified.

Once the years were classified, a compilation of Landsat satellite images was performed to observe the spectral behavior of the wetlands in the study area during the historical period. Landsat images were chosen because of their higher temporal resolution compared to others, and also because of their high accessibility and availability. These images are widely used in multi-temporal studies related to vegetation and water due to their radiometric and spatial precision characteristics (Lunneta and Balogh, 1999).

Table 2. Historical ONI anomalies in the Niño 3.4 region, that occurred between August and March, during the selected historical series.

A-ENSO			ENSO			NO EVENT		
Period	ONI(°C)	Level	Period	ONI(°C)	Level	Period	ONI(°C)	Level
1971-1972	-0.8	Weak	1972-1973	1.8	Strong	1978-1979	-0.1	Neutral
1973-1974	-1.7	Strong	1976-1977	0.7	Weak	1980-1981	-0.1	
1974-1975	-0.6	Weak	1977-1978	0.7	Weak	1981-1982	-0.1	
1975-1976	-1.4	Moderate	1979-1980	0.5	Weak	1985-1986	-0.4	
1983-1984	-0.7	Weak	1982-1983	2.0	Very strong	1989-1990	-0.1	
1984-1985	-0.8	Weak	1986-1987	1.1	Moderate	1990-1991	0.4	
1988-1989	-1.6	Strong	1987-1988	1.1	Moderate	1992-1993	0.1	
1995-1996	-0.9	Weak	1991-1992	1.2	Moderate	1993-1994	0.1	
1998-1999	-1.4	Moderate	1994-1995	0.9	Weak	1996-1997	-0.4	
1999-2000	-1.5	Strong	1997-1998	2.2	Very strong	2001-2002	-0.2	
2000-2001	-0.6	Weak	2002-2003	1.0	Moderate	2003-2004	0.4	
2005-2006	-0.6	Weak	2004-2005	0.7	Weak	2012-2013	-0.1	
2007-2008	-1.4	Moderate	2006-2007	0.7	Weak	2013-2014	-0.3	
2008-2009	-0.6	Weak	2009-2010	1.2	Moderate			
2010-2011	-1.5	Strong	2014-2015	0.5	Weak			
2011-2012	-0.9	Weak	2015-2016	2.4	Very strong			
2016-2017	-0.5	Weak	2018-2019	0.68	Weak			
2017-2018	-0.79	Weak						
2019-2020	0.20	Neutral						
2020-2021	-0.91	Weak						
2021-2022	-0.89	Weak						

Source: web: http://www.cpc.ncep.noaa.gov/products/analysis_monitoring/ensostuff/ensoyears.shtml del National Climate Prediction Center-NOAA.

Images were extracted from the EarthExplorer server of the United States Geological Survey (USGS) being selected according to the following criteria: (1) homogeneous spatial resolution with bands corresponding to the visible, near-infrared, and mid-infrared spectral ranges to ensure comparability; (2) date of scene acquisition corresponding to the dry season in Venezuela (December-March), a period when the wetlands could be more affected climatologically and hydrologically; and (3) minimal cloud cover in the useful area of interpretation. From a total of 50 initially preselected Landsat scenes, 18 images identified in Table 3 were finally selected for analysis. These images correspond to climatologically different years, hereafter referred to as "sample years".

Table 3. Images selected to monitor the dry period for the sample years.

Satélite / Sensor	Scene identifier	Date	Event	Level of intensity
LANDSAT 5 TM	LT50060541985051AAA06	20/02/1985	A-ENSO	Weak
LANDSAT 5TM	LT50060541986054XXX03	23/02/1986	S/E	Neutral
LANDSAT 4 TM	LT40060541988084XXX01	24/02/1988	ENSO	Moderate
Aerial Photo	M-10408	04/02/1989	A-ENSO	Strong
LANDSAT 5 TM	LT50060541991036AAA02	05/02/1991	S/E	Neutral
LANDSAT 5 TM	LT50060541998055CPE00	24/02/1998	ENSO	Very strong
LANDSAT 5 TM	LT50060541999090CPE01	31/03/1999	A-ENSO	Moderate
LANDSAT 7 ETM+	LE70060542000037AGS01	06/02/2000	A-ENSO	Strong
LANDSAT 7 ETM+	LE70060542001055EDC01	24/02/2001	A-ENSO	Weak
LANDSAT 7 ETM+	LE70060542003045AGS00	14/02/2003	ENSO	Moderate
LANDSAT 5 TM	LT50060542011091CHM00	01/04/2011	A-ENSO	Strong
LANDSAT 8 OLI	LC80060542014051LGN00	20/02/2014	S/E	Neutral
LANDSAT 8 OLI	LC80060542015054LGN00	23/02/2015	ENSO	Weak
LANDSAT 8 OLI	LC80060542016041LGN00	10/02/2016	ENSO	Very strong
LANDSAT 8 OLI	LC80060542017075LGN00	16/03/2017	A-ENSO	Weak
LANDSAT 8 OLI	LC80060542019033LGN00	02/02/2019	ENSO	Weak
LANDSAT 8 OLI	LC80060542020132LGN00	05/05/2020	S/E	Neutral
LANDSAT 8 OLI	LC80060542021134LGN00	14/05/2021	A-ENSO	Weak
LANDSAT 8 OLI	LC80060542022025LGN00	25/01/2022	A-ENSO	Weak

Source: EarthExplorer website (https://earthexplorer.usgs.gov/). Colors: ENSO (red), A-ENSO (blue), Neutral (green).

The images had to be preprocessed to make radiometric and atmospheric adjustments using the semi-automatic classification plug-in (SCP) method and geometrically using both the nearest neighbor and root mean square (RMS) methods (Olaya, 2016).

2.4. Image processing and NDWI estimation

The wetlands were identified and delineated from the interpretation of the Landsat 8 OLI image of February 20, 2014, with RGB combination to false color 542 (Fig. 3a), combining the mid-infrared, near-infrared, and green bands to identify the lagoons with sufficient accuracy. Since Landsat imagery have a middle resolution, the delineation process was calibrated using an aerial photograph of the area (flight mission 10408, 1989) to achieve greater accuracy (Fig. 3b). In post-processing, the results of the interpretation were verified and validated *in situ*. Eight (8) wetlands were identified: (4) swamps and (4) high Andean lagoons located in the valley bottom of the watershed.

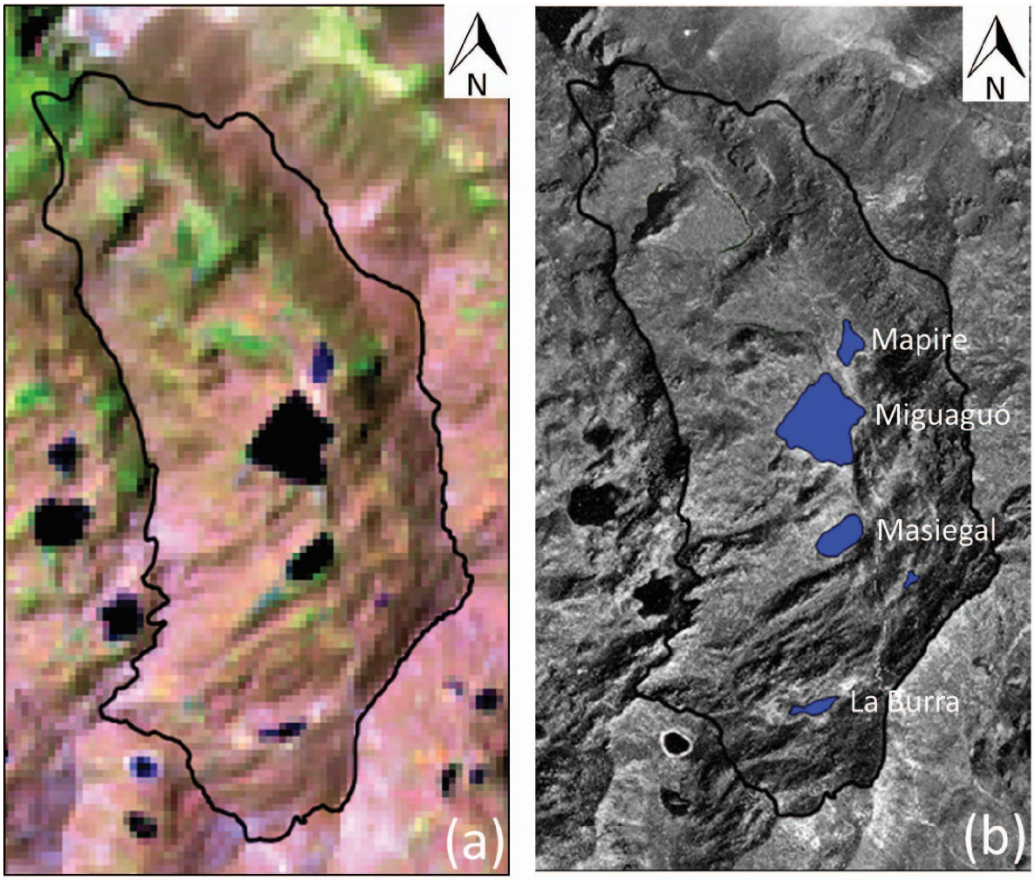

Figure 3. Identification of highland Andean lagoons in the Miguaguó watershed: (a): LANDSAT image in false color (542) of 02/20/2014, (b): lagoons delineated from aerial photo (Flight Mission 10408, 1989).

We considered the Normalized Difference Water Index (NDWI) as an indicator to evaluate perimetral water level fluctuation for the lagoons during the sample years. The degree of water extent fluctuation is considered one of the core indicators in the assessment of wetlands conditions (Fennessy *et al.,* 2004). The NDWI was developed to delineate open water features and enhance their presence in remotely sensed digital imagery. The index uses reflected near-infrared radiation and visible green light to enhance the presence of such features while eliminating the presence of soil and terrestrial vegetation features (McFeeters, 1996). For a good performance in its use, a validation process of the thresholds used to delineate water table is always required. NDWI has been widely used to identify wetlands and

water bodies, and also to delineate the surface characteristics of water (Ji *et al.,* 2009) and glaciers (López-Moreno *et al.,* 2020, 2022). It is derived from the difference between the green and near-infrared bands divided by the sum of these bands by equation (1):

$$NDWI = \frac{(\rho_{GREEN} - \rho_{NIR})}{(\rho_{GREEN} + \rho_{NIR})} \quad [1]$$

where:

ρ_{GREEN} y ρ_{NIR} correspond to the visible (green) and near-infrared reflectivity, respectively, of each NDWI image in the historical series.

NDWI values range from -1 to 1, with zero being the threshold. The cover category is water if NDWI >0 and non-water if NDWI ≤ 0.

To compare the water level oscillation for each lagoon, a vector layer was used to delineate the reference area (using aerial photographs from 1989) to identify the pixels that the NDWI counts as "WATER", and thus observe the changes in the water surface area of the lagoons from one year to another. The NDWI was derived in each selected image and the metrics and zonal statistics corresponding to the spectral index were estimated.

2.5. Statistical relationship between NDWI and ONI index

Since the SST anomalies indicate the occurrence of the ENSO phenomenon through the ONI index, the Pearson linear correlation coefficient between these anomalies and the NDWI indices was calculated for each sample year. The average NDWI values extracted from the vector polygons of the four lagoons were used to study the relationship between the oscillation of the wetlands and the possible influence of the ENSO phenomenon in the hydroperiod.

From the average NDWI values, the change or anomaly in the state of the lagoons was calculated by comparing the water surface extent in a sample year with the averaged neutral years, using equation (2):

$$\Delta NDWI\ (\%) = \left(\left(\frac{NDWI_{year\ n}}{NDWI_{referencial}}\right) * 100\right) - 100 \quad [2]$$

Where:

ΔNDWI (%): anomalies in percentage values

Reference NDWI: value corresponding to the NDWI for the averaged neutral years

NDWI year n: NDWI value for year n

According to Jiménez (2010), the percentage of variation (ΔNDWI) expresses the degree of anomaly (impact or recovery) experienced by each of the lagoons (water surface extent) quantified with respect to a reference value, and the variations are categorized as follows:

- Recovery or improvement: the value has increased compared to the averaged neutral years.
- Slight impact: the anomaly is greater than 0 and less than 10%.
- Moderate impact: the anomaly is between 10-20%.
- Severe impact: the anomaly is greater than 20%.

Thus, positive anomalies indicate an excess of rainfall resulting in a very humid rainy season, while negative anomalies indicate a deficit or low rainfall regimes with a dry season longer or more intense than usual. The purpose of calculating these anomalies was to observe the behavioral deviation of the hydroperiod respect to the neutral years, which can indicate the level of elasticity and resilience of the lentic systems due the influence of the inter annual Pacific Oscillation.

The statistical relationship between the fluctuations of the lagoons and the influence of ENSO and anti-ENSO was also evaluated by the Pearson linear correlation coefficient, comparing the average values of the NDWI of each lentic system with the values of the sea surface temperature anomalies in the Niño region 3.4.

2.6. Relationship between NDWI and local climatology

Considering the spatial dynamics of the occurrence of ENSO anomalies and the notable scarcity of climatic data recorded in the region, the degree of influence or correspondence between the surface water extent fluctuation of the lagoons and the local climatology was analyzed by comparing the normalized NDWI values observed in the sample years with the historical precipitation recorded at the INIA-Mucuchíes station (the reference station). In this case, the accumulated precipitation during the period between August - March of each year (the second half period of the rainy season plus the dry season) recorded in the reference station (1971-2015) was considered, because this period showed the best statistical performance between the surface water extent area of the lagoons and the rainfall regime.

3. Results

3.1. Chronological relationship of ENSO/anti-ENSO episodes during the time series and sample years

During the period initially considered, the temporal relationship between ENSO and anti-ENSO anomalies was heterogeneous, showing variable sequences between them according to their own episodic dynamics (Fig. 4a). In this sequential dynamic, the frequency of anti-ENSO episodes (21) was slightly higher than ENSO episodes (17), while the number of years classified as no event occurrence or neutral was lower (13). Regarding the intensity of the anomalies, a relative dominance of “weak” and “moderate” intensity events was observed, while the episodes of "strong" and "very strong" intensity seem to show a certain temporal recurrence, oscillating between 10 and 18 years for ENSO episodes and between 10 and 14 years for anti-ENSO episodes. Another trend can also be observed between the two anomalies in terms of the dynamics of their occurrence in Figure 4a, since the anti-ENSO anomalies tend to manifest themselves sequentially or successively in two (2) or three (3) years, which seems to be less frequent for the ENSO anomalies.

The sample years series chosen for the subsequent analysis (Fig. 4b) appears to adequately reproduce the temporal trend of the general period. In the sample years series were included: 9 events classified as anti-ENSO, 6 events classified as ENSO and 4 years classified as no event or neutral years.

Of the 9 anti-ENSO episodes, those of 1989, 2000 and 2011 were classified as "strong", with ONI values equal to or less than -1.5 ºC. In the remaining years: 1985, 2001, 2017, 2021 and 2022, the anomalies were of "weak" intensity (between -0.5 and -1). Meanwhile, all the intensity levels are represented for ENSO episodes, since in 1998 and 2016 there were anomalies of "very strong" intensity with a positive temperature deviation > 2 ºC; the episodes of 1988 and 2003 were of "moderate" intensity, while in 2015 and 2019 there were events of "weak" intensity. Finally, the neutral or no event years were temporally dispersed (Fig. 4b).

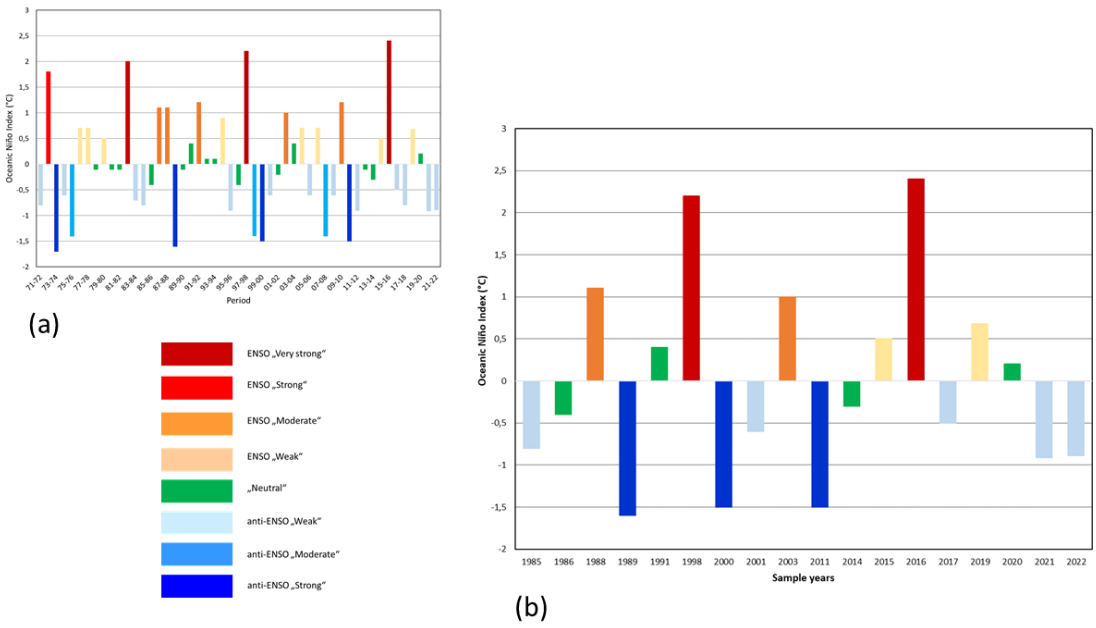

Figure 4. Chronological relationship of the occurrence of ENSO and anti-ENSO anomalies according to the Oceanic Niño Index - ONI during the initial period (a), and during the selected sample years (b).

Figure 5 shows the interannual variability of precipitation at the reference station. In the period 1971-2015, precipitation showed a high variability in occurrence (CV = 29.4%), with wet periods alternating with relatively dry periods. Between 1976 and 1990, precipitation was above the historical average, while the first decade of the 21st century was characterized by a dry period in which precipitation was significantly below the historical average (except in 2003) (Fig. 5). A maximum peak of pp occurred in 2011, coinciding with a "strong" anti-ENSO episode (Fig. 4b). On the other hand, 1992 was the driest year recorded, coinciding with an ENSO episode of "moderate" intensity (Fig. 4a).

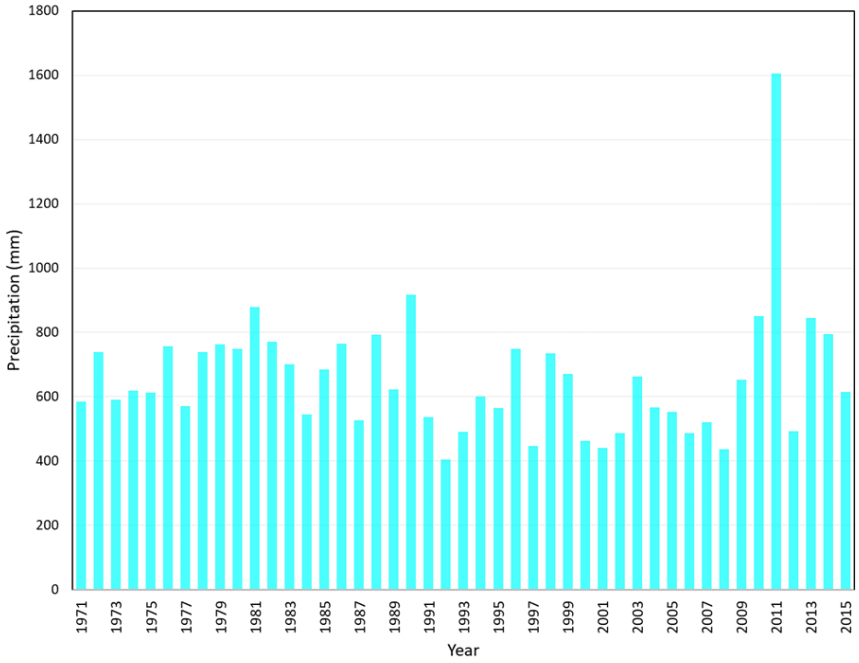

Figure 5. Total annual precipitation for the INIA-Mucuchíes weather station.

A further comparison showed, that for the 20 years with precipitation below the historical average, 8 coincided with anti-ENSO events, 2 coincided with ENSO events, while the remaining 8 were classified as no event or typologically neutral years. Meanwhile, 25 years showed precipitation values above the historical average, of which 10 coincided with ENSO events, 11 occurred during anti-ENSO events, and 4 were no event or neutral years.

3.2. Lagoon water surface extent dynamics according to NDWI results.

Figure 6 show the degree of water level fluctuation for the lagoons during the sample years classified according to ONI. The Miguaguó Lagoon has the largest surface area with 8.24 ha, followed by Masiegal Lagoon with 1.75 ha; Mapire Lagoon with 0.82 ha, meanwhile La Burra Lagoon is the smallest with only 0.57 ha.

As shown in Figure 6, the water surface extent for the four lagoons reflect a differential elastic hydrological behavior during the sample years, whose surface oscillations seemed to follow the oscillation of the climate through the relationship or combination between ENSO, anti-ENSO episodes and neutral years.

The hydrological oscillation of the water surface extent was highly dynamic among the sample years, with noticeable differences between the lagoons (Fig. 6). The CV of La Burra (45%) and Mapire (33%) lagoons clearly showed that both lentic systems had a substantial variability in their water surface extent and, therefore, the most elastic hydrological behaviour.

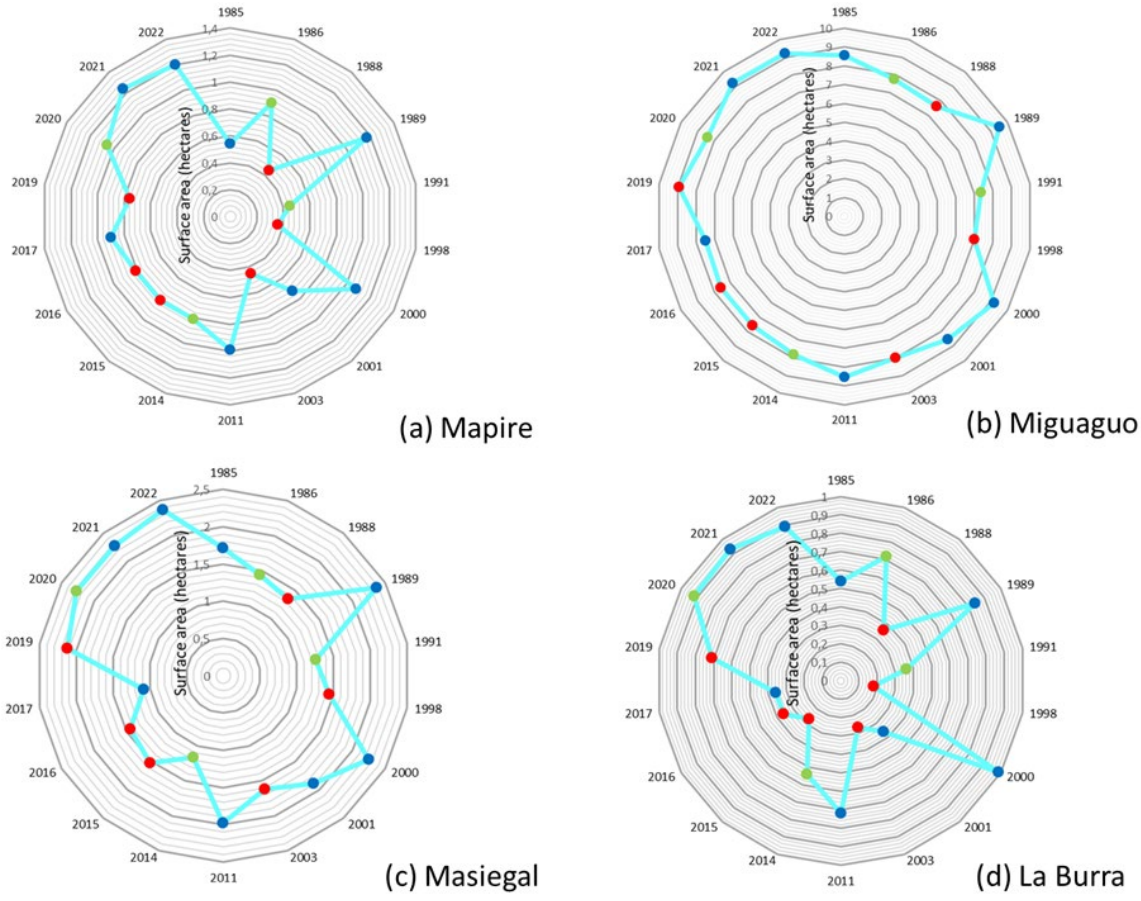

Figure 6. Water surface fluctuation during the sample years classified according to ONI index. Colors indicates: ENSO (red), A-ENSO (blue), Neutral (green) episodes.

Both lagoons are perimeter headwaters entities located downslope of a small concave "zero-order area" (see Fig. 1), so that atmospheric water reaching the rocky surface is easily concentrated there. Thus, both lagoons are highly dependent on atmospheric discharges as the primary water input, since the surface draining area is remarkably narrow and the bedrock is found at a very shallow depth, thus inhibiting subsurface inflow.

The Masiegal (CV= 24%) and Miguaguó (CV= 9%) lagoons showed a less variable and elastic statistical behavior, suggesting a lower or less evident dependence on atmospheric processes. These intra network lagoons are connected to the main channel vector of the stream, and their location in the geomorphic landscape guarantees water confinement with constant lateral subsurface flux.

As shown in Figure 6, the oscillations of the lagoons showed sensitivity to the historical alternation of the episodes of climate variability, since during the ENSO years: 1988, 1998, 2003, 2015 and 2019, the water surface level retreated and showed values below the observed mean. The greatest reduction occurred in 1998, coinciding with a "very strong" ENSO episode (see Table 2, Fig. 4b), which, according to *Corporación Andina de Fomento* [CAF] (2000), caused a rainfall deficit throughout the country. The episodes of 1988 and 2003 were of "moderate" intensity and the intra network lagoons (Masiegal and Miguaguó) did not show a significant oscillation (Fig. 6); meanwhile, the 2015 and 2019 episodes were of "weak" intensity (see Table 2, Fig. 4a and 4b).

The opposite trend occurred during the anti-ENSO years: 1989, 2000, 2011, 2021 y 2022, when the lagoons showed a significant increase in the water surface level, particularly in 2000, when a "strong" Niña event was recorded, preceded by a "moderate" one (see Table 2, Fig. 4a). During this anti-ENSO event, exceptional seasonal rainfall occurred, causing the most devastating natural disaster of the 20th century in Venezuela (Jiménez, 2007) (Córdova and López, 2015). In line with this, Artigas and Vicuña (2011) argued that the extreme rainfall that occurred in the last months of 1999 and early 2000 was a consequence of the cold phase of ENSO (La Niña), which dumped heavy rainfall on the country above the observed average. The anomalies that occurred in 1989 and 2011 were also classified as "strong" intensity events; meanwhile, “weak” anomalies occurred in 2017, 2021 and 2022 (Table 2, Fig. 4a and 4b).

For the "neutral" years, the behavioral trend of the surface water extent was less predictable, particularly for both La Burra and Mapire lagoons, which are the base of the hydrological system, showing an erratic oscillation during the sample years. On the other hand, Masiegal and Miguaguó lagoons showed a slightly decreasing trend in surface water extent (Fig. 6).

The results clearly indicate that these lagoon systems seem to be sensitive and at the same time dependent on the input of atmospheric water within the watershed, necessary to stimulate the processes of hydrological partitioning and conduction at surface and subsurface levels in the high Andean hydrological landscapes.

3.3. Statistical relationship between NDWI and ONI index

Fluctuations in water surface area and ONI are statistically inversely proportional, as can be seen from the scatter plots in Figure 7. Although the data show an adequate linear fit, the strength of this relationship is not essentially homogeneous between the lagoons. Miguaguó lagoon is the one that shows the best fit and relationship between the variables, suggesting that 50% of the variation in lagoon area can be explained by the oscillation in the occurrence of ENSO/anti-ENSO episodes. In La Burra and Mapire lagoons, the level of agreement decreases slightly to 46 and 43% respectively; finally, Masiegal lagoon is the one that shows the lowest level of fit between the variables (25%).

The statistical relationship between the two variables is more clearly reflected by the results of the Pearson correlation coefficient. The results of the "r" considering all the sample years evaluated showed a "high" negative correlation for Miguaguó Lagoon, Mapire and La Burra lagoons and a “moderate” correlation for Masiegal lagoon, indicating that the episodes of ENSO anti-ENSO can affect the lagoons differently (Table 4).

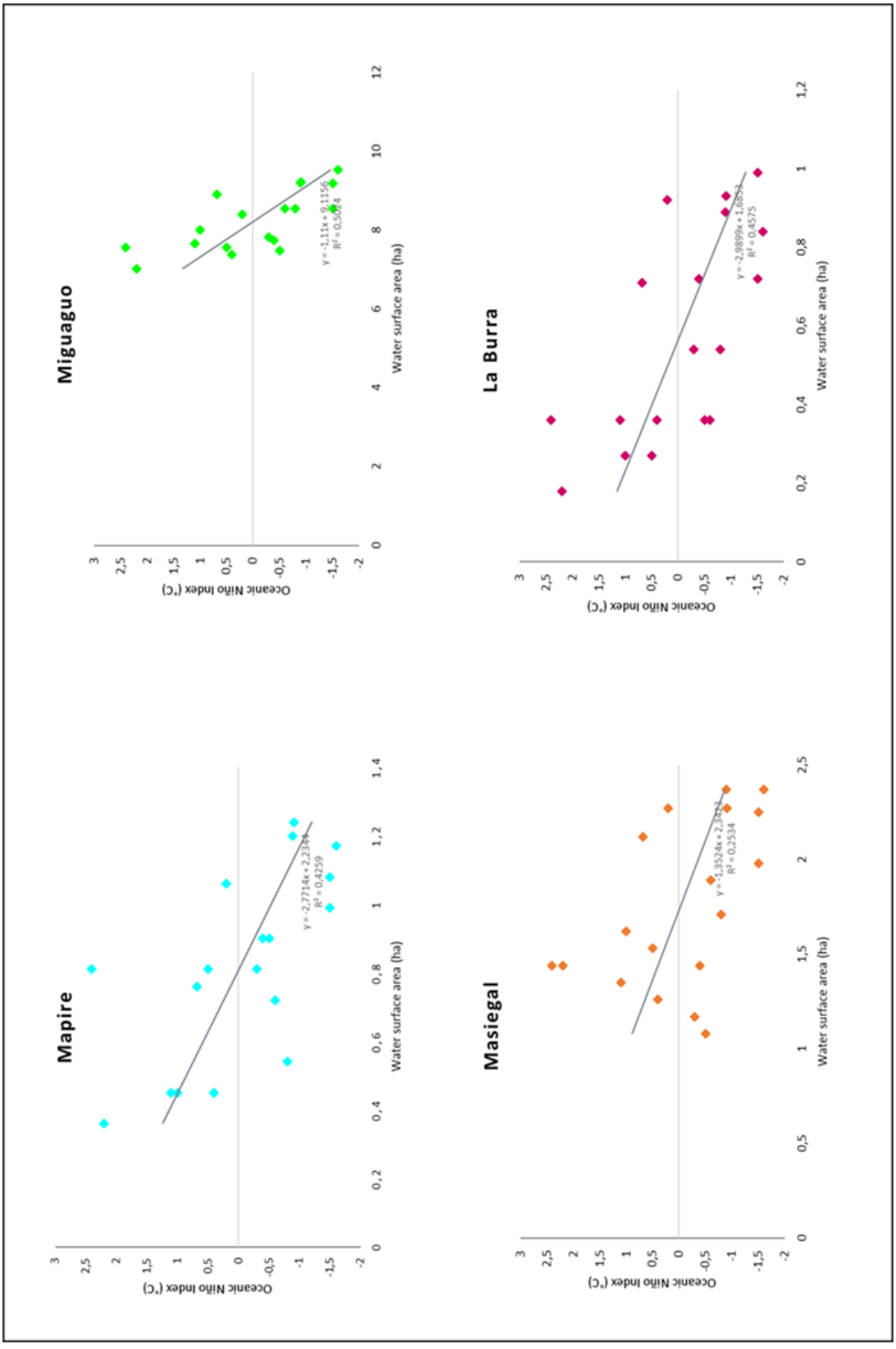

Figure 7. Statistical relationship between NDWI and ONI.

Table 4. Pearson linear correlation coefficient (r)between NDWI and ONI index for the sample years.

r considering all sample years (ENSO, anti-ENSO, Neutral)		**r considering ENSO and anti-ENSO years only**	
NDWI / ONI		NDWI / ONI	
Mapire	-0.65	Mapire	-0.69
Miguaguó	-0.71	Miguaguó	-0.77
Masiegal	-0.50	Masiegal	-0.63
La Burra	-0.68	La Burra	-0.73

Source: calculations based on the ONI index provided by the NOAA Climate Agency and water surface area as a result of the NDWI for the temporal items under study.

The resulting "r" values considering only ENSO and anti-ENSO years showed a better performance in the correlation, as a high negative correlation between the ONI and the surface water extent exist in all lagoons. This suggest that the oscillations occurred during neutral years are stochastic, introducing uncertainty to the strong relationship between the two processes.

3.4. Level of deviation of the surface water extent during ENSO / anti-ENSO episodes

Figure 8 shows the temporal variation of the percentage deviation of the NDWI (ΔNDWI) with respect to the mean accounted for the neutral years. It is clearly observed that the surface water extent of lagoons experienced a highly dynamic behaviour during the sample years, with different trends among them. La Burra and Mapire lagoons had the most elastic behaviour and higher amplitude in their surface water extent fluctuations, defining a similar temporal trend in which both lagoons show positive and negative deviations on their surfaces due to the alternation of ENSO and anti-ENSO episodes. La Burra showed the most extreme percentage of deviation, ranging from 56% for positive anomalies (anti-ENSO) to -72% for negative anomalies (ENSO). For Mapire lagoon the magnitude of the deviation is slightly lower, ranging from 54% to -55% (See Fig. 8).

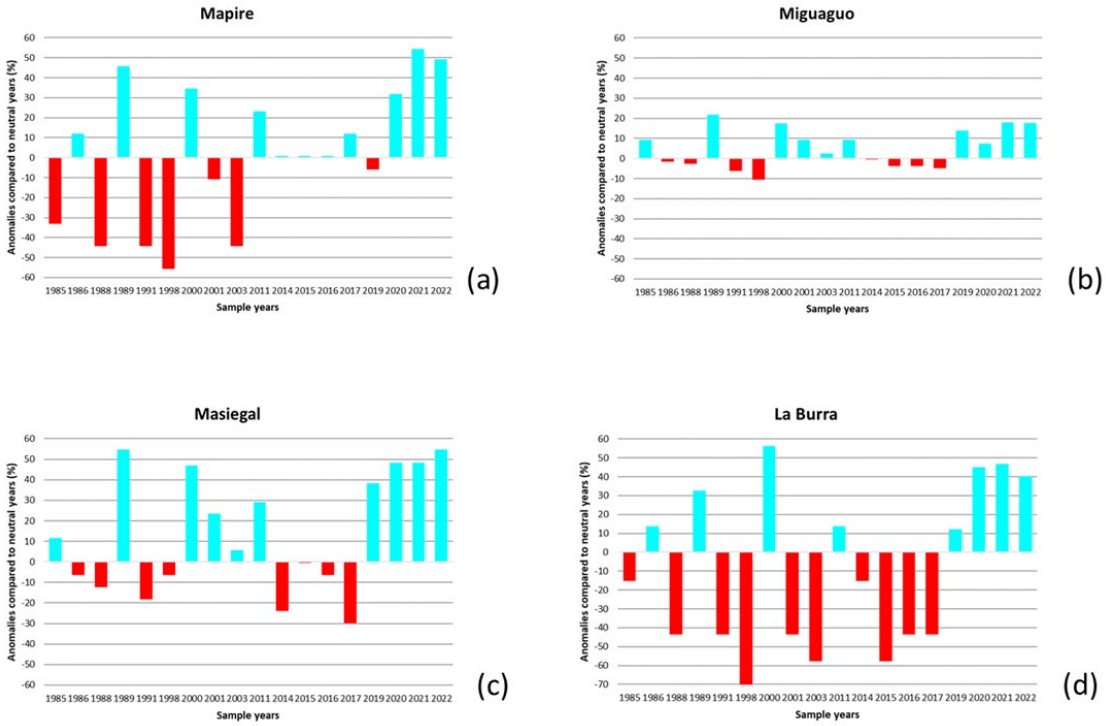

Figure 8. Percentage of variation-anomalies ΔNDWI being compared with the averaged neutral years.

The Miguaguó Lagoon showed a less elastic and more resilient behaviour during the period, with mostly positive deviations, suggesting that its surface water extent experienced relative stability during the sample period. The amplitude of the deviations with respect to the neutral years is remarkably small (between 21% and -10%), with an apparent dominance of positive deviations in its surface water extent. For the Masiegal Lagoon, the amplitude of the deviations is greater than the previous one, with values ranging between 54% and -30%.

Thus, la Burra and Mapire lagoons have the highest level of severity in anomalies related with the occurrence of ENSO and anti-ENSO events, followed by Masiegal Lagoon, meanwhile in Miguaguó Lagoon predominate the slight intensity anomalies. For La Burra Lagoon, the dominance of “severe impact” for anomalies occurred during the sample period is evident, since in 13 of the 18 sample years the surface water extent had a severe level of deviation respect to the averaged neutral years; 8 anomalies were negative, which suggests that the lagoon tends to be more prone to negative anomalies produced by ENSO. The Mapire Lagoon showed anomalies of "severe impact" intensity in 11 sample years, meanwhile Masiegal Lagoon showed this condition in 10 sample years. In Miguaguó Lagoon, a dominance of anomalies of "slight impact" intensity level was observed, thus being the lentic system that denotes high stability against the disturbances generated by the El Niño South Pacific Oscillation.

3.5. Relationship between the surface water extent and the local climatology

Figure 9 shows the relationship between the interannual precipitation recorded at the reference gauging station (INIA Mucuchíes) and the surface water extent (normalized values) of the four lagoons. Previous statistical analysis suggested that the rainfall occurring at the end of the rainy season have an important impact on the water level fluctuation of the lagoons during the dry season.

The relationship shown in Figure 9 clearly suggests that the variation in the surface water extent of the four lagoons is virtually conditioned by the direct input of atmospheric water, with La Burra and Mapire lagoons being the entities that show a more sensitive reaction to the interannual rainfall variability. The relative location of both lagoons within the hydrological landscape system, as already mentioned, seems to play an important role in this level of sensitivity.

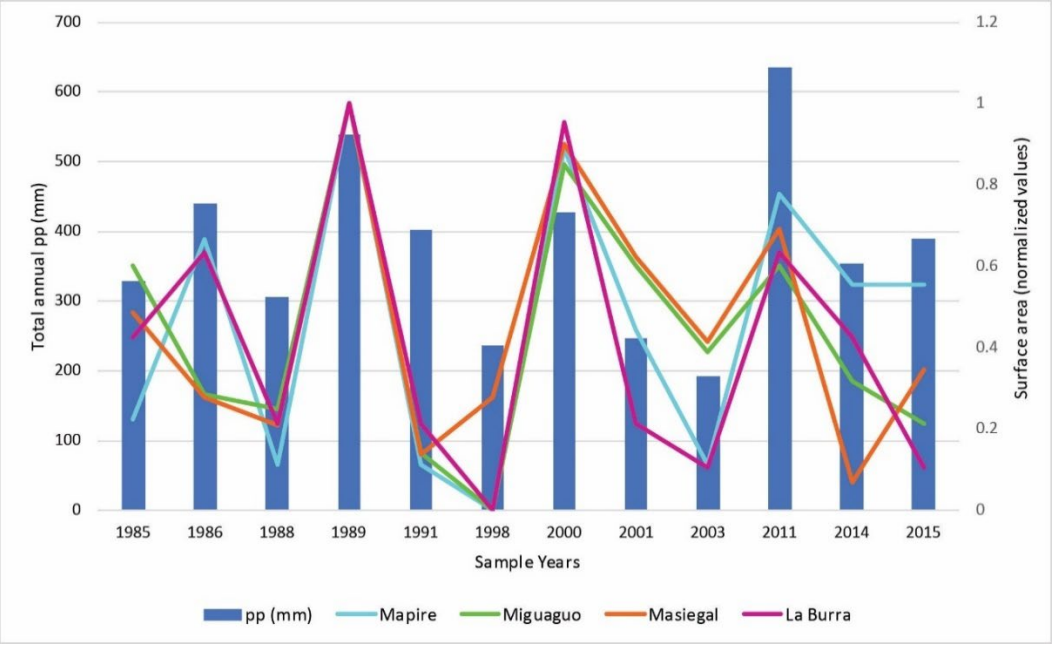

Figure 9. Ratio of accumulated precipitation between the months of August to March in the INIA-Mucuchíes reference gauge station and the surface water extent of the lagoons, according to the NDWI.

On the other hand, the Miguaguó and Masiegal lagoons showed a less evident variability of the surface water extent with respect to precipitation, which suggests that in both lentic systems the incoming runoff may be more complex and heterogeneous than in the other two lagoons, so that the hydroperiod is conditioned by the strategies of partitioning and transfer of water within the hydrological landscape.

4. Discussion

Our results clearly show that the high Andean lagoons and the headwaters of the Venezuelan Andes have a spatial and temporal dynamic that is strongly influenced by processes derived from the interannual variability of precipitation, in which the El Niño Southern Oscillation plays an important role. The results also show that climatic variability has a direct impact on the oscillation of water level of lagoons, which depends on the magnitude of the anomaly, the temporal sequence of the lagoons and the location of the lagoons in the landscape. From the results it can be concluded that the lagoons have different levels of atmospheric dependence.

4.1. El Niño Southern Oscillation and Climate Variability in the High Andes of Venezuela

The influence of ENSO/anti-ENSO on the climate of northern South America is well known, although the region is also climatically influenced by the Pacific Decadal Oscillation (PDO) on a decadal or interdecadal scale (Schoolmeester *et al.,* 2016), and there are even links or feedbacks between the two processes, as pointed out by Martínez *et al.* (2011). However, the impact of the PDO on the climate of the region has been poorly studied. On the other hand, other factors seem to modulate the climate of the region and act in close relation with ENSO (especially in its warm phase), such as changes in atmospheric pressure in the Caribbean and tropical Atlantic (Aceituno, 1988), and even the North Atlantic Oscillation exhibits an interesting coupling with the hydrometeorology of tropical South America (Poveda and Mesa, 1997).

These factors could help to explain the historical variations in precipitation observed at the reference station, which are inconsistent with the ENSO/anti-ENSO alternation. Due to the size and complexity of the Andean Mountain range, climatic processes exhibit important latitudinal differences, so that even the influence of ENSO/anti-ENSO on local climatology often shows different patterns and intensities.

4.2. Climate variability and its impact on high Andean lagoons

The relationship between ENSO/anti-ENSO events and their alternation with neutral years has a direct impact on the hydroperiod of the high Andean lagoons, which is directly reflected in the oscillations observed in their surface water extent. The location of these wetlands at the altitudinal base of the regional hydrological cycle makes them highly dependent on atmospheric dynamics, so that the hydrological response and the hydroperiod are directly related. Similar results have been obtained by Dangles *et al.* (2017) in the Cordillera Real of Bolivia, by De la Fuente *et al.* (2021) in the Chilean Andes, and recently by Carilla *et al.* (2023) in the Argentine Andes. In all these cases, the direct impact of climate variability on the wetlands studied was clearly evident, although with temporal variations imposed by latitude and climate regime.

The type of anomaly, as well as its magnitude, intensity and sequential relationship, also have an effect on the magnitude of the surface water extent in the high Andean lagoons. It is well known that anti-ENSO anomalies have more pronounced effects on the climate and hydrology of the continent than the opposite anomaly, and authors such as Poveda and Mesa (1997), Mejía (2012), Dangles *et al.* (2017), De la Fuente *et al.* (2021), Mejía *et al.* (2022) and Carilla *et al.* (2023), confirmed this. On the other

hand, the frequency of episodes is usually variable in temporal scale, and the biophysical conditions of the environment, as well as the location of lagoons in the landscape and the configuration of the drainage network, influence their hydrological response to atmospheric processes. De la Fuente *et al.* (2021) found differences in the hydroperiod of lagoons depending on the size of the wetland. Similarly, the authors previously studied the Miguaguó swamps and found differential behaviors among them respect to the climate variability, probably explained by their location in the hydrological landscape.

4.3. Influence of the hydrological landscape

Due to its topographic and hydrological position in the high Andes, the Miguaguó watershed consists of a system of wetlands (lagoons and swamps) which are directly and permanently connected to the drainage network that forms the Miguaguó stream. Conceptually, and according to Rains *et al.* (2016), it is a hydrologic landscape in which the wetlands act as nodes that receive, store, and release water to the main transmission vector of drainage flow. For Winter (2001), the hydrologic landscape with glacial landforms is perhaps the most complex to describe, since the complex topography, in addition to the type and distribution of unconsolidated geologic material in glacial terrain, can result in a wide scalar typology of hydrologic landscapes, from micro-depressions to entire moraine complexes.

These landscapes have complex surface and subsurface water flow systems, in which drainages can have very different interactions with groundwater depending on whether they cross moraine till, till plains, or pure alluvial plains. In the case of the Miguaguó watershed, the soils are basically moraine and fluvioglacial deposits, so the transmissivity of the subsurface water is probably high due to the glacial morphology.

The differences in trends observed between the lagoons may be due to their location at the landscape level and, more specifically, to their relative position in the local hydrological network. As can be seen in Figure 1, La Burra Lagoon is located in the upper zone of the watershed and channel network, specifically in the so-called transition zone between the zero-order and first-order channels (Benda *et al.,* 2005). The lagoon has a very small draining area, with very shallow soils and bedrock very close to the surface; this means that its water regulation capacity is likely limited -as suggested by Franco *et al.* (2013)- so that the hydroperiod of the lagoon is essentially controlled by atmospheric water input, rather than surface runoff.

The Masiegal and Miguaguó are intra network lagoons located in the central part of the watershed, just in the middle section of the channel network, being nodal points of surface flow convergence, thus having a higher level of hydrological connectivity and perennial inflow. The presence of glacial cirques in this sector has resulted in a predominantly concave topography, facilitating the concentration of flow at the bottom of the valley. The two well-developed lateral moraine channels on either side of the stream, surrounded by moraine and fluvioglacial deposits, suggest a complex dynamic of diffuse, laminar, and especially lateral subsurface flow towards the two lagoons. This greatly diversifies the water input, thus favoring the hydroperiod of both lentic systems, which is additionally favored by a local morphology containing coarse-textured soils with high organic matter content that facilitates hydric confinement. According to Hofstede *et al.* (2014), the soils of the paramo usually have low bulk density, high porosity and high organic matter content, making them highly suitable to retain water for long periods and to release it slowly and constantly. In addition, the shallow bedrock inhibits the vertical transmissivity of water, thus guaranteeing its persistence at the surface.

The conditions described above also apply to the Mapire Lagoon, located in the middle part of the watershed, although it is a headwater lentic system that functions as a spring being connected to the network by a single low-volume stream. Its relative location in the lower part of the watershed, very close to the abstraction of water for consumption, irrigation and extensive cattle grazing, suggests that this lagoon could be under anthropogenic pressure that could be affecting its hydroperiod. Both

topography and land use variables has been remarked by Vanderhoof *et al.* (2017) as determining the surface-water connectivity across the landscape.

For Franco *et al.* (2013), the diversity of inputs sources of water leads to greater opportunities to maintain the quantity and quality of water, thus favoring the hydroperiod of the lentic systems; this can explain the distinctive behavior of the lagoons based on the NDWI for the sample years considered.

4.4. Scope of the results in the context of the region

As mentioned above, the size and complexity of the Andes, its large latitudinal gradient and its complex climatic and biogeographical structure mean that the processes and factors that control and modulate climate at regional and local scales often vary from one region to another; similarly, ENSO/anti-ENSO episodes have different effects at spatial and temporal scales within the whole Andes range. Therefore, the results obtained may have a reduced spatial scope in their potential for spatial correlation at the regional scale. In addition, the notable scarcity of climatic records in much of the Andes and the limited access to the recorded data may in many cases affect the predictive reliability of the results. These considerations must be taken into account when studying the links between climatic variability and local hydrological or ecological processes in the Andes.

5. Conclusions

The results showed that there is a clear influence of climatic variability, specifically on the anomalies derived from ENSO and anti-ENSO events in the local climate, and on the dynamics and behaviour of the lagoons of the Miguaguó headwater watershed. The spatio-temporal behavior of the NDWI during the sample years, the statistical relationship with the Oceanic Niño Index (ONI), and its agreement with the local climatological records have helped to demonstrate this fact.

The climate variability has a different level of incidence in the surface water extent fluctuation of the lagoons. Differences are explained by: the spatial hydrological configuration, the relative position of each lagoon in the hydrological landscape, the topographic conditions, the morphology of the landforms and the soil characteristics of the environment. Similarly, the level of intensity and temporal frequency of each event also condition the dynamics of the hydroperiod of the lagoons.

The headwater lagoons showed greater hydrological elasticity and greater sensitivity to climatic anomalies, suggesting that their hydroperiod is highly dependent on atmospheric processes; the intra network lagoons appear to have greater resilience and stability to ENSO and anti-ENSO events, suggesting that their hydroperiod is structurally more complex and heterogeneous, presumably dependent on elements of the hydrological landscape.

The research demonstrated the advantage and remarkable potential usefulness of remote sensing tools and their derived indicators, such as the NDWI, in understanding the dynamics of lentic systems at different scales: spatial, temporal and climatic. Similarly, the Oceanic Niño Index seems to be a very useful indicator to be able to quantitatively and accurately delimit ENSO and anti-ENSO events, having comparability and relationship with other climatological and hydrological indicators.

Although the results of this research are clear and convincing, they are also spatially and temporally scale limited because the processes involved are inherently complex. For these reasons, additional research is needed to facilitate and complement the understanding of the climatic and atmospheric relationships in water processes typical of mountainous areas in the tropics.

Acknowledgements

The authors would like to thank the University of Los Andes and the University of Hamburg for supporting the research project, as well as the International Institute for Education IIE - SRF and the Humboldt Foundation for financial support. Special thanks to the working group "Critical Geographies of Global Inequalities" at the University of Hamburg for their valuable logistical and operational support in the development of the project. We would also like to thank the National Climate Prediction Center-NOAA and Earth Explorer - USGS for providing the open databases necessary for the research.

References

Aceituno, P., 1988. On the Functioning of the Southern Oscillation in the South American Sector. Part I: Surface Climate. *Monthly Weather Review* 116: 505-524. https://doi.org/10.1175/1520-0493(1988)116<0505:OTFOTS>2.0.CO;2

Adam, E., Mutanga, O, Rugege, D., 2010. Multispectral and hyperspectral remote sensing for identification and mapping of wetland vegetation: a review. *Wetlands Ecology Management* 18, 281-296. https://doi.org/10.1007/s11273-009-9169-z

Alibakhshi, S., Groen, Th., Rautiainen, M., Naimi, B., 2017. Remotely-Sensed Early Warning Signals of a Critical Transition in a Wetland Ecosystem. *Remote Sensing* 9, 352. https://doi.org/10.3390/rs9040352

Andressen, R., Diaz, A., Lazo, J., 2000. Influencia de la altitud y distancia al Lago de Maracaibo en la caracterización pluviométrica del estado Trujillo, Venezuela. *Revista de la Facultad de Agronomía de la UCV* 26, 107-124.

Artigas, D., Vicuña, A., 2011. La niña traerá más lluvias al norte de Sudamérica. Sala Situacional del observatorio latino americano. Centro de Modelado Científico. http://cmc.org.ve/portal/noticias.php?noticia=57 (last access: 11/07/2021).

Bedoya, M., Contreras, C., Ruíz, F., 2010. Alteraciones del régimen hidrológico y de la oferta hídrica por variabilidad y cambio climático. En: *Estudio Nacional del Agua 2010*. Instituto de Hidrología, Meteorología y Estudios Ambientales (IDEAM), pp. 282-318, Bogotá D. C., Colombia.

Benda, L., Hassan, M., Church, M., May, Ch., 2005. Geomorphology of Steepland Headwaters: The transition from Hillslopes to Channels. *Journal of American Water Resources Association (JAWRA)* 41(4), 835-851. https://doi.org/10.1111/j.1752-1688.2005.tb03773.x

Betancur-Vargas, T., García-Giraldo, D., Vélez-Duque, A., Gómez, A., Flórez-Ayala, C., Patiño, J., Ortíz-Tamayo, J., 2017. Aguas subterráneas, humedales y servicios ecosistémicos en Colombia. *Biota Colombiana* 18 (1), 1-28. https://doi.org/10.21068/c2017.v18n01a1

Cáceres, A., 2019. Estudio de los cuerpos lénticos en el escenario de cambio climático, una mirada a Colombia. *Revista Pertinencia Académica* 3(3), 29-50.

Carilla, J., Aráoz, E., Foguet, J., Casagranda, E., Halloy, St., Grau, A., 2023. Hydroclimate and vegetation variability of high Andean ecosystems. *Frontiers in Plant Science* 13,1067096. https://doi.org/10.3389/fpls.2022.1067096

Castro, M., 2019. *Influencia de la variabilidad climática en el lago de Chapala, Jalisco* (MSc Tesis). Universidad Autónoma de San Luis Potosí. San Luis Potosí, México.

Convención Internacional sobre los Humedales RAMSAR 2005. Estrategia regional de conservación y uso sostenible de los humedales altoandinos. En *9ª Reunión de la Conferencia de las Partes Contratantes en la Convención sobre los Humedales* (Ramsar, Irán, 1971). Kampala, Uganda, 8 a 15 de noviembre de 2005.

Córdoba, C., 2014. *Estudio de las características edáficas con el fin de estimar la capacidad potencial de almacenamiento hídrico en los suelos minerales de la Microcuenca Miguaguó, Mixteque estado Mérida, Venezuela* (BSc Tesis). Universidad de Los Andes, Mérida, Venezuela.

Córdova, J. López, J., 2015. Eventos extremos: inundaciones, deslaves y sequías. En: A. Gabaldón, A. Rosales, E. Buroz, J. Córdova, G. Uzcátegui, L. Iskandar (Eds.). *Agua en Venezuela: una riqueza escasa*. Fundación Polar, Caracas, Tomo 1, pp. 287-358.

Corporación Andina de Fomento - CAF. 2000. *Las Lecciones de El Niño: Memorias Del Fenómeno El Niño 1997-1998 Retos y Propuestas para la región andina*. Volumen VI. Instituto de Hidrología, Meteorología y Estudios Ambientales (IDEAM), Colombia.

Dangles, O., Rabatel, A., Kraemer, M., Zeballos, G., Soruco, A., Jacobsen, D., Anthelme, F., 2017. Ecosystem sentinels for climate change? Evidence of wetland cover changes over the last 30 years in the tropical Andes. *PLOS ONE*, https://doi.org/10.1371/journal.pone.0175814

De la Fuente, A., Meruane, C., Suárez, F., 2021. Long-term spatiotemporal variability in high Andean wetlands in northern Chile. *Science of the Total Environment* 756, 143830 https://doi.org/10.1016/j.scitotenv.2020.143830

De la Torre, C., 2014. Principales avances en la gestión del agua y la adaptación al cambio climático en los ecosistemas de montaña de América Latina. *Apuntes de Investigación* 2, 1-10.

Dos Santos, G., Meléndez-Pastor, I., Navarro-Pedreño, J., Gómez, I., 2019. A Review of Landsat TM/ETM based Vegetation Indices as Applied to Wetland Ecosystems. *Journal of Geographical Research* 2 (01), 35-49. https://doi.org/10.30564/jgr.v2i1.499

Escanilla-Minchel, R., Alcayaga, H., Soto-Alvarez, M., Kinnard, Ch., Urrutia, R. 2020. Evaluation of the Impact of Climate Change on Runoff Generation in an Andean Glacier Watershed. *Water* 12, 3547. https://doi.org/10.3390/w12123547

Esquivel, G., 2018. *Análisis integrado de variabilidad climática, dinámica de precipitación y conflictos por el agua para la gestión del recurso hídrico en Costa Rica* (PhD Dissertation). Universidad Estatal a Distancia, San José, Costa Rica.

Fennessy, M., Jacobs, A., Kentula, M., 2004. *Review of rapid methods for assessing wetland condition. EPA/620/R-04/009*. U.S. Environmental Protection Agency. Washington D.C, USA.

Franco, L., Delgado, J., Andrade, G., 2013. Factores de la vulnerabilidad de los humedales altoandinos de Colombia al cambio climático global. *Cuadernos de Geografía. Revista Colombiana de Geografía*, 22 (2), 69-85.

González, J., 2018. *Comportamiento de los humedales altoandinos en años climatológicamente distintos, usando indicadores derivados de los sensores remotos* (BSc Tesis). Universidad de Los Andes, Mérida, Venezuela.

González-Zeas, D., Erazo, B., Lloret, P., De Bièvre, B., Steinschneider, S., Dangles, O., 2019. Linking global Climate change to local water availability: limitations and prospects for a tropical mountain watershed. *Science of the Total Environment* 650 (2), 2577-2586. https://doi.org/10.1016/j.scitotenv.2018.09.309

Guerra, E., 2018. *Comportamiento de la precipitación frente al cambio climático en la microcuenca del río Escudillas* (BSc Tesis). Universidad Técnica del Norte, Ibarra, Ecuador.

Guevara, J., 2013. *Métodos de estimación y ajuste de datos climáticos*. Consejo de desarrollo científico y humanístico de la Universidad Central de Venezuela (Colección monografías 80). Caracas, Venezuela.

Hangnan, Y., Lan, L., Weihon, Z., Dongfan, P., Guishan, C., Moonil, K., Seong, W.J., Woo-Kyun, L., 2018. Drought monitoring of the wetland in the Tumen River Basin between 1991 and 2016 using Landsat TM/ETM+. *International Journal of Remote Sensing*. https://doi.org/10.1080/01431161.2018.1524604

Hernández, Z., 2005. *Modelos arquitectónicos en humedales andinos: un abanico de respuestas funcionales (Andes de Venezuela)* (MSc Tesis). Universidad de Los Andes, Mérida, Venezuela.

Herzog, S., Jorgensen, P., Martínez, R., Martius, C., Anderson, E., Hole, D., Larsen, T., Marengo, J., Carrascal, D., Tiessen, H., 2010. *Efectos del cambio climático en la biodiversidad de los Andes tropicales: el estado del conocimiento científico*. Resumen para tomadores de decisiones y responsables de la formulación de políticas públicas. São José dos Campos, Brasil, Instituto Interamericano para la Investigación del Cambio Global (IAI).

Hofstede, R., Calles, J., López, V., Polanco, R., Torres, F., Ulloa, J., Vásquez, A., Cerra, M. 2014. *Los Páramos Andinos ¿Qué sabemos? Estado de conocimiento sobre el impacto del cambio climático en el ecosistema páramo*. UICN, Quito, Ecuador.

Holden, J. (Ed.), 2017. *An Introduction to Physical Geography and the Environment*. London. Pearson Education Limited. Fourth Edition.

Ji, L., Zhang, L.,,Wylie, B., 2009. Analysis of Dynamic Threshold for the Normalized Difference Water Index. *Photogrammetric Enginnering & Remote Sensing* 75(11), 1307-1317. https://doi.org/10.14358/PERS.75.11.1307

Jiménez, V., 2007. Geografía de las catástrofes. Amenazas, vulnerabilidad y riesgos. En: GEO Venezuela. Tomo 2: Medio físico y recursos ambientales, Fundación Polar, pp. 710-748, Caracas,

Jiménez, N., 2010. *Evaluación del impacto de la sequía sobre la vegetación natural mediante teledetección en el SE español*. (BSc Tesis). Universidad Politécnica de Valencia, España.

Kashani, M., Dinpashoh, Y., 2012. Evaluation of efficiency of different estimation methods for missing climatological data. *Stoch Environ Res Risk Assess* 26, 59-71. http://doi.org/10.1007/s00477-011-0536-y

López-Moreno, J., Navarro, F., Izaguirre, E., Alonso, E., Rico, I., Zabalza, J., Revuelto, J., 2020. Glacier and climate evolution in the Pariacacá mountains, Perú. *Cuadernos de Investigación Geográfica* 46(1), 127-139. http://doi.org/10.18172/cig.4331

López-Moreno, J., Rojas-Heredia, F., Ceballos, J., Morán-Tejeda, E., Alonso-Gonzalez, E., Vidaller, I., Deschamps-Berger, C., Revuelto, J., 2022. Recent evolution of glaciers in the Cocuy-Güican Mountains (Colombian Andes) and the hydrological implications. *Land Degrad Dev*. 33, 2606-2618. http://doi.org/10.1002/Idr.4336

Lunneta, R., Balogh, M., 1999. Application of multi-temporal Landsat5TM imagery for wetland identification. *Photogrammetric Enginnering & Remote Sensing* 65(8), 1303 -1310.

Martínez, R., Ruiz, D., Andrade, M., Blacutt, L., Pabón, D., Jaimes, E., León, G., Villacís, M., Quintana, J., Montealegre, E., Euscátegui, Ch., 2011. Synthesis of the Climate of the Tropical Andes. In: S. Herzog, R. Martínez, P. Joergensen, H. Tiessen. (Ed.). *Climate Change and Biodiversity in the Tropical Andes*. Inter-American Institute for Global Change Research (IAI) and Scientific Committee on Problems of the Environment (SCOPE), pp: 97-109.

McFeeters, S., 1996. The use of Normalized Difference Water Index (NDWI) in the Delineation of Open Water Features. *International Journal of Remote Sensing* 17(7),1425-1432. https://doi.org/10.1080/01431169608948714

Mejía, J., 2012. *Evaluating the Effects of LULC Changes and Climate Variability in the Hydrological Response of a Tropical Andean River Basin. The Case of the Boconó River Basin – Venezuela.* (PhD Dissertation). Eberhard Karls Universität, Tübingen, Germany.

Mejía, J., González, J., Albarrán, A., 2022. Influencia de la variabilidad climática en los humedales altoandinos de la Microcuenca Miguaguó, Andes venezolanos. *Tropical Journal of Environmental Sciences* 56 (2), 38-62. http://doi.org/10.15359/rca.56-2.3

Meza, M., Díaz, Y., 2014. Efectos de la variabilidad climática sobre las fluctuaciones del nivel de las aguas y actividad ganadera en humedales altoandinos. *Interciencia* 39 (9), 651-658.

Middleton, B., Souter, N., 2016. Functional integrity of freshwater forested wetlands, hydrologic alteration, and climate change. *Ecosystem Health and Sustainability* 2 (1), e01200. http://doi.org/10.1002/ehs2.1200

Moncada, J., Pellegrini, N., Aranguren, J., Lugo, C., 2010. Los humedales altoandinos como elementos para el desarrollo sostenible del estado Táchira. *Geoenseñanza* 15 (2), 221-244.

Olaya, V., 2016. S*istemas de Información Geográfica. Create Space Independent Publishing Platform (Amazon)*. http://www.nosolosig.com/libros_geo/790-sistemas-de-informacion-geografica-tomo-i (last access: 11/21/2022).

Ortiz, Ch., 2016. *Impacto sobre el control de inundaciones, de la adecuación hidrogeomorfológica en humedales de Bogotá, integrando escenarios de cambio climático. Caso de estudio: Humedal Jaboque* (MSc Tesis). Pontificia Universidad Javeriana, Bogotá, Colombia.

Paredes-Trejo, F., Barbosa-Alves, H., Moreno-Pizani, M., Farías-Ramírez, A., 2020. Cambio climático: ¿altera el régimen de precipitaciones y caudales en Venezuela? En: D. Rodríguez (Ed.), *Ríos en Riesgo de Venezuela, Volumen 3. Colección Recursos hidrobiológicos de Venezuela*. Universidad Centro Occidental Lisandro Alvarado (UCLA), pp. 137-147. Barquisimeto, Venezuela.

Pinilla, M., Rueda, A., Pinzón, C., Sánchez, J., 2012. Percepciones sobre los fenómenos de variabilidad climática y cambio climático entre campesinos del centro de Santander, Colombia. *Ambiente y Desarrollo* 16 (31), 25-37.

Poveda, G., Mesa, O., 1997. Feedbacks between Hydrological Processes in Tropical South America and Large-Scale Ocean-Atmospheric Phenomena. *Journal of Climate*, 10: 2690-2702. https://doi.org/10.1175/1520-0442(1997)010<2690:FBHPIT>2.0.CO;2

Pulwarty, R., Barry, R., Hurst, C., Sellinger, K., Mogollon, L. 1998. Precipitation in the Venezuelan Andes in the Context of Regional Climate. *Meteorology and Atmospheric Physics* 67, 217-237. https://doi.org/10.1007/BF01277512

Quesada-Román, A., Mora-Vega, A., 2017. Impactos ambientales y variabilidad climática en el humedal de San Vito, Coto Brus, Costa Rica. *Revista de Ciencias Ambientales. (Tropical Journal of Environmental Sciences)* 51 (1), 16-32. http://doi.org/10.15359/rca.51-1.2

Quintero, D. 2019. *Cambio climático, un escenario de riesgo desde la mirada de las comunidades asentadas en el Páramo de Letras y el sector El Ocho de los municipios de Manizales y Villamaría* (MSc Tesis). Universidad Católica de Manizales, Manizales, Colombia.

Rains, M., Leibowitz, S., Cohen, M., Jawitz, J., Kalla, P., Lane, C., Lang, M., McLaughlin, D., 2016. Geographically isolated wetlands are part of the hydrological landscape. *Hydrological Processes* 30, 153-160. http://doi.org/10.1002/hyp.10610

Ramírez, L., Vallejo, B., 2018. *Influencia de los patrones climáticos globales en la variabilidad del clima durante el periodo 2000-2016 en los páramos del norte de Ecuador* (BSc Tesis). Universidad Técnica del Norte, Ibarra, Ecuador.

Sandoval, D., 2015. *Intercepción, evaporación desde el suelo y transpiración en un páramo andino venezolano: modelización desde la hoja al ecosistema* (MSc Tesis). Universidad de Los Andes, Mérida, Venezuela.

Schoolmeester, T., Saravia, M., Andresen, M., Postigo, J., Valverde, A., Jurek, M., Alfthan, B., Glada, S., 2016. *Outlook on Climate Change Adaptation in the Tropical Andes mountains.* Outlook Series. United Nations Environment Programme, GRID-Arendal and CONDESAN. Nairobi, Arendal, Vienna and Lima. www.unep.org.

Stolk, M., Verweij, P., Stuip, M., Baker, C., Oosterberg, W., 2006. *Valoración Socioeconómica de los Humedales en América Latina y el Caribe*. Wetlands International. Amsterdam, The Netherlands.

Uribe, D., Vera, C., Paicho, M., Espinoza, G., 2017. Observatorio ecosocial para el seguimiento del cambio climático en ecosistemas de altura en la región de Tarapacá: propuestas, avances y proyecciones. *Dialogo Andino* 54, 63-82. http://doi.org/10.4067/S0719-26812017000300063

Valencia, M., Figueroa, A., 2015. Vulnerabilidad de humedales altoandinos ante procesos de cambio: tendencias del análisis. *Revista Ingenierías Universidad de Medellín* 14 (26), 29-42.

Vanderhoof, M., Christensen, J., Alexander, L., 2017. Patterns and drivers for wetland connections in the Prairie Pothole Region, United States. *Wetlands Ecological Management,* http://doi.org/10.1007/s11273-016-9516-9

Vergara, W., Deeb, A., Leino, I., Hansen, M., 2010. *Assessment of the impact of Climate Change on Mountain Hydrology. Development of a Methodology through a case Study in Perú.* The World Bank.

Winter, T., 2001. The Concept of Hydrological Landscapes. *Journal of American Water Resources Association* 37 (2), 335-349. https://doi.org/10.1111/j.1752-1688.2001.tb00973.x

Cuadernos de Investigación Geográfica *Geographical Research Letters*	2024	Nº 50 (2)	pp. 93-113	EISSN 1697-9540

http://doi.org/10.18172/cig.6083

ANALYSIS OF FLOOD RISK IN THE LOWER HYDROGRAPHIC BASIN OF THE RÍO NEGRO (ARGENTINA)

GRETHEL GARCÍA BU BUCOGEN[1]*, VANESA Y. BOHN[2], MARIA CINTIA PICCOLO[3]

[1]*Instituto Argentino de Oceanografía (CONICET-UNS). Bahía Blanca, 8000, Buenos Aires, Argentina.*

[2]*Universidad Nacional del Sur (UNS), CONICET, DGyT, 12 de octubre y San Juan, 4to. Piso, Bahía Blanca, Argentina.*

[3]*Instituto Argentino de Oceanografía (CONICET-UNS) - Departamento de Geografía y Turismo, Universidad Nacional del Sur. Bahía Blanca, 8000, Buenos Aires, Argentina.*

ABSTRACT. The recurrent floods in the lower hydrographic basin of the Río Negro (RN), documented since 1899, have caused significant damage to the resident population settled in flood-prone areas, whose socioeconomic condition is unfavorable. The aim of this study was to analyze the risk associated with flood occurrences in this area by integrating the flood susceptibility level (hazard) of the study area and the vulnerability of the population. The risk analysis was derived from the algebraic overlay of hazard and vulnerability maps, developed according to criteria published by Renda *et al*. (2017). In the study area, floods are primarily caused by intense rainfall and winds, upstream water discharges from the Limay and Neuquén rivers, and interactions between increased upstream flow from the lower hydrographic basin of the RN and extreme meteorological events known as Sudestadas. Every certain period, such as every 2 years for winds exceeding 75 km/h and precipitation exceeding 37 mm in 24 hours, as well as every 100 years for flows exceeding 4,000 m^3s^{-1}, the occurrence of floods in the lower basin of the RN is expected to be derived from these events. Based on terrain characteristics and topography, 41.7% of the lower RN basin area showed moderate to high susceptibility to flooding. INDEC data (2010) indicated that 51.0% of the population in the study area was vulnerable to floods due to unfavorable socioeconomic conditions. According to hazard and vulnerability analyses, 43.2% of residents in the lower RN basin lived in high-risk areas, with homes located near the riverbank and on the outskirts of the Viedma-Carmen de Patagones urban conglomerate, hence being the most vulnerable. The results obtained in this research showed the influence of the natural and anthropogenic factors on the occurrence of flood-related disasters in the lower hydrographic basin of the RN. In addition, they served as a preliminary study that will enable decision-makers to create better prevention and mitigation plans contributing to improving the quality of life of its inhabitants.

Análisis del riesgo de inundaciones en la cuenca hidrográfica inferior del Río Negro (Argentina)

RESUMEN. Las recurrentes inundaciones en la cuenca hidrográfica inferior del Río Negro (RN), documentadas desde 1899, han causado daños significativos a la población residente asentada en áreas propensas a inundaciones, cuya condición socioeconómica es desfavorable. Por lo tanto, el objetivo de este trabajo fue analizar el riesgo asociado a la ocurrencia de inundaciones en esta área a través de la integración del nivel de propensión ante inundaciones (amenaza) del área de estudio y la vulnerabilidad de sus habitantes. El análisis de riesgo se obtuvo a partir de la superposición algebraica de los mapas de amenaza y vulnerabilidad, elaborados según criterios publicados por Renda *et al*. (2017). En el área de estudio, las inundaciones son principalmente causadas por intensas lluvias y vientos, descargas de agua aguas arriba de los ríos Limay y Neuquén, y la interacción entre el aumento del flujo aguas arriba de la cuenca hidrográfica inferior del RN y eventos meteorológicos extremos

conocidos como Sudestadas. Cada cierto período, tales como cada 2 años para vientos que superan los 75 km/h y precipitaciones que exceden los 37 mm en 24 horas, así como cada 100 años para caudales que sobrepasan los 4.000 $m^3 s^{-1}$, se espera la ocurrencia de inundaciones en la cuenca inferior del RN derivadas de estos eventos. Según las características del terreno y la topografía, el 41,7 % del área de la cuenca baja del RN mostró una susceptibilidad de moderada a alta a inundaciones. Los datos del INDEC (2010) indicaron que el 51,0 % de la población en el área de estudio era vulnerable a inundaciones debido a condiciones socioeconómicas desfavorables. De acuerdo con los análisis de amenaza y vulnerabilidad, el 43,2 % de los residentes en la cuenca inferior del RN habitaban en áreas de alto riesgo, en cercanías de la ribera del río y en las afueras del conglomerado urbano Viedma-Carmen de Patagones, siendo, por lo tanto, los más vulnerables. Los resultados obtenidos en esta investigación muestran que los factores naturales y antropogénicos favorecen la ocurrencia de desastres relacionados con inundaciones en la cuenca hidrográfica inferior del RN. Constituyen, también, este estudio preliminar que permitirá a los tomadores de decisiones crear mejores planes de prevención y mitigación que contribuyan a mejorar la calidad de vida de sus habitantes.

Keywords: river, floods, hazard, vulnerability, risk.

Palabras clave: río, inundaciones, amenaza, vulnerabilidad, riesgo.

Received: 29 April 2024

Accepted: 2 September 2024

***Corresponding author:** Grethel García Bu Bucogen. Instituto Argentino de Oceanografía (CONICET-UNS). Bahía Blanca, 8000, Buenos Aires, Argentina. Email: grethelgbb@gmail.com

1. Introduction

According to OEA (1993) and Lavell (2001), a disaster represents the tangible outcome of risk, which is defined as the likelihood of a hazardous event capable of causing social and economic losses to society (Moreno and Múnera, 2000). In this order, risk evaluation as an useful tool to estimate the level of danger associated with potential hazards and prevailing vulnerability conditions (Rojas Vilches and Martínez Reyes, 2011). This assessment includes the estimation of components of risks such as hazard, exposure, and vulnerability (Olcina and Ayala-Carcedo, 2002).

A hazard is recognized as a potential threat related to adverse phenomena, whether natural or human-induced. It can damage to society since a material and social point of view (Unesco, 2014; Renda *et al*., 2017). Natural events (earthquakes, floods, hurricanes, volcanic eruptions) or human-made incidents (poor flood management, dam breaches, technological origin, and pollution) become hazards when they affect populated regions (Aneas de Castro, 2000). Research about hazards includes different stages, as following (Renda *et al*., 2017):

1. Definition of the area affected by the hazard (neighborhood, district, municipality or region).
2. Identification of the origin of the hazard.
3. Definition of the magnitude of the hazard, its manifestations and return periods.
4. Physical and natural description of the affected area. This characterization includes a spatial study of the factors, which determine the susceptibility to the hazard in the study area (Liendro Moncada and Ojeda, 2018). The floods susceptibility level is expressed through a relative scale index, generated by the weighted sum of conditioning factors, ultimately classified into different levels (low, medium, and high) (SIGMA, 2023).

Vulnerability analysis are based on the social, economic, cultural, institutional, and infrastructural circumstances existing before a disaster, which render a population susceptible to a hazard (Fenoglio, 2019). The disaster occurrence and its magnitude are defined by the hazard and by the precarious conditions, respectively (Unesco, 2014). Vulnerability assessments involves various dimensions (Renda *et al*., 2017), although frequently, the exposure variable is integrated with social vulnerability in risk analysis (Rojas Vilches and Martínez Reyes, 2011):

1. Physical vulnerability (exposure): refers to the location of human settlements and physical deficiencies in structures (buildings and infrastructure).
2. Social vulnerability: is related to overall living conditions and it includes situations related to possibilities for education, health, social equity, and safety.

Globally, floods present a recurring challenge, due to the frequent occurrence of extreme hydrometeorological events and because of historical practices in settling flood-prone areas (Renda *et al*., 2017). The development of urban areas near rivers and flood-prone zones often exposes the resident population to vulnerability and increased risk (Viand and González, 2012). Moreover, the presence of infrastructures such as canals, culverts, dams, and embankments creates a false sense of security, causing the population to underestimate, neglect, or overlook the flood risk in those regions (AIC, 2020).

The risk analysis depends on both hazard occurrence and the society's vulnerability to it. For this reason, an integrated approach to both analyses is necessary (Renda *et al*., 2017). Globally, risk studies have become in a relevant tool for the decision makers. For example, research conducted by Liu *et al*. (2021), along the Dianbao River in Kaohsiung City (southern Taiwan), enabled the identification of areas with higher flood risks. Based on these results, the authors proposed various mitigation strategies to decision-makers. In Marrickville (Australia), a new flood vulnerability index, that combine high-resolution hydrological and hydraulic models with socioeconomic indicators, enabled the implementation of updated flood adaptation policies (El Zein *et al*., 2021).

In Argentina, approximately one in three inhabitants resides in flood-prone areas (Foro Ambiental, 2017). Several studies at a national scale have focused on delineating high-risk flood areas, taking into account hazard and vulnerability maps (Angheben, 2012; Herrero *et al*., 2018). A recent study revealed that floods in the Río de La Plata river and its tributaries contribute to vulnerability in more exposed areas in metropolitan area of Buenos Aires (Rotger *et al*., 2018). The extreme hydrometeorological events occurrence and scarce prevention and mitigation measures implementation showed a 22% of Santa Fe's population vulnerable to floods in 2019 (Cardoso, 2019). Moreover, the residents of Coronel Suárez (Buenos Aires province) underestimate, according to studies, the real flood risk of the town (Moretto and Gentili, 2021).

In the NE of Argentinean Patagonia, the recurrent Río Negro (RN) and the El Juncal lagoon (non-permanent water body) overflows have historically impeded economic development and population growth in the lower hydrographic basin of the RN (Pérez Morando, 2005; Marizza *et al*., 2010; Brailovsky, 2012; Zabala *et al*., 2021). Specifically, the lower sector of this basin has been affected on numerous times by river floods (AIC, 2020; Brailovsky, 2012; DesInventar, 2021; Diario Río Negro, 2021). The impact of floods has harmed economic growth in the lower RN valley, a major area for fruit and vegetable production of Argentina (Mazzulla, 1974). Floods in this region damage infrastructure like roads, railways, and irrigation networks, reduce agricultural potential through soil erosion and crop destruction, and affect nearby urban areas (AIC, 2020). The city of Viedma, located in the lower part of the RN flood valley between 3.5 and 4.5 meters above sea level (Merg and Petri, 1998), has been the most exposed to river overflow (Brailovsky, 2012).

Since the XIX century, flood mitigation measures have been undertaken by residents in response to frequent floods in the lower hydrographic basin of the RN, including building embankments and

reforesting the riverbank to shield the coast from fluvial erosion and mitigate damage during floods (Reverter *et al*., 2005). Following the catastrophic flood of July 1899 (Brailovsky, 2012; AIC, 2020), interventions such as artificial channels, embankments, and drainage of the El Juncal lagoon were implemented to reduce the impacts of RN floods (Rey *et al*., 1981). Dams located along the Limay and Neuquén rivers have regulated river flow since 1970, while anthropogenic actions stabilized riverbanks in Viedma and Carmen de Patagones during the 1970s and 1980s (Reverter *et al*., 2005). In 2012, the government, through the Departamento Provincial de Aguas de RN, decided to regulate land use along the riverbank lines for flood evacuation caused by high tides and Sudestadas (Southeast wind associated with low-pressure systems. It persists for hours, bringing rain and strong winds that counteract river drainage, leading to an increase in water levels, SMN, 2021). Additionally, in 2018, the municipality of Viedma announced filling and construction works of a slope to protect against river floods, with a maximum height of 4.5 meters above the river level at low tide (ADN, 2018). Despite these actions, the lower hydrographic basin of the RN continues to be affected by river floods (D'Onofrio *et al*., 2010; Brailovsky, 2012; AIC, 2020; DesInventar, 2021; Diario Río Negro, 2021).

According to Municipalidad de Carmen de Patagones (2019), high intensity of winds from SE are the main cause of the floods. Additionally, the increase of the flow of the tributaries (Limay and Neuquén rivers) (UNL-DPA Río Negro, 2004; Romero *et al.,* 2014), during storm pass and high tide, propitiate the flooding (D'Onofrio *et al*., 2010). Historically, the floods that exceeds the 2700 m^3s^{-1} have been recurrent every decade, showing a high probability of floods (UNL-DPA Río Negro, 2004). About the floods susceptibility areal extension and location, the coastal area of the lower hydrographic basin of RN was identified as vulnerable to sea-level rise (Kokot *et al*., 2004). According to a SSRH-INA(2002) proposal, the 46.7% of the lower RN Valley area exhibited susceptibility to river floods medium to high (García Bu Bucogen *et al*., 2021). Despite some previous studies on flooding risk in Carmen de Patagones, there is still limited research that has analyzed the flood risk of the RN in this area. This study aims to provide a flood risk map in this area, to contribute with the knowledge for the development of facilitating decision-making and of preventive and mitigation decisions in the region.

2. Study area

The lower hydrographic basin of RN belongs to the hydrographic system composed of the Neuquén, Limay, and Negro rivers (AIC, 2022) (Fig. 1a). According to Soldano (1947) and the Atlas de Cuencas y Regiones Hídricas Superficiales de la República Argentina (SSRH, 2010), the sector is extended from Segunda Angostura to the RN mouth (into the Atlantic Ocean) (Fig. 1b), at 40°- 41°S and 63°- 64°W, in the NE of Argentine Patagonia (Fig. 1c). The hydrographic basin shows NO-SE orientation, and it covers around 3,000 km^2. RN have a hydrological anastomosed pattern (Pereyra, 2003) without tributary watercourses. It is characterized by the presence of islands, non-permanent lagoons, and secondary branches, some of them correspond to paleochannels, which are activated during exceptional floods (Prates *et al*., 2019). The average streamflow of the NR is 1020 m^3s^{-1} (Gianola Otamendi, 2019). The hydrological cycle of the river starts in March (Romero and González, 2016) and show two annual maximum flows: autumn-winter and during the spring (Gianola Otamendi, 2019).

In the study area, structural plains, river terraces and flat forms at the south represent the landforms (Fabregat, 2010). Regarding the geomorphological processes, there are noted effects of fluvial erosion (Pereyra, 2003). The landscape is characterized by plains, which shows the presence of depressions, palaeochannels and non permament shallow lakes. At the river's mouth in the Atlantic Ocean, banks are formed, giving rise to an open reflux delta (Piccolo and Perillo, 1999; Longo *et al*., 2018). The most developed soil orders, according to the taxonomic classification of Soil Taxonomy (2006), are Aridisols and Entisols, characterized by moderate to poor drainage (Panigatti, 2010). Prominent pedogenetic features reflect a previous cycle of soil formation, with more humid climatic conditions that allowed for argiluviation (Pereyra, 2003). Due to topographic characteristics, permeability, surface runoff, vegetation

cover, and precipitation, the edaphic features in lower hydrographic basin of the RN are prone to water and wind erosion, as well as degradation due to overgrazing (Panigatti, 2010).

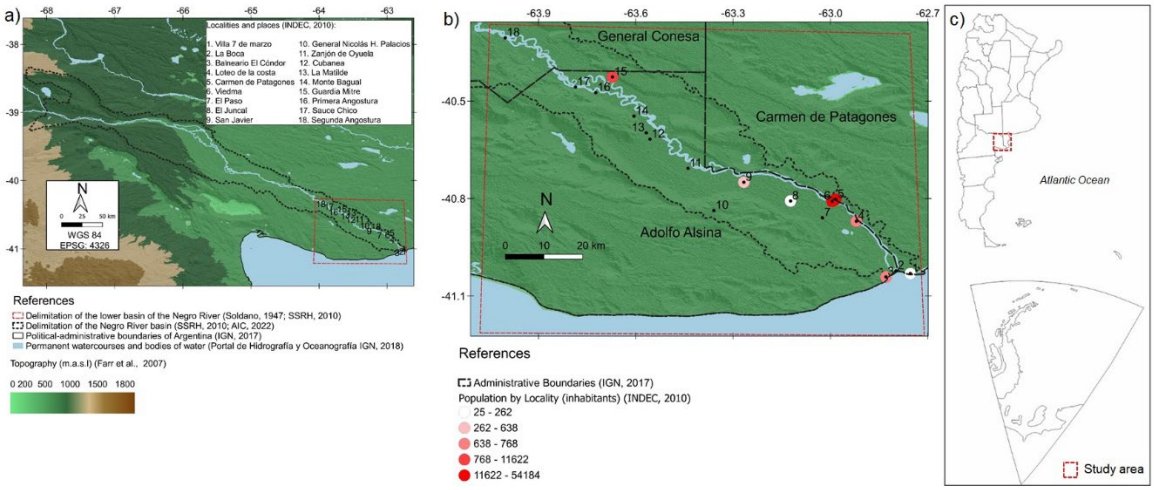

Figure 1. Study area: a) hydrographic basin of the Río Negro, b) lower hydrographic basin of the Río Negro, c) relative location of the study area in the bicontinental Argentinean Map (elaborated by Centro de Documentación Cartográfico Laboratorio de Cartografía Digital. Departamento de Geografía y Turismo, Universidad Nacional del Sur). Other cartographic data sources: Soldano (1947), Farr et al. *(2007), SSRH (2010), INDEC (2010), and IGN (2018 and 2022).*

According to Köppen-Geiger climatic classification (Chen and Chen, 2013), the study area is semi-arid temperate with dry summers. Seasonal climatological variability is defined by atmospheric circulation, topography, and proximity to the sea (Prohaska, 1976; Coronato *et al.*, 2017), with simple and persistent atmospheric patterns derived from the movement of high and low-pressure centers (Prohaska, 1976; Paruelo *et al*., 1998; Coronato *et al*., 2017). Annual precipitation is around 400 mm $year^{-1}$ (Bianchi, 2016). During summer, the movement of high-pressure systems generates arid conditions with sporadic convective precipitations (Gentile *et al.*, 2020). During winter, cold fronts and low pressures cause precipitation, while moist winds from the east, during South Atlantic blocking events, favor winter and spring rains (Gentile *et al*., 2020). The annual temperature ranges between 14 and 16°C, with maximum and minimum values in January and July, respectively (Coronato *et al*., 2017). The latitudinal position of the South Atlantic anticyclone determines the prevailing wind regime in the sector, moving southward in summer, with northeast and east winds prevailing (Musi Saluj, 2018). In winter, it moves northward, with west winds predominating (Frumento, 2017). Occasionally, the combination of high Atlantic pressure and cyclogenesis produces "Sudestadas" with strong south winds associated with a temperature decrease and precipitation. Sometimes, the described conditions cause severe flooding (UNL-DPA Río Negro, 2004).

The study area is located between Adolfo Alsina (Buenos Aires province) and Conesa (Río Negro province) districts. Some localities and cities are Loteo Costa de Río, El Juncal, San Javier, Guardia Mitre, Viedma and Carmen de Patagones cities (Table 1) (INDEC, 2010). Additionally, there are several rural settlements, such as Villa 7 de marzo, La Boca, El Paso, General Nicolás H. Palacios, Zanjón de Oyuela, Cubanea, La Matilde, Monte Bagual and Sauce Chico (Fig. 1b). According to the 2010 Census, the total population of the study area was 77,910 inhabitants (INDEC, 2010). Historically, the Viedma-Carmen de Patagones region show an increasing population (Table 1) (INDEC, 2001; 2010; 2022). The relevant economic activity in the area focuses on intensive agriculture under irrigation and livestock farming (Brailovsky, 2012).

Table 1. Demographics of the localities located in the study area (period 1960 - 2022). Based on data from INDEC (2001, 2010, and 2022)

Census/locality	Inhabitants		
	Census 2001	**Census 2010**	**Census 2022**
Viedma	46,948	52,789	62,000
Patagones	18,189	20,532	-
Viedma-Carmen de Patagones	65,137	73,322	92,914
El Juncal	61	83	-
San Javier	392	530	-
Guardia Mitre	582	856	-

3. Data and methods

A risk mapping was elaborated considering the geographical framework where the hazard and the vulnerable population interact (Ayala-Carcedo, 2000; Ribas and Saurí, 2006; Ríos and Natenzon, 2015; Renda *et al*., 2017; Zapperi and Olcina, 2021). The risk level was estimated following the methodology proposed by Renda *et al*. (2017) and its estimation was organized into three analyses: hazard, vulnerability, and risk (Fig. 2).

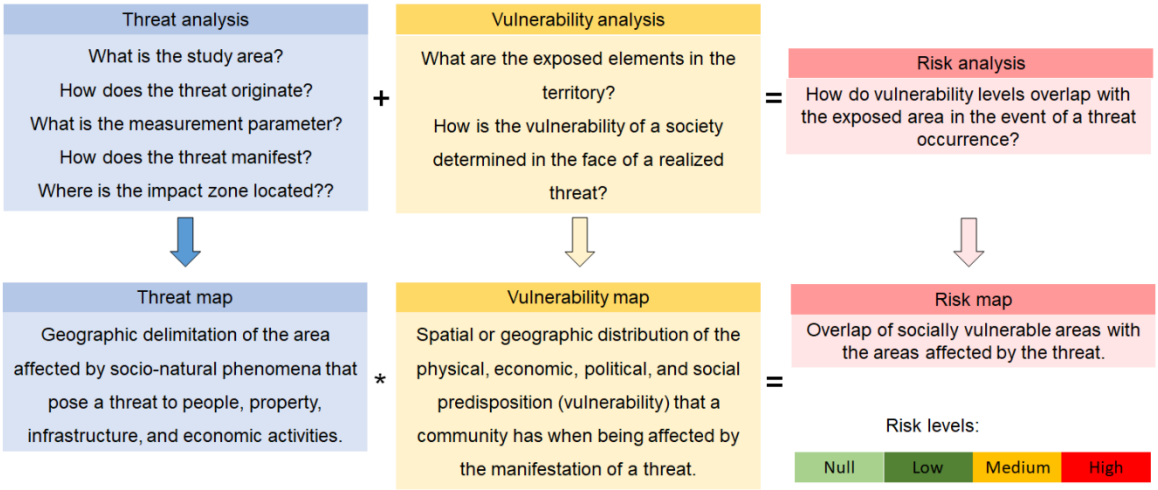

Figure 2. Methodological diagram employed for the mapping of flood risk in the study area. Based on the methodology proposed by Renda et al. *(2017).*

3.1 Hazard Analysis

In the context of hazard analysis, various stages were undertaken following the Renda *et al*. (2017) guidelines. A literature review related to the occurrence of floods and its main causes in the study area, was done. The main source of information was the DesInventar database (DesInventar, 2022) and press articles (Petri, 1992; Río Negro Online, 2001; Río Negro Online, 2003; La Nueva, 2006; Diario la Palabra, 2009; D'Onofrio *et al*., 2010; Brailovsky, 2012; Diario Río Negro, 2014; Diario Río Negro, 2018a; Diario Río Negro, 2018b; ADN, 2019; Diario Río Negro, 2019; Noticias Río Negro, 2019; Red de Alerta de sudestadas, 2020; Diario Río Negro, 2021; Livigni, 2022).

As the most common factor leading to floods is the occurrence of intense winds and precipitation, and extraordinary increases in river flow (D'Onofrio *et al*., 2010), the Gumbel distribution was calculated to model the distribution of maximum values and their return periods (Gumbel, 1941). Wind speed and precipitation data were obtained from the Servicio Meteorológico National (SMN,

2021) database, Viedma Aero station (40°52'00'' S and 63°00'00'' W). The study of RN floods was based on streamflow data analysis from the Primera Angostura (PA) station (SNIH, 2021). The function was defined according to the methodology published by USACE (2006), and Mayo and Mitrani (2022) (Eq. 1):

$$F(x) = \exp\left[\exp\left[\frac{x-B}{A}\right]\right] \quad (1)$$

where the coefficients are defined as follows: A = 0.779s and B = x − 0.45s. In this case, x is the mean value. The return period (Pr) is calculated according to the following expression (USACE, 2006) (Eq. 2):

$$P_r = \frac{1}{1-P_a} \quad (2)$$

where P_r and P_a are the return period in years and the cumulative probability.

The delimitation of the affected area by flooding was carried out through a Multicriteria Evaluation (MCE). This approach involved the precise delineation of the flood-prone area, using spatial assessments of factors that determine the susceptibility of the area to the phenomena occurrence (Olivera Acosta *et al*., 2011; Carrascal *et al*., 2018; García Bu Bucogen *et al*., 2021). As the main limitation for the MCE estimation was the accessibility to historical flood maps, the Maximum Extent of Water Coverage (MEWC) was delineated. MEWC's estimation was done using extremely humid periods and for this purpose, the Standardized Precipitation and Evapotranspiration Index (SPEI) data (spei.csic.es) (Vicente-Serrano *et al*., 2010) was employed. The SPEI time series acquisition was performed specifically for the geographic coordinates 40°45'00" S and 63°15'00" W (the available grid close to Viedma). For the areal analysis of the water coverage, satellite data were analysed during the periods in which the SPEI indicated extremely wet (SPEI ≥ 2.00) and very wet (1.99 ≥ SPEI ≥ 1.50) conditions (Vicente-Serrano *et al*., 2010). The satellite data, corresponding to Landsat 8 OLI/TIRS Level 2 product (freely accessible), were provided by the United States Geological Survey (USGS) (https://earthexplorer.usgs.gov) (USGS, 2021) (Fig. 3). Satellite images with cloud coverage of less than 10% were utilized from 1998 to 2021, with a spatial resolution of 30 meters.

The Normalized Difference Water Index (NDWI) was employed to delineate water bodies and flows from satellite images corresponding to very and extremely wet periods, using the near-infrared and shortwave bands of the Landsat 8 OLI/TIRS product through the SNAP software (Fig. 3). The digital processing was performed considering NDWI values greater than 0.0 in the QGIS GIS, an open-source tool (QGIS, 2024) (https://qgis.org/es/site/). Subsequently, a reclassification was done to assign the weights for every variable in the MCE. The assigned values were from 10 (areas covered by water) to 1 (areas with absence of water coverage).

Also, MCE using geographic, geomorphological and geospatial characteristics from freely accessible repositories of official organizations (SAGyP-INTA, 1990; Volante *et al*., 2009; SSRH, 2010). Geomorphological features, drainage, and soil texture were derived from soil maps (Scale 1: 250,000) (Carta de suelos de la República Argentina, SAGyP-INTA, 1990). The digital cartography of land cover was elaborated based on the Mapa de Cobertura del Suelo de la República Argentina (Volante *et al.* 2009). The delimitation of the lower hydrographic basin of RN was according the criteria published by Soldano (1947) and the Atlas de Cuencas y Regiones de Aguas Superficiales de Argentina (SSRH, 2010). Subsequently, the assignment of weights, the prioritization of variables, and the mapping of the flood-affected area were based on previous research (Olivera Acosta *et al.*, 2011; Carrascal *et al.*, 2018; García Bu Bucogen *et al.*, 2021). Based on the results obtained, subzones were delineated according to estimated level of susceptibility to the flood hazard, as following: non susceptible, low, medium, and high.

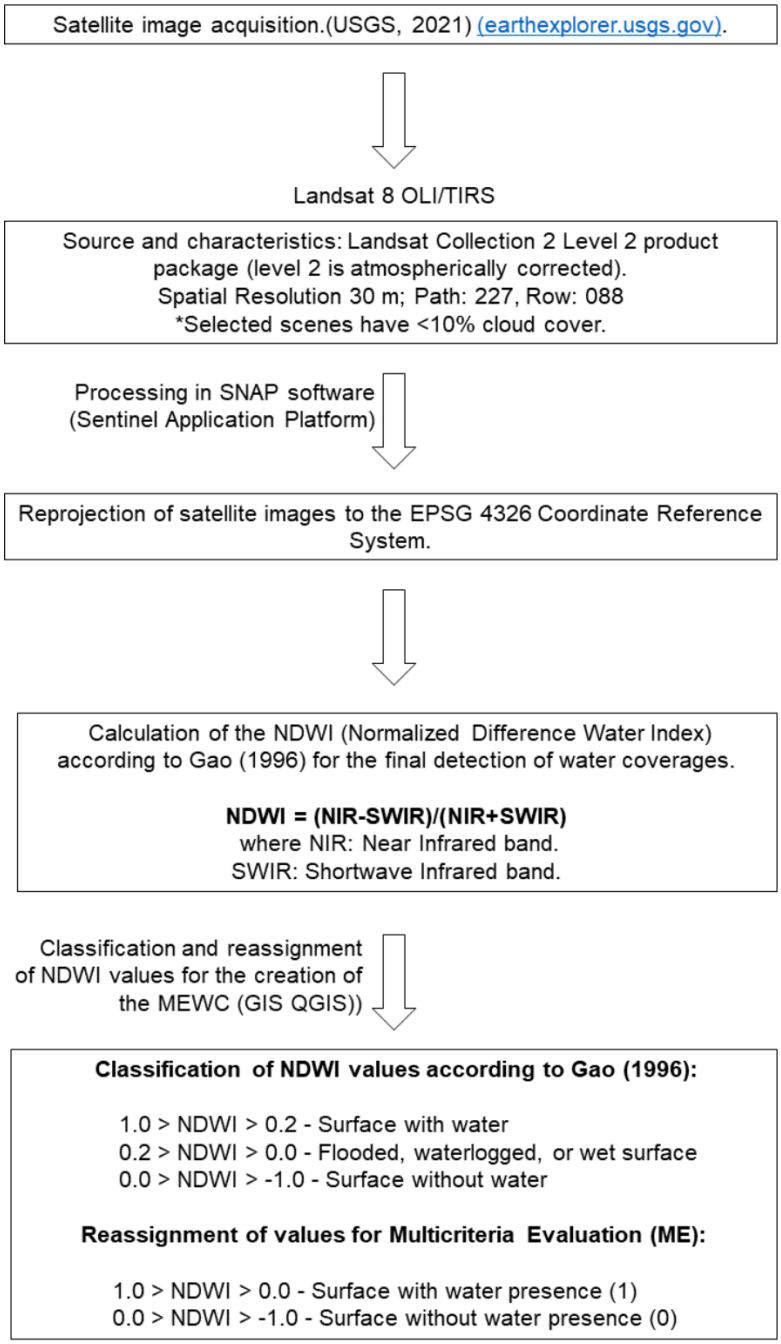

Figure 3. Methodological framework to delineate the Maximum Extent of Water Coverage.

3.2 Vulnerability Analysis

Data on demographics, public service infrastructure, housing construction quality, population overcrowding, individuals with private health coverage (social security), and illiteracy were sourced from the 2010 Population Census provided by the Instituto Nacional de Estadística y Censos (INDEC) of Argentina and compiled by AEROTERRA (2022) (https://datosabiertos.aeroterra.com). The results were based on the 2010 Census data due to the unavailability of socio-economic indicators—such as the percentage of the population with unmet basic needs, housing condition, overcrowding, and unemployment—necessary for vulnerability studies. Additionally, information on streets and roads was obtained from the IGN Transport Portal (2022). The analysis was conducted at the department/municipality level for most indicators, while literacy data were analyzed at the census zone level.

The vulnerability analysis involved evaluating structural poverty conditions (structural poverty refers to entrenched and persistent poverty conditions deeply rooted in the socio-economic structure of a society, often characterized by a lack of access to basic resources such as education, healthcare, adequate housing, decent employment, and economic opportunities). To estimate the vulnerability, the physical, social, and organizational indicators were analyzed according to the Renda *et al*. (2017). The Unsatisfied Basic Needs Index (in Spanish, NBI) was used to map vulnerability to floods, considering households with at least one of the five essential deprivations described in INDEC (2013). Additionally, following the criteria of Renda *et al*. (2017), other vulnerability indicators summarized in Table 2 were considered. The classification of indicators was done by assigning values of 0 and 1, where 0 represented non-vulnerable conditions and 1 indicated high vulnerability. To analyze the population vulnerability associated to the access to the road network were utilized Daga *et al*. (2015) criteria.

Table 2. Criteria used to calculate the degree of vulnerability. Based on the criteria published by Renda et al. (2017)

Indicator	Analysis Unit	Categories	Source
Population concentration	Census zone	0: Moderately populated areas. 1: Densely populated areas and sparsely populated areas.	INDEC (2010)
Access to road network	Department / municipality	0: Distance to road network less than 300 m. 1: Distance to road network greater than 300 m.	Portal Transporte IGN (2022)
Access to basic services	Census zone	0: Low percentage of households with access to public services. 1: High percentage of households with inaccessibility or deficiency in access to public services.	INDEC (2010)
Housing construction status	Census zone	0: Limited number of houses with construction deficiencies. 1: High number of houses with construction deficiencies.	INDEC (2010)
Population age structure	Census zone	0: High percentage of population aged between 14 years <= age <= 65 years. 1: High percentage of population aged <=14 years and >= 65 years.	INDEC (2010)
Overcrowding	Census zone	0: Low percentage of households with critical overcrowding. 1: High percentage of households with critical overcrowding.	INDEC (2010)
Access to medical coverage	Census zone	0: Low percentage of population without health insurance. 1: High percentage of population without health insurance.	INDEC (2010)
Literacy level	Departament / Municipality	0: Low percentage of population over 10 years old who are illiterate 1: High percentage of population over 10 years old who are illiterate	INDEC (2010)

Population concentration is considered when analyzing vulnerability to floods, as densely populated areas can result in a greater number of people being affected by these events, while in sparsely populated areas, such as dispersed rural areas, rescue and assistance efforts may be more difficult due to limited accessibility. Access to road networks influences the population's mobility capacity. Inaccessibility or lack of access to basic services, along with precarious housing conditions, play a significant role in vulnerability to floods as they hinder the population's ability to cope with and recover from the impacts of these events. The population whose age is lower than 14 years old and highest than 65 years old is considered more vulnerable to floods effects than the other age's stages. Overcrowding

is a condition of fragility that provides crucial information for effective evacuations. Additionally, it was found that the population without medical coverage is highly exposed to suffering from diseases after floods. High levels of illiteracy due to their impact on job opportunities, economic conditions, and access to housing can increase the population's vulnerability in disaster situations.

Vulnerability map was generated by a map algebra for the criteria mentioned in Table 2 and QGIS GIS (QGIS.org) software. Vulnerability subzoning was defined using Delménico *et al*. (2018) classification criteria, where non-vulnerable areas have only one high indicator, while sectors with at least two, four, and five indicators are classified as low, medium, and high vulnerability, respectively.

3.3 Risk Analysis

After conducting the hazard and vulnerability analyses and obtaining their respective maps, the subzoning of the study area according to its flood risk levels was delimited according the methodological steps shown at the Figure 2 and QGIS GIS functions. The resulting layer was obtained by sum of variables of the affected area (HM) and vulnerability (MV). The risk map (RM) was obtained according to the criteria identified in Table 3.

The number of households and inhabitants residing in high and medium-risk areas in 2010 was identified using INDEC (2010) data. The sensitivity of the results found in the risk analysis was evaluated qualitatively, comparing the results obtained in the RM with flood records provided by Desinventar database (2021) and several newspapers.

Table 3. Applied criteria to calculate the level of flooding risk

Hazard's level	Vulnerability's level	Risk's level
High or High / Medium	High or Medio/ High	High
Medium or Medium /Non susceptible	Medium or Low/ Medium	Medium
Low or Low /Non susceptible	Low or Non vulnerablel/ Low	Low
Non susceptible	Non vulnerable	Null

4. Results

4.1. Floods: recurrence and causes

Between 1899 and 2021, a total of 32 floods were reported by several sources (Table 4). These reports showed that 50% of the cases were triggered by the combination of intense rainfall and winds. Additionally, upstream water discharges from the Limay and Neuquén rivers (Fig. 1a) were responsible of 25% of the floods. Finally, the remaining 25% occurred resulting of the interaction between increased upstream flow from the lower hydrographic basin of the RN and the occurrence of extreme meteorological events.

The recurrence of intense winds, precipitation, and high flows was calculated using the Gumbel statistical distribution at a 95% confidence level, taking into account that floods in the lower RN basin are caused by strong south winds, intense precipitation, and increased upstream flow (Table 4). The results showed that, over a period of 100 years, there is a 1% probability of wind speeds exceeding 120 km/h, while winds exceeding 95 km/h have a 10% probability, and winds exceeding 75 km/h have a 50% probability (Fig. 4a). In terms of precipitation, events surpassing 37 mm in 24 hours have a 50% probability of occurring within a 2-year return period (Fig. 4b). Furthermore, for return periods of 20 and 50 years, the maximum precipitation can exceed 70 mm and 84 mm. The analysis of extreme values reveals that, over a period of 100 years, there is a 1% probability of floods with flows exceeding 4000 m^3/s, while events with flows greater than 2800 m^3/s and 2415 m^3/s have 10% and 20% probabilities, respectively (Fig. 4c).

Table 4. Reports of floods and waterlogging events in the lower Río Negro basin (1829-2021). In the 'Flooding Causes' column, a '' indicates that the cause of the flood was not found referenced in the literature."*

Date	Flooding causes	Affected localities	Source of data
1829	Strong winds and intense precipitation	Viedma	Rey *et al*., (1981)
1870	*	Viedma	Rey *et al*., (1981)
19 - 22/07/ 1899	upstream flow increases ($9{,}000\ m^3s^{-1}$)	San Javier, Guardia Mitre, Zanjón de Oyuela and Viedma	Brailovsky (2012) Livigni (2022)
1904	*	Viedma	Brailovsky (2012)
1914	*	Viedma and San Javier	Brailovsky (2012)
1922	*	Viedma	Brailovsky (2012)
1930	Increase in upstream flow	Viedma	Brailovsky (2012) Rey *et al*., (1981)
1932	*	Viedma	Brailovsky (2012)
1937	*	Viedma	Brailovsky (2012)
1940	*	Viedma	Brailovsky (2012)
1945	Increase in upstream flow ($6{,}500\ m^3s^{-1}$)	Viedma	Brailovsky (2012)
1949	*	Viedma	Brailovsky (2012)
1951	*	Viedma	Brailovsky (2012)
1958	*	Viedma and Guardia Mitre	Brailovsky (2012) Río Negro (2001)
1974	*	Viedma	Brailovsky, 2012
2/02/1976	Intense precipitation	Viedma	DesInventar (2021)
27/09/1976	Intense precipitation (30 mm) and strong winds	Viedma	DesInventar (2021)
8/10/1977	Intense precipitation	Viedma	DesInventar (2021)
03/1992	*	Viedma	Petri (1992) D'Onofrio *et al*. (2010)
6/08/2001	upstream flow increases and intense precipitation (50 mm)	Guardia Mitre	Río Negro (2001)
20/02/2003	Extraordinary tides associated with permanent S winds	Viedma	Diario Río Negro (2003)
10/07/2003	Intense SE winds	Viedma	Río Negro Online (2003)
29/07/2006	Release of water flow from dams located on the Limay and Neuquén rivers in conjunction with strong south winds (60 km/h) and high tide	Viedma	La Nueva (2006)
22/07/2009	Strong S winds	Viedma and Carmen de Patagones	Diario la Palabra (2009)
22/02/2010	Intense precipitation	Carmen de Patagones	DesInventar (2021)
4/01/2014	Conjunction of extraordinary tides and SE winds	Viedma	Diario Río Negro (2014)
21/06/2018	Release of 600 m³ of water from dams on the Limay and Neuquén rivers	Viedma and Carmen de Patagones	Diario Río Negro (2018a)
24/06/2018	Strong winds (Sudestada)	Viedma	Diario Río Negro (2018b)
23/02/2019	Increase in river flow combined with an extraordinary tide and strong southerly winds	From RN mouth to San Javier	ADN (2019) Diario Río Negro (2019)
3-4/09/2019	Strong winds (Sudestada)	Viedma	Noticias Río Negro (2019)
4/07/2020	Release of upstream flow in interaction with high tide	Viedma	Red de Alerta de sudestadas (2020)
26-27/05/2021	Increase in flow rates in conjunction with high tide and southerly winds.	Viedma and Carmen de Patagones	Diario Río Negro (2021)

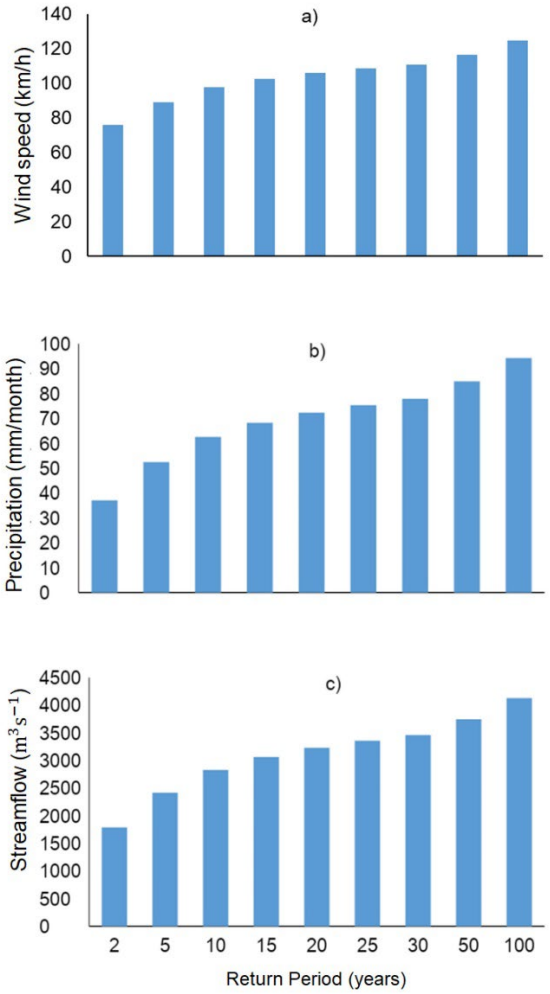

Figure 4. Recurrence of events capable of favor floods through by Gumbel Distribution (1981 - 2020): a) wind speed, b) precipitation, c) streamflow. Based on SMN (2021) and SNIH (2021) data.

4.2. Delimitation of the area affected by floods: hazard map

During 2015, the SPEI (12-month scale) categorized the period of January to August as extremely humid whereas the period from September to December was defined as very humid. For this reason, for the delineation of the maximum area affected by floods, the MEWC was defined according to the climatic conditions of 2015. Satellite data corresponding to the following dates: January, 18th; March, 23rd; July, 13rd and October, 17th, were selected for the analysis. MEWC was delineated by NDWI calculation for the previously mentioned images. Finally, the satellite images were averaged to obtain the representative value of MEWC for the period 1998-2021.

After obtaining the MEWC, the weights were assigned to the geographical, geomorphological, and geospatial shapes according to the criteria published by García Bu Bucogen et al. (2021). Finally, the MCE was completed. In this step, the study area was classified based on its flood susceptibility levels (Table 5), using the criteria adapted from Montecelos Zamora (2010) for this investigation.

High and medium levels of susceptibility were observed in a large portion of the northern area (Fig. 5), with 44.7% of the study area exhibiting these susceptibility levels to floods (Fig. 6). The subzones with medium levels covered 1,396.5 km^2, representing 41.7% of the study area's surface. Areas with high hazard levels were extended over 101.2 km^2 (3.0%). Finally, the subzones with low susceptibility and non-susceptibility to the occurrence covered 1,847.3 km^2 (55.3% of the total study area).

Table 5. Hazard's levels obtained from Multicriteria Evaluation. Based and adapted from Montecelos Zamora (2010) criteria

Hazard's levels	Values range
Non susceptible	0 – 3
Low	3.1 – 5
Medium	5.1 – 8
High	≥ 8.1

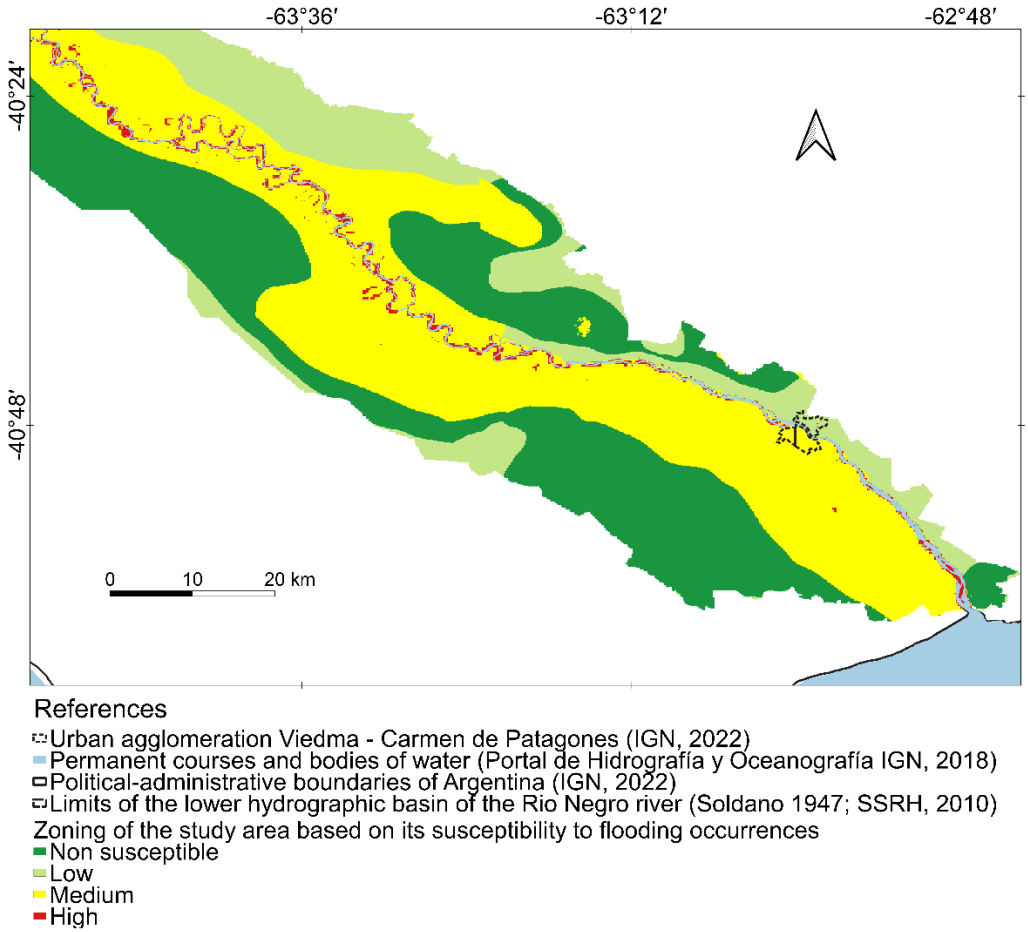

Figure 5. Subzones of flooding susceptibility in the lower hydrographic basin of the Río Negro.

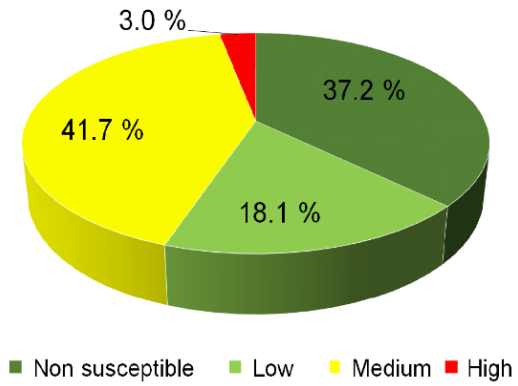

Figure 6. Areal extension (%) of the estimated susceptibility classes in the lower hydrographic basin of the Río Negro.

4.3. Vulnerability analysis

The vulnerability classes were estimated based on the 2010 Population Census data and evaluation criteria proposed by Daga *et al.* (2015), Renda *et al.* (2017) and Delménico *et al*. (2018). In this case, the objective was determining the magnitude of the vulnerability of the local population. The final map showed a spatial resolution of 122 x 149 meters.

The spatial distribution of vulnerability levels showed (Fig. 7) high vulnerability in areas close to the banks of the RN. The peripheral zones of the urban conglomerate Viedma - Carmen de Patagones were identified as high vulnerability areas. Carmen de Patagones town exhibited a low to medium vulnerability level. The area close to the riverbank showed a medium to high vulnerability level. Moderate vulnerability levels were detected in the SW and NW of the study area.

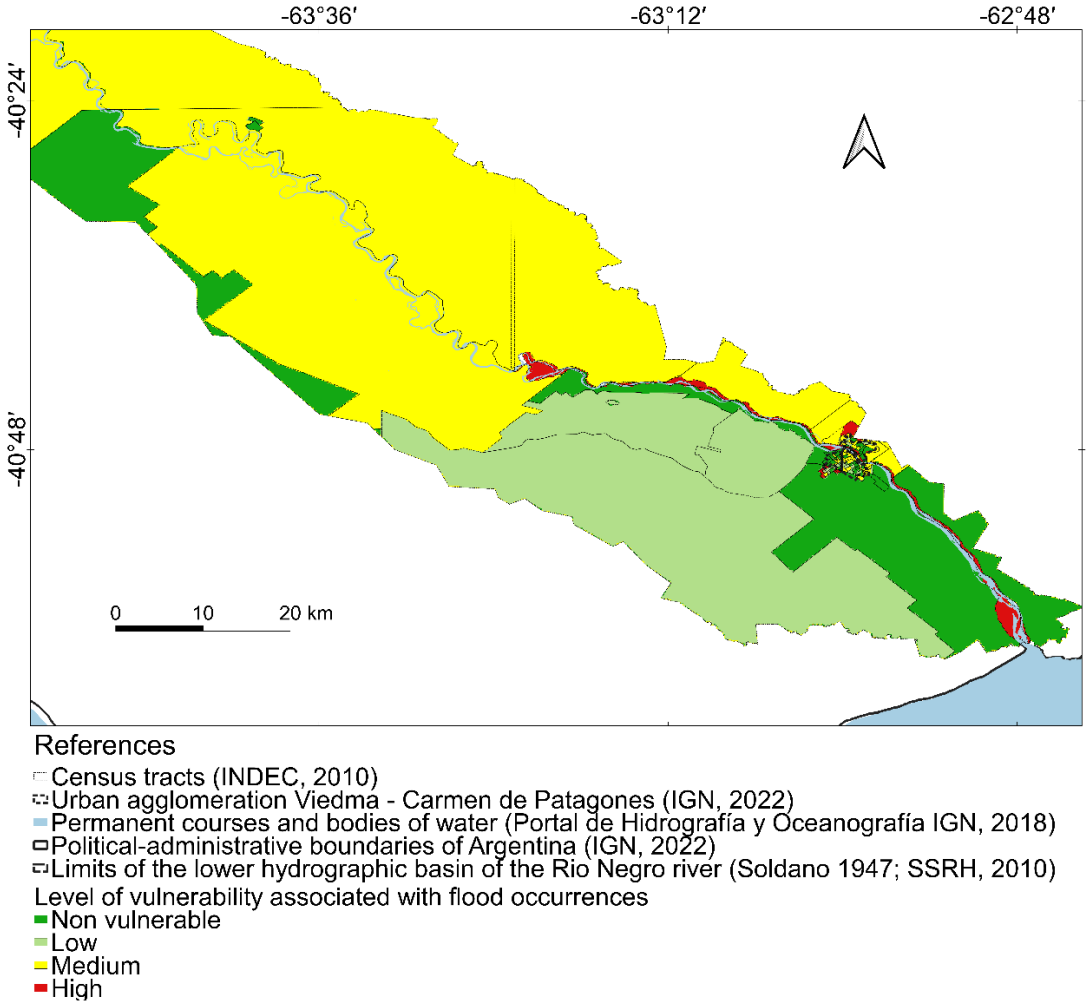

Figure 7. Vulnerability map of the occurrence of riverine floods in the study area.

According to INDEC data (2010), the 51.0% (~ 33,636 inhabitants) of the population in the study area was classified with medium and high vulnerability to RN overfloods (Fig. 8). The 49.0% (~ 44,274 inhabitants) of the total population was included at the low or non-vulnerable levels of vulnerability.

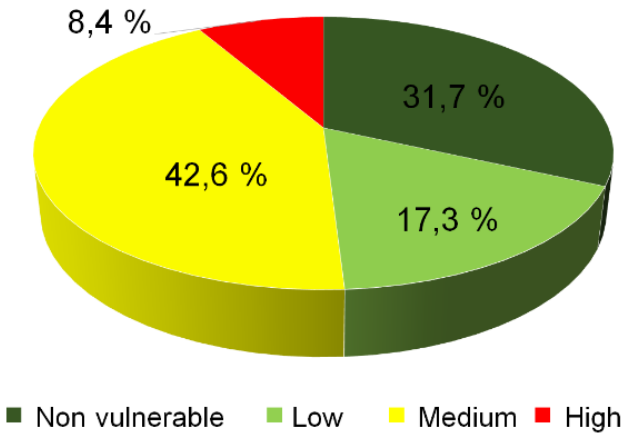

Figure 8. Percentage of inhabitants who lived in vulnerable areas. Based on INDEC data (2010).

4.4. Risk analysis

After conducting hazard and vulnerability analyses, the algebraic sum of both maps allowed the mapping of the risk of flooding occurrences (Renda *et al*., 2017). The RM showed a spatial resolution of 136x176 m, and risk levels were classified according to the criteria identified in Table 3. High-risk zones for flooding were detected on the banks and mouth of the RN (Fig. 9). Additionally, areas with a medium level of risk were located on the outskirts of Viedma. The risk derived from RN floods was medium on the Viedma riverbank, while the risk was low for the rest of the city. The risk distribution in Carmen de Patagones town was heterogeneous.

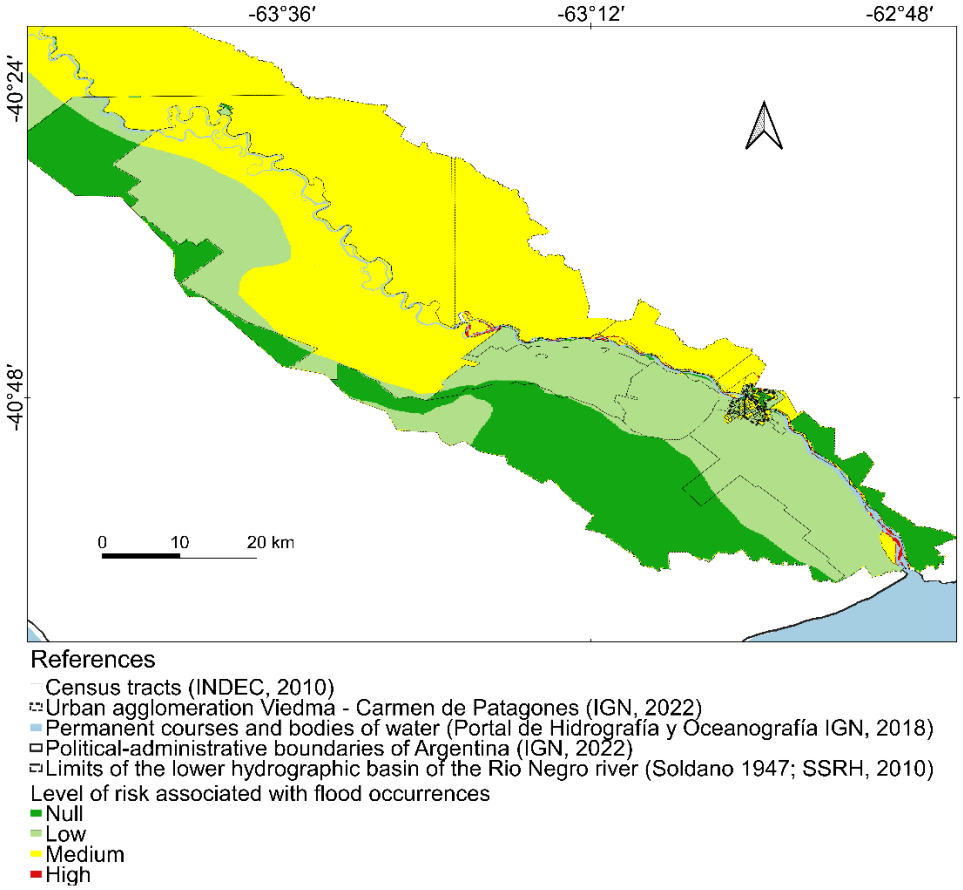

Figure 9. Flood risk map in the study area.

In 2010, 43.2% of the total population of the study area was located in areas categorized as high and medium-risk levels (Fig. 10). The population who lives in high-risk areas were quantified at 1,239 people, while 32,397 residents (41.6% of the total population of the study area) lived in areas with a medium level of risk. The high-risk conditions reported in the lower basin of the RN were due to the location of homes in areas with high levels of susceptibility to flooding (Fig. 5) and unfavorable socioeconomic conditions (Fig. 8). Viedma, Carmen de Patagones, and Guardia Mitre towns showed medium and high-risk levels.

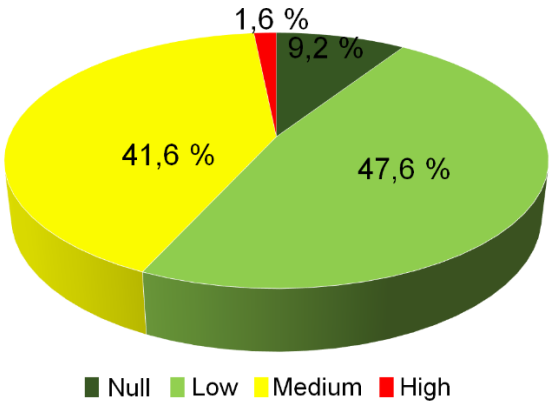

Figure 10. Percentage of inhabitants who lived in flooding risk areas in the lower basin of the Río Negro River in areas with no risk, low, medium and high risk. Developed based on INDEC data (2010).

5. Discussion

Floods are extreme events that have devastating consequences, especially in areas where the vulnerability of the population is high. In the lower basin of the RN, historical floods have caused devastating effects (Petri, 1992; Río Negro, 2002; La Nueva, 2006; D'Onofrio *et al.,* 2010; Brailovsky, 2012). Despite ongoing efforts to regulate floods in the study area (Reverter *et al.,* 2005), the danger persists, as the risk of river overflow cannot be completely mitigated (AIC, 2020).

The complexity of these events requires a holistic understanding that not only considers environmental and geophysical factors but also the social and economic components that influence the vulnerability of communities. This integrated approach allows for a more comprehensive risk assessment and facilitates the design of more effective and equitable mitigation strategies. By simultaneously addressing the physical dimensions of the phenomenon and the socioeconomic conditions, a more accurate view of high-risk areas is obtained, and the most vulnerable populations are better identified, which is essential for disaster planning and management.

Internationally, several authors have conducted risk studies that combine extreme events with social, economic, and physical indicators to estimate risk levels (Birkmann *et al.,* 2013; Godfrey *et al.,* 2015). For example, in Germany, the use of this conceptual framework allowed the observation that low-income populations near the Rhine, Elbe, and Danube rivers are especially vulnerable to flooding (Fekete, 2010). In the USA, it was found that residents of mobile homes and racial minorities are more vulnerable to these phenomena (Tate *et al.,* 2021). In Kaohsiung (Taiwan), mitigation strategies were proposed following an urban flood risk assessment (Liu et al., 2021). In Marrickville (Australia), flood emergency policy and service planning were improved after estimating a vulnerability index that combines hydrological models with socioeconomic indicators (El Zein *et al.,* 2021).

In Argentina, risk indicators have been established that relate adverse phenomena to physical and social vulnerability (Angheben, 2012; Herrero *et al.,* 2018). An example of this, embedded in the study area, was the study conducted by the Municipalidad de Carmen de Patagones (2019), which

identified high and medium vulnerability levels in the peripheral areas of the urban core. On the other hand, in the town center and most of the eastern bank of the RN, vulnerability was low, except for the western bank of the river, where vulnerability was high. The risk of flooding was high in peripheral sectors of the city. Studies more focused on the susceptibility analysis of flood occurrence showed that the coastal sector presents moderate to high vulnerability to sea level rise (Kokot *et al.,* 2004), while approximately 46.7% of the lower valley shows medium to high susceptibility to flooding (García Bu Bucogen *et al.,* 2021). Finally, adverse meteorological conditions, such as storms and heavy rains, can trigger floods in the study area (Table 4).

In this study, a conceptual framework was established to understand the area's susceptibility to hazards and the vulnerability of its inhabitants, allowing for a flood risk study. The subsequent development of flood risk maps identified areas with a higher probability of disaster events. The findings of this study regarding the vulnerability of the peripheral sector and the western sector of the Río Negro bank for Carmen de Patagones are consistent with the results of the Municipalidad de Carmen de Patagones (2019) study, although they differ with the vulnerability detected on the eastern bank of the river, which was indicated as medium-high. The detected differences may be attributable to variations of indicators, scales, or data used. Furthermore, differences in data spatial resolution, information availability, and analysis methods may contribute to the observed variations. The Gumbel distribution analysis shows a 50% probability of floods due to strong winds (return period of 2 years) and a 10% probability of floods due to heavy rainfall (return period of 10 years). Additionally, it was estimated that floods associated with flows exceeding 2800 m^3/s in Primera Angostura have a 10% probability of occurrence (return period of 10 years), surpassing the flood susceptibility threshold (2700 m^3/s) established by UNL-DPA Río Negro (2004).

The main limitation of this study was the use of outdated data (INDEC, 2022). Although data from the 2010 National Population and Housing Census (INDEC, 2010) were used, the population's vulnerability may have changed since then. However, the results obtained are a valuable precedent for studying flood risk in this area. With the population growth reported by the 2022 Census (INDEC, 2022) in the urban conglomerate of Viedma-Carmen de Patagones (Table 1), the number of vulnerable individuals has likely increased. Therefore, the methodology used remains relevant and can be applied in the future after the final publication of the 2022 Census data.

The areas of highest flood risk in the study area are coincident with the zones where the most flood occurrences were reported (Table 4), demonstrating that the methodology used provides an accurate representation of the areas at greatest flood risk. This suggests that it can be a useful tool for decision-makers in disaster risk management. However, it is important to note that risk validation is an ongoing process that requires constant monitoring to ensure the accuracy and relevance of the results.

6. Conclusions

Despite significant efforts in constructing various defensive structures that have mitigated flood-related damages in the RN region, the level of risk remains considerable. The analysis results showed that 43.2% of the population in the study area was residing in medium and high-risk zones in 2010. Of this total, 1.6% of the inhabitants were in high-risk areas, with their homes located near the riverbank and on the outskirts of the Viedma-Carmen de Patagones region.

The susceptibility of areas near the river is due to geomorphological characteristics, including a natural propensity for flooding and river flow dynamics. This risk is exacerbated by social factors such as population density, infrastructure quality, and socioeconomic conditions. These results highlight the need for a comprehensive and multidimensional flood risk assessment that integrates both physical and social aspects. Such integration will enhance understanding of risk factors and support the development of more effective mitigation strategies. Risk management policies and urban development plans should incorporate these findings to address flood preparedness and response deficiencies.

The study's information can guide future research and the implementation of measures to reduce risk in vulnerable areas. Collaboration among local authorities, urban planners, and the community is essential for designing and implementing solutions that improve resilience to flooding. Continuous monitoring and adjustment of strategies are also crucial as new data emerges and local conditions evolve.

Acknowledgments

This work is supported by the Research Project (PGI) Hydrological vulnerability and environmental problems in plain hydrographic basins (Argentina), funded by UNS. The authors also thanks to the Consejo Nacional de Investigaciones Científicas y Técnicas Institución (CONICET) and Centro de Documentación Cartográfico Laboratorio de Cartografía Digital (Departamento de Geografía y Turismo, UNS) for their support.

References

ADN (Agencia Digital de Noticias), 2018. *Construirán la defensa del río en costanera sur de Viedma.* https://www.adnrionegro.com.ar/2018/04/construiran-la-defensa-del-rio-en-costanera-sur-de-viedma/

ADN (Agencia Digital de Noticias), 2019. *Alertan por crecidas extraordinarias en el río y el mar.* https://www.adnrionegro.com.ar/2019/02/alertan-por-crecidas-extraordinarias-en-el-rio-y-el-mar/

AIC, 2020. *El control de las crecidas. Sistema de Emergencias Hídricas y Mitigación del Riesgo.* Autoridad Interjurisdiccional de las Cuencas de los Ríos Limay, Neuquén y Negro.

AIC, 2022. *Autoridad Interjurisdiccional de las Cuencas de los ríos Limay, Neuquén y Negro.* http://www.aic.gob.ar/sitio/laaic

Aneas de Castro, S. D., 2000. *Riesgos y peligros: una visión desde la Geografía. Scripta Nova* 60. http://www.ub.edu/geocrit/sn-60.htm

Angheben, E., 2012. *Estudio Ecohidrológico de la Cuenca Urbana de La Cava de Villa Itatí. Quilmes, Provincia de Buenos Aires.* [Master's thesis]. Universidad Nacional de La Plata. Buenos Aires. http://sedici.unlp.edu.ar/handle/10915/25864

Ayala-Carcedo, F. J., 2000. La ordenación del territorio en la prevención de catástrofes naturales y tecnológicas. Bases para un procedimiento técnico-administrativo de evaluación de riesgos para la población. *Boletín de la Asociación de Geógrafos Españoles* 30, 37-49.

Bianchi, E., 2016. *Dinámica espacio-temporal de la relación entre el clima y el funcionamiento de los ecosistemas de Patagonia Norte.* [Doctoral thesis]. Universidad Nacional de COMAHUE. Centro Regional Universitario Bariloche.

Birkmann, J., Cardona, O., Tibaduiza, M., Barbat, A., Pelling, M., Schneiderbauer, S., Kienberger, S., Keiler, M., Alexander, D., Zeil, P., Kienberger, S., Keiler, M., Alexander, D., Zeil, P., Welle, T., 2013. Framing vulnerability, risk and societal responses. *Natural Hazards* 67, 193-211. https://doi.org/10.1007/s11069-013-0558-5

Brailovsky, A. E., 2012. *Viedma, la capital inundable* (primera parte). Avaliable at: http://noqueremosinundarnos.blogspot.com/2012/08/viedma-la-capital-inundable-primera.html

Cardoso, M. M., 2019. *Estudio de la vulnerabilidad y la resiliencia en la ciudad de Santa Fe, Argentina: El rol de los servicios urbanos en general y del transporte de pasajeros en particular. Revista de Geografía Norte Grande* 73, 133-159. https://dx.doi.org/10.4067/S0718-34022019000200133

Carrascal, C. N., Bohn, V. Y., Piccolo, M. C., Perillo, G. M. E., 2018. Análisis de la susceptibilidad hídrica en una cuenca de llanura (Buenos Aires, Argentina). *XII Jornadas Nacionales de Geografía Física. Universidad Nacional de la Patagonia San Juan Bosco* - Red Argentina de Geografía Física, Trelew, Argentina.

Coronato, A., Mazzoni, E., Vazquez, M., Coronato, F., 2017. *Patagonia. Una síntesis de su Geografía Física. Río Gallegos*. Ediciones Universidad Nacional de la Patagonia Austral.

DesInventar., 2021. *Inventario de desastres.* https://www.desinventar.org/es/desinventar.html

Diario Río Negro, 2021. *La crecida del rio Negro se hizo notar en la costa de Viedma.* https://www.rionegro.com.ar/la-crecida-del-rio-negro-se-hizo-notar-en-la-costa-de-viedma-1833438/

D'Onofrio, E., Fiore, M., Di Biase, F., Grismeyer, W., Saladino, A., 2010. Influencia de la marea astronómica sobre las variaciones del nivel del Río Negro en la zona de Carmen de Patagones. *Geoacta* 35 (2).

El Zein, A., Ahmed, T., Tonmoy, F., 2021. Geophysical and social vulnerability to floods at municipal scale under climate change: The case of an inner-city suburb of Sydney. *Ecological Indicators* 121, 106988. https://doi.org/10.1016/j.ecolind.2020.106988

Fabregat, E. H., 2010. *La construcción de las representaciones mentales en los alumnos de nivel medio que habitan el valle inferior de Rio Negro.* [PhD thesis]. Departamento de Geografía y Turismo. Universidad Nacional del Sur.

Farr, T. G., Rosen, P. A., Caro, E., Crippen, R., Duren, R., Hensley, S., Kobrick, M., Paller, M., Rodríguez, E., Roth, L., Seal, D., Shaffer, S., Shimada, J., Umland, J., Werner, M., Oskin, M., Burbank, D., Alsdorf, D., 2007 The Shuttle Radar Topography Mission. *Rev. Geophys.* 45 (2), 1-33. https://doi.org/10.1029/2005RG000183

Fenoglio, E. P, 2019. *Inundaciones urbanas y cambio climático: recomendaciones para la gestión.* Secretaría de Ambiente y Desarrollo Sustentable de la Nación, 154 pp., Ciudad Autónoma de Buenos Aires. https://www.argentina.gob.ar/sites/default/files/manualinundaciones.pdf

García Bu Bucogen, G., Piccolo, M. C., Bohn, V. Y., 2021. Estimación de la susceptibilidad a inundaciones en la cuenca inferior de Río Negro (Argentina). *Finisterra – Revista Portuguesa de Geografía* LVI (118). https://doi.org/10.18055/Finis21647

Gianola Otamendi, A. 2019. El Río Negro. Su uso como vía navegable. *Boletín del Centro Naval* 851, 173-174. https://www.centronaval.org.ar/boletin/BCN851/851-GIANOLA-RIO-NEGRO.pdf

Godfrey, A., Ciurean, R. L., Van Westen, C. J., Kingma, N. C., Glade, T., 2015. Assessing vulnerability of buildings to hydrometeorological hazards using an expert based approach – an application in Nehoiu Valley, Romania. I*nternational Journal of Disaster Risk Reduction* 13, 229-241. https://doi.org/10.1016/j.ijdrr.2015.06.001

Herrero, A. C., Natenzon, C. Y., Miño, M. L., 2018. *Vulnerabilidad social, amenazas y riesgos frente al cambio climático en el Aglomerado Gran Buenos Aires.* Programa de Ciudades Área de Desarrollo Económico. https://www.cippec.org/wp-content/uploads/2018/10/DT-172-CDS-Vulnerabilidad-social-amenazas-y-riesgos-frente-al-cambio-climático-Herrero-Natenzon-Miño-septiembre-2018.pdf

INDEC (Instituto Nacional de Estadísticas y Censos. República Argentina), 2010. *Mapas temáticos Censo 2010* (GEOCENSO). https://sig.indec.gob.ar/censo2010/?_ga=2.224146587.1293401755.1651671405-2097421635.1647274886

INDEC (Instituto Nacional de Estadísticas y Censos. República Argentina), 2013. *Definiciones de los indicadores del Censo Nacional de Población Hogares y Viviendas 2010.* Base de Datos REDATAM.

INDEC (Instituto Nacional de Estadísticas y Censos. República Argentina), 2022. *Censo 2022: resultados provisorios.* Instituto Nacional de Estadística y Censos (INDEC). https://censo.gob.ar/index.php/censo-2022-resultados-provisorios/

Kokot, R. R., Codignotto, J. O., Elissondo, M., 2004. Vulnerabilidad al ascenso del nivel del mar en la costa de la provincia de Río Negro. *Revista de la Asociación Geológica Argentina* 59 (3), 477-487.

La Nueva, 2006. El río Negro, a un metro de desbordarse. https://www.lanueva.com/nota/2006-7-29-9-0-0-el-rio-negro-a-un-metro-de-desbordarse (Last access: 20/07/2023).

Liendro Moncada, J.V., Ojeda, E. C., 2018. Aproximación al mapa de susceptibilidad a inundación en la cuenca del río Boconó, Estado Trujillo, Venezuela. *Terra Nueva Etapa,* 34 (55). https://www.redalyc.org/articulo.oa?id=72156172012

Liu, W.C., Hsieh, T.H., Liu, H.M., 2021. Flood Risk Assessment in Urban Areas of Southern Taiwan. *Sustainability* 13, 3180. https://doi.org/10.3390/su13063180

Longo, A.C., Moreira, S., Perillo, G. M. E., 2018. Estudio del impacto de la actividad de los diques de la cuenca del río Negro sobre la evolución geomorfológica de los bancos de sedimentos de su estuario inferior, Río Negro, Patagonia Argentina. [Resumen extendido]. *Séptimo Congreso Argentino de Cuaternario y Geomorfología* (GEOCUAR 2018).

Marizza, M. S., Rapacioli, R., Vives, L., 2010. La problemática aluvional en el Alto Valle del Río Negro, Argentina. *Tecnología, Ciencia y Agua* 1(1), 21-34.

Mazzulla, J., 1974, *El valle inferior del Río Negro como polo de desarrollo.* Tesis doctoral. Universidad de Buenos Aires, Buenos Aires. http://bibliotecadigital.econ.uba.ar/download/tesis/1501-1045_MazzullaJ.pdf

Merg C., Petri D., 1998. *Red Alerta Sudestadas en el Valle Inferior del Río Negro* Departamento Provincial de Aguas. Provincia de Río Negro, Viedma, 21p.

Montecelos Zamora, Y., 2010. *Evaluación de la peligrosidad por tasa de escorrentía superficial en la Cuenca del Río Cauto. Sector Provincia Granma. Cuba.* [Master Thesis]. Instituto de Investigaciones Agropecuarias Jorge Dimitrov.

Moretto, B., Gentili, J. O., 2021. Percepción del riesgo de inundación y anegamiento en el partido de Coronel Suárez (Argentina). *Investigaciones Geográficas* 61, 57-77.

Noticias Río Negro, 2019. *Una sudestada inundó calles de la costanera y afectó varios inmuebles.* https://www.noticiasrionegro.com.ar/noticia/32896/una-sudestada-inundo-calles-de-la-costanera-y-afecto-varios-inmuebles

Olivera Acosta, J., Morales G., García Rivero, A., Salgado, E., López M., Estrada, R., Campos Dueñas, M., 2011. *El uso de los SIG y la evaluación multicriterio (EMC) para la determinación de escenarios peligrosos de inundaciones en cuencas fluviales. Estudio de caso cuenca Guanabo.* Proyección 10, 143-163.

Olcina, J., Ayala-Carcedo, F., 2002. Riesgos naturales, conceptos fundamentos y clasificación. En: F. Ayala-Carcedo y J. Olcina (coord.). *Riesgos Naturales.* Ariel. Barcelona.

ORSEP, 2017. *Organismo Regulador de Seguridad de Presas* - ORSEP https://www.argentina.gob.ar/orsep

Panigatti, J.L., 2010. *Argentina. 200 años. 200 suelos.* Ediciones INTA. Buenos Aires:

Pérez Morando, H., 2005. Inundaciones y mudanzas de pueblos. *Diario Rio Negro.* https://www.rionegro.com.ar/inundaciones-y-mudanzas-de-pueblos-FFHRN05102416241401/

Pereyra, F., 2003. *Ecoregiones de la Argentina.* Anales del SEGEMAR, Buenos Aires.

Petri, D., 1992. *Informe Crecida 1992 en el Curso Inferior del Río Negro.* Departamento Provincial de Aguas. 10p.

Piccolo, M.C., Perillo, G. M. E., 1999. Estuaries of Argentina: a review. In: G.M.E. Perillo, M.C., Piccolo, M. Pino Quivira (eds.). *Estuaries of South America: their geomorphology and dynamics.* Environmental Science Series, Springer-Verlag, pp. 101-132, Berlin.

Portal Geodesia y Demarcación IGN, 2022. *Geodesia y demarcación.* Instituto Geográfico Nacional. https://www.ign.gob.ar/NuestrasActividades/ InformacionGeoespacial/CapasSIG

Portal Hidrografía y Oceanografía IGN, 2022. *Hidrografía y oceanografía.* Instituto Geográfico Nacional. https://www.ign.gob.ar/NuestrasActividades/ InformacionGeoespacial/CapasSIG

Portal Transporte IGN., 2022. *Transporte.* Instituto Geográfico Nacional. https://www.ign.gob.ar/NuestrasActividades/InformacionGeoespacial/CapasSIG

Prates, L. R., Martinez, G. A., Belardi, J. B., 2019. Los ríos en la arqueología de Norpatagonia (Argentina). *Revista del Museo de La Plata* 4(2), 633-656.

Prohaska, F. 1976, The Climate of Argentina, Paraguay and Uruguay. *World Survey of Climatology* 2, 532.

Renda, E., Rozas Garay, R, Moscardini, O., Torchia, N. P., 2017. *Manual para la elaboración de mapas de riesgo.* Ministerio de Seguridad de la Nación, Buenos Aires

Rey, H., Entraigas, J., Vovcon, R., 1981. *De la laguna el Juncal a las chacras del Idevi.* Instituto de Desarrollo del Valle Inferior. https://inta.gob.ar/sites/default/files/libro_laguna_el_juncal_en_pdf.pdf

Reverter, M., Gonzalo Ginés, A., Magnin, S., 2005. Estabilización de márgenes y defensa contra inundaciones en la ciudad de Viedma – Rio Negro. Principios y Aplicaciones en Hidráulica de Ríos. En: H. D. Farias, J. D. Brea y R. Cazeneuve (Editores). *Segundo Simposio Regional sobre Hidráulica de Ríos, Neuquén, Argentina,* 2-4 nov. 2005. http://irh-fce.unse.edu.ar/TC/TC_Reverter_et_al__Estab_Margenes_Viedma.pdf

Ribas, A., Saurí, D., 2006. De la geografía de los riesgos a las geografías de la vulnerabilidad. En: J. Nogué, J. Romero (eds.). *Las otras geografías.* Tirant lo Blanc, pp. 285-300, Valencia.

Rojas Vilches, O., Martínez Reyes, C., 2011. Riesgos naturales: evolución y modelos conceptuales. *Revista Universitaria de Geografía* 20(1), 83-116.

Rotger, D. V., Aversa, M., Jáuregui, E., 2018. Cambio climático, inundaciones y "lagunas" de información. Análisis de inundaciones a través del rastreo de artículos periodísticos en el Gran La Plata (Buenos Aires, Argentina). *Cadernos Metropole* 20 (42), 305-324. https://doi.org/10.1590/2236-9996.2018-4201

SIGMA, 2023. *Mapas de Susceptibilidad.* https://experience.arcgis.com/experience/eedd0b9a835041efbaf04dcaae7bea6f/page/Susceptibilidad/

SSRH–INA, 2002. *Subsecretaría de Recursos Hídricos. Descripción de cuencas hídricas superficiales.* Fecha de consulta: febrero 2020.

SSRH, 2010. *Atlas de Cuencas y Regiones Hídricas Superficiales de la República Argentina.* Subsecretaría de Recursos Hídricos. https://www.argentina.gob.ar/obras-publicas/hidricas/cartografia-hidrica-provincial

Soldano, F. A., 1947. *Régimen de aprovechamiento de la red fluvial argentina.* Módulo III: Región Patagónica. Editorial Cimera. 159 – 219.

UNESCO, 2014. *Gestión del Riesgo de Desastres para el Patrimonio Mundial.* Organización de las Naciones Unidas para la Educación, la Ciencia y la Cultura, https://unesdoc.unesco.org/ark:/48223/pf0000228134

Viand, J., González, S., 2012. Crear riesgo, ocultar riesgo: gestión de inundaciones y política urbana en dos ciudades argentinas. P*rimer Encuentro de Jóvenes Investigadores en Formación en Recursos Hídricos.* Ezeiza, Instituto Nacional del Agua. http://www.ina.gov.ar/pdf/ifrrhh/01_027_Viand.pdf

Zabala, P. L., Aravena, J., Jurio, E., 2021. Urbanización de áreas ribereñas del río Limay en Neuquén y Plottier. *Boletín Geográfico* 43(1), 91-110.

Cuadernos de Investigación Geográfica *Geographical Research Letters*	2024	Nº 50 (2)	pp. 115-134	EISSN 1697-9540

http://doi.org/10.18172/cig.6052

ESTUDIO DE LOS USOS DEL SUELO PARA EVALUACIÓN DE ÁREAS ELEGIBLES EN PROYECTOS MDL: CUENCA HIDROGRÁFICA DEL RÍO SOROCABUÇU, IBIÚNA-SP (BRASIL)

MAYRA VANNESSA LIZCANO TOLEDO,
ROBERTO WAGNER LOURENÇO,
DARLLAN COLLINS DA CUNHA E SILVA

Instituto de Ciência e Tecnologia – ICTS.
Universidade Estadual Paulista (UNESP). Câmpus de São, Brasil.

RESUMEN. El constante crecimiento de población que demanda recursos naturales pone bajo presión la capacidad que tienen los bosques para capturar CO_2, entre otros beneficios. Surge así la necesidad de implementar medidas de monitorización y conservación. Considerando lo anterior, el objetivo de este estudio fue identificar áreas degradadas que sean elegibles para el desarrollo de proyectos de MDL (Mecanismo de Desarrollo Limpio) en la cuenca hidrográfica del Río Sorocabuçu, localizada en el estado de São Paulo, Brasil. Para esto, se clasificó el uso del suelo para los años 2000 y 2020 a través del uso de redes neuronales del tipo multicapa. Éstas fueron evaluadas a partir de una matriz de confusión e índice Kappa, en donde las mencionadas clasificaciones realizadas permitieron la obtención del potencial de transición utilizando la herramienta LCM (*Land Change modeler*). Junto con cálculo del NDVI (Índice de Vegetación de Diferencia Normalizada), la metodología permitió la determinación de las áreas elegibles para la implementación de proyectos MDL a través de un sistema Fuzzy. En la clasificación de usos del suelo se identificó una pérdida de áreas de vegetación natural, indicando el NDVI que no hay presencia de áreas con vegetación que se encuentre en la categoría de extremamente saludable. Para el potencial de transición, se determinó que el área de estudio presenta mayormente un potencial bajo; no obstante, existen áreas que presentan un alto potencial. Finalmente, se determinó que el área de estudio comprende un 1,38% de áreas degradadas con alta elegibilidad para la implementación de proyectos MDL.

Study of land uses in the Sorocabuçu River watershed, Ibiúna-SP, (Brazil) for the evaluation of eligible areas in MDL projects

ABSTRACT. The constant population growth along with the demand for natural resources put pressure on forests' capacity to capture CO_2, among other benefits, thus arising the need to implement monitoring and conservation measures. Considering the above, the objective of this study was to identify degraded areas eligible for the development of CDM projects in the Sorocabuçu River watershed, Brazil. To achieve this, land use was classified for the years 2000 and 2020 using Multi-layer Perceptron neural networks, which were evaluated using a confusion matrix and Kappa index. These classifications allowed the determination of transition potential using the LCM tool, which, along with NDVI calculation, enabled the identification of areas eligible for CDM project implementation through a Fuzzy system. In the land use classification, a loss of natural vegetation areas was identified, while the NDVI indicated the absence of areas with vegetation in the extremely healthy category. As for transition potential, it was determined that the study area mostly exhibits low potential; however, there are areas with high potential. Finally, it was found that the study area comprises 1.38% degraded areas with high eligibility for CDM project implementation.

Palabras clave: Geoprocesamiento, bosque atlántico, Modelación ambiental, Índice de vegetación.

Key words: Geoprocessing, Atlantic Forest, environment modelling, vegetation index.

Received: 24 May 2024

Accepted: 26 August 2024

Corresponding author: Mayra Vannessa Lizcano Toledo. Instituto de Ciência e Tecnologia – ICTS. Universidade Estadual Paulista (UNESP). Câmpus de São, Brasil**.** Email: mayra.lizcano@unesp.br

1. Introducción

Los bosques, que constituyen el 31% de la superficie terrestre, son ecosistemas fundamentales para el secuestro de dióxido de carbono y equilibrio climático e hidrológico, lo que mejora la calidad de vida. Sin embargo, la desforestación ha afectado estos beneficios, con consecuencias graves para la biodiversidad y la salud pública. Esto subraya la importancia de mitigar las emisiones de gases de efecto invernadero (GEI) para limitar el aumento de la temperatura. Las actividades humanas han provocado un incremento exponencial en la concentración de estos gases, generando preocupación en la comunidad científica (Attia *et al.*, 2019; Ugas Pérez *et al.*, 2022).

Algunos estudios abordan la pérdida de servicios ecosistémicos debido a actividades humanas como la minería y la deforestación. Xiang *et al.* (2021) encontraron una disminución en servicios de regulación y suministro, como la retención de agua y la producción de alimentos en áreas mineras. Por otro lado, Bera *et al.* (2022) observaron una reducción en el suministro de servicios ecosistémicos, especialmente en la disponibilidad de plantas medicinales y materiales de construcción, debido a la deforestación entre 2006 y 2020. Estos cambios tienen efectos significativos en las cuencas hidrográficas, ya que los bosques desempeñan un papel crucial en la prevención de la erosión y la sedimentación en los ríos, así como en la regulación de la evapotranspiración del agua. Además, la pérdida de cobertura vegetal contribuye al aumento de la temperatura global, lo que afecta la conservación de la biodiversidad (FAO, 2000).

Hay que mencionar que el crecimiento y desarrollo poblacional han causado una alta demanda de recursos naturales, lo que generó, a lo largo de los años, aumento en las tasas de deforestación; en el periodo entre 1990 y 2020, la pérdida de superficie vegetal en el mundo disminuyó en un total de 178 millones de hectáreas; de igual manera, el Panel Intergubernamental sobre Cambio Climático (IPCC), que realiza evaluaciones sobre el cambio climático, estimó que la variación climática causada por acciones antrópicas desde 2000 es de aproximadamente 0,8°C a 1,2°C, lo que representa un aumento del 20%. Esto se debe, mayormente, al aumento de la concentración de CO_2 en el ambiente; en 2015 era de 400 ppm, mientras que en junio de 2022 era de 417 ppm (FAO y PNUMA, 2020; IPCC, 2020).

Dada la importancia de los bosques en el secuestro de carbono y la gestión hídrica en las cuencas hidrográficas, es crucial desarrollar modelos que optimicen los esfuerzos e inversiones económicas para estudiar su potencial de secuestro de carbono. Estos bosques son vitales para monitorear los cambios en el uso del suelo, que afectan el ciclo climático e hidrológico, especialmente en el balance de energía y la variabilidad del flujo de carbono (Lefebvre *et al.*, 2019; Samaniego *et al.*, 2022).

Existen acuerdos que tienen como objetivo la promoción de alternativas de reducción de emisiones, entre ellos el mecanismo de desarrollo limpio (MDL), propuesto en el protocolo de Kyoto en 1997, que entró en vigor en 2004 con el objetivo de implementar proyectos que permitan la reducción de emisiones de gases efecto invernadero (Kiessling, 2021).

Brasil es uno de los países con mayor biodiversidad del mundo, poseedor de más del 20% del total de especies del planeta, según el Ministerio del Medio Ambiente (MMA, 2020); además, el país lidera la lista en términos de biodiversidad de mamíferos y peces de agua dulce; en cuanto a las florestas del país, tienen una capacidad de absorción de carbono de 3,05 Mg C ha^{-1} $año^{-1}$, pero esa capacidad ha sido afectada por la deforestación a lo largo de los años (Silva *et al.*, 2020; UNESCO, 2019).

En el período entre 1985 y 2018, hubo una reducción del 12% en la cobertura vegetal en el país; sin embargo, en 2016, Brasil firmó el Acuerdo de París, comprometiéndose a reducir sus emisiones en un 43% hasta 2025, en comparación con las emisiones de 2005. Para cumplir con esta meta, se establecieron objetivos de reforestación (Silva *et al.*, 2020; UNESCO, 2019). No obstante, la selección de áreas que posean potencial para este tipo de proyectos representa la principal problemática debido a la expansión de áreas urbanas y agrícolas, entre otras actividades que ponen en riesgo la inversión efectuada. Se exige, pues, el desarrollo de metodologías que evalúen el potencial de captura de carbono de los bosques, permitiendo la eficiencia y eficacia de dichos proyectos a largo plazo (Meza y Rodríguez, 2021; Wei *et al.*, 2012).

A partir de lo señalado anteriormente, el presente estudio plantea como objetivo identificar áreas elegibles para el desarrollo de proyectos que contribuyan al mecanismo de desarrollo limpio, con ayuda de técnicas de geoprocesamiento e inteligencia artificial (IA).

2. Materiales y métodos

2.1. Área de estudio

El estudio, como se observa en la Figura 1, fue realizado en la cuenca hidrográfica del Río Sorocabuçu (BHRS), que se encuentra dentro del área de preservación ambiental de Itupararanga, localizada en el municipio de Ibiúna, en el estado de São Paulo, Brasil. La BHRS está conformada por los ríos Sorocabuçu, Sorocamirim y Una, siendo utilizada para el abastecimiento del recurso hídrico y generación de energía eléctrica (Maia y Lourenço, 2020).

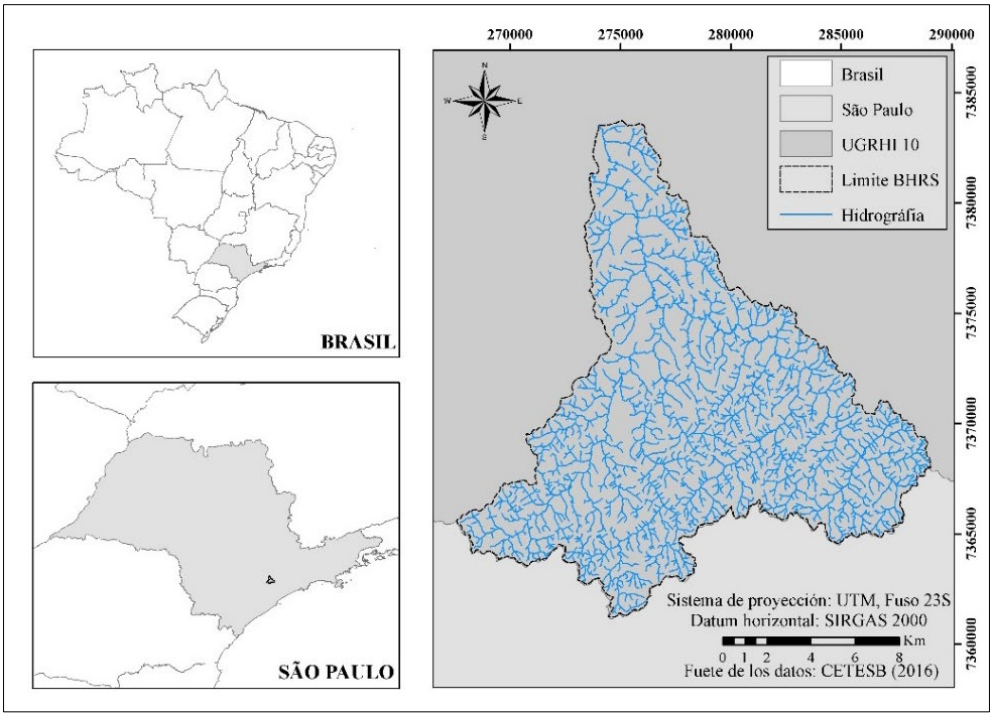

Figura 1. Cuenca hidrográfica del Río Sorocabuçu.

La BHRS ocupa un área de 202,67 km^2, lo que representa el 19% del territorio del municipio de Ibiúna, que cuenta con 79479 habitantes y cuya economía se basa en actividades agrícolas, industrias procesadoras de madera y producción hortícola y frutícola (Maia y Lourenço, 2020; Vasques *et al.*, 2021).

En cuanto a sus condiciones climáticas, la zona se caracteriza por un clima templado de montaña, con invierno seco (Cwb) según la clasificación de Köppen-Geiger (1928); con precipitación media anual de 1330 mm, variación de temperatura entre 14,2 °C y 21,3 °C y humedad relativa del 84%; los suelos predominantes en la región son latosoles rojo amarillo - orto y podzolicos con guijarros (Maia y Lourenço, 2020; Vasques *et al.*, 2021).

Por otro lado, en lo que respecta a la vegetación, el área de estudio se encuentra en el bioma mata atlántica, que comprende el 20% del sistema costero del país, caracterizado por cadenas montañosas, mesetas, valles y llanuras. Además de bosques ombrófilos (asociados a clima cálido y húmedo), debido a los altos índices de humedad relativa y luz, predominan varias familias vegetales como Myrtaceae, Caesalpiniaceae, Fabaceae, Mimosaceae, Rutaceae, Lauraceae, Meliaceae, Apocinaceae y Arecaceae (Andreoti, 2012; IBGE, 2019).

2.2. Elaboración de los mapas de la clasificación del uso del suelo

Los datos utilizados fueron adquiridos del Servicio Geológico de los Estados Unidos (USGS), obteniéndose imágenes de satélite con resolución de 30 metros, para los años 2000 y 2020 de Landsat 5 y Landsat, respectivamente. La zona de interés corresponde a la órbita 219 con puntos 076 y 077.

El primer procedimiento realizado fue una corrección radiométrica y atmosférica que permitió el tratamiento de los pixeles para la obtención de valores con intensidad homogénea, corrigiendo las perturbaciones atmosféricas, removiendo los efectos de dispersión y absorción de la atmosfera.

Como método de clasificación se utilizó el algoritmo Redes Neuronales artificiales (RNA), basado en IA. Este procedimiento, junto con el sensoramiento remoto, es una alternativa para obtener información precisa y fiable ante la clara necesidad de desarrollar una metodología que permita integrar diferentes fuentes de entrada de datos para la misma salida, y que realice el ajuste de manera automatizada (Izadkhah, 2022).

El tipo de red neuronal artificial utilizada fue de tipo MLP (Multi-layer Perceptron), disponible en el software TerrSet, donde las clases de uso de suelo empleadas se establecieron en base a la clasificación definida en el Manual Técnico del Uso de la Tierra del IBGE (2013) de nivel I, visualizadas en la Tabla 1 (Meneses y Almeida, 2012; Defige *et al*., 2018).

Tabla 1. Descripción de las clases de uso del suelo.

Nº	USO DEL SUELO	DESCRIPCIÓN
1	Agua	Caracterizada por la presencia de aguas continentales y costeras.
2	Áreas de vegetación natural	Representa áreas forestales y campestres.
3	Áreas antrópicas agrícolas	Corresponde a áreas de culturas temporales, permanentes, pastos y silvicultura.
4	Áreas antrópicas no agrícolas	Áreas urbanizadas y áreas destinadas a actividades mineras.
5	Otras áreas	Representa aquellas áreas que no poseen cobertura vegetal.

Fuente: Modificado de IBGE (2013).

Para la clasificación del uso del suelo se emplearon siete capas de neuronas, seis de las cuales estaban ocultas, con una muestra mínima de 1000 píxeles y 10000 interacciones para el entrenamiento

del sistema. Se utilizaron muestras de las clases establecidas para el uso del suelo, y se realizaron diversas composiciones de bandas para mejorar la identificación de las clases, lo que facilitó el muestreo y aumentó la precisión en la clasificación.

La calidad y precisión de los resultados de las clasificaciones generadas por la RNA fueron evaluados de manera cuantitativa a través de una matriz de confusión, la cual consiste en una tabla cuya cantidad de filas y columnas depende de las clases evaluadas. Esto permite una mejor apreciación del desempeño de la clasificación a partir del registro de la clasificación de cada píxel, donde la clasificación errónea de un píxel puede ser categorizada como error de comisión (ErroC) o error de omisión (ErroO) (Cozo, 2022; Jaramillo y Antunes, 2018).

En relación con los tipos de errores, el ErroC representa aquellos datos catalogados a una clase a la que no pertenecen, mientras que el ErroO representa aquellos valores que fueron omitidos por el algoritmo (Verma *et al.*, 2020). Finalmente, a partir de la matriz de confusión, se calculó el índice Kappa (k) (1960), que permite conocer la exactitud global de la clasificación, contando con cuatro clases (Tabla 2) definidas por Landis y Koch (1997). Estas métricas permiten la comparación de la precisión de dos clasificaciones diferentes en un área de estudio considerándose que los dos poseen el mismo coeficiente de precisión (k1 = k2), determinándose cual clasificador presenta una mayor precisión (Mosca, 2017).

Una vez obtenidas las clasificaciones, fue ejecutada una reclasificación de áreas en función de su potencial para contribuir al MDL. Dividiéndose en tres categorías: áreas restringidas (AR), áreas de interés (AI) y áreas estabilizadas (AE). Las áreas restringidas tienen bajo potencial para proyectos de desarrollo limpio, ya que están caracterizadas por la presencia de centros urbanos y actividades mineras; las áreas de interés necesitan ser recuperadas para contribuir a la captura de carbono y ser aptas para el desarrollo sostenible y las áreas estabilizadas tienen alta densidad forestal y ya contribuyen a la captura de carbono, por lo que no necesitan recuperación y son aptas para el desarrollo sostenible.

Tabla 2. Interpretación del índice Kappa.

VALOR DE KAPPA	CONCORDANCIA
<0	Pésima
0-0,2	Mala
0,2-0,4	Razonable
0,4-0,6	Buena
0,6-0,8	Muy buena
0,8-1	Excelente

Fuente: Landis y Koch (1997).

2.3. Determinación y categorización del índice de vegetación por diferencia normalizada

Fue realizado el cálculo del NDVI utilizando las bandas correspondientes al rojo e infrarrojo próximo, del satélite Landsat 8 para el año 2020, cuyos resultados fueron clasificados (Tabla 3) y utilizados para la identificación de áreas potenciales para la implementación de proyectos MDL. Cabe resaltar que, debido a la alta cobertura de nubes en el área, fueron utilizadas imágenes de satélite de los años 2019 y 2021 para los meses de febrero, noviembre y diciembre en lugar de utilizar la metodología propuesta por Pauleto *et al.* (2019), que consiste en la media del NDVI a lo largo de un año.

Una vez obtenidos los valores del NDVI, estos fueron clasificados y denominados NDVIclass, con valores negativos que indican áreas sin cobertura vegetal y valores positivos que indican vegetación fotosintéticamente activa. La clasificación fue adaptada de Menezes *et al.* (2019) y se agregó el potencial para la aplicación del MDL para cada clase presentada.

Tabla 3. Clasificación del NDVI.

CLASES DE COBERTURA VEGETAL	INTERVALO	POTENCIAL
Sin cobertura	<0	Potencial bajo
Vegetación no saludable	>0-0,33	Potencial medio
Vegetación poco saludable	>0,33-0,66	Potencial alto
Vegetación saludable	>0,66-1	Potencial altísimo

Fuente: Menezes *et al.* (2019).

2.4. Modelación de los escenarios viables

El potencial de transición se calculó utilizando la herramienta LCM (*Land Change Modeler)*, que se basa en submodelos de transición evaluados empíricamente. Se empleó el método MLP para el cálculo. Los mapas resultantes del potencial de transición se generaron utilizando variables como altitud, pendiente, *Evidence Likelihood* y distancia a vías principales, centros urbanos y cuerpos de agua. Estas variables se obtuvieron de bases de datos gubernamentales o se calcularon a partir de clasificaciones previas del uso del suelo, lo que mejoró la precisión de la predicción del modelo de transición.

Hay que mencionar que existen diversas variables que pueden ser utilizadas para mejorar el rendimiento y precisión de los potenciales de transición, sin embargo, el estudio realizado por Wang *et al.* (2021) argumenta como las variables de tipo natural (Altitud, Pendiente, entre otras) tienen influencia elevada para el incremento de la precisión.

Las variables potenciadoras fueron evaluadas utilizando el Test Cramer's V (1750), que determina la fuerza de relación de estas variables con el submodelo de transición. Los valores cercanos a 1 indican una relación significativamente mejor para el modelo, pero es importante destacar que un valor alto no garantiza un alto rendimiento del modelo (Ronald Eastman, 2006; Sankarrao *et al.*, 2021).

Se generaron mapas que representan el potencial de transición de AI para AR y AE en un rango de 0 a 1. Estos resultados se combinaron en un mapa final de potencial de transición con un rango de -1 a 1, luego se normalizaron a valores entre 0 y 1 para obtener el mapa de transición final normalizado (PTFn). Este mapa se reclasificó (Tabla 4) en cinco categorías de igual amplitud, mostrando el potencial de las áreas para convertirse en zonas adecuadas para la aplicación del MDL, con el objetivo de fortalecer territorios con una gran cobertura vegetal.

Tabla 4. Potencial de consolidación

CLASES	INTERVALO
Potencial de consolidación altísimo	0,8-1
Potencial de consolidación alto	0,8-0,6
Potencial de consolidación medio	0,6-0,4
Potencial de consolidación bajo	0,4-0,2
Potencial de consolidación bajísimo	0,2-0

Se utilizó un sistema Fuzzy (Zadeh, 1965) para identificar las áreas elegibles, utilizando las variables lingüísticas de NDVIclass y PTFn (Fig. 2 A y Fig. 2 B) como entradas, y generando una variable de salida que indica la elegibilidad de las áreas (Fig. 2 C). Esta variable se clasificó en un rango de 0 a 1 (Tabla 5), según el potencial de recuperación de la vegetación y, por lo tanto, la viabilidad para el desarrollo de proyectos MDL.

Se aplicó un sistema Fuzzy (Zadeh, 1965) de tipo Mamdani y Assilian (1975), utilizando principalmente funciones triangulares. Las reglas se basaron en el sistema If A Then B (si A entonces B), y el número total de reglas se determinó según la cantidad de clases de cada variable. Estas clases pueden visualizarse en el Anexo I.

Finalmente, la defuzzificación de los datos fue a través del método Centroide, basado en la suma de los centros para generar un valor Crisp, para luego crear un mapa de las áreas que presenten potencial de elegibilidad a la aplicabilidad del MDL, siendo este último proceso realizado en el sotfware ArcGis.

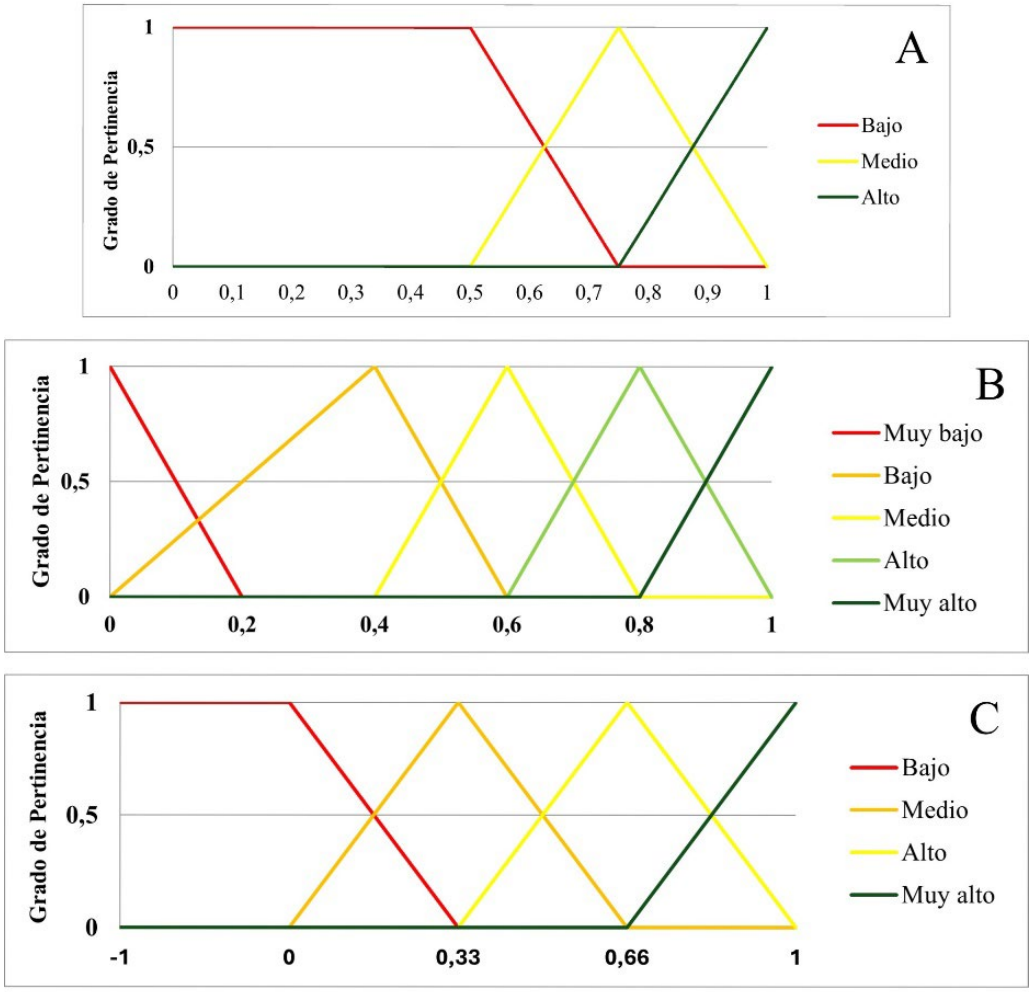

Figura 2. Variables del sistema. A) PTFn; B) NDVIclass; C) Elegibilidad de las áreas.

Tabla 5. Elegibilidad de las áreas.

CLASES	INTERVALO
Potencial bajo	0-0,50
Potencial medio	0,50-0,75
Potencial alto	0,75-1

3. Resultados y discusión

3.1. Clasificación del uso del suelo para los años 2000 y 2020

La clasificación del uso del suelo tuvo una tasa de aprendizaje del algoritmo medida para los años 2000 y 2020 de, respectivamente, 99,38% y 99,91%, con una tasa de precisión del 99,26% para el año 2000 y 99,89% para 2020; los mapas del uso del suelo para los años 2000 y 2020 son presentados en la Figura 3.

Los cambios en el uso del suelo entre 2000 y 2020 se detallan en la Tabla 6. Se observó una expansión de áreas antrópicas no agrícolas, con un aumento de 15,7 km² (7,74%) en el área de estudio. Las áreas de vegetación natural experimentaron una pérdida del 10% en 2020 en comparación con 2000, mientras que las áreas antrópicas agrícolas disminuyeron en un 13,1%.

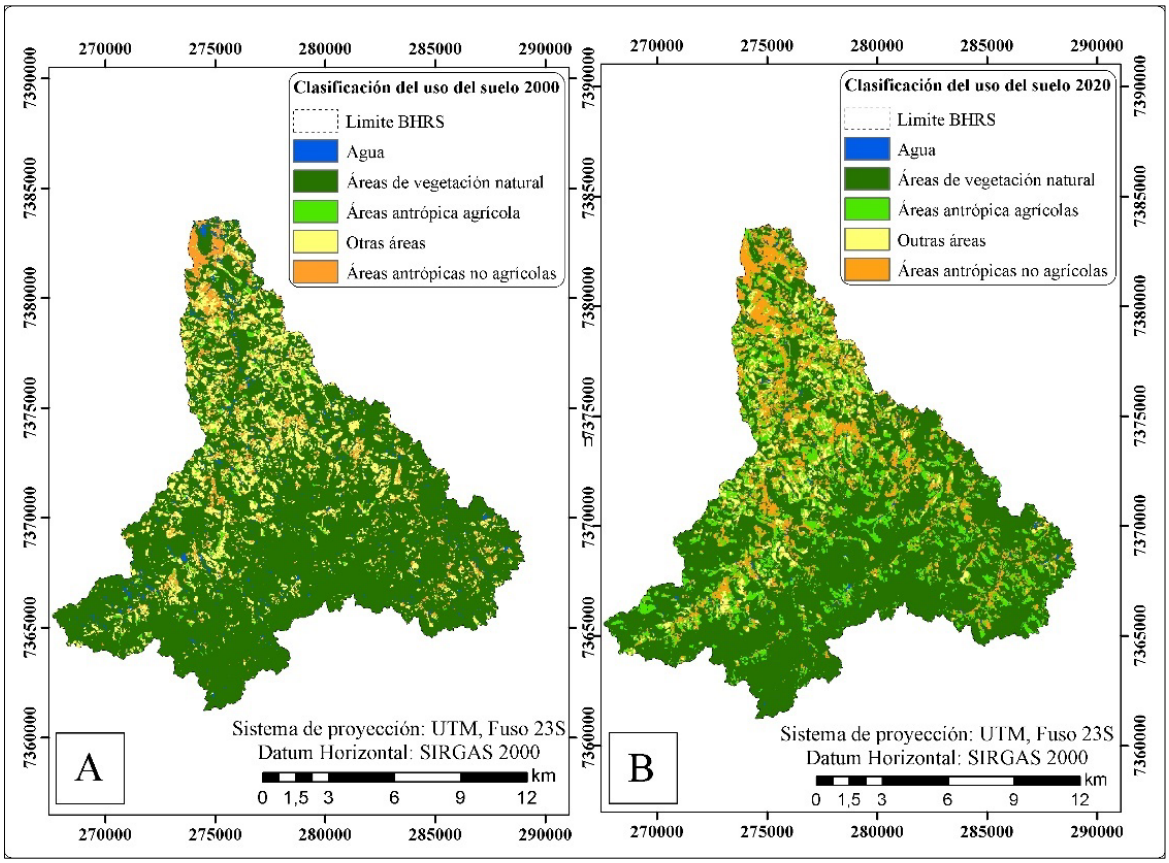

Figura 3. Clasificación del uso del suelo. A) 2000; B) 2020.

Tabla 6. Cambio del uso del suelo entre el año 2000 y 2020.

CLASE	2000		2020	
	ÁREA (km²)	%	ÁREA (km²)	%
Agua	4,08	2,00	2,34	1,15
Área de vegetación natural	155,4	76,69	130,46	64,38
Áreas antrópicas agrícolas	3,92	1,93	29,58	14,59
Áreas antrópicas no agrícolas	12,76	6,30	28,46	14,04
Otras áreas	26,52	13,08	11,83	5,84

La matriz de confusión de la clasificación del año 2000 (Tabla 7) muestra que las clases de agua, áreas antrópicas no agrícolas y otras áreas tienen un mayor error de omisión, mientras que el error de comisión solo está presente en las clases de áreas antrópicas no agrícolas y otras áreas. El error global fue de 0,003 y el índice Kappa (1960) de la clasificación del uso de la tierra fue de 0,99, calificándose como excelente.

En la matriz de confusión (Tabla 8) para la clasificación del uso de la tierra del año 2020, se observan errores de omisión en las clases de áreas antrópicas agrícolas y áreas antrópicas no agrícolas, mientras que las clases de áreas antrópicas agrícolas y otras áreas presentan errores de comisión. Sin embargo, estos errores tienen valores menores a 0,001. Además, el error global y el índice Kappa (1960) son menores a 0,001 y 0,99, respectivamente, lo que indica una clasificación excelente.

Tabla 7. Matriz de confusión para la clasificación del uso del suelo del año 2000.

	1	**2**	**3**	**4**	**5**	**6**	**TOTAL**	**ERROC**
1	70	0	0	0	0	0	70	0
2	0	3390	0	0	0	0	3390	0
3	0	0	108	0	0	0	108	0
4	2	0	0	146	5	0	153	0,046
5	1	0	0	6	355	0	362	0,019
6	0	0	0	0	0	241	241	0
TOTAL	73	0	0	152	360	241	4324	
ERRO0	0,041	0	0	0,039	0,0139	2		0,003

Tabla 8. Matriz de confusión para la clasificación del uso del suelo del 2020.

	1	**2**	**3**	**4**	**5**	**6**	**TOTAL**	**ERROC**
1	93	0	0	0	0	0	93	0
2	0	3589	1	0	0	0	3590	0
3	0	0	248	0	2	0	250	0,003
4	0	0	0	186	0	0	186	0,008
5	0	0	0	0	660	0	660	0
6	0	0	0	0	0	105	105	0
TOTAL	93	3589	249	186	662	105	4884	
ERRO0	0	0	0,004	0	0,003	0		0,0001

3.2. Determinación y reclasificación del NDVI medio

La reclasificación del uso del suelo para los años 2000 y 2020, representada en la Figura 4, muestra un aumento de las AR y AI durante el período de estudio seleccionado. Las AR experimentaron una expansión de 13,96 km^2, equivalente al 6,89% del área de estudio, mientras que las AI aumentaron en un 5,42% (10,98 km^2). Se observa que las AI están cercanas a las AR y al cauce principal del río, lo que es un patrón común para el desarrollo de actividades humanas.

La Figura 5 muestra el estado de la vegetación mediante el NDVI para el año 2020 en la cuenca hidrográfica del Río Sorocabuçu. Una vez obtenido el NDVI medio, este fue reclasificado.

Con la reclasificación del NDVI, se identificó la ausencia de áreas clasificadas como de altísimo potencial, mientras que las clases de alto potencial representan 81,37 km^2, y las clases de potencial medio abarcan 121,13 km^2, siendo predominantemente en el área de estudio y representando principalmente el área de interés.

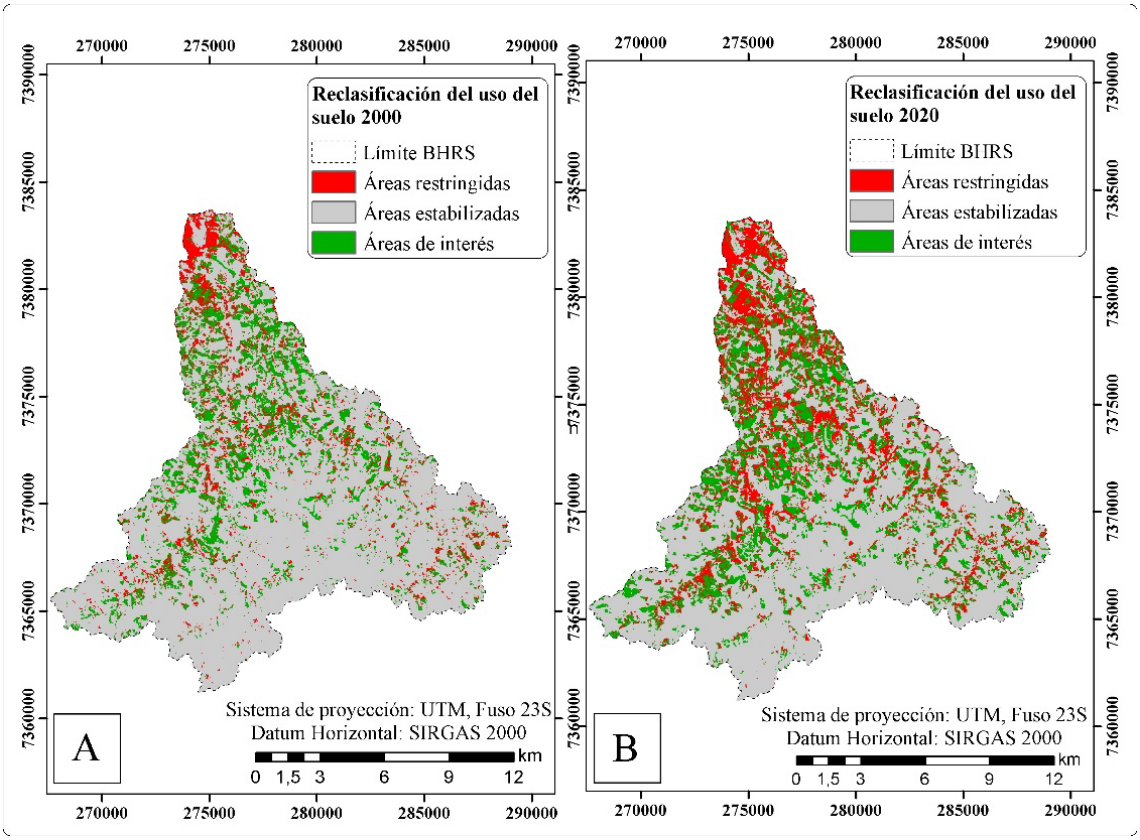

Figura 4. Reclasificación del uso del suelo. A) 2000; B) 2020.

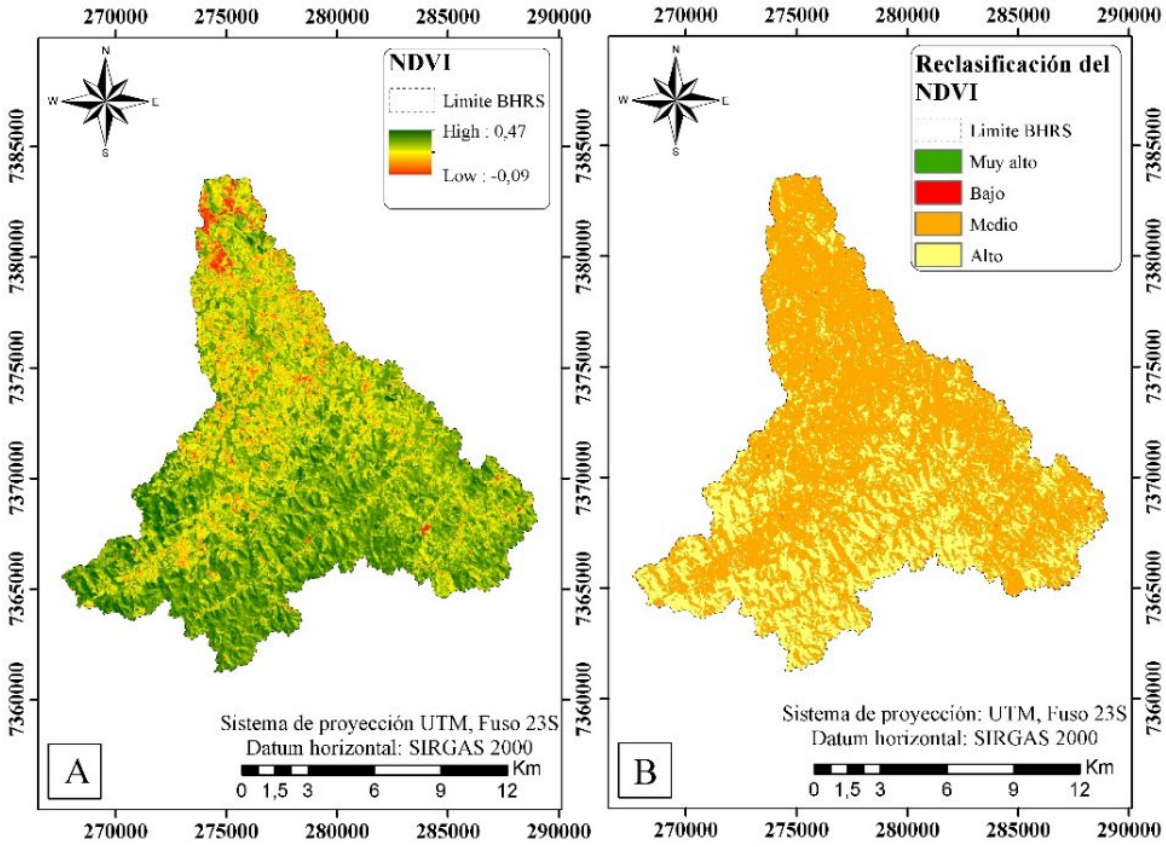

Figura 5. Índice de vegetación por diferencia normalizada. A) Medio; B) Reclasificación.

3.3. Identificación de las áreas elegibles

En la Figura 6 A se presenta la variable *Evidence Likelihood*, que muestra la frecuencia relativa donde ocurrieron las transiciones entre las diferentes clases de uso del suelo entre 2000 y 2020. Un aumento en el valor indica una mayor probabilidad de encontrar el uso del suelo en un píxel en caso de ser un área de transición en donde los valores más altos se observan principalmente en las áreas de vegetación natural.

Además, se pueden ver otras variables utilizadas para construir el submodelo de transición, obtenidas y calculadas a partir del Modelo de Elevación Digital (MED) del estado de São Paulo obtenido en la página de la Secretaría de Medio Ambiente.

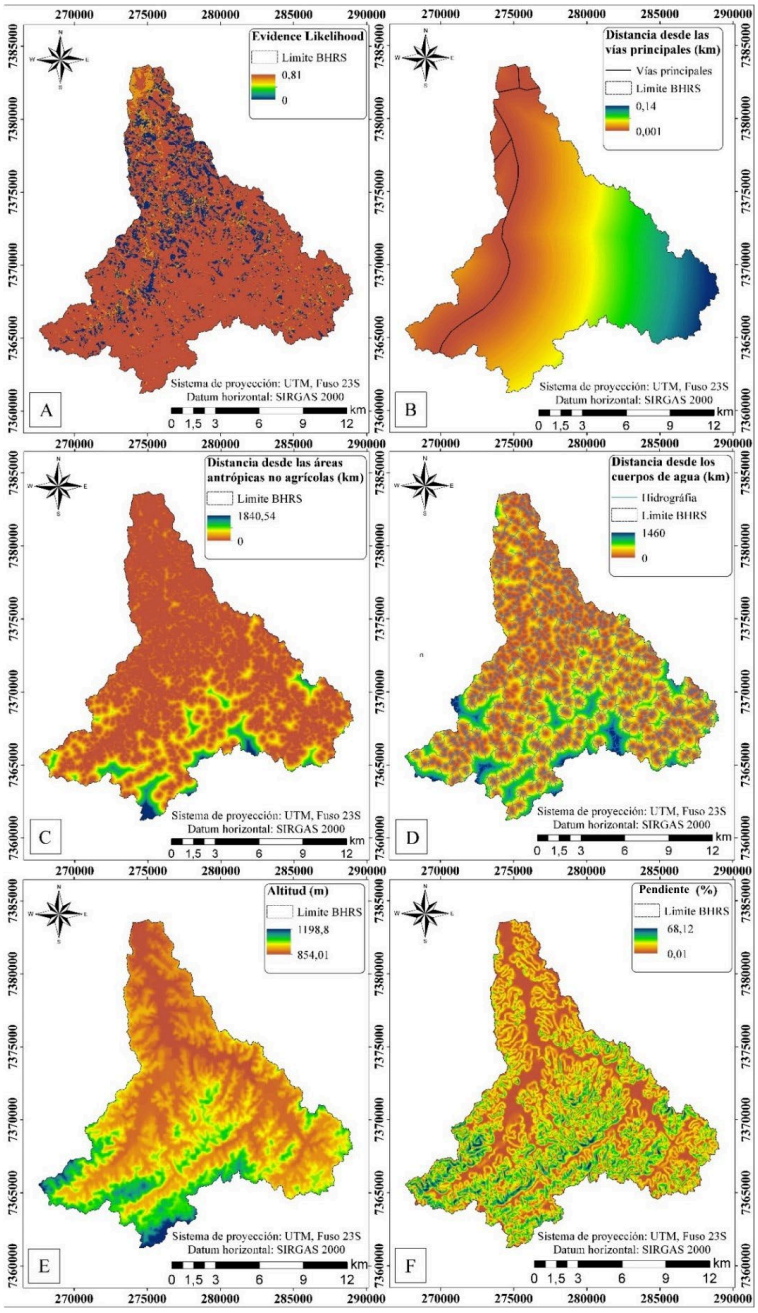

Figura 6. Variables potenciadoras. A) Evidence Likelihood; B) Distancia desde las vías principales; C) Distancia desde las áreas antrópicas no agrícolas; D) Distancia desde los cuerpos de agua; E) Altitud; F) Pendiente.

En cuanto a la altitud (Fig. 6 E) y la pendiente (Fig. 6 F), se puede ver que las áreas de mayor valor pertenecen a la clase de vegetación natural. En el caso de las áreas antrópicas no agrícolas (Fig. 6 C), se observa que la menor distancia se encuentra en áreas con menor pendiente y altitud cercanas a la carretera principal (Fig. 6 B), lo que refleja un patrón de desarrollo de la población. De igual manera, los cuerpos de agua (Fig. 6 D) se encuentran más cerca de las áreas antrópicas no agrícolas.

En la Tabla 9 se pueden ver los resultados del test de Cramer's V (1750) para cada variable, tanto para los valores obtenidos de manera general como para cada tipo de cobertura del suelo. Los valores más significativos, en general, fueron presentados por las variables de distancia a las áreas urbanas y evidencia de similitud, con 0,60 y 0,37, respectivamente, mientras que los valores más bajos pertenecen a las variables de pendiente (0,16) y distancia a las carreteras (0,16).

La Figura 7 muestra el potencial de transición de áreas de interés a áreas estabilizadas, alcanzo una tasa de precisión del 84,25% cumpliendo el valor mínimo recomendado del 80% para los resultados modelados (Sankarrao *et al.*, 2021). Se reveló que las áreas con mayor potencial se encuentran alejadas de los centros urbanos, mientras que las áreas restringidas muestran un menor potencial de transición (0,48), especialmente en regiones con menor pendiente.

Tabla 9. Test de Cramer's V.

1	2	3	4	5	6	7
Áreas restringidas	0	0	0	0	0	0
Áreas estabilizadas	0,39	0,31	0,22	0,21	0,96	0,28
Áreas de interés	0,59	0,36	0,24	0,25	0,65	0,31
General	0,37	0,23	0,16	0,16	0,60	0,21

1. Usos del suelo; 2. Evidencia de semejanza; 3. Altitud; 4. Pendiente; 5. Distancia desde las vías principales; 6. Distancia desde las áreas antrópicas no agrícolas; 7. Distancia desde los cuerpos de agua

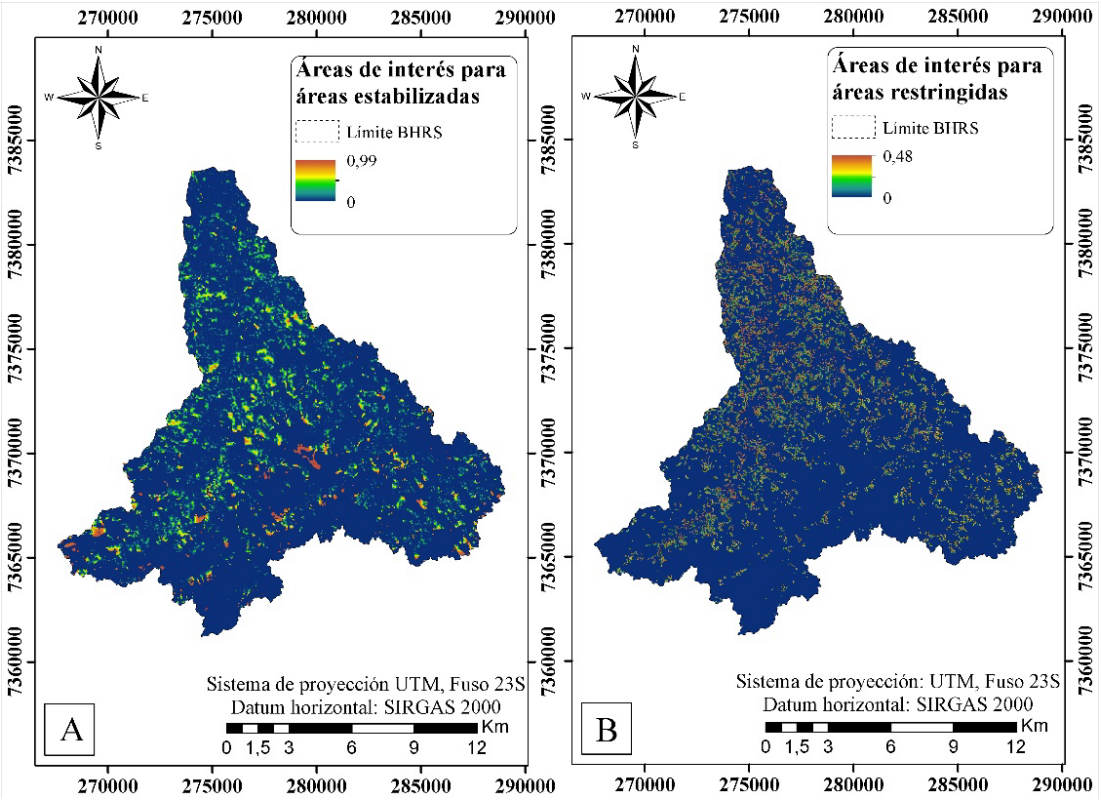

Figura 7. Potencial de transición. A) Áreas estabilizadas; B) Áreas restringidas.

En la Figura 8 se muestra el potencial de transición final, donde se puede ver que el potencial categorizado como bajo predomina en el área de estudio; sin embargo, hay áreas con un potencial altísimo que representan el 2,21% del total del área de estudio.

La Figura 9 muestra los valores obtenidos a través del sistema Fuzzy (Zadeh, 1965), representando la elegibilidad de las áreas en la BHRS para el desarrollo de proyectos de MDL y, por ende, la identificación de áreas con una alta capacidad de captura de CO_2. Se observa que la mayoría del área de estudio tiene una elegibilidad baja para proyectos MDL, con 192,67 km^2 en esta categoría, mientras que solo el 1,38% de las áreas (2,81 km^2) se identificaron con una elegibilidad alta y el 3,55% (7,19 km^2) con una elegibilidad media.

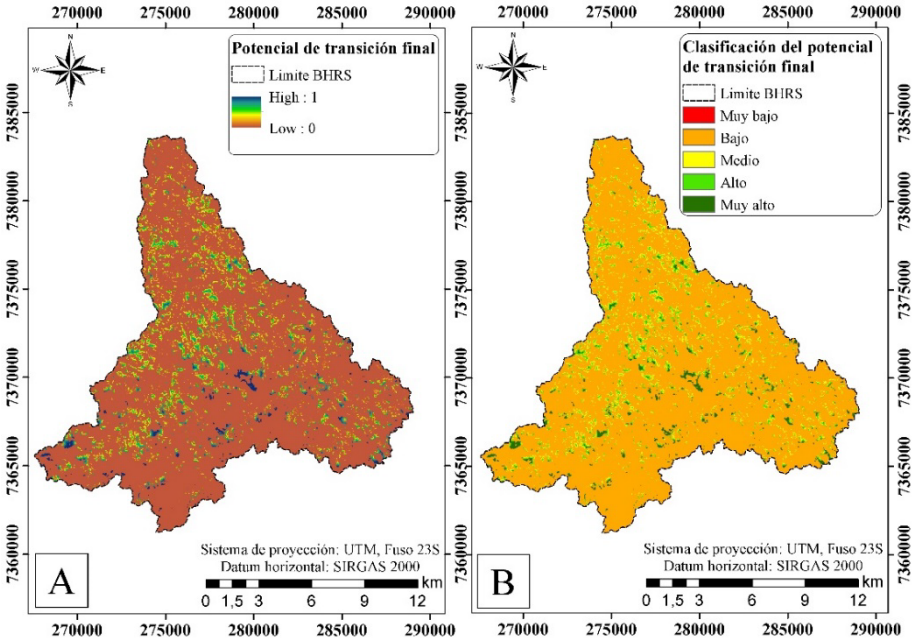

Figura 8. A) PTF normalizado; B) PTF reclasificado.

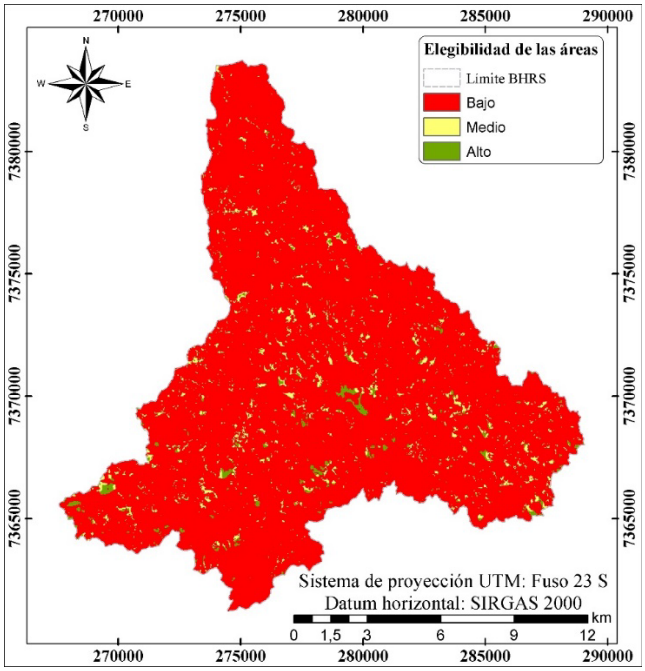

Figura 9. Elegibilidad de las áreas.

4. Discusión

El estudio de Simonetti *et al.* (2019) señaló una expansión significativa en la clase "otras áreas" en la APA de Itupararanga en 2017, sugiriendo un aumento de riesgos y degradación forestal. En contraste, Maia y Lourenço (2020) encontraron una pérdida del 2,5% de vegetación natural en la BHRS en 2018, atribuida a la alta pendiente que dificulta las actividades humanas. Comparativamente, Sales *et al.* (2022) identificaron un desarrollo económico y agrícola pronunciado en la cuenca del Río Una, mientras que Padovanni *et al.* (2018) observaron una expansión de actividades agrícolas en años anteriores, indicando una intensa interferencia humana en el área de estudio.

Asimismo, se observó una deforestación significativa en el cerrado brasileño, especialmente en la cuenca hidrográfica del río Uruçuí-Preto, donde entre 1984 y 2007 se perdió el 13,48% de la vegetación nativa, con pérdidas de entre el 20% y el 50% en algunas subcuencas. Este cambio refleja una conversión del uso del suelo para la expansión agrícola, principalmente para el cultivo de soja. Además, en 2019 se detectó una tendencia negativa en el estado fotosintético de la vegetación debido a la expansión de las actividades agrícolas (Barbosa *et al.*, 2019; Santana *et al.*, 2020).

Desde la década de 1980, Brasil ha experimentado cambios significativos en el uso del suelo, con bosques sometidos a intensas perturbaciones humanas, incluida la extracción de recursos naturales. Sin embargo, se han propuesto diversas alternativas para reducir la deforestación. Estudios recientes, como los de Azevedo *et al.* (2022) y Silva *et al.* (2021), han demostrado la relación entre el aumento de la eficiencia agrícola y la reducción de la deforestación, aunque la efectividad varía entre diferentes áreas. Se recomienda ampliar los esfuerzos de conservación mediante estrategias que promuevan el desarrollo sostenible del país.

En áreas con alta fragilidad ambiental como la BHRS, el estado fotosintético de la vegetación depende de su respuesta a las perturbaciones o su resiliencia. En esta zona, se ha observado un rápido crecimiento de centros urbanos y, como resultado, la expansión de áreas dedicadas a actividades humanas, especialmente la agricultura (Silva *et al.*, 2021).

El estudio de Simonetti *et al.* (2019) identificó que la región sur de la cuenca del alto Sorocaba, en la APA de Itupararanga, se clasifica como "Muy fuerte" en términos de fragilidad ambiental. Esta clasificación es crucial para la implementación de políticas de gestión, ya que las perturbaciones humanas pueden tener un mayor impacto negativo en estas áreas vulnerables. Se observó un ligero aumento en el valor máximo del estado fotosintético de la vegetación, pero no fue significativo. Además, se registró un aumento en los valores negativos, lo que indica una expansión de las áreas urbanas debido al crecimiento de la población.

El bioma de la Mata Atlántica se caracteriza por su alta fragilidad ambiental. Varios autores han destacado cómo las características regionales influyen en el comportamiento fotosintético de la vegetación, con áreas de mayor pendiente y menor intervención humana mostrando valores más altos que indican un mejor estado fotosintético, como se observa en la BHRS. Un estudio en el noreste de Brasil entre 1982 y 2001 encontró una disminución en el vigor de la vegetación a lo largo de dos décadas, atribuida al crecimiento poblacional y al desarrollo de actividades agrícolas e industriales (Silva *et al.*, 2021).

Las variables potenciadoras (Fig. 6) mostraron comportamientos que reflejan un patrón de desarrollo esperado, ya que a lo largo de los años el establecimiento de centros urbanos se ha realizado cerca de los cuerpos de agua para tener un mayor acceso al recurso (Sankarrao *et al*., 2021).

En el estudio realizado por Milhomem *et al.* (2022) en el bioma del cerrado, fueron evaluados los impactos causados por los cambios en el uso del suelo entre 1986 y 2016 y generó escenarios futuros, también se determinó que entre las principales causas de los cambios abruptos en el uso del suelo se encuentran las actividades agropecuarias, que representan el principal sector del país. Estas actividades pueden ser más invasivas con el tiempo debido al aumento de la demanda de recursos naturales si no

son adoptadas técnicas de bajo carbono y sostenibles, lo que puede llevar a un aumento del uso del suelo del 49% entre 2033 y 2100 (Rodrigues *et al*., 2021).

En un estudio realizado por Díaz-Pacheco y Hewitt (2014), se destacó la utilidad de los modelos de simulación basados en inteligencia artificial para generar mapas del potencial de uso de la tierra, lo que facilita la identificación de patrones de comportamiento, como el potencial de un área para adquirir un uso diferente del suelo en el futuro.

Según Nogueira (2018), el potencial del Mecanismo de Desarrollo Limpio (MDL) es crucial para Brasil dada la importancia de los bosques en la mitigación del cambio climático al absorber CO_2. Sin embargo, al implementarlo en políticas públicas, existen dos desafíos principales: primero, la necesidad de crear alternativas que cumplan con los criterios de adicionalidad para garantizar beneficios a través de prácticas sostenibles; segundo, la garantía de la permanencia de los bosques para asegurar la absorción continua de CO_2, ya que las actividades del MDL están limitadas a la forestación y reforestación.

Brasil se sitúa en la tercera posición en número de proyectos MDL, seguido de China e India, habiendo desarrollado el primer proyecto registrado en el mundo en Aterro Novagerrar, Rio de Janeiro. Sin embargo, su contribución aún es insuficiente para alcanzar la meta de reducción del 43% establecida para 2030 en relación con las emisiones de 2005, especialmente en un mercado incipiente para la implementación de nuevos proyectos (Torres *et al.*, 2016).

De igual manera, Barbosa *et al*. (2021) realizaron un estudio para evaluar el potencial de secuestro de CO_2 de áreas elegibles para proyectos de MDL en la cuenca del río Pardo, en Minas Gerais, simulando diferentes escenarios de reforestación y recuperación forestal, identificándose que la recuperación forestal por 20 años presentó un secuestro de 10,22 millones de Mg de CO_2, mientras que, para la reforestación por seis años, el secuestro de carbono fue de 12 millones de Mg.

Entre las dificultades para implementar proyectos MDL se destaca la falta de información sobre áreas viables. Aunque Brasil no tiene obligación en reducir las emisiones de GEI, estos proyectos atraen inversión extranjera y generan créditos de carbono que pueden venderse a países desarrollados para cumplir sus metas. Según Lima (2019), esto podría impulsar una economía de bajo carbono, especialmente porque Brasil supera su meta de 0,05 t CO_2 por millón de PIB. La implementación de proyectos MDL no solo ayudaría a reducir GEI, sino que también promovería la sustentabilidad social y económica mediante la generación de empleo y la asistencia a comunidades en actividades sociales (Benites-Lazaro *et al.*, 2018).

Finalmente, Brasil es fundamental para el Mecanismo de Desarrollo Limpio (MDL), ya que fue uno de los primeros en proponer este mecanismo y ha mantenido una alta participación a lo largo de los años, ejecutando numerosos proyectos que contribuyen a esta medida (Mudrovitsch *et al.*, 2018).

5. Conclusiones

La clasificación del uso del suelo en la BHRS mostró una pérdida significativa de la vegetación natural y una expansión del uso de la tierra no agrícola y agrícola entre 2000 y 2020. El crecimiento de la población y el desarrollo tecnológico, científico y económico son considerados las principales causas de esta tendencia, a pesar de los esfuerzos por conservar los recursos naturales a través de medidas como el Protocolo de Kyoto; además, el estudio obtuvo excelentes resultados para la validación de la clasificación del uso del suelo y demostró un alto grado de confiabilidad.

En cuanto al cálculo del Índice de Vegetación con Diferencia Normalizada, se puede inferir que no hay áreas en la clase saludable y la vegetación con el mayor nivel de salud se encuentra principalmente en áreas con la mayor pendiente, las cuales representan una mayor dificultad para el establecimiento de cultivos además de que pueden representar áreas de protección ambiental cuya eficiencia no es suficiente para que el estado fotosintético se encuentre en la categoría saludable.

La integración de una amplia variedad de información ha permitido el cálculo y análisis de tendencias para el futuro, proporcionando conocimiento sobre los escenarios que puedan favorecer en la toma de decisiones; sin embargo, el potencial de transición ha demostrado que hay un mayor potencial de transición de áreas de interés a áreas estabilizadas en lugar de las áreas restringidas.

Finalmente, es importante destacar la relevancia de estudios que buscan la mejora de proyectos MDL teniendo en consideración la incipiente producción de material bibliográfico que permita dar soporte a los gestores públicos para así contribuir a la toma de decisiones e implementación de medidas.

Referencias

Andreoti, C., 2012. Avaliação da eficiência de um sistema agroflorestal na recuperação de um solo degradado por pastoreio. São Paulo, 131 p. Disertación (Maestría en Geografía física), Universidade de São Paulo, São Paulo. Disponible en: http://www.teses.usp.br/teses/disponiveis/8/8135/tde-09012013-121619/pt-br.php

Attia, A., Nouvellon, Y., Cuadra, S., Cabral, O., Laclau, J., Guillemot, J., Campoe, O., Stape, J., Galdos, M., Lamparelli, R., Maire, G., 2019. Modelling carbon and water balance of Eucalyptus plantations at regional scale: Effect of climate, soil and genotypes. *Forest Ecology and Management* 449, 117460. https://doi.org/10.1016/j.foreco.2019.117460

Azevedo, W. C., Rodrigues, M., Correia, D., 2022. Does agricultural efficiency contribute to slowdown of deforestation in the Brazilian Legal Amazon? *Journal for Nature Conservation* 65, 126092. https://doi.org/doi:10.1016/j.jnc.2021.126092

Barbosa, K., Batista, J., Rocha, S., Santos, K., Santos, G., Ratke, R., 2019. Mudança no uso do solo na bacia hidrográfica do rio Uruçuí-Preto, Piauí. Brazilian *Journal of Development* 5(11), 25490-25511. https://doi.org/10.34117/bjdv5n11-211

Barbosa, G., Santos, M., Lima, V., Vicente, M., Martins, T., 2021. Avaliação de áreas elegíveis à implantação de projetos de MDL florestais na bacia de Rio Pardo, em Minas Gerais. *Pesquisas Agrarias e Ambientais* 9(1). https://doi.org/10.31413/nativa.v9i1.11173

Benites-Lazaro, L., Mello-Théry, N., Simões, A., Gnaccarini, I., 2018. Gorvernança e desenvolvimento sustentável: a participação dos stakeholders locais nos projetos de mecanismo de desenvolvimento limpo no Brasil. *Revista Colombiana de Geografía* 27(2), 227-241, https://doi.org/10.15446/rcdg. v27n2.66336

Bera, D., Chatterjee, N., Gosh, S., Dinda, S., Bera, S., Mandal, M., 2022. Assessment of forest cover loss and impacts on ecosystem services: Coupling of remote sensing data and people's perception in the dry deciduous forest of West Bengal, India. *Journal of Cleaner Production* 356, 131763. https://doi.org/10.1016/j.jclepro.2022.131763

Cozo Narvaez, C. M., 2022. *Análisis de cambio de uso de suelo por actividad minera mediante percepción remota en el distrito de Ananea, períodos 2015-2021.* Disponible en: http://repositorio.upsc.edu.pe/handle/UPSC/380

Cramer, 1750. *Introduction A L'Analyse Des Lignes Courbes Algébriques.* Geneve: Cramer & Philibert, 1750. http://eudml.org/doc/203906

Defige, A., Zabel, F., Mauser, W., 2018. Assessing land use and land cover changes and agricultural farmland expansions in Gambella Region, Ethiopia, using Landsat 5 and Sentinel 2a multispectral data. *Heliyon* 4(11), e00919. https://doi.org/10.1016/j.heliyon.2018.e00919.

Díaz-Pacheco, J., Hewitt, R., 2014. Modelado de cambios de usos de suelo urbano a través de redes neuronales artificiales: Comparando dos aplicaciones de software. *Geofocus* 14, 1-22. https://www.geofocus.org/index.php/geofocus/article/view/298

FAO y PNUMA, 2020. E*l estado de los bosques del mundo: Los bosques, la biodiversidad y las personas.* https://doi.org/10.4060/ca8642es.

FAO, 2000. *Bosques, seguridad alimentaria y medios de vida sostenibles.* Disponible en: http://fao.org/3/x7273s/x7273s01.htm

IBGE-Instituto Brasileiro de Geografia e Estatística, 2013. *Manual Técnico de Uso da Terra.*

IBGE-Instituto Brasileiro de Geografia e Estatística, 2019. *Biomas e sistema costerio- marinho do Brasil. Rio de Janeiro.*

IPCC, 2020. *Climate change and land.* Disponible en: http://ipcc.ch/site/assets/uploads/2019/11/SRCCL-Full-Report-Compiled-191128.pdf

Izadkhah, H., 2022. Basic structure of neural networks. In: *Deep Learning in Bioinformatics,* cap. 4, 67-93, https://doi.org/10.1016/B978-0-12-823822-6.00011-1

Jaramillo, L., Antunes, A., 2018. Detección de cambios en la cobertura vegetal mediante interpretación de imágenes Landsat por redes neuronales artificiales (RNA). Caso de estudio: Región Amazónica Ecuatoriana. *Revista de Teledetección* 51(33), 33-46. https://doi.org/10.4995/raet.2018.8995

Köppen, W., Geiger, R., 1928. *Klimate der Erde.* Gotha: Verlag Justus Perthes.

Kiessling, C. K., 2021. Principio de las Responsabilidades Comunes pero Diferenciadas: un análisis de la internalización de la norma por parte del sector privado en Brasil (2005-2015). *Estudios Internacionales* 53(198), 63-88. https://doi.org/10.5354/0719-3769.2021.58261

Landis, J., Koch, G., 1977. The measurement of observer agreement for categorical data, *Biometrics* 33(1), 159-174. https://doi.org/10.2307/2529310

Lefebvre, D., Goglio, P., Williams, A., Manning, D., De Azevedo, A., Bergmann, M., Meersmans, J., Smith, P., 2019. Assessing the potential of soil carbonation and enhanced weathering through Life Cycle Assessment: A case study for Sao Paulo State, Brazil. *Journal of Cleaner Production* 233, 468-481. https://doi.org/doi:10.1016/j.jclepro.2019.06.099

Lima, R., 2019. *Cenário do mercado regulado de MDL no nordeste do Brasil.* Disertación (Maestría en Ciencias Economicas), Serra Talhada.

Maia, L., Lourenço, R., 2020. Impactos das mudanças no uso e cobertura da terra sobre a variabilidade do albedo na bacia hidrográfica do Rio Sorocabuçu (Ibiúna - SP). *Revista Brasileira de Climatologia* 27(16), 443-462. https://doi.org/10.5380/abclima.v27i0.72761

Mamdani, E., Assilian, S., 1975. An experiment in linguistic synthesis with a fuzzy logic controller. *International Journal of Man-Machine Studies* 7(1), 1-13. https://doi.org/10.1016/S0020-7373(75)80002-2

Meneses, P., Almeida, T., 2012. *Introdução ao processamento de imagens de sensoriamento remoto.* UnB-CNPq

Menezes, A., Cabral, J., Linhares, M., 2019. A aplicação do índice de vegetação por diferença normalizada (NDVI) para análise da degradação ambiental da área de influência direta do açude castanhão. *Revista Casa de Geografia de Sobral* 21(2), 674- 685. https://doi.org/10.35701/rcgs.v21n2.602

Meza, L. E., Rodríguez, A. G., 2021. *Soluciones basadas en la naturaleza para la sostenibilidad de la agricultura: ruta para la sinergia entre las convenciones de Río y la recuperación pos-Covid-19.* Disponible en: http://repositorio.cepal.org/handle/11362/47574

Milhomem, D., Alvarado, S., Marques, M., Ribeiro, M., 2022. Alterações do uso e cobertura da terra entre os anos de 1986 e 2018: estudo de caso da bacia do rio Lajeado no cerrado Maranhense. *Open Science Research VI* (1), 34-51. https://doi.org/10.37885/220909951

MMA, Ministério do Meio Ambiente, 2020. Biodiversidades e Biomas. Disponíble em: https://www.gov.br/mma/pt-br/assuntos/biodiversidade

Mosca, N., Reno, V., Marani, R., Nitti, M., D'Orazio, T., Stella, E., 2017. *Human Walking Behavior detection with a RGB-D Sensors Network for Ambient Assisted Living Applications.* CEUR-ws (pp. 17-29).

Mudrovitsch, S., Busch, S., Rojas, M., 2018. *O mecanismo de desenvolvimento limpo no Brasil.* Disponible en: http://repositorio.ipea.gov.br/bitstream/11058/9474/1/O%20Mecanismo.pdf

Nogueira, F., 2018. *O MDL florestal no Brasil: fundamentos, legado e elementos para o futuro.* p.131-178. Disponible en: http://repositorio.ipea.gov.br/handle/11058/9484

Padovanni, N., Reis, E., Souza, J., Matias, M., Lourenço, R, 2018. Análise Espacial da Temperatura e Albedo de Superfície na Bacia Hidrográfica do rio Uma-Ibiúna/São Paulo, a partir de imagens MODIS. *Revista Brasileira de Geografia Física* 11(5), 1832-1845. https://doi.org/10.26848/rbgf.v11.5.p1832-1845

Pauleto, H., Hoff, R., Costacurta, L., Portella, M., Alberti, R., 2019. *Investigação do ciclo de pomares de macieira pelo NDVI de imagens Sentinel-2 na região dos campos de cima da serra, Rio Grande do Sul, Brasil.* XIX Simpósio Brasileiro de Sensoriamento Remoto.

Rodrigues, E., Guimarães, C., Marques, R., Bacani, V., Pott, A., 2021. Future scenarios based on a CA-Markov land use and land cover simulation model for a tropical humid basin in the Cerrado/Atlantic forest ecotone of Brazil. *Land Use Policy* 101, 105141 https://doi.org/10.1016/j.landusepol.2020.105141.

Ronald Eastman, J., 2006. *Idrisi Andes: Guide to GIS and Image Processing. Worcester, MA:* IDRISI Production. Disponible en: http://gis.fns.uniba.sk/vyuka/DTM_ako_sucast_GIS/Kriging/1/Andes_Manual.pdf

Sales, V., Strobl, E., Elliott, R., 2022. Cloud cover and its impact on Brazil's deforestation satellite monitoring program: Evidence from the Cerrado biome of the Brazilian Legal Amazon. *Applied Geography* 140, 102651. https://doi.org/10.1016/j.apgeog.2022.102651

Samaniego, J., Lorenzo, S., Rondón Toro, E., Krieger Merico, L. F., Herrera Jiménez, J., Rouse, P., Harrison, N., 2022. *Soluciones basadas en la naturaleza y remoción de dióxido de carbono.* United Nations CEPAL, Santiago, Chile, 84 pp. https://oceanrep.geomar.de/id/eprint/57645

Sankarrao, L., Kumar, D., Rathinsamy, M., 2021. Predicting land-use change: Intercomparison of different hybrid machine learning models. *Environmental Modelling and Software* 145, 105207. https://doi.org/10.1016/j.envsoft.2021.105207

Santana, R., Delgado, R., Schiavetti, A., 2020. The past, present and future of vegetation in the Central Atlantic Forest Corridor, Brazil. *Remote Sensing Applications: Society and Environment* 20, https://doi.org/10.1016/j.rsase.2020.100357

Silva, C., Heinrich, V., Freire, A., Broggio, I., Rosan, T., Doblas, J., Anderson, L., Rousseau, G., Shimabukuro, Y., Silva, C., House, J., Aragão, L., 2020. Benchmark maps of 33 years of secondary forest age for Brazil. *Scientific Data* 7(269). https://doi.org/10.1038/s41597-020-00600-4

Silva, R., Santos, A., Batista, J., Fiedler, N., Juvanhol, R., Barbosa, K., Figueira, E., 2021. Vegetation trends in a protected area of the Brazilian Atlantic Forest. *Ecological Engineering* 162, 106180. https://doi.org/10.1016/j.ecoleng.2021.106180

Simonetti, V., Silva, D., Rosa, A., 2019. Proposta metodológica para identificação de riscos associados ao relevo e antropização em áreas marginais aos recursos hídricos. *Scientia Plena* 15(2). https://doi.org/10.14808/sci.plena.2019.025301

Torres, C., Fermam, R., Sbragia, I., 2016. Projetos de MDL no Brasil: Oportunidade de mercado para empresas e para novas entidades operacionais designadas. *Ambiente & Sociedade* 19(3), 199-214. https://doi.org/10.1590/1809-4422ASOC142054V1932016

Ugas Pérez, M., Calderón Castellanos, R., Rivas Meriño, F., Núñez Ravelo, F., 2022. Cuantificación del flujo de CO_2 en el suelo colonizado por Avicennia germinans, emplazado en el humedal Laguna Grande, sector Los Totumos, estado Miranda, Venezuela. LA GRANJA. *Revista de Ciencias de la Vida* 35(1), 85-97. https://doi.org/10.17163/lgr.n35.2022.07

UNESCO, 2019. http://pt.unesco.org/fieldoffice/brasilia/expertise/biodiversity-brazil

Vasques, E., Silva, A., Almeida, E., Gomes, G., Foloni, M., 2021. Queima De Resíduos Domiciliares A Céu Aberto Em Lageadinho, Ibiúna/SP: Causas, Consequências, Propostas De Melhoria. *Multidisciplinar Núcleo do Conhecimento* 3(4), 22-44. https://www.nucleodoconhecimento.com.br/engenharia-ambiental/ceu-aberto

Verma, P., Raghubanshi, A., Srivastava, P., Raghubanshi, A., 2020. Appraisal of kappa-based metrics and disagreement indices of accuracy assessment for parametric and nonparametric techniques used in LULC classification and change detection. *Modelling Earth Systems and Environment* 6(2), 1045-1059. https://doi.org/10.1007/s40808-020-00740-x

Wang, Q., Guan, Q., Lin, J., Luo, H., Tan, Z., Ma, Y., 2021. Simulating land use/land cover change in an arid region with the coupling models. *Ecological Indicators* 122, https://doi.org/10.1016/j.ecolind.2020.107231

Wei, T., Yang S., Moore, J., Shi, P., Cui, X., Duan, Q., Xu, B., Dai., Y., Yuan, W., Wei, X., Yang, Z., Wen, T., Teng, F., Gao, Y., Chou, J., Yan, X., Wei, Z., Gou, Y., Jiang, Y., Gao, X., Wang, K., Zheng, X., Ren, F., Lv, S., Yu, Y., Liu, B., Luo, Y., Li, W., Ji, D., Feng, J., Wu, Q., Cheng, H., He, J., Fu, C., Ye, D., Xu, G., Dong, W., 2012. Developed and developing world responsibilities for historical climate change and CO_2 mitigation. *Proceedings of the National Academy of Sciences of United States of America* 109 (32), 12911-12915. https://doi.org/10.1073/pnas.1203282109

Xiang, H., Wang, Z., Mao, D., Zhang, J., Zhao, D., Zeng, Y., Wu, B., 2021. Surface mining caused multiple ecosystem service losses in China. *Journal of Environmental Management* 290, 112618. https://doi.org/10.1016/j.jenvman.2021.112618

Zadeh, L., A., 1965. Fuzzy sets. *Information and control* 8(3), 338-353 https://doi.org/10.1016/S0019-9958(65)90241-X

Anexo I. Reglas del sistema para la elección de áreas elegibles

POTENCIALIDAD DE CONSOLIDACIÓN	NDVI	ELEGIBILIDAD
Muy alto	Bajo	Medio
	Medio	Alto
	Alto	Alto
	Muy alto	Alto
Alto	Bajo	Medio
	Medio	Alto
	Alto	Alto
	Muy alto	Alto
Medio	Bajo	Medio
	Medio	Alto
	Alto	Alto
	Muy alto	Alto
Bajo	Bajo	Medio
	Medio	Alto
	Alto	Alto
	Muy alto	Alto
Muy bajo	Bajo	Medio
	Medio	Alto
	Alto	Alto
	Muy alto	Alto

Cuadernos de Investigación Geográfica *Geographical Research Letters*	2024	Nº 50 (2)	pp. 135-156	EISSN 1697-9540

http://doi.org/10.18172/cig.6289

AN INTEGRATED METHODOLOGICAL APPROACH FOR THE BALANCE BETWEEN CONSERVATION AND TRADITIONAL USE IN A PROTECTED AREA: THE CASE OF THE PICO AZUL-LA ESCALERA ENVIRONMENTAL PROTECTION ZONE

ADONIS M. RAMÓN PUEBLA[1], CARLOS TROCHE-SOUZA[2]*, MANUEL BOLLO MANENT[1]

[1]*Universidad Nacional Autónoma de México-Campus Morelia: Morelia, Michoacán, México.*

[2] *Comisión Nacional para el Conocimiento y Uso de la Biodiversidad (CONABIO), Tlalpan, México.*

ABSTRACT. Protected Natural Areas often impose restrictions that require a delicate balance between conservation and the traditional uses upheld by local communities. This study presents a novel integrated methodological approach using anthropo-natural landscapes as the primary unit of analysis. The methodology evaluates natural suitability for various appropriate uses within the protected area, considering legal compatibility, environmental sustainability, socioeconomic benefits, and technical-financial feasibility. Our case study of the Pico Azul – La Escalera Environmental Protection Zone reveals that 59.2% of the territory is primarily suited for conservation activities, 38.3% for the rehabilitation of degraded areas, and only 2.5% for extensive livestock farming and rainfed agriculture. Additionally, 24% of the area, comprising mainly non-degraded sectors, is designed for the sustainable use of non-timber forest resources. Furthermore, alternative tourism is identified as a viable secondary use in 10.2% of the most preserved landscapes. This research underscores the importance of a comprehensive and balanced approach to managing protected areas, ensuring both conservation goals and the livelihoods of local communities are met.

Aproximación metodológica integrada para el balance entre conservación y uso tradicional en un área protegida: el caso de la Zona de Protección Ambiental Pico Azul-La Escalera

RESUMEN. Las áreas naturales protegidas a menudo imponen restricciones que requieren un delicado equilibrio entre la conservación y los usos tradicionales defendidos por las comunidades locales. Este estudio presenta un nuevo enfoque metodológico integrado que utiliza los paisajes naturales antropógenos como unidad principal de análisis. La metodología evalúa la idoneidad natural para diversos usos dentro del área protegida, considerando la compatibilidad legal, la sostenibilidad ambiental, los beneficios socioeconómicos y la viabilidad técnico-financiera. Nuestro caso de estudio, la Zona de Protección Ambiental Pico Azul-La Escalera, revela que el 59,2% del territorio es apto para actividades de conservación, el 38,3% para la rehabilitación de áreas degradadas y solo el 2,5% para la ganadería extensiva y la agricultura de secano. Además, el 24% de la superficie, que comprende principalmente sectores no degradados, está destinado al uso sostenible de recursos forestales no madereros. Además, el turismo alternativo se considera un uso secundario viable en el 10,2% de los paisajes más preservados. Esta investigación subraya la importancia de un enfoque integral y equilibrado para el manejo de las áreas protegidas, asegurando tanto los objetivos de conservación como los medios de vida de las comunidades locales.

Keywords: protected natural areas, environmental management, landscape approach, land use suitability, Mexico.

Palabras clave: áreas naturales protegidas, gestión ambiental, aproximación al paisaje, uso sostenible del suelo, México.

Received: 04 July 2024

Accepted: 12 November 2024

***Corresponding author:** Carlos Troche-Souza, Comisión Nacional para el Conocimiento y Uso de la Biodiversidad (CONABIO), Tlalpan, México. E-mail: ctroche@conabio.gob.mx

1. Introduction

Protected natural areas (PNAs) are defined geographical areas aimed at achieving specific conservation objectives (Maldonado *et al*., 2020). According to the International Union for Conservation of Nature (IUCN, 2020), they form the basis of biodiversity conservation, and aim to safeguard nature and cultural resources, improve the livelihoods of resident communities, and promote balanced development between nature protection and the needs of the people living there.

Although PNAs restrict and regulate certain traditional activities, they also open up new avenues for development. If carefully planned and managed, these areas can contribute to economic growth and enhance the well-being of local communities (Botana, 2022). The declaration of a PNA in a territory entails a series of protocols to be followed, primarily aimed at restricting land uses through increased limitation and monitoring of traditional activities previously carried out, upon which local communities often depend for their subsistence (Rienmann *et al*., 2011; Engen *et al*., 2019).

Faced with this issue, specialists suggest that organizing a territory based on its potential suitability allows for long-term growth and development opportunities for rural communities (Lee-Cortés and Delgadillo-Macías, 2018). Rezende *et al*. (2017) and Sosa-Montes *et al*. (2012) highlight the need for residents in PNAs, regardless of conservation objectives, to have spaces to develop their economic activities without affecting the conservation of protected areas, or even participating in the rehabilitation of degraded areas essential for maintaining ecosystem services.

Consistent with these above considerations, in Mexico, there is a recognized need to establish an integrated methodology that considers the social and environmental needs of these territories (Espinoza and Bollo, 2015; Pablo and Hernández, 2016; Azuela de la Cueva *et al*., 2019). The lack of Management Plans (MPs) and Zoning schemes is recognized in about 62 Federal PNAs, accounting for 34.1% of those in the country (CONANP, 2024), which are under various land tenure regimes. This leads to incompatible land uses with the natural suitability of the soils, resulting in degradation and loss of conservation attributes and characteristics which led to their categorization as PNAs.

The natural suitability of a territory is framed within the conceptual and methodological contributions made by the FAO (1993) to define the analytical process that allows the selection of optimal land use forms based on their natural characteristics (Pablo and Hernández, 2016). The potential of the landscape, derived from its natural suitability, is defined by Bollo *et al.* (2010) and Pablo and Hernández (2016) as the set of natural, socioeconomic, and cultural conditions suitable for the development of a particular activity within a territory space called a landscape. The term "landscape" refers to a territorial system integrated by natural and anthropic elements socially conditioned, where the original properties of the landscape are modified (Mateo, 2011; Martínez and Bollo, 2023).

The use of these landscape units as a foundation for environmental research (Izakovicová *et al*., 2019; Martínez and Bollo, 2023) has been demonstrated to be applicable in planning. They serve as environmental management units in zoning exercises across various scales, given their nature as

anthropo-natural systems (Fry *et al*., 2009; Skřivanová, 2014; Cirer *et al*., 2009; Mejías, 2015; López, 2019; Martínez and Bollo, 2023).

Maldonado *et al*. (2020) point out that local communities present in a PNA can interact with their natural resources and use them sustainably. In addition to tourism, activities linked to maintenance, rehabilitation, and utilization can establish other sources of economic income. Thus, the identification of the natural potential of landscapes and their compatible activities may constitute the fundamental approach for proper planning in these protected spaces and avoid their degradation.

In this context, the study aims to evaluate the natural potential of landscapes within the Pico Azul-La Escalera Environmental Protection Zone in Michoacán, Mexico, for various uses. The assessment will consider legal compatibility, environmental feasibility, socioeconomic factors and the technical-financial viability of land use. This approach aims to promote sustainable practices that conserve natural resources while benefiting local communities engaged in socioeconomic activities.

2. Methodology

2.1. Study Area

The Pico Azul-La Escalera Environmental Protection Zone (Fig. 1) was declared in 2011 as an Environmental Protection Zone due to its physical, climatic, and conservation characteristics. It provides a series of environmental services focused on regulating water flow, purifying and retaining water, and infiltration for aquifer recharge. Additionally, it contributes to flood control and prevention, as well as sediment regulation and climatic regulation in the region. Furthermore, it offers areas with scenic beauty for recreation, which is of great importance to the population of the city of Morelia (Official Newspaper of the Constitutional Government of the State of Michoacán de Ocampo, 2011).

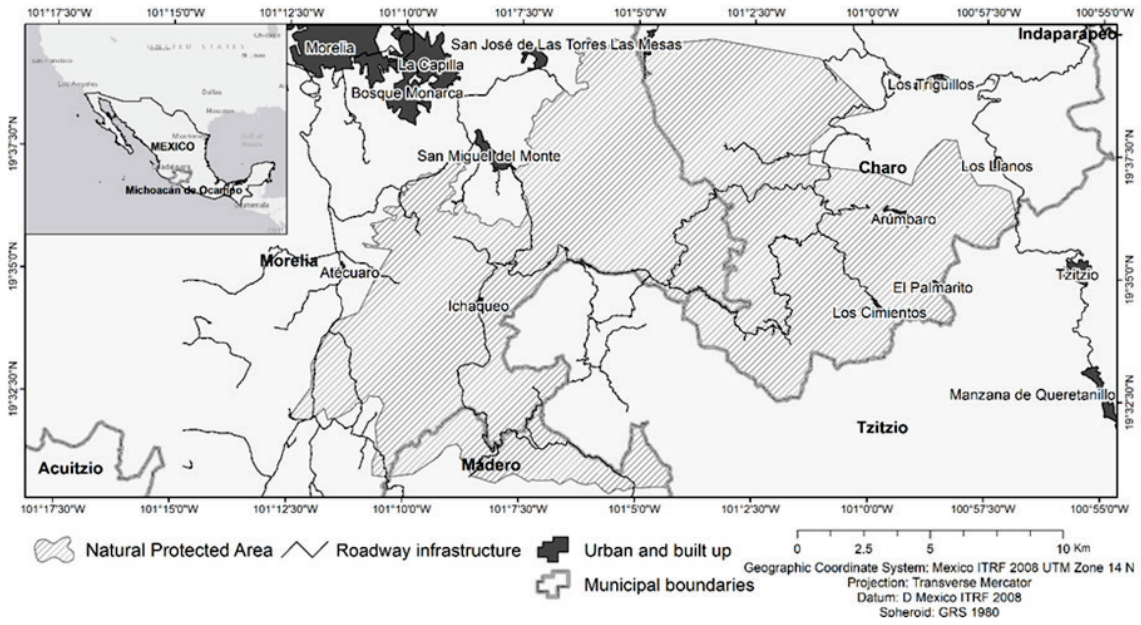

Figure 1. Geographic location of the Pico Azul-La Escalera Environmental Protection Zone.

It spans an area of 224 km² and is located in the transition zone between the mountains of the Neovolcanic Transverse Axis and the Sierra Madre del Sur, in the central-southern region of Mexico. The geographical coordinates of the area range between 19° 39' 48.52" - 19° 30' 31.33" N and 101°

12'24.77" - 100° 56' 48.57" W (Ramón and Bollo, 2023). Its altitude ranges from 1,171 to 2,640 meters above sea level.

The region has a temperate climate, with an annual temperature ranging between 12 and 18°C, and precipitation fluctuating between 200 and 1800 mm (García, 1988). The predominant soils are andosols (34.76%), luvisols (27.82%), and acrisols (26.40%) (INEGI, 2004). The main vegetation cover is forested, covering 85.5% of the studied area, with 86.7 km² considered primary vegetation, mainly in the north, northwest, and southwest. Of the total forested area, 40.9% (78.4 km²) shows a high degree of disturbance, and 30.9% exhibits a predominance of shrub species. Induced grasslands occupy 9.8% of the total area, areas allocated to rainfed agriculture cover 2.7%, and permanent crops cover the remaining 1.50% (Ramón and Bollo, 2023). Human settlements encompass only 0.5% of the total study area, with 27 established populations housing 2,789 inhabitants according to the official census (INEGI, 2020).

2.2. Territorial Analysis Unit: Anthropo-natural Landscapes

This research uses anthropo-natural landscape units within the PNA at a 1:50,000 scale as the basic analysis unit. These units were derived from overlaying the physical-geographical landscape map (Ramón and Bollo, 2023) and the land cover and land use map of 2021, generated from supervised classification of a Landsat-8 satellite image (Legend of the landscape units in Supplementary Material A).

2.3. Stages of Landscape Potential Assessment

The present study bases the assessment of landscape potential on Land Use Types (LUTs), which encompass the purposes and actions through which individuals engage with land and terrestrial ecosystems (Meyfroidt *et al.*, 2018). The selection and description of each LUTs, is a planning process that takes into account development objectives and the natural and socio-economic conditions of the territory. Palacio-Prieto and Sánchez-Salazar (2003) suggest considering criteria that guide government development objectives and policies, current land use, current markets, cultural acceptance of LUTs by local communities, and the availability of physical infrastructure, among others.

The process of identifying of landscapes potential was divided into three stages: a) identifying natural suitability regarding LUTs; b) evaluating the implementation of LUTs and the legal, environmental, socio-economic, and technical-financial compatibility of the study area; and c) determining the potential use of landscapes.

2.4. Natural Suitability of Landscape for Proposal Land Use Types

Based on the compatibility of permitted uses according to the category of the study area (Environmental Protection Zone), and the availability of information, the selection of LUTs was carried out following the methodological proposals of various authors (Bollo *et al*., 2010; Ramón *et al*., 2013; Pablo and Hernández, 2016). The selected LUTs are described below, and Table 1 shows the indicators and methods used for their identification:

- Conservation: This aspect focuses on identifying landscapes with high natural and conservation values that play a fundamental role in providing environmental services (Bollo *et al*., 2010; Chávez and González, 2015; Teixeira *et al*., 2018).
- Alternative Tourism: This includes non-conventional and non-massive tourism modalities, which aim to offer participants a more direct and active involvement with nature, local culture, and other special interest resources they visit (Báez and Acuña, 2003; Ramón *et al*., 2020; Bassan, 2022).

- Rehabilitation: This aspect aims to identify landscapes that require intentional intervention to initiate or accelerate the recovery of their natural conditions due to loss or deterioration in their environment. This is vital to ensure the environmental services that the PNA must provide according to its management category and declaration motive, based on the criteria of Keenleyside *et al.* (2014).
- Forestry: This aspect aims to promote the permanence of forests and maintain their environmental functions through the sustainable use of Non-Timber Forest Products such as resins, wild plants, medicinal plants, edible mushrooms, certain shrubs, and firewood (Anastacio-Martínez, 2016).
- Extensive Livestock Farming: This focuses on ensuring the sustainability of economic activity in the PNA for the resident population through the existence of induced pastures and certain soil properties (Bollo *et al*., 2010; Pablo and Hernández, 2016; Ramón *et al*., 2017).
- Rainfed Agriculture: This aims to ensure the sustainability of economic activity in the PNA for the resident population. The same indicators as for extensive livestock farming were established, except for those related to the presence of induced pastures and secondary forests dominated by herbaceous vegetation.

All indicators and variables were weighted on a scale of 1 to 5. The highest value was assigned to attributes that favored the LUT, while the lowest value was assigned when the attribute did not favor the evaluated LUT. The score of each indicator was summed up, and the result was reclassified into four suitability categories using the natural break method (Jenks, 1976): A1 (Suitable), A2 (Moderately Suitable), A3 (Marginally Suitable), and N (Not Suitable).

Table 1. Indicators used to identify the natural potential of the landscape according to the proposed land use type.

Indicator	Evaluation Method		Land Use Type	Reference
Degree of Naturalness	$Dn = \left(\frac{Sveg_{nat}}{A}\right) * 100$	Where: Dn = Degree of Naturalness $Sveg_{nat}$ = Primary vegetation area A = Landscape unit area	Conservation Alternative Tourism Rehabilitation Forestry	Bollo and Velazco (2018)
Landscape Degradation	$IAVC = \frac{\sum_{i=1}^{n} r_i * A_{ij}}{A_j}$	Where: $IAVC$ = Index of Vegetation Cover Anthropization r_i = Weighting value of land cover type *"i"* A_{ij} = Area of land use type in landscape unit A_j = Total area of landscape	Conservation Alternative Tourism Rehabilitation Forestry	Shishenko (1988)
Water recharge	$Water\ recharge = \lfloor 0.27(S) + 0.23(ST) + 0.12(TR) + 0.25(PVC) + 0.13(LU) \rfloor$	Where: S = Slope ST = Soil Type TR = Type of rock PVC = Permanent vegetation cover LU = Land use	Conservation Rehabilitation Forestry	Matus *et al*. (2009)
Soil loss	$Soil\ loss = R * K * LS * S * P$	Where: R = Rainfall and runoff factor K = Soil erodibility factor LS = Topographic factor C = Cover and management factor P = Support practice factor	Conservation	Wischmeier and Smith (1978)
Slope Degree	Topographic maps (scale 1:50 000)		Alternative Tourism Rehabilitation Forestry	INEGI (2018)
Soil fertility	Soil maps (scale 1:50 000)		Rehabilitation Extensive Livestock Rainfed Agriculture	INEGI (1983)
Soil physical limitations	Soil maps (scale 1:50 000)		Rehabilitation Extensive Livestock Rainfed Agriculture	INEGI (1983)

Soil pH	Soil maps (scale 1:50 000)	Rehabilitation Extensive Livestock Rainfed Agriculture	INEGI (1983)
Soil depth	Soil maps (scale 1:50 000)	Rehabilitation Extensive Livestock Rainfed Agriculture	INEGI (1983)
Soil erodibility	Soil maps (scale 1:50 000)	Rehabilitation Extensive Livestock Rainfed Agriculture	INEGI (1983)
Carbon Sequestration	Carbon Storage and Sequestration model (InVEST)	Conservation	Natural Capital Project (2023)
Nutrient Delivery	Nutrient Delivery Ratio model (InVEST)	Conservation	Natural Capital Project (2023)
Primary Ecotourism activities	- Number of waterfalls per analysis unit - Number of rivers per analysis unit - Number of mountain peaks	Alternative Tourism	This study
Complementary Ecotourism activities	- Number of trails - Lodging capacity - Dining Options	Alternative Tourism	This study
Traditional economic activities or festivities	Surveys on Local Agricultural and Religious Festival Dates	Alternative Tourism	This study
Induced pastures	Area of induced pasture (Land cover and land use map 2021)	Extensive Livestock	This study
Secondary forest with herbaceous vegetation	Area of secondary forest with herbaceous vegetation (Land cover and land use map 2021)	Extensive Livestock	This study

2.5. Landscape Use Viability

The assessment of different viabilities is conducted through a comprehensive review of existing information. This includes analyzing the results of variables and indicators. These results facilitate an understanding of the temporal dynamics and interrelationships among sociodemographic factors, socioeconomic aspects, and the characteristics of the natural-physical environment.

Legal Compatibility: It assesses the presence of any potential legal restriction on the implementation of the LUT. This assessment is exclusive, meaning that if a landscape unit has certain natural suitability but is subject to legal regulations, it automatically renders such suitability as *Not Suitable*.

The criteria for assessing legal compatibility are based on the provisions set forth in the Decree declaring the study area, Pico Azul – La Escalera, as an Environmental Protection Zone (EPZ). Additionally, the assessment considers the local legal framework in Michoacán de Ocampo, given that it falls under state jurisdiction. Federal regulations on land use allocation are also taken into account. Table 2 summarizes all laws, regulations, and official standards considered in the analysis.

After analyzing the legal compatibility of each landscape unit, those units deemed 'Suitable' undergo a viability assessment process. Viability refers to the possibility of effectively and sustainably implementing the proposed LUTs. Three fundamental areas were defined for viability analysis: environmental, socioeconomic, and technical-financial. Landscape units that were deemed 'unsuitable' for socioeconomic use were classified according to their conservation or restoration characteristics.

Environmental Viability: This criterion was used to assess the ability of landscape units to support and maintain the proposed LUTs without compromising their long-term sustainability (Palacio-Prieto and Sánchez-Salazar, 2003). Given that it is a PNA, proposed LUTs that support management objectives (conservation and rehabilitation) received a positive evaluation and proceeded to further viability analyses. For landscape units with productive or natural resource use LUTs (Forestry, Extensive Livestock, and Agriculture), the criteria from Table 3 were used. Ecotourism, proposed and developed with low impact, had no recorded usage limitations. If any LUT showed no environmental viability, it was excluded from further evaluations.

Table 2. Federal and State laws, Federal and State regulations, analyzed to determine the legal compatibility of landscape units in the Pico Azul – La Escalera Environmental Protection Zone.

Application Level	Oficial Law / Regulation	Reference
Study Area	- Decree establishing the Environmental Protection Zone	POGMICH, 2011
State (Michoacán de Ocampo)	- Climate Change Law and its regulations - Sustainable Forestry Development Law and its regulations - Sustainable Integral Rural Development Law and its regulations - Livestock Law - Water and Watershed Management Law and its regulations - Land Conservation and Restoration Law - Environmental Conservation and Sustainability Law - Regulation of the Environmental Law and Protection of Natural Heritage	POGMICH, 2014, 2018 POGMICH, 2004a, 2007a POGMICH, 2006a, 2006b POGMICH, 2007b POGMICH, 2004b, 2008 POGMICH, 2007c POGMICH, 2021 POGMICH, 2004c
Federal (Mexico)	- Regulation for the exploitation of Fungi - Regulation for the exploitation of Wild Soil - Regulation for the exploitation of Forest Roots and Rhizomes - Regulation for the exploitation of Moss, Hay, and Clubmoss - Regulation for the Rehabilitation and Conservation of Grazing Forest Lands - Regulation for the exploitation of Pine Resin - Regulation for Content of Forest Management Programs	SEMARNAT, 1996a SEMARNAT, 1996b SEMARNAT, 1996c SEMARNAP, 1996 SEMARNAT, 2001 SEMARNAT, 2005 SEMARNAT, 2006

Table 3. Environmental valuation criteria for productive land use types.

Land Use Viability	Criterion	Description
Environmental	Long-term degrading potential	The ability of a use or activity to cause environmental degradation over time.
	Carrying capacity for land use	Maximum amount of a specific type of use that a territory can sustainably support.
	Natural and anthropogenic threat limitations	Constrains due to the presence of phenomena occurring from natural processes (such as floods, seismic activity, landslides) and those caused by human actions (soil and water contamination, deforestation, etc.).
	Degradation process constrains.	Limitations due to the deterioration of the natural environment caused by the excessive exploitation of natural resources.
	Anthropogenic pressures	Factors or actions resulting from human activity that affect land use and management (agriculture, deforestation, hunting, logging, construction, livestock farming, and development of housing, service infrastructure, and transportation).
Socioeconomic	Inertia from traditional land uses	Deep-rooted and persistent trends in how a territory has been historically utilized.
	Job creation	Job creation for local community residents.
	Population needs	Requirements, necessities of a community or group of people living in a particular area. These needs can include various aspects such as access to healthcare, employment opportunities, infrastructure, and other resources necessary for sustaining and improving quality of life.
	Availability of labor force	Number of skilled labor for the land use type selected.
	Accessibility	Concerns the ease of reaching and utilizing a specific area, relying on transportation routes like roads, pathways, and transportation to connect various parts within the territory.
Technical-financial	Availability of technical and technological resources	Access to the knowledge, tools, and technologies necessary for the intended land use.
	Financial resource availability	Existence and accessibility of required financial resources.
	Availability of required infrastructure	Existence and accessibility of necessary facilities and services for the development of the corresponding land use.

Source: Modified and adapted from Aguiló-Alonso *et al.,* 2009, and Palacio-Prieto *et al.,* 2004.

Socioeconomic viability: Used to assess whether the landscape unit can generate long-term economic and social benefits while maintaining environmental sustainability (Ramírez *et al*., 2016). Evaluation criteria were derived from fieldwork data.

Technical and financial viability: assesses the ability to effectively implement the LUT from a technical standpoint, as well as the capacity to finance and sustain the LUT over time. It relies on the availability of government funding programs or support provided by Non-Governmental Organizations (NGOs). Existing technological means for the proposed LUT should be sustainable and cost-effective for conservation, protection, and production in these areas.

With the information obtained according to the criteria in Table 3, the information is used to assess the viability of each landscape unit for each LUT within a suitability range, as per the values in Table 4.

These results are reflected in a data matrix that includes landscape units, natural suitability values, and environmental, socioeconomic, and technical-financial viability assessments.

Table 4. Measurement scale for viability categories.

Viability category	Value
Non-viable	0
Viable with conditions	50
Viable	100

Source: Developed from Palacio-Prieto and Sánchez-Salazar (2003)

2.5.1. Assessment of Landscape Use Potential

Following the previous procedure, the quantitative assessment of the suitability of each landscape polygon for each LUT is continued. In this process, the categories obtained in Natural Suitability (Suitable, moderate, marginal, and not suitable) are converted into a numerical value with a common maximum of 100, as shown in Table 5.

With the values obtained for each landscape polygon and the results of the evaluation of each viability, the Land Use Suitability Index (LUSI) is calculated for different LUTs using Eq. (1) (Palacio-Prieto and Sánchez-Salazar, 2003)

$$LUSI = \frac{LNP+SEV+EV+TFV}{4} \quad (1)$$

Where LNP: Landscape natural potential; SEV: Socioeconomic viability, EV: Environmental viability, TFV: Technical-financial viability.

The index value will range from 0 to 100. Categories were established as Suitable (75.1-100), Moderately Suitable (50.1 – 75), Marginally Suitable (25.1 – 50), and Not Suitable (0-25) for each specific LUT.

Table 5. Equivalent value scale with a maximum of 100 according to natural suitability.

Category	Value
Suitable (S1)	100
Moderately Suitable (S2)	67
Marginally Suitable (S3)	33
Not Suitable (N)	0

Source: Palacio-Prieto and Sánchez-Salazar (2003)

The results obtained generate a matrix that identifies primary and secondary potential uses for each landscape polygon in relation to the evaluated LUTs. To determine the primary or potential primary uses, the LUTs with category S1 are selected from each landscape unit. If there is none, those in category

S2 are considered. The same procedure is applied to determine secondary potentials, where if category S1 is chosen as the primary potential, category S2 is considered as the secondary potential.

Both potentials were assessed with the aim of providing a wide range of options to decision-makers in territorial planning. The primary potential aligns with the highest natural aptitude and environmental, socio-economic, and technical-financial viabilities of the polygon in relation to the analyzed LUTs. The secondary potential refers to possible uses to maintain or develop but requires specific conditions and periodic monitoring to prevent degradation of the area's natural conditions. This matrix forms the basis for the development of maps of primary and secondary use potentials of the territory.

3. Results and Discussion

3.1. Anthropo-natural Landscapes

The land cover and land use map derived from the Landsat-8 satellite imagery classification for 2021 identified five categories of land cover or use and three subclasses within the Forest category (Table 6).

The resulting map was overlaid with regions from the physical-geographical landscape map (Ramón and Bollo, 2023), revealing 24 different types of anthropogenic landscapes within the PNA, totaling 136 polygons (See Fig. 2 and complete legend in Supplementary Material A).

Table 6. Land cover and land use types for the year 2021.

Category	Area (ha)
Forest	19,151
-Primary forests	8,681
- Shrubland secondary forests	2,644
- Herbaceous secondary forests	7,826
Induced pastures	2,192
Rainfed agriculture	613
Peremanent crops	336
Urban and built up	108
Total	22,401

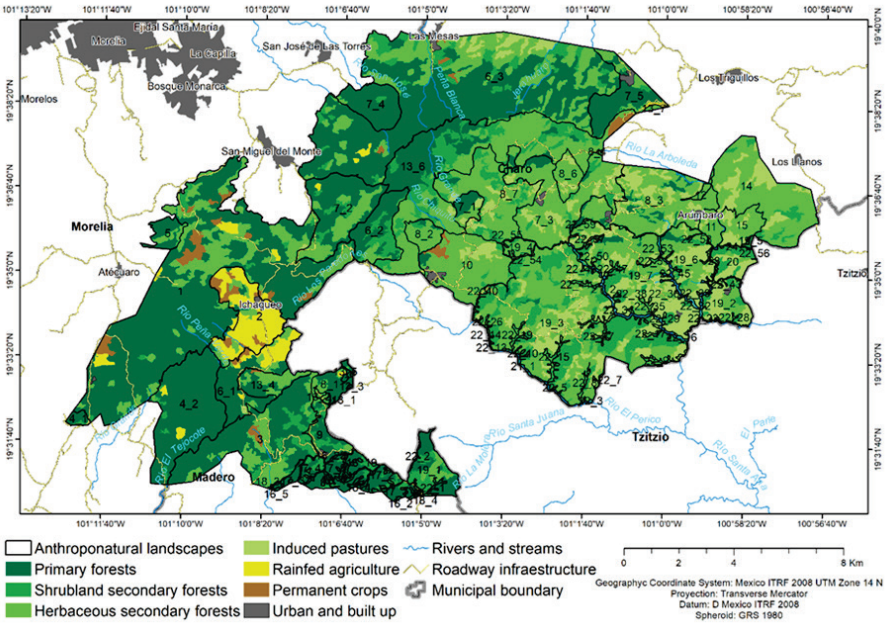

Figure 2. Anthropo-natural Landscape Units for the year 2021.

3.2. Landscape Suitability and Viability for Proposed Land Use Types

The spatial evaluation of landscape suitability for the proposed LUTs is depicted in Fig. 3. *Conservation, Alternative Tourism, and Restoration LUTs* demonstrated legal compatibility across all landscape units, as they prioritize environmental conservation, protect natural resources, and entail low environmental impact. However, the legal analysis revealed limited compatibility for the Non-timber Forest Products Harvesting in landscapes with slopes exceeding 45 degrees and riparian vegetation protection zones. *Extensive Livestock Farming* and *Rainfed Agriculture* faced legal restrictions in forested areas and riparian zones due to soil erosion prevention and restoration regulations.

Viability assessment for *Conservation* considered opportunities provided by payment for ecosystem services (PES) and Sustainable Forest Development programs, which support market creation for forest landowners (CONAFOR, 2022; Wunder *et al.,* 2007). The landscape units with higher conservation potential (Fig. 3A) consist of 51 polygons, representing 56.9% of the territory (see Table 7). These landscapes are mainly located in the north, northwest, and southwest, associated with less degraded forest cover, which enhances the viability for implementing the PES scheme. Categories S2 and S3, covering 24.3% of the area (43 polygons), are linked to forested landscapes with moderate degradation levels, with lower chances for PES scheme application. The remaining 18.8% of the PNA (42 polygons) comprises landscapes with the highest degradation levels, primarily used for agricultural and livestock activities, with minimal forest cover.

For *Alternative Tourism*, the PES scheme presented financing opportunities, particularly where ecotourism is considered an effective environmental service (Ruiz-González *et al.,* 2022). This incentive could represent, for some communities with traditions of mezcal production (a type of tequila) or religious practices, an influx of visitors, making the socio-economic and technical-financial viability of this LUT feasible. Landscape units with the highest tourism potential (Fig. 3B) encompass nine polygons, representing 51.8% of the PNA (Table 7). They extend to the north and northwest, coinciding with regions of high conservation potential (Fig. 3A) and having higher feasibilities for implementing PES scheme. In the central and western regions (Fig. 3B), some landscapes, despite low forest cover, show high suitability values due to cultural traditions and the presence of primary ecotourism activities, lodging facilities, and restaurants. The S2 category, representing only 4.0% of the landscape area, is associated with the presence of some service infrastructure and good accessibility. The remaining 44.2% of the PNA (Table 7) comprises landscapes located in the south and west (Fig. 3B). These areas exhibit low significance for tourism activity (S3 and N), primarily due to accessibility challenges, absence of primary activities, or degradation resulting from agricultural and livestock activities.

The results regarding the socioeconomic viability for the *Rehabilitation* LUT indicate job creation and opportunities, stemming from the accessibility to the areas targeted for rehabilitation. The technical and financial viability was confirmed as positive. This was attributed to the availability of knowledge, technical and technological resources, and financial support from existing programs on forest and sustainable productive development by the central government (Cravioto, 2019). The S1 category for Rehabilitation (Fig. 3C) covers 95 landscape polygons, representing 70.0% of the territory (Table 7), mainly extending to the north, south, east, and a group of polygons to the southwest (Fig. 3C). These coincide with polygons exhibiting some level of forest cover degradation, high water recharge capacity, topography, and soils unsuitable for other uses. Landscape classified with S2 comprise 37 polygons, accounting for 8.7% of the total area. These landscapes are mainly located in the southwest, featuring preserved forest cover. However, they encounter challenges in socioeconomic viability due to low population density and limited accessibility. The S3 category is absent, and the remaining 21.3% of the territory consists of polygons in the northwest (Fig. 3C) with high conservation levels.

The use of non-timber *Forest* resources (NTFR) demonstrated excellent socioeconomic viability due to the employment opportunities and economic prospects it provides for the land use. The technical and financial viability is also very high, as it generally does not rely on substantial resources to be implemented. The S1 category of the NTFR LUT covers 17 landscape polygons (Fig. 3D), representing

57.5% of the territory (Table 7), primarily extending to the north, northwest, and south. It coincides with polygons characterized by higher forest cover, better accessibility, and lower slope ranges. The polygons categorized as S2 (six polygons), representing 1.1%, encompass some isolated polygons in the northwest, center, and southeast (Fig. 3D), with moderate values of forest cover and degradation, as well as limited accessibility. The remaining categories S3 and N, accounting for 41.4%, consist of polygons with very little or no forest cover or with legal restrictions on exploitation.

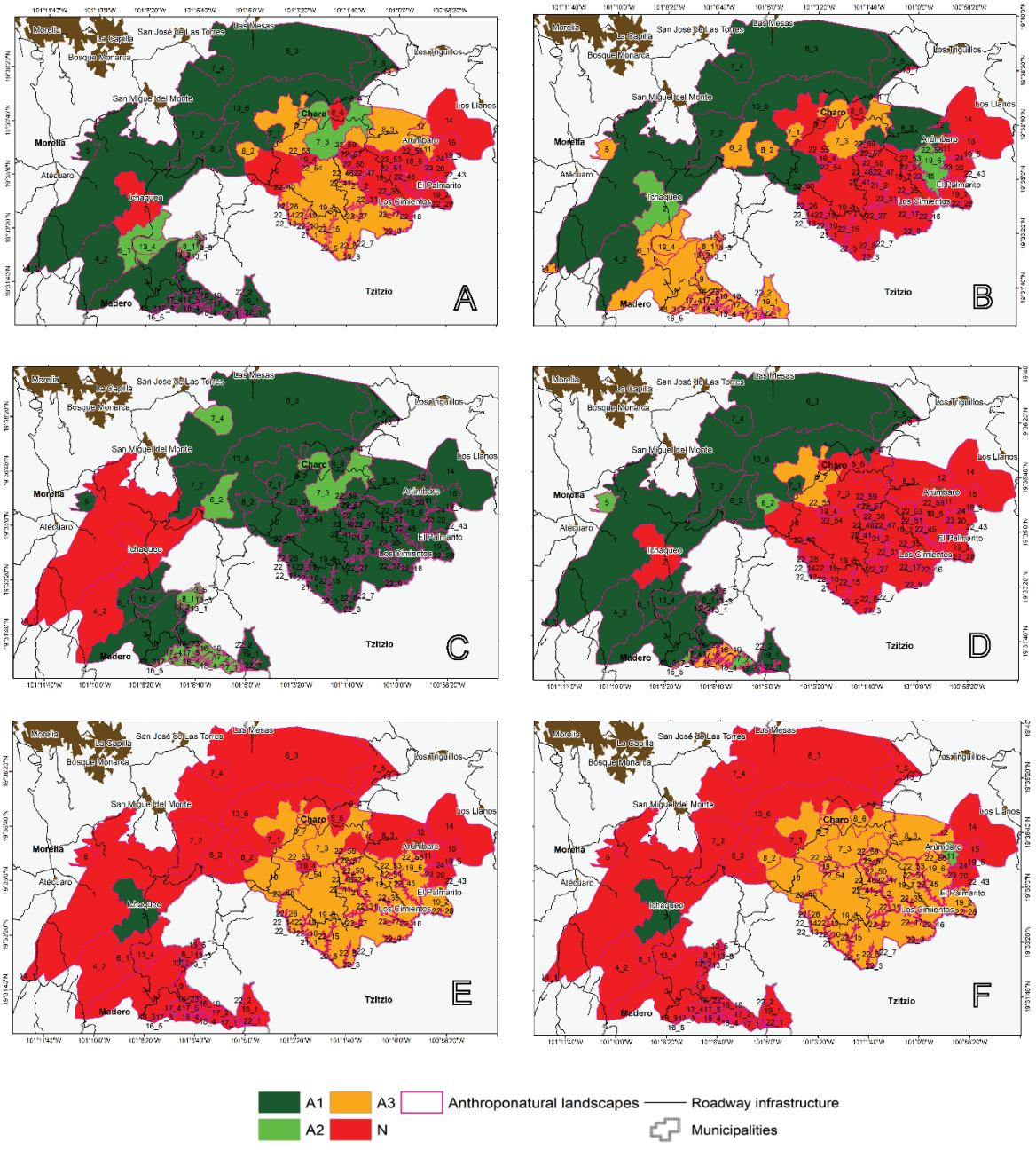

Figure 3. Spatial distribution of landscape potential on Land Use Types in PNA Pico Azul-La Escalera Environmental Protection Zone. Land Use Types: A) Conservation; B) Alternative Tourism; C) Rehabilitation; D) Forestry; E) Extensive Livestock Farming; F) Rained Agriculture.

Table 7. Surface area of potential suitability for each proposed land use type.

Land Use Type / Suitability	Conservation	Alternative Tourism	Rehabilitation	Forestry	Extensive livestock farming	Rainfed Agriculture
Suitable (S1)	12,743.0 ha 56.9% 51 LP	11,610.8 ha 51.8% 9 LP	15,675.5 ha 70.0% 95 LP	12,886.5 ha 57.5% 17 LP	549.1 ha 2.5% 2 LP	550.7 ha 2.4% 4 LP
Moderately Suitable (S2)	1,451.2 ha 6.5% 15 LP	898.3 ha 4.0% 2 LP	1,958.0 ha 8.7% 37 LP	238.8 ha 1.1% 6 LP	729.5 ha 3.2% 1 LP	82.0 ha 0.4% 1 LP
Marginally suitable (S3)	4,001 ha 17.8% 28 LP	4,126.7 ha 18.4% 68 LP	-	881.2 ha 3.9% 26 LP	657.8 ha 2.9% 1 LP	940.9 ha 4.2% 2 LP
No Suitable (N)	4,205.3 ha 18.8% 42 LP	5,764.7 ha 25.8% 57 LP	4,767.1 ha 21.3% 4 LP	8,394.0 ha 37.5% 87 LP	20,464.2 ha 91.4% 132 LP	20,827.0 93.0% 129 LP

LP: Landscape polygons

The socioeconomic viability for *Extensive Livestock Farming* largely depends on the accessibility of the areas to be occupied. The technical and financial viability is positive due to the availability of knowledge and technical resources, which generally require low economic inputs. The land area categorized as S1 for livestock farming represents 2.5% of the total area. However, this suitability is limited due to its topographical characteristics, soils, and environmental viability. The two landscape units with this suitability are located in the central-western part (Fig. 3E), coinciding with polygons of lower slope, induced grasslands, and better accessibility. The moderate category (S2) represents 3.2% of the PNA, located in the central-eastern part, with some areas of high slopes, which is what gives it this category. The remaining 133 polygons of landscape units, covering practically the entire territory (94.3% of the total area); belong to categories S3 and N. These units have high slopes, primarily in the northern and northwestern sectors (Fig. 3E), with abundant primary or secondary forest vegetation dominated by shrubs.

The socioeconomic and technical-financial viability for *Rainfed Agriculture,* similar to extensive livestock farming, proved positive owing to job creation and opportunities, along with low-cost input requirements. However, its success hinges largely on accessibility to suitable areas for this use. Category S1 represents 2.4% of the territory (Table 7) and mainly located in the north and northwest (Fig. 3F). This area coincides with land already dedicated to rainfed agriculture and induced pastures, better accessibility, and low slope ranges. The polygons under category S2 (one polygon) represent 0.4% and is located to the east, exhibiting the same characteristics as category S1, but with more restrictive slope ranges for the development of this activity. The Remaining 129 landscape polygons, representing 97.2% fall under categories S3 and N, covering virtually the entire PNA (Fig. 3F). These units have slopes unsuitable for this LUT or abundant primary or secondary forest vegetation.

3.3. Landscape Use Potential

The results obtained from the evaluation of the landscape use potential for each landscape unit with respect to the evaluated LUTs (*Conservation, Alternative Tourism, Rehabilitation, Forestry, Extensive Livestock Farming,* and *Rainfed Agriculture*) form the basis for determining the primary and secondary potential of the territory. Figure 4 shows the spatial distribution of primary and secondary use potential by polygon for the year 2021.

Due to its designation as a Protected Natural Area, conservation, ecotourism, and rehabilitation were prioritized as primary potentials (solid colored Fig. 4). As secondary potentials (hatched and cross-hatched lines Fig. 4), emphasis was placed on the utilization of territorial resources, particularly for

forestry purposes. Additionally, primary suitability was prioritized for socioeconomic uses in landscape units with higher resident populations and better environmental, socioeconomic, and technical-financial conditions for implementation. In these units, secondary uses were determined as those that could be carried out without destroying or degrading natural values.

The Figure 4 and Table 8 show that landscapes with primary conservation potential are the most abundant, collectively representing 59.3% of the territory's landscape area. They are distributed across the north, northwest, west, southwest, and south. In terms of categories, landscapes with exclusive primary conservation potential cover 13.6% of the PNA and are characterized by the highest conservation levels and minimal or no resident population. They are mainly found in the southwest and south, with isolated units in the center and northwest. Within this category, 1.2% exclusively have primary conservation potential, while 98.8% have secondary potential for rehabilitation due to some degree of deterioration in primary forest cover (3,008.7 ha). Additionally, 85.3%, regardless of their secondary potential for restoration, can be exploited under regulatory guidelines for obtaining non-timber forest products.

In the Conservation-Tourism category, which represents 45.7% of the total, landscapes exhibit a higher level of forest degradation compared to those in the previous category. They also feature better accessibility and scattered settlements within them, while still retaining values attractive to alternative tourism. These landscapes are distributed in the north, northwest, and west regions. Within this category, all units have rehabilitation as a secondary potential, and 52.4% have the possibility of exploiting non-timber forest resources according to regulations governing their use.

Suitable for forest cover rehabilitation encompasses 38.3% of the area, primarily located in the eastern and central regions, historically more exploited for timber extraction and agricultural production despite suboptimal conditions for these activities.

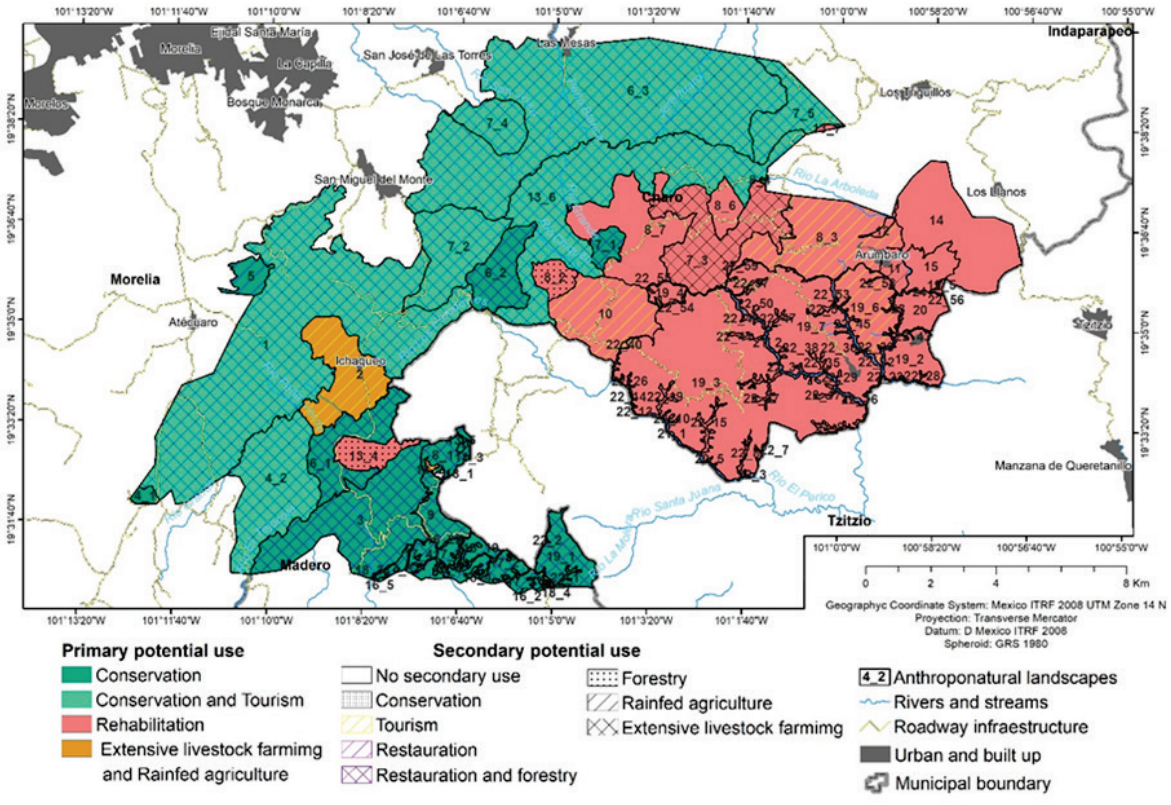

Figure 4. Primary and secondary landscape potential use.

Table 8. Landscape Use Potential.

Primary Use	Area (ha)	Landscape units	Secondary Use	Area (ha)	Landscape units
Conservation	3,043.6	44	No secondary use	34.9	1
			Rehabilitation	413.1	31
			Rehabilitation-Forestry	2,595.6	12
Subtotal	**3,043.6**	**44**	**Subtotal**	**3,043.6**	**45**
Conservation – Alternative Tourism	10,230.3	7	Rehabilitation- Forestry	4,864.0	2
			Forestry	5,366.2	5
Subtotal	**10,230.5**	**7**	**Subtotal**	**10,230.5**	**7**
Rehabilitation	8,576.0	81	No secondary use	5,720.3	61
			Conservation	21.4	12
			Alternative Tourism	1,737.3	4
			Forestry	285.5	2
			Extensive Livestock Farming	729.5	1
			Rainfed agriculture	82.1	1
Subtotal	**8,576.0**	**81**	**Subtotal**	**8,576.0**	**81**
Rainfed Agriculture – Extensive Livestock Farming	550.7	4	Alternative Tourism	541.5	1
			Rehabilitation-Forestry	7.5	1
			Rehabilitation	1.6	2
Subtotal	**550.7**	**4**	**Subtotal**	**550.7**	**4**
Total	**22,400.6**	**136**	**Total**	**22,400.6**	**136**

Within this category, 66.7% of landscape units are solely designated for rehabilitation (5,720 ha), while 0.3% still maintain some forest cover suitable for conservation (21.4 ha) as secondary use. Additionally, 20.3% possess values for alternative tourism (1,737.3 ha) linked to local cultural traditions or existing infrastructure (such as restaurants and lodges). Furthermore, 3.3% of the area (285.5 ha) is suitable for non-timber forest product harvesting in residual forests, in compliance with current regulations, while 9.5% can accommodate extensive livestock farming (729.5 ha) and rainfed agriculture (82.1 ha) in appropriate areas as secondary landscape potential uses.

Regarding productive activities, 2.5% have common primary potential for both rainfed agriculture and extensive livestock farming (550.1 ha). These areas are located in the flattest zones of the territory, featuring better soil for such activities and significant human settlements traditionally linked to these land uses. Within this category, 98.3% possess secondary potential for alternative tourism (541.5 ha), attributed to factors such as accessibility, existing infrastructure, and proximity to key attractions within the PNA. The remaining 1.7% of landscape units could potentially shift to rehabilitation if agricultural activity were abandoned and 1.4% could serve as secondary potential for non-timber forest resource utilization within their forest remnants.

The use of landscape units to assess the potential of a PNA for various LUTs has not been previously addressed. There are references to the use of landscape units to assess the natural potential of the territory (aptitude) in the works of Bollo *et al*. (2010) and Ramírez-Sánchez *et al.* (2016), applied to state-level studies in Mexico. However, the analyses proposed here of viability and landscape potential to address possible types of use are not addressed in those studies. These aptitude assessments are characteristic of works that address environmental land management and follow the execution proposal of Palacio-Prieto and Sánchez-Salazar (2003) during their execution phases, as seen in the work conducted by Ramón *et al*. (2011).

Ramón *et al*. (2013) made a methodological proposal for the use of landscape units, involving the evaluation of use aptitude and the various feasibilities discussed here to assess landscape potential in ANPs, without documentation of its use or references to its application being found. The evaluation conducted here could be considered an initial validation of the methodology proposed by the aforementioned authors, which builds upon the proposal of Palacio-Prieto and Sánchez-Salazar (2003),

with adjustments made within the context of Mexico and the category of the Pico Azul-La Escalera PNA for its application.

Studies on landscape potentials in various regions of the world have been extensively conducted to evaluate the tourism potential of landscapes (Cetin, 2015; Mikulec and Antoušková, 2011; Martínez-Rodríguez *et al*., 2021; Torres *et al*., 2015; Huerta and Sánchez, 2011). Therefore, the evaluation conducted in this study in the context of a PNA can be considered the first assessment from this perspective, with results that support its implementation.

4. Conclusions

The assessment conducted constitutes a comprehensive methodological proposal for assessing land use potential that can contribute to the zoning of protected natural areas. Including social, legal, and natural factors in this assessment provides administrators of these spaces with solid arguments to support and diversify proposed land uses according to existing physical-geographic and socioeconomic conditions. The use of anthropo-natural landscapes as the fundamental unit of analysis for evaluating territorial potential offers the opportunity to zone potential landscape uses into categories for various purposes. These units represent a synthesis of the physical-geographic and socioeconomic components and processes that characterize the homogeneity of the protected natural area's surface.

Based on the designed indicator evaluation procedure, it was found that the Pico Azul - La Escalera Environmental Protection Zone has a primary potential for conservation activities on 59% of its territory. This percentage comprises preserved forests maintaining the environmental services and natural processes specified in the creation decree.

On the other hand, the incompatibility of uses assessed through environmental, legal, socio-economic, and technical-financial indicators determined that 38% of the Pico Azul - La Escalera Environmental Protection Zone has a primary potential for rehabilitation. This Land Use Type, aligned with the objectives of the protected area, could emerge as a pivotal revenue stream for local communities.

Tourism is often regarded as a low-impact alternative activity within NPA, offering socio-economic benefits to local communities. Typically, these tourist activities prioritize showcasing the natural attractions of the region. However, this study demonstrates that by considering comprehensive planning criteria and appropriate land use, tourism can emerge as a secondary and marginal potential only linked to the presence of infrastructure and cultural-religious themes.

Acknowledgement

The authors express their gratitude to the Postgraduate Program in Geography and the Center for Research in Environmental Geography, both institutions belonging to the National Autonomous University of Mexico (UNAM). They also extend their acknowledgement to the National Council of Humanities Science and Technology of Mexico (CONAHCYT), for their financial support in carrying out this research. Additionally, they are thankful to all those who, with their suggestions, contributed to the completion of this work.

References

Aguiló-Alonso, M., Albaladejo-Montoso, J., Aramburu-Maqua, M.P., Valero-Huete, F., 2009. *Guía para la elaboración de estudios del medio físico. Contenido y metodología.* Fundación Conde del Valle de Salazar (ETSI Montes) y Ministerio de Agricultura, Alimentación y Medio Ambiente. https://oa.upm.es/55224/1/Guia_para_la_elaboracion_de_estudios_del_medio_fisico_2.pdf

Anastacio-Martínez, N.D., Franco-Maass, S., Valtierra-Pacheco, E., Nava-Bernal, G., 2016. Aprovechamiento de productos forestales no maderables en los bosques de montaña alta, centro de México. *Revista mexicana de ciencias forestales* 7(37), 21-38. https://www.scielo.org.mx/pdf/remcf/v7n37/2007-1132-remcf-7-37-00021-en.pdf

Azuela de la Cueva, A., Cano, I., Rabasa, A., Alcántar, E., Gil, M., Villasís, A., 2019. *Estudios sobre el cumplimiento e impacto de las recomendaciones generales, informes especiales y pronunciamientos de la CNDH (2001-2017)*. Tomo VI Áreas naturales protegidas y derechos humanos. México, Comisión Nacional de Derechos Humanos / UNAM. https://www.cndh.org.mx/sites/all/doc/Informes/Especiales/ANP-DH.pdf

Báez, A, Acuña, A., 2003. *Guía para las mejores prácticas de ecoturismo en áreas protegidas*. Comisión Nacional para el Desarrollo de los Pueblos Indígenas, México, DF. https://gc.scalahed.com/recursos/files/r161r/w25434w/sem5_guiaparalamejorespracticasdecoturismo.pdf

Bassan, C., 2022. Turismo Científico: Conceptualización, modalidades y desafíos. *Realidad, Tendencias y Desafíos en Turismo* 20 (2) 33-48. https://revele.uncoma.edu.ar/index.php/condet/article/view/4507

Bollo, M., Hernández, J.R., Méndez, A.P., 2010. Evaluación de potencialidades naturales en el ordenamiento ecológico territorial: Noroeste del estado de Chiapas, México. *Boletín de la Asociación de Geógrafos Españoles* 53, 191-218. http://bage.age-geografia.es/ojs/index.php/bage/article/download/1198/1121

Botana, M.D., 2022. Situación y oportunidades de desarrollo socioeconómico en un área protegida transfronteriza. El caso de la RBTGX. *Minius* 27, 297-340. https://doi.org/10.35869/mns.v0i27.4414

Cetin, M., 2015. Evaluation of the sustainable tourism potential of a protected area for landscape planning: a case study of the ancient city of Pompeipolis in Kastamonu. *International Journal of Sustainable Development & World Ecology 22*(6), 490-495. https://doi.org/10.1080/13504509.2015.1081651

Chávez, H., González, M.D.J., 2015. Metodologías para identificar áreas prioritarias para conservación de ecosistemas naturales. *Revista mexicana de ciencias forestales* 6(27), 8-23. https://www.scielo.org.mx/pdf/remcf/v6n27/v6n27a2.pdf

CONANP (Comisión Nacional de Áreas Naturales Protegidas), 2024. *Programas de Manejo.* https://www.gob.mx/conanp/acciones-y-programas/programas-de-manejo

CONAFOR (Comisión Nacional Forestal), 2022. *Reglas de operación 2023 del programa desarrollo forestal sustentable para el bienestar.* Diario Oficial de la Federación. https://www.conafor.gob.mx/apoyos//docs/adjuntos/c973f53fba23d9b486bd63939008b358.pdf

Cravioto, F., 2019. Análisis de las Reglas de Operación del programa Apoyos para el Desarrollo Forestal Sustentable 2019. *Nota informativa*. Consejo Civil Mexicano para la Silvicultura Sostenible. https://www.ccmss.org.mx/wp-content/uploads/ 2019/03/2019_03_ApoyoForestal-1.pdf

Engen, S., Fauchald, P., Hausner, V., 2019. Stakeholders' perceptions of protected area management following a nationwide community-based conservation reform. *PloS one* 14(4), e0215437. https://doi.org/10.1371/journal.pone.0215437

Espinoza, A., Bollo, M., 2015. La tipología de los paisajes antroponaturales como base para el ordenamiento ecológico territorial a diferentes escalas. En V. Sorani, M.A. Alquicira (comp.). *Perspectivas del ordenamiento territorial ecológico en América y Europa*. México, Arlequín, 155-195.

FAO (Food and Agriculture Organization of the United Nations, Agriculture), 1993. *Guidelines for land-use planning* (Vol. 1). Organization of the United Nations. Soil Resources, Management, Conservation Service, & Agriculture Organization of the United Nations. Interdepartmental Working Group on Land Use Planning. https://urban.pusan.ac.kr/bbs/urban/3420/424820/download.do

Huerta, M.A., Sánchez, A., 2011. Evaluación del potencial ecoturístico en áreas naturales protegidas del municipio de Santa María Huatulco, México. *Cuadernos de Turismo* 27, 541-560. https://www.redalyc.org/pdf/398/Resumenes/Abstract_39820898030_2.pdf

INEGI (Instituto Nacional de Estadística, Geografía e Informática), 1983. *Conjunto de las cartas de edafología (escala 1:50 000) de la República Mexicana*. Aguascalientes, México: Instituto Nacional de Estadística, Geografía e Informática. https://www.inegi.org.mx/temas/edafologia/#descargas

INEGI (Instituto Nacional de Estadística, Geografía e Informática), 2004. *Guía para la interpretación de Cartográfica Edafológica*, México. https://www.inegi.org.mx/contenidos/productos/prod_serv/contenidos/espanol/bvinegi/productos/historicos/1329/702825231736/702825231736_1.pdf

INEGI (Instituto Nacional de Estadística, Geografía e Informática), 2018. *Conjunto de las cartas de topografía (escala 1:50 000) de la República Mexicana*. Aguascalientes, México: Instituto Nacional de Estadística, Geografía e Informática. https://www.inegi.org.mx/programas/topografia/50000/#descargas

INEGI (Instituto Nacional de Estadística y Geografía), 2020. *Censo de Población y Vivienda 2020.* Instituto Nacional de Estadística y Geografía. México. https://www.inegi.org.mx/programas/ccpv/2020/#Datos_abiertos

IUCN (International Union for Conservation of Nature-Protected Areas), 2020. *How we engage.* https://www.iucn.org/theme/protected-areas

Izakovicová, Z., Miklós, L., Miklósová, V., Petrovic, F., 2019. The Integrated Approach to Landscape Management. Experience from Slovakia. *Sustainability* 11, 4554. https://doi.org/10.3390/su11174554

Jenks, G.F., 1967. The data model concept in statistical mapping. *International yearbook of cartography* 7, 186-190.

Keenleyside, K.A., Dudley, N., Cairns, S., Hall, C.M., Stolton, S., 2014. *Ecological restoration for protected areas: principles, guidelines and best practices*, Gland, Suiza: UICN. https://www.iucn.org/resources/publication/ecological-restoration-protected-areas-principles-guidelines-and-best

Lee-Cortés, J.V., Delgadillo-Macías, J., 2018. El potencial territorial como factor del desarrollo. Modelo para la gestión rural. *Agricultura, sociedad y desarrollo* 15(2), 191-213. https://www.scielo.org.mx/pdf/asd/v15n2/1870-5472-asd-15-02-191.pdf

Maldonado, O.A., Chávez, R.M., Bravo, M.L., 2020. Áreas naturales protegidas y participación social en América Latina: problemas y estrategias para lograr la integración comunitaria. *Región y sociedad* 32. https://doi.org/10.22198/rys2020/32/1277

Martínez, A., Bollo, M. 2023. *El paisaje. Una Mirada a través del análisis espacial,* Universidad Nacional Autónoma de México, (1ra edición), Universidad Nacional Autónoma de México, Morelia, Michoacán. https://publicaciones.ciga.unam.mx/index.php/ec/catalog/book/104

Martínez-Rodríguez, A.A., Juárez-López, J.F., Ortiz-Salaz, L., Galmiche-Tejeda, A., 2021. El paisaje como recurso turístico en Áreas Naturales Protegidas: Caso Ranchería Chilapa 2da.Sección (Cañaveralito), Centla, Tabasco. *Ecosistemas y Recursos Agropecuarios* 8(I). https://doi.org/10.19136/era.a8nI.2680

Mateo, J.M., 2011. *Geografía de los paisajes, primera parte, Paisajes Naturales*. Editorial Universitaria. La Habana.

Matus, O., Faustino, J., Jiménez, F., 2009. *Guía para la identificación participativa de zonas con potencial de recarga hídrica. Aplicación práctica en la subcuenca del río Jucuapa, Nicaragua*. Centro Agronómico de Investigación y Enseñanza, División de Investigación y Desarrollo, Turrialba, Costa Rica. https://repositorio.catie.ac.cr/handle/11554/8339

Meyfroidt, P., Chowdhury, R.R., de Bremond, A., Ellis, E.C., Erb, K.H., Filatova, T., Garrett, R.D., Grove, J.M., Heinimann, A., Kuemmerle, T., Kull, C.A., Lambin, E.F., Landon, Y., le Polain de Waroux, Y., Messerli, P., Müller, D., Nielsen, J.O., Peterson, G.D., Rodriguez García, V., Schlüter, M., Turner, B.L., Verburget, P.H., 2018. Middle-range theories of land system change. *Global Environmental Change* 53, 52-67. https://doi.org/10.1016/j.gloenvcha.2018.08.006

Mikulec, J, Antoušková, M., 2011. Landscape and tourism potential in the protected landscape areas. *Agricultural Economics* 57(6), 272. https://www.agriculturejournals.cz/pdfs/age/2011/06/02.pdf

Natural Capital Project, 2023. *InVEST™ (Integrated Valuation of Ecosystem Services and Tradeoffs)*, Stanford University, USA. https://naturalcapitalproject.stanford.edu/software/invest

Pablo, M.A., Hernández, J.R., 2016. Evaluación de la aptitud natural de los paisajes físico-geográficos en la cuenca del río Grande, Oaxaca, México. *Investigaciones Geográficas* 91, 7-24. https://doi.org/10.14350/rig.49203

Palacio-Prieto, J.L., Sánchez-Salazar, M.T. (coords.), 2003. *Segunda Generación de Guías Metodológicas para la elaboración de Planes Estatales de Ordenamiento Territorial,* Memoria Escrita, Convenio específico de colaboración SEDESOL/Instituto de Geografía-UNAM, México. Distrito Federal, México.

Palacio-Prieto, J.L., Sánchez-Salazar, M.T., Casado, J., Propin, E., Sancho, J., Valdez, C., Cacho, R. (coords.), 2004. *Indicadores para la caracterización del territorio y el ordenamiento territorial*. Secretaría de Desarrollo Social (SEDESOL)-Instituto de Geografía/UNAM. http://www.publicaciones.igg.unam.mx/index.php/ig/catalog/view/161/149/818-1

POGMICH (Periódico Oficial del Estado de Michoacán), 2004a. *Ley de Desarrollo Forestal Sustentable del Estado de Michoacán de Ocampo*. Número 476 sección 11, 22 de noviembre. http://congresomich.gob.mx/file/Ley-de-Desarrollo-Forestal-Sustentable-del-Estado-de-Michoacán-de-Ocampo.pdf

POGMICH (Periódico Oficial del Estado de Michoacán), 2004b. *Ley del Agua y Gestión de Cuencas para el Estado de Michoacán*. Número 504, sección 14, 5 de julio. http://www.publicaciones.igg.unam.mx/index.php/ig/catalog/view/161/149/818-1

POGMICH (Periódico Oficial del Estado de Michoacán de Ocampo), 2004c. *Reglamento de la Ley General del Equilibrio Ecológico y la Protección del Ambiente del Estado de Michoacán de Ocampo*. México, Secretaría de Gobierno. http://www.ordenjuridico.gob.mx/Estatal/MICHOACAN/Reglamentos/MICHREG12.pdf

POGMICH (Periódico Oficial del Estado de Michoacán), 2006a. *Ley de Desarrollo Rural Integral Sustentable del Estado de Michoacán de Ocampo*. Número 43. Periódico Oficial del Estado de Michoacán, sección 9, 18 de enero. http://congresomich.gob.mx/file/LEY-DE-DESARROLLO-RURAL-INTEGRAL-SUSTENTABLE-DEL-ESTADO-REF-30-DE-JUNIO-DE-2020.pdf

POGMICH (Periódico Oficial del Estado de Michoacán), 2006b. *Reglamento de la Ley de Desarrollo Rural Integral Sustentable del Estado de Michoacán de Ocampo*, tomo CXL, número 21, 4 de diciembre. http://congresomich.gob.mx/file/LEY-DE-DESARROLLO-RURAL-INTEGRAL-SUSTENTABLE-DEL-ESTADO-REF-30-DE-JUNIO-DE-2020.pdf

POGMICH (Periódico Oficial del Estado de Michoacán), 2007a. *Reglamento de la Ley de Desarrollo Forestal Sustentable del Estado de Michoacán de Ocampo*, tomo CXLI, número 5, 28 de marzo. https://laipdocs.michoacan.gob.mx/?wpfb_dl=334841

POGMICH (Periódico Oficial del Estado de Michoacán), 2007b. *Ley de Ganadería del Estado de Michoacán de Ocampo*. Número 129, sección 4, 2 de marzo. http://congresomich.gob.mx/file/LEY-DE-GANADER%C3%8DA-DEL-ESTADO-REF-17-OCTUBRE-DE-2018.pdf

POGMICH (Periódico Oficial del Estado de Michoacán), 2007c. *Ley para la Conservación y Restauración de Tierras del Estado de Michoacán de Ocampo*. Numero 223 (*2007*), sección 3, 9 de octubre. http://www.ordenjuridico.gob.mx/Documentos/Estatal/Michoacan/wo33317.pdf

POGMICH (Periódico Oficial del Estado de Michoacán), 2008. *Reglamento de la Ley del Agua y Gestión de Cuencas para el Estado de Michoacán de Ocampo*, tomo CXLIII, número 44, 25 de febrero. https://aguaysaneamiento.cndh.org.mx/Content/doc/Normatividad/16Reglamento_LAGCE_Mich.pdf

POGMICH (Periódico Oficial del Estado de Michoacán), 2011. *Decreto por el que se declara como zona de protección ambiental el área de Pico Azul-La Escalera, en los municipios de Charo, Madero y Morelia, Michoacán*. Número 56, cuarta sección, Morelia, Michoacán. https://implanmorelia.org/site/wp-content/uploads/2022/02/8_7_DECRETO_PICO_AZUL_LA_ESCALERA.pdf

POGMICH (Periódico Oficial del Estado de Michoacán), 2014. *Ley de cambio climático del estado de Michoacán de Ocampo*. Número 273 *sección 7, 21 de enero.* http://congresomich.gob.mx/file/LEY-DE-CAMBIO-CLIMATICO-REF-07-NOV-2017.pdf

POGMICH (Periódico Oficial del Estado de Michoacán), 2018. *Reglamento de la Ley de Cambio Climático del Estado de Michoacán de Ocampo*. (*28 de diciembre*), tomo CLXXI, número 52. http://congresomich.gob.mx/file/Reglamento-de-la-Ley-de-Cambio-Clim%C3%A1tico.pdf

POGMICH (Periódico Oficial del Estado de Michoacán), 2021. *Ley para la Conservación y Sustentabilidad Ambiental del Estado de Michoacán de Ocampo*. *Número 513* (*2021*), sección 9, 5 de abril. http://congresomich.gob.mx/file/NUEVA-LEY-PARA-LA-CONSERVACIÓN-Y-SUSTENTABILIDAD-AMBIENTAL-5-ABRIL-2021.pdf

Ramírez, L., Priego, A., Bollo, M., Castelo, D., 2016. Potencial para la conservación de la geodiversidad de los paisajes del Estado de Michoacán, México. *Perspectiva Geográfica* 21(2), 321-344. https://doi.org/10.19053/01233769.5856

Ramón, A.M., Salinas Chávez, E., Acevedo Rodríguez, P., 2011. La determinación de los conflictos de uso del territorio: Cuenca Alta del Río Cauto. Cuba. *Terra* 27 (42), 47-71. https://ve.scielo.org/scielo.php?script=sci_arttext&pid=S1012-70892011000200003

Ramón, A.M., Salinas, E., Lorenzo, C., 2013. Propuesta metodológica para la zonificación funcional de áreas naturales protegidas terrestres desde la perspectiva del paisaje. *Revista Instituto Forestal* 25(1), 7-23. https://doaj.org/article/f3233ca1f3f747799d022c98e09b0f41

Ramón, A.M., Salinas, E., Martínez, L., Suárez, C., 2017. La determinación de potencialidades agropecuarias y silvícolas en zonas de montaña. Municipio Buey Arriba. Cuba. *Entorno Geográfico* 14, 92-105. https://hdl.handle.net/10893/11592

Ramón, A.M., Martínez, L., Suárez, C., Salinas, E., 2017. La determinación de potencialidades agropecuarias y silvícolas en zonas de montaña: municipio Tercer Frente, Cuba. *Cuadernos de Geografía: Revista Colombiana de Geografía* 26(1), 65-75. https://doi.org/10.15446/rcdg.v26n1.52754

Ramón, A.M., Salinas, E., Millán, M., Labrada, O., Rosales, Y., 2020. Evaluación de los recursos paisajísticos e históricos para el desarrollo del turismo de naturaleza en las zonas de uso público del Parque Nacional Pico Bayamesa. Cuba. *Investigaciones Turísticas* 19, 213-239. https://doi.org/10.14198/INTURI2020.19.10

Ramón, A., Bollo, M., 2023. El índice de antropización de la cubierta vegetal como medida de la antropización de áreas naturales protegidas: Caso Pico Azul-La Escalera, México. *Revista de Ciencias Ambientales* 57(2), 1-25. https://doi.org/10.15359/rca.57-2.4

Rezende, M.G.G., Canalez, G.D.G., Fraxe, T.D.J.P., 2017. Protected areas in the Amazon: forest management, conflict and social participation. A*cta Scientiarum. Human and Social Sciences* 39(1), 63. https://doi.org/10.4025/actascihumansoc.v39i1.33206

Ruiz-González, J. L., Aguirre-Calderón, O. A., Jiménez-Pérez, J., Treviño-Garza, E. J., Alanís-Rodríguez, E., 2022. Pago por servicios ambientales: esquemas y experiencias de éxito. *e-CUCBA* 19, 33-44. https://doi.org/10.32870/ecucba.vi19.261

SEMARNAP (Secretaría de Medio Ambiente, Recursos Naturales y Pesca), 1996. *NOM-011-SEMARNAT-1996: Que establece los procedimientos, criterios y especificaciones para realizar el aprovechamiento, transporte y almacenamiento de musgo, heno y doradilla*. Diario Oficial de la Federación. Ciudad de México. https://www.profepa.gob.mx/innovaportal/file/3318/1/nom-011-semarnat-1996.pdf

SEMARNAP (Secretaría de Medio Ambiente y Recursos Naturales), 1996a. *NOM-010-SEMARNAT-1996: Que establece los procedimientos, criterios y especificaciones para realizar el aprovechamiento, transporte y almacenamiento de hongos*. Diario Oficial de la Federación. Ciudad de México. https://www.profepa.gob.mx/innovaportal/file/3316/1/NOM-010-SEMARNAT-1996.pdf

SEMARNAP (Secretaría de Medio Ambiente y Recursos Naturales), 1996b. *NOM-027-SEMARNAT-1996: Que establece los procedimientos, criterios y especificaciones para realizar el aprovechamiento, transporte y almacenamiento de tierra de monte*. Diario Oficial de la Federación. Ciudad de México. https://www.profepa.gob.mx/innovaportal/file/3341/1/nom-027-semarnat-1996.pdf

SEMARNAP (Secretaría de Medio Ambiente y Recursos Naturales), 1996c. *NOM-028-SEMARNAT-1996: Que establece los procedimientos, criterios y especificaciones para realizar el aprovechamiento, transporte y almacenamiento de raíces y rizomas de vegetación forestal*. Diario Oficial de la Federación. Ciudad de México. https://www.profepa.gob.mx/innovaportal/file/3342/1/NOM-028-SEMARNAT-1996.pdf

SEMARNAP (Secretaría de Medio Ambiente y Recursos Naturales), 2001. *NOM-020-RECNAT-2001: Procedimientos y lineamientos para la rehabilitación, mejoramiento y conservación de terrenos*

forestales de pastoreo. Diario Oficial de la Federación. *C*iudad de México. https://www.dof.gob.mx/nota_detalle.php?codigo=757042&fecha=10/12/2001#gsc.tab=0

SEMARNAP (Secretaría de Medio Ambiente y Recursos Naturales), 2005. *NOM-026-SEMARNAT-2005: Que establece los criterios y especificaciones técnicas para realizar el aprovechamiento comercial de resina de pino*. Diario Oficial de la Federación. Ciudad de México. https://biblioteca.semarnat.gob.mx/janium/Documentos/Ciga/agenda/PPD02/DO863_1.pdf

SEMARNAP (Secretaría de Medio Ambiente y Recursos Naturales), 2006. *NOM-152-SEMARNAT-2006: Lineamientos, criterios y especificaciones de los contenidos de los programas de manejo forestal para el aprovechamiento de recursos forestales maderables en bosques, selvas y vegetación de zonas áridas*. Diario Oficial de la Federación. Ciudad de México. https://vlex.com.mx/vid/maderables-bosques-selvas-vegetacion-43468492

Shishenko, P.G., 1988. *Estabilidad de los paisajes a las cargas económicas. Geografía Física Aplicada*. Editorial de la Escuela Superior, Kiev, Ucrania.

Sosa-Montes, M., Durán-Ferman, P., Hernández-García, M., 2012. Relaciones socioambientales entre comunidades y áreas naturales protegidas, Reserva de la Biósfera Calakmul: entre el conflicto y la conservación. *Revista Chapingo, Serie de Ciencias Forestales y del Ambiente* 18(1), 111-121. https://www.scielo.org.mx/pdf/rcscfa/v18n1/v18n1a10.pdf

Torres, K.L., López, J.F.J., Quevedo, M.L.M., 2015. Valoración paisajística del potencial turístico de la reserva Río Playa de Comalcalco, Tabasco. *Teoría y Praxis* 138-157. https://www.redalyc.org/pdf/4561/456144904008.pdf

Wischmeier, W.H., Smith, D.D., 1978. *Predicting rainfall erosion losses-a guide to conservation planning, agriculture handbook No. 537 USDA*/Science and Education Administration, US. Govt. Printing Office, Washington D.C.

Wunder, S., Wertz-Kanounnikoff, S., Sánchez, R.M., 2007. Pago por servicios ambientales: una nueva forma de conservar la biodiversidad. *Gaceta ecológica* 84, 39-52. https://dialnet.unirioja.es/descarga/articulo/2873782.pdf

Supplementary Material A

Legend of the anthropo-natural landscape map of the year 2021 (from Ramón and Bollo, 2023)

A. Physiographic Province Neovolcanic Transmexican Axis, Mil Cumbres subprovince

I. Volcano-tectonic mountains, denudative-erosive, conical in shape with horseshoe-shaped collapse structures (calderas), (1,800-2,641 masl) in a subhumid temperate climate, ranging from slightly to heavily dissected (200<Vd<500), with slopes ranging from slightly to heavily inclined (0-30º), composed of andesite-volcanic breccia, basalts, acidic extrusive igneous rocks, limolites, and conglomerates, with Andosol, Acrisol, and Luvisol soils, and mixed coniferous and broadleaf forests, broadleaf forests, and cloud forests coverages.

1. Volcanic cone and domes, with slopes ranging from flat to very steep (0-30º), composed of andesite-volcanic breccia, with humic Andosol and chromic Luvisol soils, and primary pine-oak forests, primary pine forests, and secondary forests predominantly of pine-oak herbaceous species.

2. Foothills with slopes ranging from flat to steep (0-20º), composed of andesite-volcanic breccia with humic Andosol soil, and coverages of rainfed agriculture, permanent crops, secondary pine-oak forests with herbaceous predominance.

3. Foothills with slopes ranging from flat to steep (0-45º), composed of acidic extrusive igneous rocks with humic Andosol and orthic Acrisol soils, and coverages of primary pine-oak forests, secondary pine-oak forests with herbaceous predominance, primary pine forests, and secondary pine-oak forests with shrub predominance.

4. (4_1 - 4_2) Foothills with slopes ranging from flat to steep (0-30º), composed of basalts, with humic Andosol soil, and coverages of primary pine-oak forests and secondary pine forests.

5. Volcano-erosive depression, with steep slopes (10-30º), composed of andesite-volcanic breccia, with chromic Luvisol, humic Andosol, and orthic Acrisol soils, and coverages of primary pine-oak forests and secondary pine-oak forests.

II. Volcano-tectonic mountains, denudative-erosive, with horseshoe-shaped collapse structures (calderas), (1,965-2,608 masl) in a subhumid temperate climate, ranging from slightly to heavily dissected (200<Vd<500), with slopes ranging from slight to very steep (0-45º), composed of andesite-volcanic breccia, basalts, acidic extrusive igneous rocks, limolites, and conglomerates, with Acrisol, Andosol, Luvisol, and Ranker soils, and mixed coniferous and broadleaf forests, broadleaf forests, and cloud forests coverages.

6. (6_1 - 6_3) Volcanic cone, with slopes ranging from flat to very steep (0-45º), composed of andesite-volcanic breccia, with orthic Acrisol, humic Andosol, and Ranker soils, and coverages of primary pine-oak forests, secondary pine-oak forests, primary pine forests.

7. (7_1 - 7_5) Volcanic domes, with slopes ranging from flat to steep (0-45º), composed of andesite-volcanic breccia, with humic Andosol, orthic Acrisol, and chromic Luvisol soils, and coverages of primary pine-oak forests, secondary pine-oak forests, induced grasslands, primary pine forests.

8. (8_1 - 8_7) Foothills with slopes ranging from flat to steep (0-45º), composed of andesite-volcanic breccia, with chromic Luvisol and orthic Acrisol soils, and coverages of secondary pine-oak forests, induced grasslands, and primary pine-oak forests.

9. Foothills with slopes ranging from flat to steep (0-30º), composed of acidic extrusive igneous rocks, with orthic Acrisol soil, and coverages of primary pine-oak forests, secondary pine forests, and primary pine forests.

10. Foothills with slopes ranging from flat to steep (0-30º), composed of conglomerates, with chromic Luvisol and orthic Acrisol soils, and coverages of secondary pine-oak forests, induced grasslands, and permanent crops.

11. Foothills with slopes ranging from flat to steep (0-30º), composed of limolite-sandstone, with chromic Luvisol soil, and coverages of secondary pine-oak forests and induced grasslands.

12. Foothills with slopes ranging from flat to steep (0-30º), composed of rhyolitic tuffs, with chromic Luvisol soil, and coverages of secondary pine-oak forests.

13. (13_1 - 13_7) Volcano-erosive depression, with slopes ranging from flat to steep (0-45º), composed of andesite-volcanic breccia, with orthic Acrisol, humic Andosol, and chromic Luvisol soils, and coverages of secondary pine-oak forests and primary pine-oak forests.

III. Polygenetic volcano-tectonic mountains, denudative-erosive, in a subhumid temperate climate, ranging from slightly to heavily dissected (200<VD<500), (1,294-2,837 masl) with slopes ranging from slight to heavily inclined (1-30º), composed of andesite-volcanic breccia, basalts, acidic extrusive igneous rocks, limolites, and conglomerates, with Luvisol and Regosol soils, and mixed coniferous and broadleaf forests, broadleaf forests.

14. Foothills with slopes ranging from flat to steep (0-30º), composed of andesite-volcanic breccia, with chromic Luvisol and dystrophic Regosol soils, and coverages of secondary pine-oak forests with herbaceous predominance, induced grasslands, and secondary pine-oak forests with shrub predominance.

15. Foothills with slopes ranging from flat to steep (0-30º), composed of limolite-sandstone, with chromic Luvisol soil, and coverages of secondary pine-oak forests with herbaceous predominance and induced grasslands.

IV. Denudative volcano-tectonic mountains (1,327-2,302 masl) in a subhumid temperate climate, moderately dissected (200<Dv<300), with slopes ranging from slight to steep (0-30º), composed of acidic extrusive igneous rocks and andesite-volcanic breccia, with Acrisol and Andosol soils, and mixed coniferous and broadleaf forests, broadleaf forests.

16. (16_1 - 16_23) Summits with slopes ranging from flat to steep (0-30º), composed of acidic extrusive igneous rocks, with orthic Acrisol soil, and coverages of primary pine-oak forests and secondary pine-oak forests.

17. (17_1 - 17_5) Slopes, with slopes ranging from flat to steep (0-30º), composed of acidic extrusive igneous rocks, with orthic Acrisol soil, and coverages of primary pine forests, secondary pine forests, and secondary pine forests with herbaceous predominance.

18. (18_1 - 18_4) Fluvio-denudative, erosive, V-shaped valleys, with slopes ranging from slight to steep (5-30º) and intermittent river currents, composed of acidic extrusive igneous rocks, with orthic Acrisol soil, and coverages of primary pine forests and secondary pine forests.

B. Physiographic province Sierra Madre del Sur, subprovince Balsas Depression. V. Denudative volcano-erosive mountains (984-2,384 masl), in a subhumid temperate climate, moderately to heavily dissected (300<VD<500), with moderately to heavily inclined slopes (10-45º), composed of andesite-volcanic breccia and conglomerates, with Luvisol, Feozem, Regosol, and Acrisol soils, and mixed coniferous and broadleaf forests, deciduous lowland forests, and broadleaf forests.

19. (19_1 - 19_7) Denudative volcano-mountains with slopes ranging from flat to steep (0-30º), composed of andesite-volcanic breccia, with chromic Luvisol, haplic Feozem, and eutric Regosol soils, and coverages of secondary pine-oak forests, induced grasslands, and secondary deciduous lowland forests.

20. Denudative volcano-mountains with slopes ranging from strong to very steep (30-45º), composed of conglomerates, with chromic Luvisol soil, and coverages of induced grasslands and secondary pine-oak forests with shrub predominance.

21. (21_1 - 21_2) Fluvio-denudative-erosive valleys, V-shaped, with slopes ranging from slight to very steep (5-45º), and permanent river currents, composed of andesite-volcanic breccia, with chromic Luvisol, haplic Feozem, and eutric Regosol soils, and coverages of induced grasslands, secondary pine-oak forests, and secondary deciduous lowland forests.

22. (22_1 - 22_59) Fluvio-denudative valleys, erosive, V-shaped, with slopes ranging from slight to very steep (5-45º), and intermittent river currents, composed of andesite-volcanic breccia, with chromic Luvisol, haplic Feozem, and eutric Regosol soils, and coverages of secondary pine-oak forests, secondary deciduous lowland forests, and induced grasslands.

23. Fluvio-denudative valleys, erosive, V-shaped, with slopes ranging from slight to very steep (5-45º), and permanent river currents, composed of conglomerates, with chromic Luvisol soil, and coverages of secondary deciduous lowland forests, secondary pine-oak forests, and induced grasslands.

24. Fluvio-denudative valleys, erosive, V-shaped, with slopes ranging from slight to very steep (5-45º), and intermittent river currents, composed of conglomerates, with chromic Luvisol soil, and coverages of secondary pine-oak forests.

Cuadernos de Investigación Geográfica *Geographical Research Letters*	2024	Nº 50 (2)	pp. 157-177	EISSN 1697-9540

http://doi.org/10.18172/cig.6273

REMOTE SENSING OF ILLEGAL DUMPS THROUGH SUPERVISED CLASSIFICATION OF SATELLITE IMAGES: APPLICATION IN OAXACA, MEXICO

JAVIER GÓMEZ MATURANO[1]*, JOSÉ DAVID MENDOZA SANTANA[2], ANA LILIA AGUILAR-GARCÍA[2], MAYRA SERNA HERNÁNDEZ[2]

[1] *Centro de Investigación en Materiales Avanzados, Chihuahua, México.*

[2] *Centro de Investigaciones y Estudios Superiores en Antropología-Golfo, México.*

ABSTRACT. Various economic, social, and cultural factors have contributed to the proliferation of illegal dumps, causing urban image degradation, population health impacts, and soil, air, and water contamination. Scientists developed remote sensing techniques to identify these red spots and thus contribute to their mitigation and control. They recently used these techniques to detect large areas of illegal waste dumping instead of using expensive field monitoring. Artificial intelligence algorithms have been used to process satellite images due to the availability of satellite images and the increase in the processing capacity of computer systems. This work presents the results of a satellite remote-sensing procedure to detect illegal dumps in one hydrographic subbasin in Oaxaca, Mexico, through a supervised land cover classification using a Random Forest classifier. Two hundred and fifty-six control polygons were used to train the classifier. The classification criteria were the twelve bands of the Sentinel 2A satellite images with a spatial resolution of 10x10 meters, the spectral indices NDVI, MNDWI, SAVI, NDBI, BSI, and the surface slope. Google Earth Engine platform was used to process satellite images. There were 288,100 hectares classified in this way: 65.4% classified as vegetation, 31.5% like bare soil, 2.7% was urban soil and the rest was classified as water or garbage. A confusion matrix calculated the accuracy of the model in 0.9517. The model was not able to accurately distinguish between urban soil, bare soil and garbage due to the similarity of their spectral fingerprints. NDVI and SAVI were the most important spectral indices for detecting litter, and those might contribute to building a spectral fingerprint of litter in the future. Poorly classified areas were discarded through photointerpretation work and post-processing. Finally, thirty-two probable illegal dumps were identified, twelve of which were confirmed on the territory.

Teledetección de vertederos ilegales mediante clasificación supervisada de imágenes de satélite: aplicación en Oaxaca, México

RESUMEN. Diversos factores económicos, sociales y culturales han contribuido a la proliferación de vertederos ilegales, ocasionando degradación de la imagen urbana, afectaciones a la salud de la población y contaminación del suelo, aire y agua. Diversas técnicas de percepción remota se han desarrollado para identificar estos focos rojos y así contribuir a su mitigación y control. La percepción remota de satélites ha sido utilizada en los últimos años para detectar amplias zonas de vertido ilegal de residuos, en lugar de los costosos monitoreos en campo. Se han utilizado algoritmos de inteligencia artificial para procesar imágenes de satélite gracias a su disponibilidad y al aumento en la capacidad de procesamiento de los sistemas informáticos. Este trabajo presenta los resultados de un procedimiento de teledetección por satélite para detectar vertederos clandestinos en una subcuenca hidrográfica en Oaxaca, México, a través de una clasificación supervisada de cobertura terrestre utilizando el clasificador *Random Forest*. Se utilizaron doscientos cincuenta y seis polígonos de control para entrenar al clasificador. Los criterios de clasificación fueron las doce bandas de las imágenes del Sentinel 2ª, con una resolución espacial de 10x10 metros, los índices espectrales NDVI, MNDWI, SAVI, NDBI, BSI y la pendiente de la superficie. Para el procesamiento de las imágenes de satélites se utilizó la plataforma Google Earth Engine. Se obtuvieron 288.100

hectáreas clasificadas de esta manera: 65,4% clasificadas como vegetación, 31,5% como suelo desnudo, 2,7% como suelo urbano y el resto como agua o basura. Una matriz de confusión calculó la precisión del modelo en 0,9517. El modelo no fue capaz de distinguir con precisión entre suelo urbano, suelo desnudo y basura debido a la similitud de sus huellas espectrales. Los índices espectrales más importantes para detectar basura fueron el NDVI y SAVI, los cuales podrían contribuir a construir una huella espectral de basura en el futuro. Las áreas mal clasificadas se descartaron mediante trabajos de fotointerpretación y posprocesamiento. Finalmente, se identificaron treinta y dos probables vertederos clandestinos, doce de los cuales fueron confirmados en el territorio.

Keywords: remote sensing, illegal dumps, supervised classification, urban solid waste, artificial intelligence.

Palabras clave: teledetección, vertederos clandestinos, clasificación supervisada, residuos sólidos urbanos, inteligencia artificial.

Received: 30 May 2024

Accepted: 15 October 2024

***Corresponding author:** Javier Gómez Maturano, Centro de Investigación en Materiales Avanzados, Chihuahua, México. E-mail: jgomezma@uaemex.mx

1. Introduction

In developing countries like Mexico, it is difficult to find cases in which urban solid waste (MSW) is adequately confined to avoid impacts on the natural and social environment. MSW Final Disposal Sites (FDS) have become one of the main sources of air, soil, and water pollution with strong health, economic, and legal impacts (Semarnat, 2020; Sedema, 2021). Instead, open-air landfills predominate without any type of control.

The lack of space for the final deposit of waste generated in cities, the high costs of managing these sites (Kaza *et al.*, 2018), and their poor operation (Gill *et al.,* 2019) contribute to the formation of illegal dumps. An illegal dump is a place that, without environmental considerations, is chosen by a group of people to deposit their waste without obtaining permission from the competent authority (Karimi and Richter, 2022). Likewise, the deficiency of waste collection systems and the involvement of uncontrolled private agents cause the proliferation of illegal dumps on the outskirts of urban centers (Ferronato *et al.*, 2021; Vu *et al.*, 2019). Rapid industrial and urban growth during the last century has also contributed to the emergence of illegal dumps, making them a central environmental problem in all developed and developing countries (You *et al.*, 2020; Karimi and Richter, 2022; Silvestri and Omri, 2008).

Mexico reports that 16% of the MSW generated is not collected (Semarnat, 2020), so a fraction of it could end up in illegal dumps. These illegal dumps increased by 10.8% between 2019 and 2021 in Mexico City (Sedema, 2021), and they are generally found on public roads, common areas, parks, vacant lots, ravines, and streams. The State of Mexico illegally deposes of more than 220 tons/day of waste in 50 landfills and pours nearly 5 thousand tons on the metropolitan area's periphery (Rodríguez, 2023).

Illegal dumps are a source of air, soil, and water pollution (Karimi and Richter, 2022). The pollutants generated in these sites are mobilized and dispersed in broad areas due to topographic conditions, drainage systems, and soil types (Angelino *et al.*, 2018; Glanville and Chang, 2015). Illegal dumps pollute due to the emission of greenhouse gases generated by decomposing the organic fraction of the dumped waste (Cusworth *et al.*, 2020). They also pollute by the dissolution of solid polluting materials, such as heavy metals, by meteoric water that falls on them and its subsequent integration into

surface or underground water currents (Padubidri *et al.,* 2022; Mahmood *et al.*, 2023). The spread of biological-infectious agents and the proliferation of harmful fauna directly affect the population living near illegal dumps (Mahmood *et al.*, 2023; Cusworth *et al.*, 2020).

Dumps not only cause environmental damage but also impose significant financial burdens on managers: in Australia, the management of more than nine thousand tons of illegally dumped waste in 2011-2012 cost more than 6 million dollars (Glanville and Chang, 2015); the Chartered Institution of Wastes Management estimated that the associated annual costs with the detection and remediation of illegal dumps in the United Kingdom were 100 to 150 million pounds in 2014 (Karimi and Richter, 2022) and the costs associated with their remediation in the USA were estimated at over $10 million dollars in 2016 (Quesada-Ruiz *et al.*, 2019). This underscores the urgent need for effective strategies to combat this issue.

Illegal dumps are not easily detected and frequently are in hidden locations or areas with low vehicular or pedestrian traffic. The detection of these sites is not only costly but also ineffective (Karimi and Richter, 2022). Identifying them is the crucial first step for their control and remediation, but the lack of public data in this regard presents a significant challenge (You *et al.*, 2020). Various methods exist to identify these dumps, with field surveys being the most effective but also the most expensive (Karimi and Richter, 2022; Angelino *et al.*, 2018). This complexity underscores the need for interdisciplinary collaboration and innovative solutions.

A relevant line of research consists of developing predictive models to identify probable areas of illegal dumps based on quantitative and qualitative information on the natural and social characteristics of the area (Matsumoto and Takeuchi, 2011). Glanville and Chang (2015) suggest a binary logistic regression model to identify explanatory variables, such as population density, land use, nearby waste facilities, and accessibility, that help predict the distribution of illegal dumps processed through geographic information systems (GIS). Additionally, methods that include social participation and the use of collective intelligence through social networks and applications, which provide georeferenced databases to influence authorities (Torres *et al.*, 2021), are explored. However, these approaches may have biases and inaccuracies, and their effectiveness on a large scale may be limited because they do not always reflect recent changes in landfills and the environment.

Satellite remote sensing, a precise and effective tool, is instrumental in detecting illegal dumps in large geographical areas (Shrivastava *et al.,* 2015; Niu *et al.,* 2023). It offers an alternative for analyzing relevant natural environmental features, which can be complemented with GIS (Ahmed *et al.,* 2006). This technology allows the spectral reflectance of topographic features to be recorded at visible and infrared wavelengths. The temperature difference at the earth's surface has been used to detect illegal waste dumping activities (Gill *et al.,* 2019; Yan, 2014) since areas where organic waste decomposes tend to have higher temperatures due to exothermic chemical reactions (Mahmood *et al.*, 2023). Gill *et al.* (2019) used Landsat images to identify regions most prone to waste discharge, with an overall accuracy of 72%. Mahmood *et al.* (2023) evaluated thermal energy release in FDSs through remote sensing, measuring thermal anomalies with Landsat 8 images.

Silvestri and Omri (2008) and Karimi and Richter (2022) used remote sensing with Landsat-8 and Suomi NPP satellite images to develop multi-criteria decision models to identify illegal dumps in large areas. Their model included spectral indices and surface temperatures as quantitative decision variables.

A common way to identify illegal dumps and monitor areas impacted by waste is by using spectral indices, although mainly as another decision variable (Mahmood *et al.*, 2023). One of the most useful indices is the Normalized Difference Vegetation Index (NDVI), which evaluates the health and vegetation cover, revealing areas affected by waste. Although effective, NDVI may be less reliable over large areas where diversified environmental factors influence the index (Niu et al., 2023). The Normalized Difference Water Index (NDWI) and its modified variant (MNDWI) are crucial for

identifying water accumulations and wet areas impacted by dumps, which is critical to understanding environmental damage. However, these indices face challenges in urbanized areas where they can be confused with built infrastructure (Papale *et al.*, 2023; Xu, 2006).

The Normalized Difference Urbanized Index (NDBI) distinguishes urbanized areas with high-resolution data from the Sentinel-2A satellite, highlighting the need to carefully select indices and bands for accurate identifications (Vigneshwaran and Kumar, 2018; Xi *et al.*, 2019). The Bare Soil Index (BSI) is essential for detecting areas without vegetation cover using near-infrared and shortwave wavelengths, which can indicate the presence of dumps (Nguyen et al., 2021). Finally, the Soil Adjusted Vegetation Index (SAVI) adjusts soil brightness, improving the accuracy of vegetation measurement. Its use together with NDWI and MNDWI has proven effective in assessing erosion and deposition in places such as the Ping River in Thailand, highlighting its ability to improve environmental monitoring strategies (Laonamsai *et al*., 2023). The studies reviewed have shown the usefulness of spectral indices to detect illegal dumps; however, they have been used as another variable in decision models, which constitutes a limited application of them.

Artificial intelligence, a cutting-edge technology, has been effectively used to analyze satellite images of the earth's surface; one of its potential uses is the identification of illegal dumps. Niu *et al*. (2023) proposed a deep learning model for FDS mapping based on remote sensing of high spatial resolution images (0.5 meters) and a dual-stream deep neural network. Their model achieved high performance with an average accuracy of 90.62% and could be used to recognize landfills in large-scale regions. Dabholkar *et al*. (2017) also applied artificial intelligence, particularly neural networks, to analyze high-resolution satellite images to detect illegal dumps.

In addition to the neural networks used by Niu et al. (2023) and Dabholkar et al. (2017), supervised classification algorithms can be used for remote sensing of illegal dumping sites, as done by Perumal and Bhaskaran (2010) and Wang *et al.* (2024). Random forests is an artificial intelligence algorithm used for classifying remotely sensed images and outperforms individual decision tree classifiers (Zhou *et al.,* 2021). Also, it performs identically or better than several advanced pattern recognizers, such as artificial neural networks, support vector machines, and bagging and boosting methods (Shi and Yang, 2016; Zhou *et al.,* 2021).

Remote sensing can provide crucial information for identifying contaminated sites, but there are few rigorously validated approaches (Silvestri and Omri, 2008). This work addresses the use of remote sensing with multispectral images taken from the Sentinel-2 satellite to analyze the earth's surface and, using a supervised classification algorithm, identify probable illegal dumps of solid waste in hydrographic subbasins surrounding the metropolitan area of Oaxaca, Mexico. A classifier model was trained with random forests from a set of control polygons on known surfaces with waste in the open. The study area's image collection, processing, and supervised classification were done on the Google Earth Engine platform. The results were verified in the office using geographic information systems and, in the field, taking a sample of the probable illegal dumps identified in the office.

2. Materials and methods

This section describes the five stages used to identify probable illegal dumps in hydrographic subbasins bordering the Metropolitan Area of Oaxaca, Mexico. The diagram in Figure 1 shows the research process used in this work.

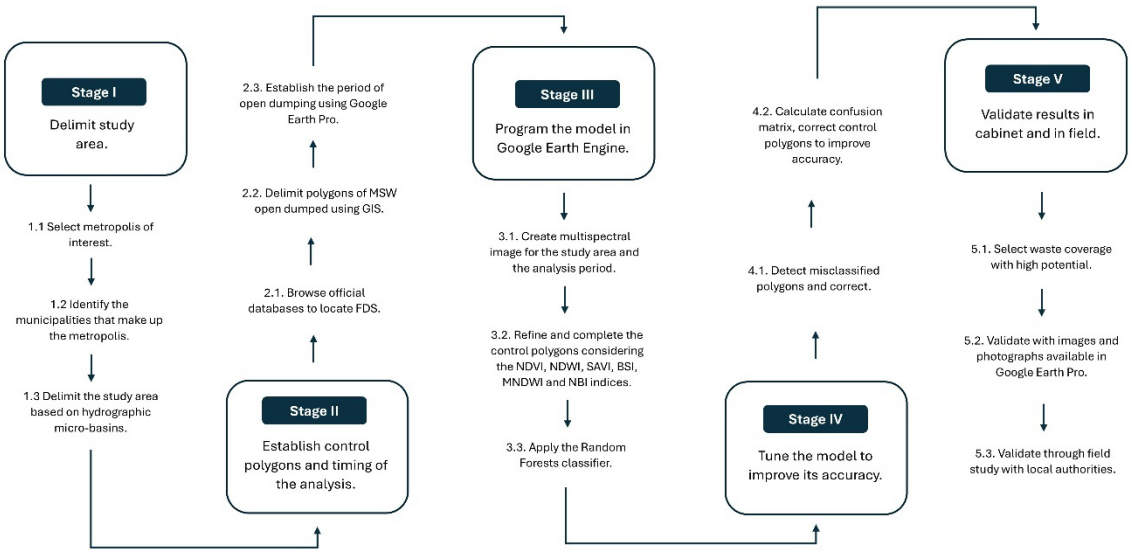

Figure 1. Research process to identify potential illegal dumps.

2.1. Stage I. Delimit study area

This research analyzed the metropolitan area of Oaxaca, which is one of the priority regions to address the problem of MSW since it represents the problem faced throughout Mexico. The area is one of the distributed MSW management systems studied by the National Research and Advocacy Project (Pronaii, by its acronym in Spanish) called "Transdisciplinary Strategy for Research and Resolution of the National Problem of Urban Solid Waste" in Mexico. This project aims to contribute to the transformation of solid waste management systems with a supportive, social, inclusive and circular economy approach.

The limit of the study area was carried out considering geohydrological and not administrative criteria. A delimitation of hydrographic micro-basins bordering the metropolitan area of Oaxaca was used. The hydrographic basin as a basic planning unit allows for the quantification of some natural and anthropic processes, such as the hydrological cycle, soil erosion processes, and dispersion of pollutants and nutrients, among others.

Figure 2 shows the three micro-basins surrounding the metropolitan area of Oaxaca that were analyzed to identify illegal dumps. The polygonal product of hydrographic basins used in this study is HydroBASINS (Lehner and Grill, 2013) on a global scale. This product was developed on behalf of the United States World Wildlife Fund with the support of international organizations and is part of the HydroSHEDS database (Hydrographic data and maps based on Shuttle Elevation Derivatives).

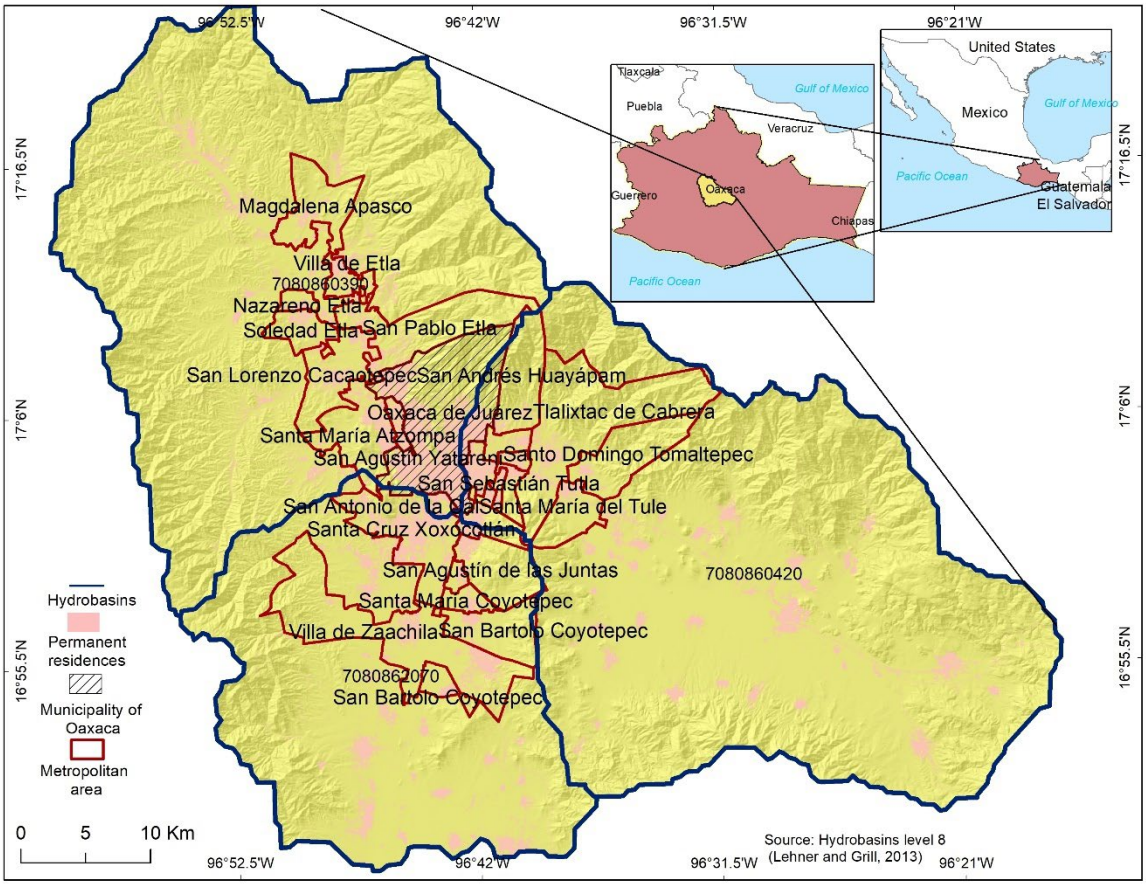

Figure 2. Microbasins of the metropolitan area of Oaxaca.

2.2. Stage II. Establish control polygons and timing of the analysis

The determination of official FDS that could contain surfaces covered by MSW deposited in the open was derived from the census of municipal governments and territorial demarcations of Mexico City in 2021 (INEGI, 2022). Thirty-nine FDS were identified, located, and analyzed using ArcGIS Pro to create the vector layer with the geolocation of the official FDS.

Photo interpretation work of the satellite images in the Google Earth Pro software identified surfaces covered with MSW deposited in the open between December 15, 2022, and January 15, 2023. These surfaces served as initial control polygons to train the supervised classification model and consisted of fifty-six control polygons for MSW coverage. This stage resulted in a vector layer of polygons covered by open-air MSW and a period of analysis.

2.3. Stage III. Program the model in Google Earth Engine

The supervised classification model of the multispectral images of the study area was programmed using Google Earth Engine. This online platform offers unparalleled access to an extensive catalog hosting millions of satellite images such as Sentinel-1, -2, -3, and -5P. This tool can also process large volumes of data efficiently and quickly in the cloud, which is of enormous value considering the size of the study area.

Figure 3 shows the process flow diagram of the model based on the methodologies presented in the End-to-End Google Earth Engine course (Gandhi, 2021) to identify probable illegal dumps used to process the images acquired from the Sentinel-2 MSI sensor, calculate spectral indices, and perform supervised classification. The first part of the model allows access to vector resources on the location of

control polygons and delimitation of the study area. Next, multispectral images from the COPERNICUS_S2_SR collection of the Sentinel-2 sensor were acquired and preprocessed. Image preprocessing includes corrections to remove atmospheric effects, geometric and radiometric correction, and image harmonization to ensure consistency between images from different dates and paths. The choice of these images and their proper processing are essential to obtain reliable data.

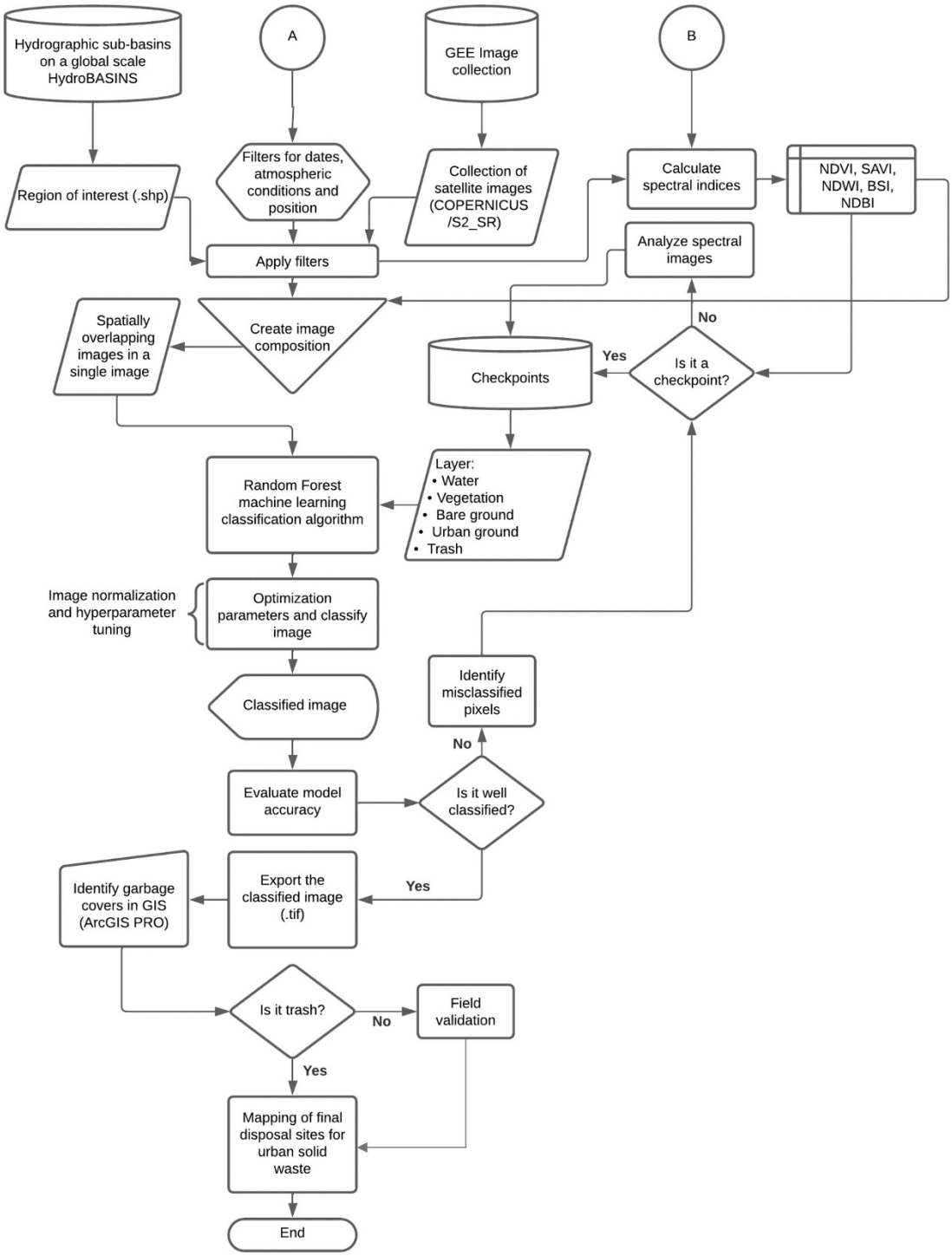

Figure 3. Flowchart of the supervised classification model in Google Earth Engine. Source: Own elaboration based on the supervised classification model proposed by Gandhi (2021).

The next block of the model uses spectral indices for the identification and differentiation of land cover. Land cover is a biophysical indicator that describes the materials that cover the territory, although it is understood differently depending on the discipline, the joint use of the concepts of land use and land cover is very common (Torres *et al.*, 2023). This study established five categories of land cover:

1) built structures or urban coverage; 2) bare soil or soil devoid of vegetation; 3) bodies of water; 4) surfaces with vegetation cover; and 5) surfaces covered with MSW.

In this part, the spectral indices NDVI, MNDWI, SAVI, NDBI, and BSI are calculated, with which the control polygons were precisely defined. Figure 4 shows the spectral image of the study area. Each of these indices provides critical information for the analysis, such as the amount and health of vegetation, the detection of the presence of water, the identification of areas with vegetation, and the characterization of areas without vegetation cover. The analysis of spectral indices is presented as an essential component of the procedure since it allows the precise delineation of specific characteristics on the Earth's surface, which is essential for the subsequent identification of probable illegal dumps.

The random forest classifier was the supervised machine learning algorithm used for classification and regression tasks in this work. This classifier integrated fifty decision trees into the forest. This classifier used 70% of the polygons for training and the remaining 30% for validation tests. The decision criteria were the values of the 13 bands of the optical images, the spectral indices NDVI, MNDWI, SAVI, NDBI, and BSI, and the slope and altitude of the surface.

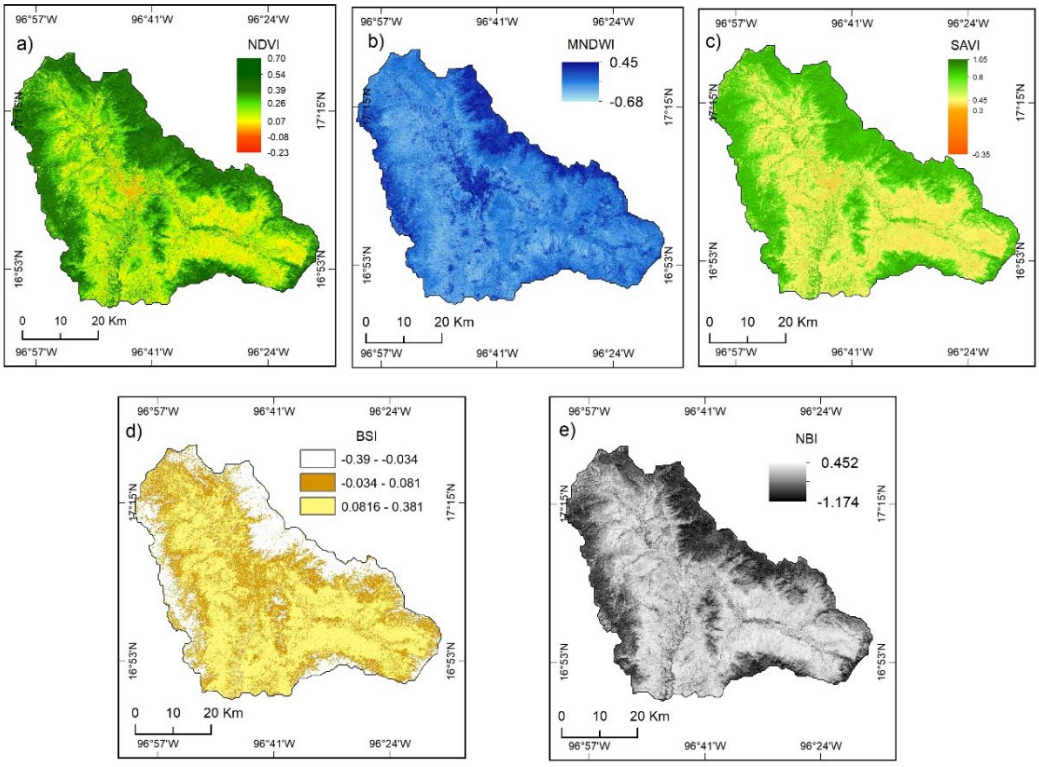

Figure 4. Images of the spectral indices in the study area: a) NDVI, b) MNDWI, c) SAVI, d) BSI and e) NBI.

2.4. Stage IV. Tune the model to improve its accuracy

After classification, model accuracy was evaluated using a confusion matrix, and the misclassified polygons were determined. The validation of supervised classification accuracy was executed through a Confusion Matrix, like an overall accuracy metric. Depending on the results

obtained, the polygons were reclassified, eliminated, or others were included, using information from the spectral indices and satellite images available in Google Earth Engine. This run, fix, tune, and test loop consumed considerable research time. Due to this iterative process of improving accuracy, it was not considered necessary to use other metrics, such as ROC or the McNemar test, to validate the cartographic products.

2.5. Stage V. Validate results in cabinet and in field

The classification results were subjected to a rigorous validation process that included both cabinet photo interpretation techniques and field validation. The main objective of this validation was to ensure the accuracy of the classification. The validation in the cabinet was based on photo interpretation techniques to make a visual and detailed evaluation of the areas classified as illegal dumps. Figure 5a shows the supervised classification results on a property in the study area. Pixels classified as waste are shown in black color. Figure 5b shows the Google Earth Pro satellite image in which characteristic features of a surface covered with irregularly deposited waste are detected. Finally, Figure 5c shows a street-view photograph that seems to confirm the accumulation of waste in the area. The polygons with the greatest remote evidence were presented to the municipal authority of Oaxaca de Juárez for field validation.

From this stage, a map was obtained with the location of probable illegal dumps, with which the field visit was planned with the endorsement of the corresponding municipal and state authorities. The field validation consisted of visiting the polygons with the highest probability of being illegal dumps at the end of October 2023. To carry out this visit, an approach was made with the competent authorities, to whom the information obtained was presented and accompaniment was requested to tour their territory.

Figure 5. Validation process by photointerpretation.

3. Results and discussion

From a 5x5 confusion matrix shown in Table 1, it was possible to determine the performance of the supervised classification model. The matrix took the coverage established at the checkpoints and compared it to the classification assigned by Random Forests. The overall accuracy for the study area of Oaxaca was 0.9517, which indicates that the classifier's performance is good. Although the results in Table 1 show that the model is not capable of accurately distinguishing between urban soil, bare soil, and garbage, it does not mean that the classifier selected was the wrong one. Future works may use other classifiers to discriminate the classes, for example, Maximum Likelihood Estimation or Support Vector Machines, which were already used by Torres *et al.* (2023) in land cover classification. These classifiers could improve the performance of the current model. However, as Perumal and Bhaskaran (2010) point out, it is impossible to state only one classifier for all situations since the characteristics of each image and the circumstances of each study vary significantly (Table 1).

Table 1. Confusion matrix of the classification model.

	Urban	Bare ground	Water	Vegetal	Waste
Urban	354	8	0	6	0
Bare ground	73	950	0	1	8
Water	8	0	250	0	0
Vegetal	2	3	0	1320	0
Waste	10	20	0	2	68

The classifier's confusion between bare soil and vegetation can be explained by the seasonal changes in vegetation cover during the analysis period. The model's confusion in classifying urban coverage as water confirms what Xu (2006) points out: that the MNDWI works poorly in urbanized areas, confusing constructions with bodies of water.

More relevant to the objective of this work is the model's confusion when predicting the surfaces covered with waste. Waste is a mixture of various materials, so obtaining a spectral fingerprint of it is difficult. The spectral fingerprint depends on the composition of the waste at the selected control points. The most significant confusion in the model is between waste cover and bare ground. Despite the use of the BSI index as proposed by Nguyen *et al.* (2021), this classification error was not possible to avoid. Therefore, more research is necessary on the spectral fingerprint of urban solid waste.

The graph in Figure 6 shows the relative importance of the nineteen decision criteria for classifying land cover. As can be seen, the value of the NDVI and SAVI spectral indices, as well as the B1 spectral band of aerosols, is the most important characteristic when making the classification. The importance that the model gives to the spectral indices is consistent with what Mahmood *et al.* (2023) stated regarding their usefulness in detecting illegal dumps. The NDVI and SAVI indices had already been identified by Karimi and Richter (2022) as relevant metrics for remote sensing of these dumpsites.

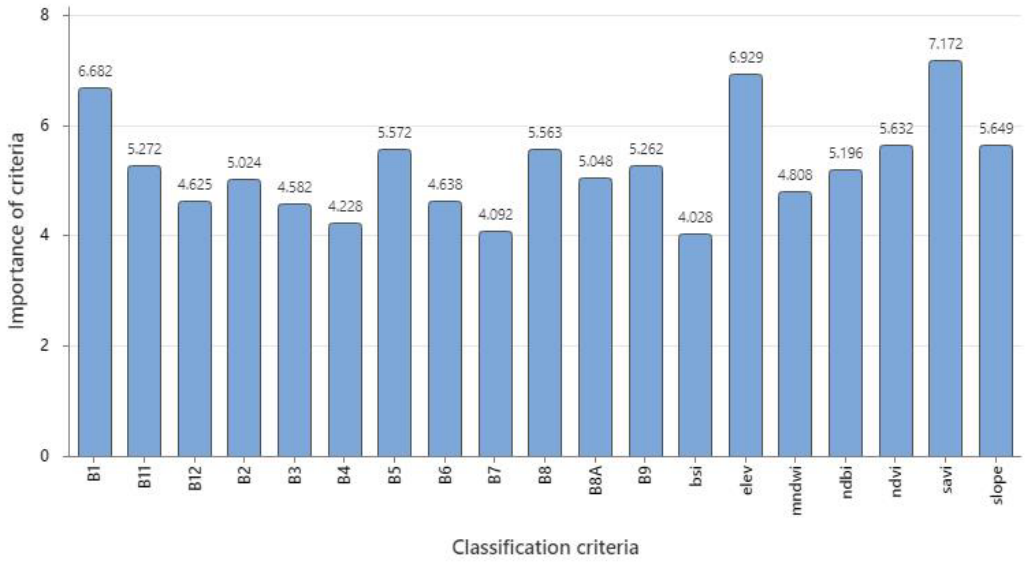

Figure 6. Importance of criteria in supervised classification.

Understandably, NDVI is a vital criterion for vegetal cover, bare ground, and even water bodies. Being a simple indicator of photosynthetically active biomass, the NDVI helps soil classification with high degrees of certainty, as Silvestri and Omri (2008) found. The SAVI helps mitigate the impact of ground shine, so its importance in classification is also consistent with the literature review. The SAVI

index improves the precision of identifying areas affected by erosive processes, as Laonamsai *et al.* (2023) suggested.

The B1 band of aerosols stands out as a significant characteristic in the classification, and this result invites us to investigate the spectral fingerprint of solid waste further. Bands B4, B5, B6, and B7 were the least important in classifying. These bands are associated with red, infrared, and near-infrared, an optical characteristic of little relevance among the five coverages analyzed in this work. Future models could remove these bands.

The graph in Figure 7 shows the mean, maximum, and minimum values of the pixels classified based on the criteria in Figure 6. The graph 7a shows the spectral fingerprint of the urban coverage for 363 data points. The adjustment of the NDBI index for this type of coverage is confirmed, as is the usefulness of the NDVI and the SAVI, whose values show a dispersion of less than 5%. Graph 7b shows the spectral fingerprint for 1187 bare ground data points. The adjustment of the BSI, NDBI, NDVI, and SAVI indices for this coverage stands out.

Graph 7c shows the spectral footprint of residues for 94 data points. For this cover, the NDVI, NDBI and SAVI indices present more significant adjustments, along with the bands B03, B11 and B12. The adjustment of the NDVI and SAVI spectral indices shown in the figure confirms what Karimi and Richter (2022) point out regarding the reduction of vegetation cover due to large-scale soil disturbances caused by residues. As shown in Figure 7c, the values of these indices are lower.

The similarity between the spectral fingerprints of urban cover, bare ground, and waste should be appreciated, which partially explains the classifier's confusion and the difficulty of finding illegal dumps.

The graphs 7d and 7e show the spectral fingerprint of the vegetation cover and water bodies, respectively. The 1030 vegetative cover data points analysis permitted to represent the spectral fingerprint that fits well to the first six bands. In general, the model distinguished wellvegetation and bodies of water cover. The analysis of 258 data points predicted by the model built the clear spectral fingerprint of the water.

Graph 7c is an example of how remote sensing can be used as a discrimination tool to recognize the unique spectral reflectance of clandestine dumpsites. This graph is the first approximation of the spectral fingerprint that, according to Karimi and Richter (2022), is of capital importance to delve deeper into the topic of detection and control of illegal dumpsites. Graph 7c is the first approximation of the spectral fingerprint of waste, but future work should delve into the topic, as well as the construction of a spectral index of waste.

Figure 8 shows the supervised classification results in the study area: urban cover represents 2.7%, 31.5% is bare ground, and 65.4% is vegetal cover. Only 200 hectares in the territory could correspond to bodies of water, which is consistent with the climate of the study area. Around 288 thousand 100 hectares of land surface were analyzed, supporting what Shrivastava *et al.* (2015) and Niu *et al*. (2023) pointed out, that satellite remote sensing is a powerful tool for analyzing large geographic areas.

Regarding the surface classified as covered with waste, the model produced a result of 400 hectares, which represents only 0.14% of the surface. This area is equivalent to fifteen times the size of the Zaachila Landfill, which served the municipality of Oaxaca de Juárez. This area was explored in the cabinet through photo interpretation to discard those areas with low potential to be illegal dumps.

The photo interpretation work after supervised classification was arduous because the model yields a large surface with probable waste coverage. Of the total area classified with waste coverage, only 4% had sufficient evidence in satellite images to establish probable illegal dumps. At this stage, using predictive models could further reduce the areas to be explored, such as the one proposed in Glanville and Chang (2015), which considers variables such as population density, land use, nearby waste facilities, and access roads; this improvement would make the process of detecting illegal dumps more efficient.

Figure 7. Spectral footprint of the types of coverage: a) urban, b) bare ground, c) waste, d) vegetal and e) water.

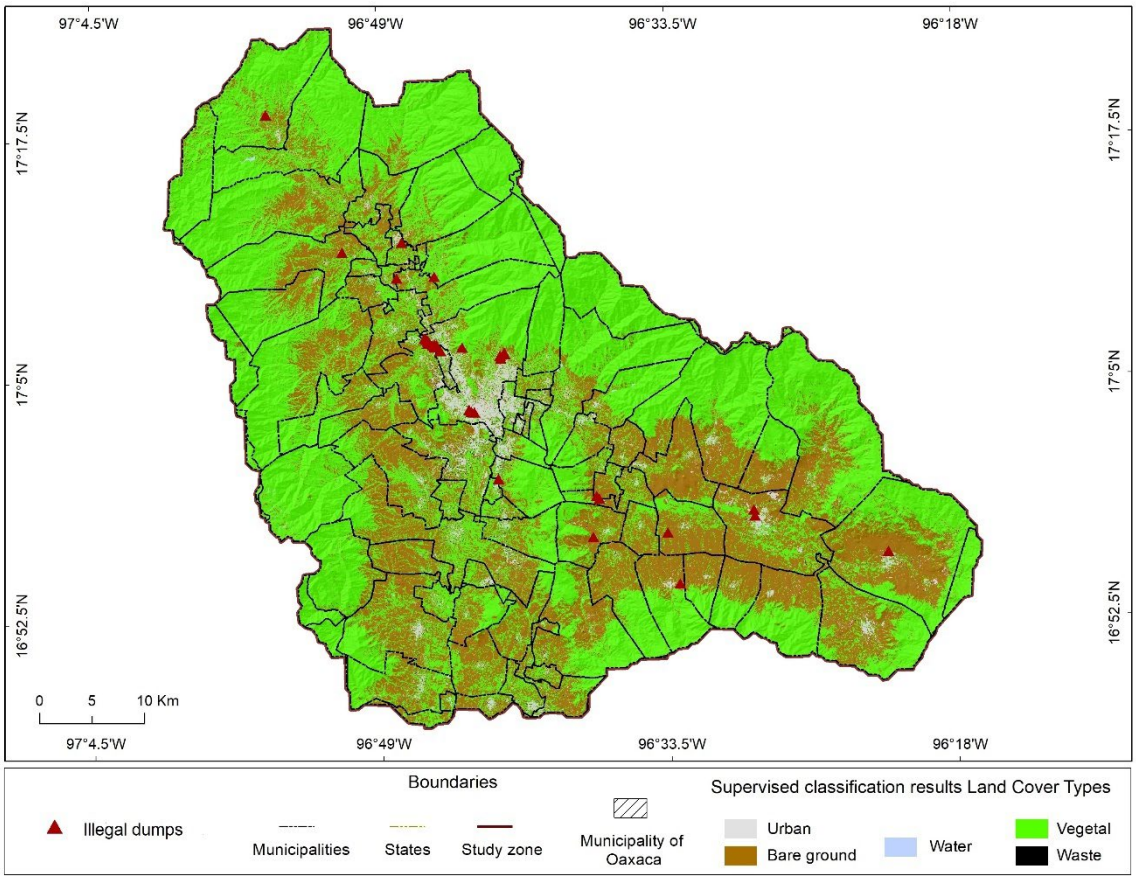

Figure 8. Results of supervised classification in the study area and location of probable illegal dumping sites.

In the end, 32 probable illegal dumps were detected, which cover approximately seventeen hectares (Fig. 8). Fifteen of these sites are in the municipality of Oaxaca de Juárez or its surroundings. This number is understandable, given that Oaxaca de Juárez has the largest population of the twenty-four municipalities that comprise the Metropolitan Zone of Oaxaca. Figures 9, 10, 11, and 12 show the result of supervised classification and the five land cover categories with the color indicated on the legend of each image. As a background, the available satellite image does not correspond to the model's analysis period. So, this produced several discrepancies between the coverage predicted by the model and the background image. Also, these figures illustrate the model confusion discussed in previous paragraphs.

The thirty-two probable illegal dumps could not be corroborated in the field since it was impossible to obtain the support of the municipal or state authorities of the region. Only the city council of Oaxaca de Juárez provided the conditions to tour its territory and carry out the field validation of seventeen sites. In this tour, the team discarded some probable illegal dumps; for example, sites 29 and 32 were banks of stone materials instead of waste, and their reflectance was like that of MSW. Site 30 contained construction and demolition waste, but this waste was on private property, so it cannot be considered a dump itself. At site 31, there was no trace of a waste deposit, and at site 28, only remains of burned waste were found.

The rocks identified at sites 29 and 32 showed hydrothermal alteration. During hydrothermalism, water reacts with the original rock-forming minerals, such as feldspars, pyroxenes, and amphiboles, to form micas and clays (Frost and Frost, 2019). Rocks display characteristic spectral signatures in multispectral and hyperspectral RS systems based on their mineralogy and texture (Girijaa and Mayappana, 2019). Girijaa and Mayappana (2019) report that it is possible to identify minerals

formed by hydrothermal alteration from band ratios (BR) and Principal component analysis (PCA). For the same purpose, Abdel-Rahman (2023) used selective band ratios (BR), directed principal component analysis (DPCA), feature-oriented false color composites (FFCC), and constrained Energy Minimization (CEM) using ASTER and Sentinel 2 data. Using BR and PCA can reduce the confusion model between residues and altered rocks in future studies.

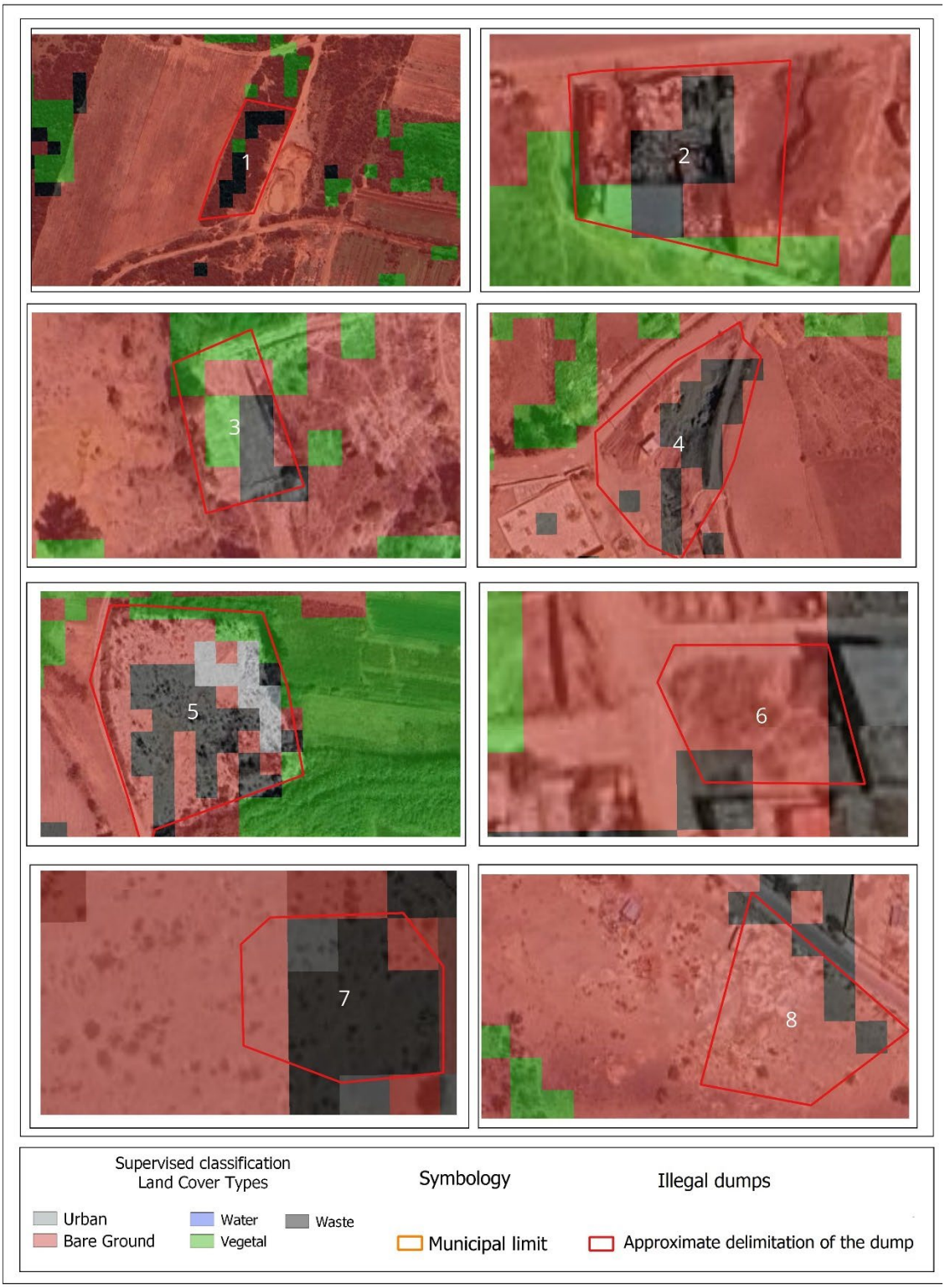

Figure 9. Probable illegal dumps 1-8.

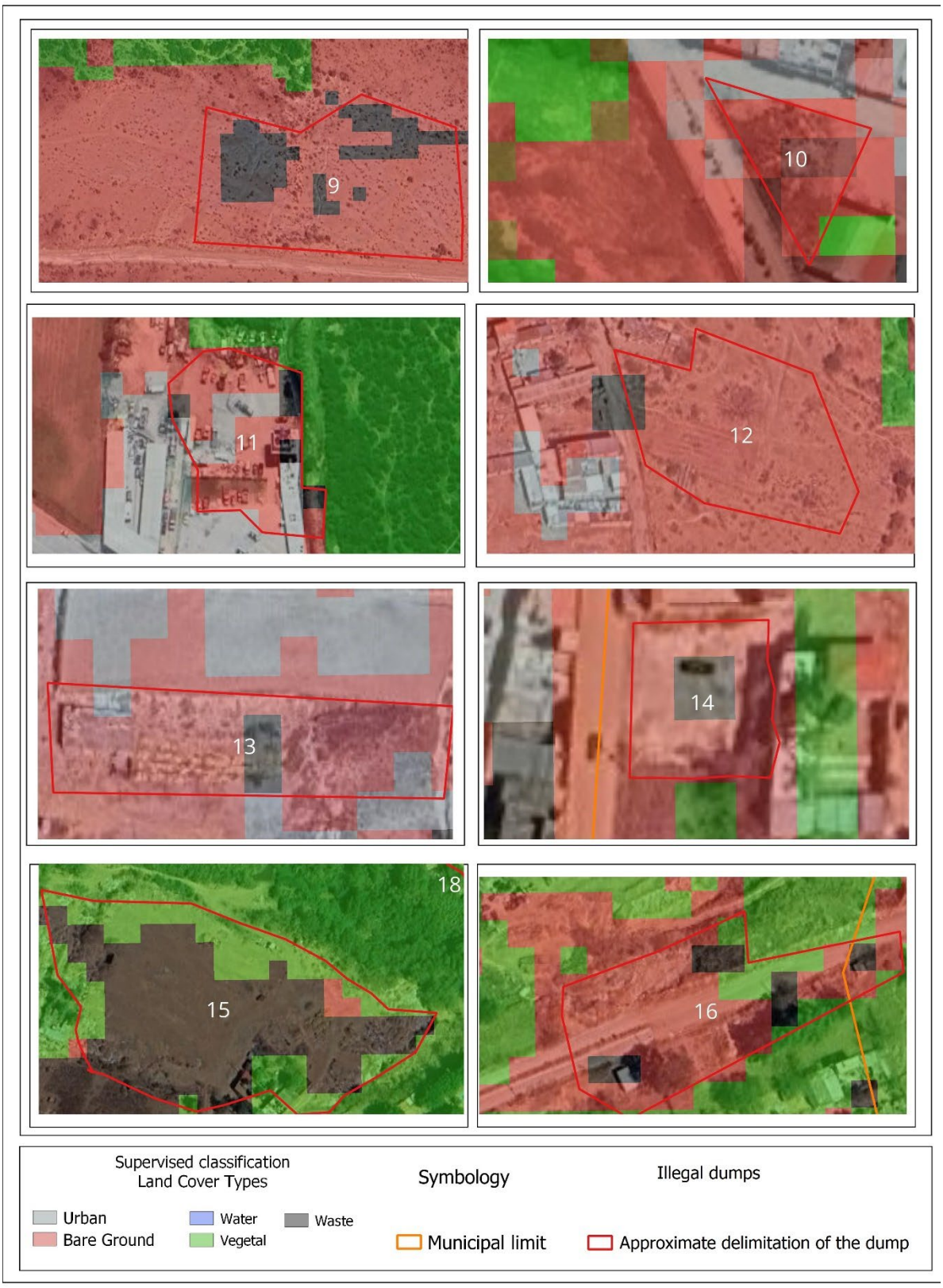

Figure 10. Probable illegal dumps 9-16.

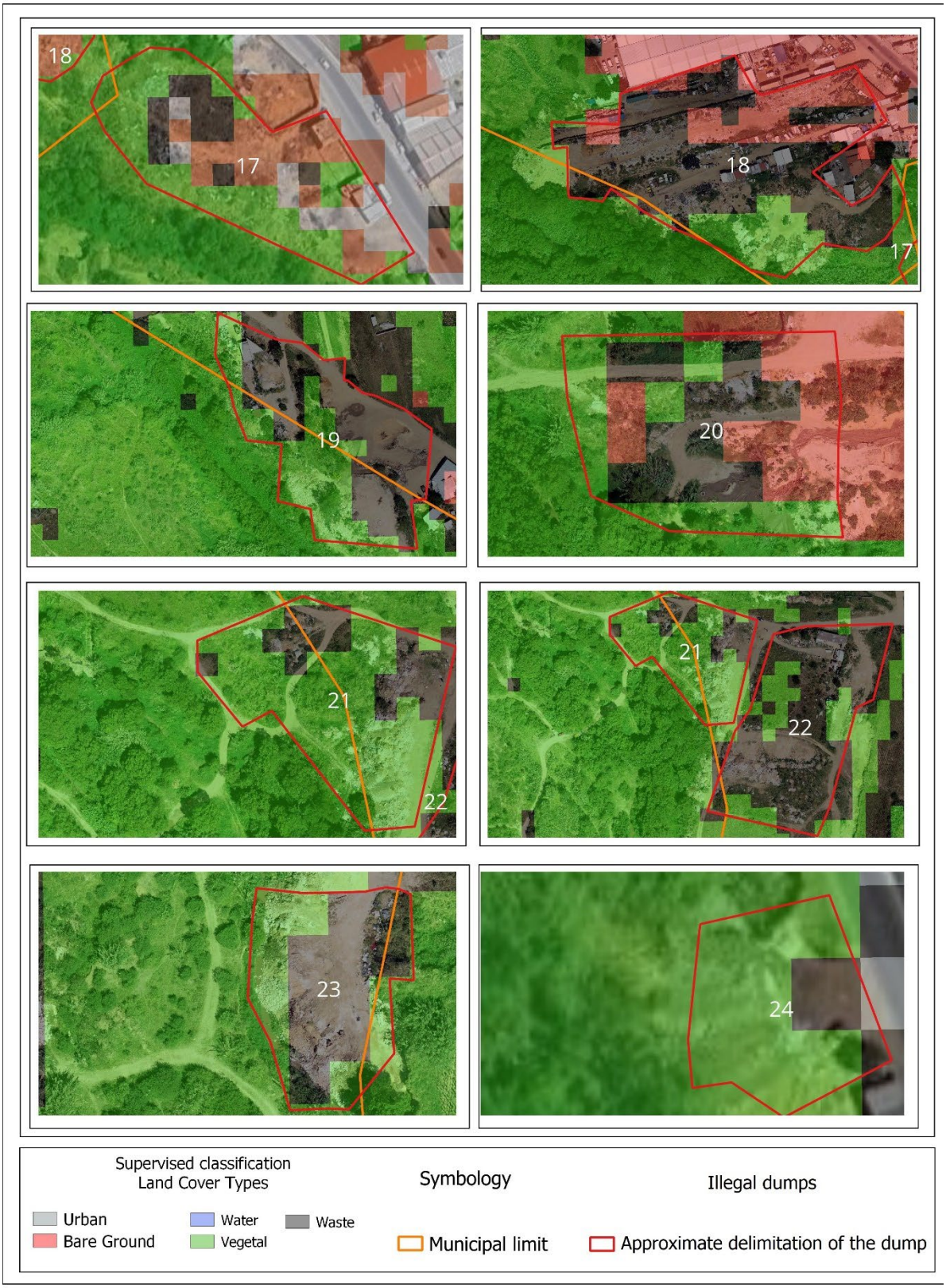

Figure 11. Probable illegal dumps 17-24.

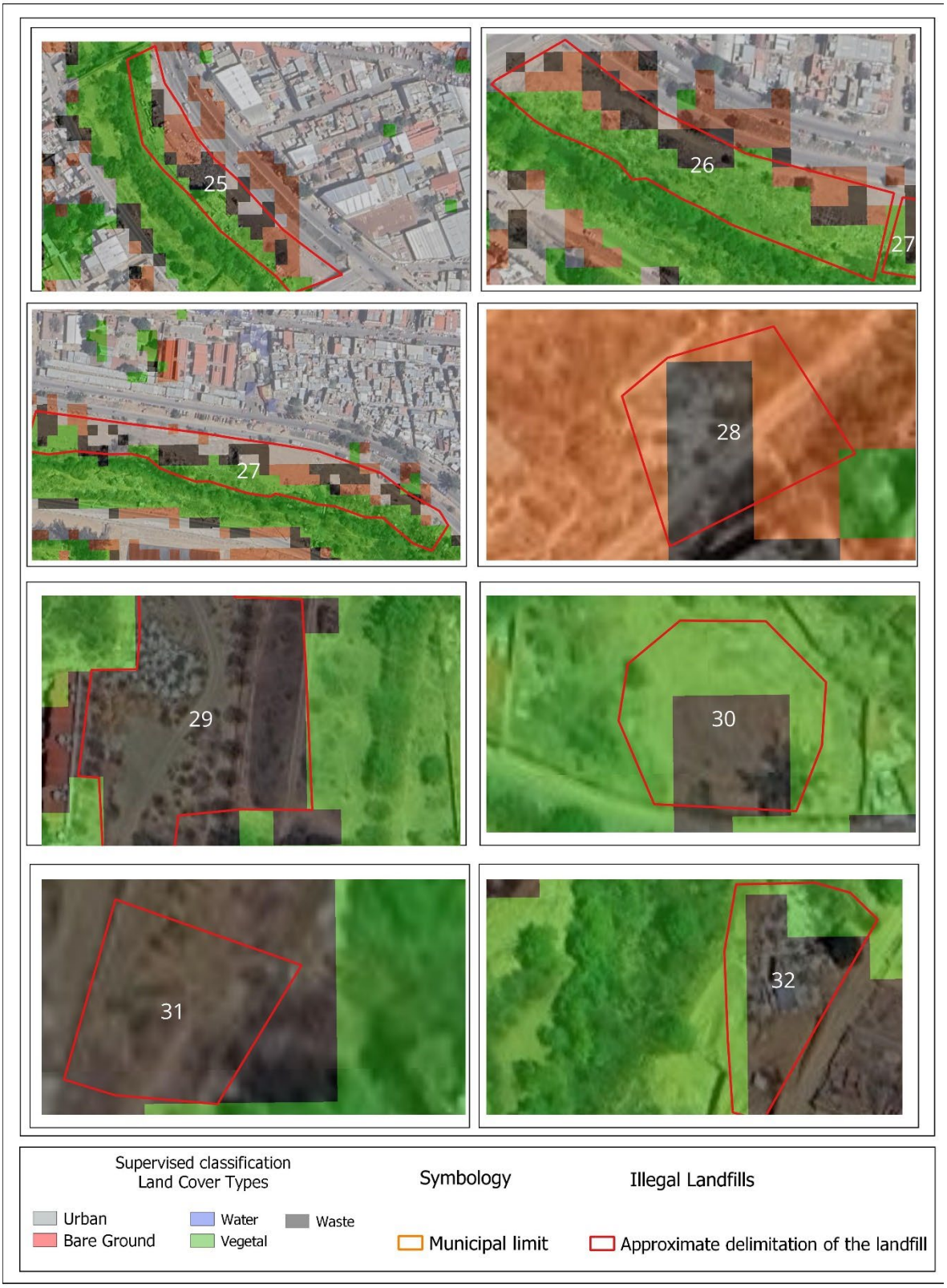

Figure 12. Probable illegal dumps 25-32.

In twelve properties identified as probable illegal dumps, there was evidence of irregular solid waste deposits. Fieldwork confirmed the possible illegal dumps 15, 16, 17, 18, 19, 20, 21, 22,23, 25, 26, and 27. Some of the background images of these sites correspond to an orthophoto obtained with a drone flight during the field validation carried out between October 24 and 26, 2023. The area of validation was the bank of the Atoyac River was poses a high risk of contamination for this body of water. People regularly and clandestinely dump urban solids and special handling waste in this area.

Future research should review the impacts of irregular discharge on the banks of the Atoyac River in depth. Unfortunately, the lack of resources allocated to monitoring and controlling waste dumping causes clandestine practices with strong environmental impacts. The results of this work required arduous validation work in the office but less than traditional classification methods, which require expensive and time-consuming field studies, as Perumal and Bhaskaran (2010) pointed out. Using collective intelligence and social participation can improve the validation process in the field (Torres *et al.*, 2021).

This work improved classification models by using spectral indices as relevant characteristics. Although Niu *et al.* (2023) pointed out that the effectiveness of these indices decreases in large territories, the results of this work show that the post-processing techniques can correct the effectiveness of discarding poorly classified areas.

The model presented in this investigation does not reach the level of precision of other models such as those developed by Gill *et al.* (2019) and Niu *et al.* (2023). However, one of its benefits is the possibility of exploring large geographical areas, and that in combination with photointerpretation and GIS techniques, it can successfully detect illegal dumps.

It is important to mention that other artificial intelligence algorithms, such as artificial neural networks, have been used, obtaining greater precision (Gill *et al.*, 2019; Niu *et al*., 2023; Dabholkar *et al*., 2017; Zhou *et al.,* 2021; Wang *et al.* (2024)). However, these models require high-resolution images, which limits their large-scale applicability.

An important line of research is to develop predictive models to identify probable areas of illegal dumping sites. Although this work provides relevant information for this, a model of this type usually ignores spatial heterogeneity and local contamination characteristics, so this work did not follow this line.

4. Conclusions

The traditional approach to garbage management in Mexico is inefficient and fails to fully protect the environment and the health of the population. Proof of this are the dozens of illegal dumps found in the study area. Technological tools such as the presented in this work can help managers and decision makers develop actions to control and mitigate pollution in these sites. The development of these models requires technical skills that could be beyond the reach of local authorities; however, collaboration between the academic sector and the authorities, as exemplified by the Pronaii in Mexico, can bridge this gap.

This work has shown how artificial intelligence, satellite remote sensing, and geographic information systems constitute powerful tools for identifying illegal dumps. The availability of satellite images over increasingly shorter periods and tools to process them, such as Google Earth Engine, can contribute to the development of remote sensing in solid waste management. This study is the one first approach to regional studies for detecting illegal dumps, through of the solid methodology that could replicated in other regions in Mexico.

Although the model presented does not achieve the level of precision of other models, such as those developed by Gill *et al.* (2019) and Niu *et al.* (2023), one of the benefits is that it can be expanded to explore large geographical areas and, combined with photointerpretation and GIS techniques, it can

be successful in detecting illegal dumps. It should also be noted that other artificial intelligence algorithms such as artificial neural networks have been used, obtaining greater precision (Gill *et al.,* 2019; Niu *et al.,* 2023; Dabholkar *et al.,* 2017); however, these models require high-resolution images, which limits their large-scale applicability.

The surfaces covered with solid waste occupied as control polygons allowed us to explore the spectral fingerprint of the solid waste and identify the bands and indices that are characteristic of it. This is a contribution to the remote sensing of illegal dumps. Future work will be able to specify the spectral fingerprint of the waste, and even construct a spectral index for the detection of solid waste on a large scale.

Others research should focus on improving spectral techniques for waste and integrating social participation mechanisms to enhance the detection and management of illegal dumps.

Acknowledgements

Financial support for this study was provided by the National Council of Humanities, Sciences and Technologies (Conahcyt) of Mexico, through the National Research and Advocacy Project (Pronaii) with number 321379, entitled like "Transdisciplinary Strategy for Research and Resolution of the National Problem of Urban Solid Waste." Thanks to the efforts of the Center for Research and higher Studies in Social Anthropology (Ciesas) Golfo, the resources for the development of this research were made available. The authors thank Vicente Torres Rodríguez and Miguel Ángel Blancas Reza for their advice on technical and methodological aspects. Finally, we would like to thank the authorities of the municipality of Oaxaca de Juárez for their support.

References

Ahmed, S. M., Muhammad, H., Sivertun, A., 2006, September. Solid waste management planning using GIS and remote sensing technologies case study Aurangabad City, India. In *2006 International Conference on Advances in Space Technologies* (pp. 196-200). IEEE. https://doi.org/10.1109/ICAST.2006.313826

Angelino, C. V., Focareta, M., Parrilli, S., Cicala, L., Piacquadio, G., Meoli, G., De Mizio, M., 2018. A case study on the detection of illegal dumps with GIS and remote sensing images. In *Earth Resources and Environmental Remote Sensing/GIS Applications IX* (Vol. 10790, pp. 165-171). SPIE. https://doi.org/10.1117/12.2325557

Cusworth, D. H., Duren, R. M., Thorpe, A. K., Tseng, E., Thompson, D., Guha, A., Newman, S., Koster, K.T., Miller, C. E., 2020. Using remote sensing to detect, validate, and quantify methane emissions from California solid waste operations. *Environmental Research Letters* 15(5), 054012. https://doi.org/10.1088/1748-9326/ab7b99

Dabholkar, A., Muthiyan, B., Srinivasan, S., Ravi, S., Jeon, H., Gao, J., 2017. Smart illegal dumping detection. In *2017 IEEE Third International Conference on Big Data Computing Service and Applications (BigDataService)* (pp. 255-260). IEEE. https://doi.org/10.1109/BigDataService.2017.51

Ferronato, N., Portugal Alarcón, G.P., Guisbert Lizarazu, E.G., Torretta, V., 2021. Assessment of municipal solid waste collection in Bolivia: Perspectives for avoiding uncontrolled disposal and boosting waste recycling options. *Resources, Conservation and Recycling* 167, 105234. 2021. https://doi.org/10.1016/j.resconrec.2020.105234

Frost, B.R. Frost, C.D., 2019. *Essentials of Igneous and Metamorphic Petrology.* Second edition. Cambridge University Press, New York, 297 pages.

Gandhi, U. 2021. End-to-End Google Earth Engine Course. Spatial Thoughts. Available: https://courses.spatialthoughts.com/end-to-end-gee.html

Glanville, K., Chang, H. C., 2015. Mapping illegal domestic waste disposal potential to support waste management efforts in Queensland, Australia. *International Journal of Geographical Information Science*, 29(6), 1042-1058. https://doi.org/10.1080/13658816.2015.1008002

Gill, J., Faisal, K., Shaker, A., Yan, W. Y., 2019. Detection of waste dumping locations in landfill using multi-temporal Landsat thermal images. *Waste Management and Research*, 37(4), 386-393. https://doi.org/10.1177/0734242X18821808

Instituto Nacional de Estadística y Geografía (INEGI), 2021. *Censo Nacional de Gobiernos Municipales y Demarcaciones Territoriales/Delegacionales, 2021.* https://www.inegi.org.mx/programas/cngmd/2021/

Karimi, N., Ng, K. T. W., Richter, A., 2022. Development and application of an analytical framework for mapping probable illegal dumping sites using nighttime light imagery and various remote sensing indices. *Waste Management*, 143, 195-205. https://doi.org/10.1016/j.wasman.2022.02.031

Kaza, S., Yao, L., Bhada-Tata P., Van Woerden, F., 2018. *What a waste 2.0: a global snapshot of solid waste management to 2050.* Urban Development Series. World Bank Group, Washington, D.C. https://doi.org/10.1596/978-1-4648-1329-0

Laonamsai, J., Julphunthong, P., Saprathet, T., Kimmany, B., Ganchanasuragit, T., Chomcheawchan, P., Tomun, N., 2023. Utilizing NDWI, MNDWI, SAVI, WRI, and AWEI for Estimating Erosion and Deposition in Ping River in Thailand. *Hydrology* 10(3), 70. https://doi.org/10.3390/hydrology10030070

Lehner, B., Grill G. 2013. Global river hydrography and network routing: baseline data and new approaches to study the world's large river systems. *Hydrological Processes* 27(15), 2171–2186. https://doi.org/10.1002/hyp.9740

Mahmood, K., Iftikhar, W., Faizi, F., 2023. Geospatial indices as an alternative for environmental impact assessment of dumped waste. *Acta Geophysica* 71(1), 309-322. https://doi.org/10.1007/s11600-022-00974-6

Matsumoto, S., Takeuchi, K., 2011. The effect of community characteristics on the frequency of illegal dumping. *Environmental Economics and Policy Studies* 13 (3), 177–193. https://doi.org/10.1007/s10018-011-0011-5

Nguyen, C. T., Chidthaisong, A., Kieu Diem, P., Huo, L. Z., 2021. A Modified Bare Soil Index to Identify Bare Land Features during Agricultural Fallow-Period in Southeast Asia Using Landsat 8. *Land* 10(3), 231. https://doi.org/10.3390/land10030231

Niu, B., Feng, Q., Yang, J., Chen, B., Gao, B., Liu, J., Li, Y., Gong, J., 2023. Solid waste mapping based on very high-resolution remote sensing imagery and a novel deep learning approach. *Geocarto International* 38(1), 2164361. https://doi.org/10.1080/10106049.2022.2164361

Papale, L. G., Guerrisi, G., De Santis, D., Schiavon, G., Del Frate, F., 2023. Satellite Data Potentialities in Solid Waste Landfill Monitoring: Review and Case Studies. *Sensors*, 23(8), 3917. https://doi.org/10.3390/s23083917

Padubidri, C., Kamilaris, A., Karatsiolis, S., 2022. Accurate Detection of Illegal Dumping Sites Using High Resolution Aerial Photography and Deep Learning. *2022 IEEE International Conference on Pervasive Computing and Communications Workshops and other Affiliated Events (PerCom Workshops)*, Pisa, Italy, pp. 451-456. https://doi.org/10.1109/PerComWorkshops53856.2022.9767451

Perumal, K., Bhaskaran, R., 2010. Supervised classification performance of multispectral images. *arXiv preprint arXiv:1002.4046*. https://doi.org/10.48550/arXiv.1002.4046

Quesada-Ruiz, L. C., Rodriguez-Galiano, V., Jordá-Borrell, R., 2019. Characterization and mapping of illegal landfill potential occurrence in the Canary Islands. *Waste Management* 85, 506-518. https://doi.org/10.1016/j.wasman.2019.01.015

Girija, R. R., Mayappan, S., 2019. Mapping of mineral resources and lithological units: a review of remote sensing techniques. *International Journal of Image and Data Fusion* 10, 79–106. https://doi.org/10.1080/19479832.2019.1589585

Rodríguez, A., 2023. Edoméx cuenta con al menos 50 tiraderos clandestinos. *Capital Media*. https://www.capitaledomex.com.mx/local/edomex-cuenta-con-al-menos-50-tiraderos-clandestinos/ (último acceso: 28/05/2024)

Secretaría de Medio Ambiente y Recursos Naturales (Semarnat), 2020. *Diagnóstico básico para la gestión integral de los residuos. 2020.* https://www.gob.mx/cms/uploads/attachment/file/554385/DBGIR-15-mayo-2020.pdf

Secretaría del Medio Ambiente de la Ciudad de México (Sedema), 2021. *Inventario de Residuos Sólidos de la Ciudad de México 2021.* https://www.sedema.cdmx.gob.mx/storage/app/media/DGCPCA/residuos/InventariodeResiduosSolidos2021.pdf

Shi, D., Yang, X., 2016. An assessment of algorithmic parameters affecting image classification accuracy by random forests. *Photogrammetric Engineering and Remote Sensing* 82(6), 407-417. https://doi.org/10.14358/PERS.82.6.407

Shrivastava, P., Mishra, S., Katiyar, S. K., 2015. A review of solid waste management techniques using GIS and other technologies. In *2015 International conference on computational intelligence and communication networks (CICN)* (pp. 1456-1459). IEEE. https://doi.org/10.1109/CICN.2015.281

Silvestri, S., Omri, M., 2008. A method for the remote sensing identification of uncontrolled landfills: formulation and validation. *International Journal of Remote Sensing* 29 (4), 975-989. https://doi.org/10.1080/01431160701311317

Torres, R. G., Bezada, M., Santalla, I. R., 2023. Cartografía de cobertura del suelo mediante datos de teledetección en la planicie de desborde del río Apure (Venezuela). *Cuadernos de Investigación Geográfica (Geographical Research Letters)* 49(1), 113-137. http://doi.org/10.18172/cig.5607

Torres, R. N., Fraternali, P., Biscontini, A., 2021. On the Use of Class Activation Maps in Remote Sensing: the case of Illegal Landfills. *2021 IEEE 8th International Conference on Data Science and Advanced Analytics (DSAA).* Porto, Portugal, 2021, pp. 1-10, https://doi.org/10.1109/DSAA53316.2021.9564243

Vigneshwaran, S., Vasantha Kumar, S., 2018. Extraction of built-up area using high resolution sentinel-2a and Google satellite imagery. *The International Archives of the Photogrammetry, Remote Sensing and Spatial Information Sciences*, XLII-4/W9, 165–169. https://doi.org/10.5194/isprs-archives-xlii-4-w9-165-2018 .

Vu, H.L., Bolingbroke, D., Ng, K.T.W., Fallah, B., 2019. Assessment of waste characteristics and their impact on GIS vehicle collection route optimization using ANN waste forecasts. *Waste Management* 88, 118-130. https://doi.org/10.1016/j.wasman.2019.03.037

Wang, Y., Zou, B., Zuo, X., Zou, H., Zhang, B., Tian, R., Feng, H., 2024. A remote sensing analysis method for soil heavy metal pollution sources at site scale considering source-sink relationships. *Science of The Total Environment* 946, 174021. https://doi.org/10.1016/j.scitotenv.2024.174021

Xi, Y., Thinh, N. X., Li, C., 2019. Preliminary comparative assessment of various spectral indices for built-up land derived from Landsat-8 OLI and Sentinel-2A MSI imageries. *European Journal of Remote Sensing* 52(1), 240–252. https://doi.org/10.1080/22797254.2019.1584737

Xu, H., 2006. Modification of normalised difference water index (NDWI) to enhance open water features in remotely sensed imagery. *International Journal of Remote Sensing*, 27(14), 3025–3033. https://doi.org/10.1080/01431160600589179

Yan, W. Y., Mahendrarajah, P., Shaker, A., Faisal, K., Luong, R., Al-Ahmad, M., 2014. Analysis of multi-temporal Landsat satellite images for monitoring land surface temperature of municipal solid waste disposal sites. *Environmental monitoring and assessment* 186, 8161-8173. https://doi.org/10.1007/s10661-014-3995-z

You, T., Chen, W., Wang, H., Yang, Y., Liu, X., 2020. Automatic Garbage Scattered Area Detection with Data Augmentation and Transfer Learning in SUAV Low-Altitude Remote Sensing Images. *Mathematical Problems in Engineering* 2020, 1-13. https://doi.org/10.1155/2020/7307629

Zhou, L., Luo, T., Du, M., Chen, Q., Liu, Y., Zhu, Y., He, C., Wang, S., Yang, K., 2021. Machine learning comparison and parameter setting methods for the detection of dump sites for construction and demolition waste using the google earth engine. *Remote Sensing* 13(4), 787. https://doi.org/10.3390/rs13040787

Cuadernos de Investigación Geográfica *Geographical Research Letters*	2024	Nº 50 (2)	pp. 179-202	EISSN 1697-9540

http://doi.org/10.18172/cig.6356

PASTOREO EN LA MEDIA MONTAÑA MEDITERRÁNEA PARA MITIGAR EL CAMBIO CLIMÁTICO: UNA EXPERIENCIA EN EL SISTEMA IBÉRICO NOROCCIDENTAL

TEODORO LASANTA, MELANI CORTIJOS-LÓPEZ, ESTELA NADAL-ROMERO*

Instituto Pirenaico de Ecología (CSIC). Campus de Aula Dei. Avda. de Montañana, 1005. Apdo. 1034, 50080-Zaragoza (España).

RESUMEN. El sector ganadero, en especial en su modalidad intensiva, se considera de gran relevancia en el contexto de cambio climático por su contribución a las emisiones de gases de efecto invernadero. Sin embargo, la producción ganadera es necesaria para alimentar a la población y la conservación de ecosistemas y paisajes culturales. Por otro lado, la ganadería extensiva puede ayudar a mitigar el cambio climático a través del pastoreo. En este trabajo se analiza cómo el binomio desbroce de matorrales–pastoreo contribuye a reducir los incendios forestales y a incrementar el almacenamiento de carbono orgánico en el suelo. El trabajo se ha realizado en un sector del Sistema Ibérico Noroccidental (norte de España), un área de media montaña mediterránea muy despoblada. En su paisaje abundan matorrales en distintas fases de sucesión vegetal tras el abandono rural, siendo la ganadería extensiva la principal actividad económica. Desde 1986 el gobierno regional ha desbrozado aproximadamente el 30% de la superficie de matorrales, disminuyendo el material combustible. La superficie quemada ha pasado de un promedio de 1.060 ha/año en el periodo 1968-1986 a 222,6 ha/año entre 1987 y 2023. Se comprueba también que los pastos regenerados tras el desbroce y las repoblaciones forestales gestionadas (aclareos y pastoreo) acumulan más carbono orgánico en el suelo que los matorrales. En estas montañas marginadas hay personas que quieren seguir viviendo de los recursos locales. La ganadería extensiva puede ayudar a fijar población, contribuyendo también a mitigar el cambio climático y a suministrar servicios ecosistémicos a la sociedad.

Grazing in the Mediterranean Mid-Mountains to Mitigate Climate Change: An Experience in the Northwestern Iberian System

ABSTRACT. The livestock sector, especially in its intensive form, is considered highly relevant in the context of climate change due to its contribution to greenhouse gas emissions. However, livestock production is necessary to feed the population and to conserve ecosystems services and cultural landscapes. On the other hand, extensive livestock farming can help to mitigate climate change through grazing. This study analyses how the combination of shrub clearing and grazing contributes to reducing forest fires and increasing organic carbon (SOC) storage in the soil. The study was conducted in the Northwestern Iberian System (Spain), a sparsely populated Mediterranean mid-mountain region. In the landscape predominates shrubs in different stages of plant succession after rural abandonment, with extensive livestock farming being the main economic activity. Since 1986, the regional government has cleared approximately 30% of shrublands, reducing the amount of available combustible material. The burned area has decreased from an average of 1,060 ha/year in the period 1968-1986 to 222.6 ha/year between 1987 and 2023. It has also been found that pastures regenerated after clearing, as well as managed forest plantations (thinning and grazing), accumulate more SOC than the shrublands. In these marginalized mountains there are people who want to continue living off local resources. Extensive livestock farming can help retain the population, while also contributing to climate change mitigation and providing ecosystem services to society.

Palabras clave: ganadería extensiva, paisaje en mosaico, incendios forestales, secuestro de carbono en el suelo, La Rioja (España).

Keywords: extensive stockbreeding, mosaic landscape, forest fires, SOC stocks, La Rioja (Spain).

Received: 20 September 2024

Accepted: 2 December 2024

***Corresponding author**: Estela Nadal Romero. Instituto Pirenaico de Ecología. Campus de Aula Dei. Avda. Montañana, 1005. 50080-Zaragoza. estelanr@ipe.csic.es

1. Introducción

La existencia de complejas interacciones entre producción ganadera y cambio climático (CC, en adelante) es un asunto científico y técnico de gran trascendencia y controversia en la actualidad (Hoffmann, 2010; Rojas-Downing *et al.,* 2017; Herrera, 2020). Por un lado, la cría de animales es una actividad productora de gases de efecto invernadero (GEIs): dióxido de carbono, metano y óxido nitroso, sobre todo. Por otro lado, la ganadería es un sector vulnerable al CC, ya que se ve condicionada por la producción y calidad de pastos, así como por el bienestar y la salud de los animales (Rubio y Roig, 2017). Es decir, la ganadería contribuye al CC, pero también se ve afectada por él (Hoffman, 2010).

La ganadería extensiva es un sector clave para la conservación de ecosistemas y paisajes culturales, así como para el suministro de servicios ecosistémicos: producción y calidad de pastos, control de incendios, regulación hídrica, conservación de la biodiversidad o incremento de la fertilidad edáfica del suelo y de sus funciones (Bernués *et al.,* 2014; Fernández-Rebollo *et al.,* 2015; Lasanta *et al.,* 2024). Por otra parte, se trata de un sector clave en la seguridad alimentaria y en la producción de alimentos a escala global. Todo esto en un contexto en el que se prevé que alimentar a la humanidad requerirá incrementar un 50% la producción para mediados del siglo XXI, a la par que se espera que aumente el consumo de proteína animal, lo que exigirá una mayor producción ganadera (FAO, 2017). Además, la ganadería extensiva y el pastoreo cumplen con prácticas beneficiosas para el medio ambiente, incluidas en los objetivos de la Política Agraria Común (PAC), 2023-2027 (PEPAC, 2023).

Se estima que la ganadería es responsable de entre el 7% y el 18% de los GEIs de origen antrópico (Gerber *et al.,* 2013), debido a las emisiones de los animales domésticos, los consumos de energía (piensos, transportes, electricidad…), el manejo de estiércol y purines; y el uso de antibióticos (Rojas-Downing *et al.,* 2017; Rubio y Roig, 2017). Pero no todos los sistemas ganaderos emiten la misma cantidad de GEIs. Los sistemas ganaderos se pueden agrupar en dos grandes bloques: ganadería extensiva o pastoralista y ganadería intensiva o industrial, con variantes entre uno y otro. La ganadería extensiva aprovecha recursos forrajeros locales mediante pastoreo con escasa incorporación de insumos externos, tanto materiales (piensos y otros alimentos) como energéticos. La ganadería industrial, por el contrario, se desarrolla en recintos cerrados, utilizando alimentos (tortas de semillas de oleaginosas, cereales, forrajes y pajas, fundamentalmente) procedentes de otros lugares, a veces incluso de otros países. Genera residuos perjudiciales cuando se acumulan en grandes cantidades (nitratos, por ejemplo, que contaminan acuíferos y suelos) y consume gran cantidad de energía (una parte considerable en el transporte) y otros insumos externos (González, 2012; Herrera, 2020).

La mayor parte de la literatura científica sobre ganadería y CC no diferencia la emisión de GEIs entre sistemas ganaderos, ni entre producción intensiva y extensiva (Gerber *et al.,* 2013; Rojas-Downing *et al.,* 2017; Aguilera *et al.,* 2018). Afortunadamente, en los últimos años algunas investigaciones analizan individualmente la contribución de los sistemas de producción al CC. Es una información esencial para determinar su contribución a los GEIs y para impulsar iniciativas específicas de adaptación y mitigación al CC. En este sentido, Zhu *et al.* (2020) han estimado que las emisiones de óxido nitroso del vacuno

extensivo en Kenia son hasta 14 veces inferiores a las estimadas por el IPCC (2020). Otros estudios demuestran que la emisión de metano por los rumiantes disminuye entre un 15-25% cuando en la dieta se incluye el ramoneo de matorrales ricos en taninos (Tang *et al.,* 2028; Aboagye y Beachemin, 2019). Este tipo de estudios coinciden en que los GEIs atribuidos a la ganadería han penalizado de manera notable a los sistemas extensivos, ya que su aporte a los GEIs es mínimo, derivados del cambio de uso del suelo, la gestión de purines y estiércol, la utilización de fertilizantes químicos para la producción agrícola, incluyendo la de piensos para alimentar al ganado, además del consumo de energía en las instalaciones ganaderas y el transporte de piensos, entre otras variables (Rojas-Downing *et al.,* 2017; Herrera, 2020).

La media montaña mediterránea es un territorio muy afectado por el CC y muy sensible a sus efectos, entre otras razones por el incremento de las sequías climáticas e hidrológicas, el mayor riesgo de incendios, la pérdida de recursos pastorales y la disminución de la biodiversidad (Nogués-Bravo *et al.,* 2008; García-Ruiz *et al.,* 2011; Pascual Sánchez y Pla Ferrer, 2024). La media montaña mediterránea española tuvo una explotación muy intensa desde la Baja Edad Media hasta bien entrado el siglo XX. Muchas laderas fueron deforestadas para aprovechamiento ganadero, casi siempre mediante ganadería trashumante, y agrícola. Algunos bosques se deforestaron también para obtener leña para los hornos de la industria textil, la construcción y la venta al exterior (Moreno Fernández, 1994; Sabio Alcutén, 1997; García-Ruiz *et al.,* 2015). En estas condiciones los bosques quedaron recluidos en enclaves con escasas posibilidades para usos agropecuarios: laderas muy pendientes, poco accesibles o alejadas de los pueblos, y suelos de baja calidad o muy pedregosos.

Bajo las exigencias (elevada competitividad y rentabilidad de los productos, así como buena accesibilidad a los mercados) del sistema reciente de gestión del territorio, la media montaña mediterránea tiene enormes dificultades para desarrollar actividades económicas competitivas, por sus condiciones topográficas en las que dominan las fuertes pendientes y escasean los espacios llanos, la degradación de sus suelos tras siglos de gestión intensiva, la escasez de infraestructuras y servicios, y la lejanía de los núcleos dinamizadores del territorio (Lasanta y Ruiz-Flaño, 1990; García-Ruiz *et al.,* 2015). Por ello, desde al menos mediados del siglo XX, la media montaña mediterránea ha experimentado un proceso de marginación socioeconómica con emigración de la población (muchos pueblos y aldeas han desaparecido y otros han visto reducida su población en el 70-80%), abandono de la agricultura y brusca caída de los censos ganaderos. En el paisaje, esta evolución se manifiesta en un proceso de sucesión vegetal, con avance de matorrales y bosques (García-Ruiz y Lana-Renault, 2011), y por la reforestación de muchas laderas con pinos por parte de la Administración (Ortigosa, 1990). Los campos abandonados, especialmente los bancales, se han visto afectados por procesos de erosión y degradación del suelo (Arnáez *et al.,* 2015).

Con las condiciones ambientales y sociales de la media montaña mediterránea, la ganadería extensiva es actualmente la principal actividad económica, en algunos municipios la única. La mayor parte del territorio solo puede ser aprovechado mediante pastoreo. En cambio, la agricultura no deja de ser una actividad secundaria, por sus condiciones climáticas, pendientes pronunciadas y suelos poco fértiles. La ganadería extensiva, por el contrario, consume fibras vegetales ligno-celulósicas en tierras no aptas para la agricultura, incorporando estas montañas al sistema productivo. Sin la ganadería quedarían al margen y los recursos pastorales se deteriorarían progresivamente (Lasanta, 2009; Herrera, 2020).

Desde 1986 el Gobierno de La Rioja elimina matorrales en áreas seleccionadas para reducir el material combustible y crear un paisaje más fragmentado, con el fin de disminuir el número de incendios y la superficie quemada. También persigue incrementar la oferta pascícola mediante la regeneración de pastos en áreas de matorral (Lasanta *et al.,* 2013). Es un plan (*Plan Shrub Clearing*; PSC en adelante) muy riguroso, que se ejecuta cada año, siguiendo una normativa que compagina la conservación de suelos y aguas con el mantenimiento de la biodiversidad, el desarrollo ganadero y el impulso de varios servicios ecosistémicos (Lasanta *et al.,* 2024). La financiación corre a cargo del propio gobierno, si bien cuenta con el apoyo fluctuante de la Unión Europea, el gobierno nacional o los ayuntamientos. El coste durante los últimos años ronda los 400 euros/ha.

Una cuestión poco estudiada y muy importante es que la ganadería se considera emisora de GEIs, pero no se tiene en cuenta que los ecosistemas y paisajes creados o mantenidos por la ganadería extensiva pueden tener una elevada capacidad para mitigar el CC. Así, por ejemplo, no se tiene en cuenta el carbono que acumulan los pastos y el metano que oxidan. En este sentido, los objetivos de este trabajo son: (i) comprobar, a partir de imágenes, la disminución de combustible y la fragmentación del paisaje como consecuencia de la eliminación de matorrales y del pastoreo; (ii) conocer la evolución de la superficie quemada en La Rioja, y (iii) analizar la calidad de suelo y almacenamiento de carbono orgánico en diferentes usos y cubiertas del suelo (en adelante LULC, por sus siglas en inglés) relacionados con el pastoreo en comparación con otros LULC que actúan de control. Nuestra hipótesis es que el pastoreo contribuye a mitigar el CC, por un lado, reduciendo las emisiones de CO_2 a la atmósfera a través de la disminución de los incendios forestales y, por otro lado, incrementando la acumulación de carbono orgánico en el suelo (en adelante SOC, por sus siglas en inglés).

2. Área de estudio

El trabajo se ha realizado en el Sistema Ibérico Noroccidental, en concreto en las montañas de La Rioja (Fig. 1), que abarcan una superficie de 1879,5 Km^2. En estas montañas (la Sierra en adelante) se suceden siete valles estrechos, con laderas de elevada pendiente en el sector occidental (Sierra de la Demanda) y más suaves en los valles centrales (Cameros) y orientales, separados por divisorias de escasa pendiente o llanas (Fig. 2). La altitud de la Sierra disminuye desde las divisorias meridionales hacia el norte y hacia el este. Las líneas de cumbres carecen de relieves enérgicos, alcanzando la máxima altitud en el Pico de San Lorenzo (2.265 m s.n.m.) en la Sierra de la Demanda, mientras que las montañas más orientales apenas superan los 1.000 m. s.n.m. La suavidad de las cumbres ha favorecido la explotación ganadera, al permitir el fácil aprovechamiento de los pastos en verano.

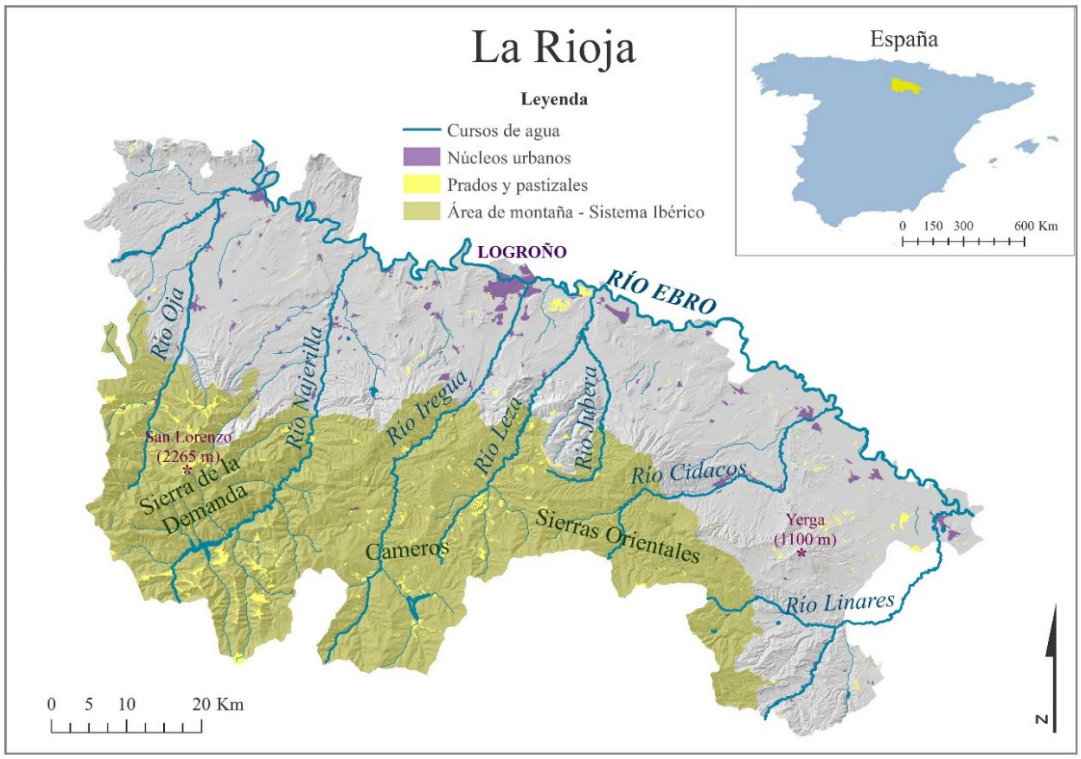

Figura 1. Área de estudio, La Rioja (España).

Figura 2. Campos abandonados en las proximidades de Hornillos (Camero Viejo). Las cimas de la mayor parte de las montañas de La Rioja son relieves prácticamente planos o alomados. En muchas de ellas los campos de cultivo llegaron hasta la parte más alta. En la actualidad son pastos, en algunos casos regenerados mediante la eliminación de matorrales.

El área de estudio tiene un clima submediterráneo, matizado por los rasgos orográficos y por la mayor o menor distancia a la influencia atlántica. El sector más occidental recibe una precipitación superior a los 1000 mm anuales, con rasgos próximos al clima oceánico, con inviernos fríos y sin apenas déficit hídrico estival. En los valles centro-orientales el clima es mucho más mediterráneo, con temperaturas más elevadas, largos periodos de sequía durante el verano y notable contraste térmico anual. Las precipitaciones oscilan entre 600 y 800 mm/año y la temperatura media entre 10-12ºC, en función de la altitud y exposición (Cuadrat y Vicente-Serrano, 2008).

El paisaje del Sistema Ibérico noroccidental ha sido modificado por las sociedades humanas desde hace miles de años. El análisis polínico en turberas muestra que el bosque experimentó un notable descenso a partir de 5.060 ± 90 yr BP (Gil-García *et al.,* 1996). De igual forma, el estudio de dólmenes datados entre 6.000 y 3.500 cal yr BP por debajo de 1.400 m s.n.m. indica la presencia de sociedades agropastorales desde épocas relativamente tempranas (López de Calle y Tudanca, 2014). Desde la Baja Edad Media se incrementó el aprovechamiento ganadero, basado en la trashumancia, lo que favoreció el desarrollo de la industria textil. Su decadencia desde el siglo XVIII impulsó la roturación y cultivo de tierras en laderas marginales, para sustituir a la economía ganadero-industrial (Gómez Urdáñez, 1986). Todo ello llevó a la deforestación de la mayor parte del territorio (Sanjuán *et al.,* 2018).

A lo largo del siglo XX, especialmente entre los años cincuenta y ochenta, se asiste a la caída de los censos demográficos y a la despoblación total de 50 pueblos y aldeas. En 1900 la montaña riojana contaba con 33.632 habitantes (17,9 hab./Km^2), y en 2022 con tan solo 7.762 habitantes (4,1 hab./Km^2), y valores extremos de 10 hab./Km^2 en el valle del Oja, gracias a la localización del municipio de Ezcaray, y 2 hab./Km^2 en el valle del Leza. A lo largo del siglo XX, el progresivo hundimiento de la ganadería lanar se vio acompañado por un incremento del ganado vacuno, a la vez que el espacio agrícola se dejó de cultivar casi completamente (Lasanta y Errea, 2001). El paisaje cultural tradicional dio lugar a otro más homogéneo y naturalizado, con matriz de bosques y matorrales (Lasanta y Arnáez, 2009). Dominan

los robledales (*Quercus pyrenaica* y *Quercus faginea*), hayedos (*Fagus sylvatica*) y pinares (*Pinus sylvestris* y *Pinus nigra*) distribuidos en diferentes pisos de altitud (Fernández Aldana, 2015), si bien los matorrales de sucesión (*Calluna vulgaris*, *Cytisus scoparius*, *Genista scorpius*, *Cistus laurifolius*, *Buxus sempervirens*, *Rosa sp*….) ocupan la mayor parte del territorio en los valles centro-orientales (Arizaleta *et al.*, 1990). Por otro lado, entre 1941 y 1982 se reforestaron más de 40.000 ha de coníferas: *P. sylvestris*, *P. nigra*, *P. halepensis* y *P. douglasii* (Ortigosa, 1991). Después de los años noventa del pasado siglo se siguió repoblando con subvenciones de la PAC (Fernández Aldana, 2015).

La ganadería extensiva es la principal actividad económica en la Sierra desde las últimas décadas del pasado siglo. En 2022 pastaban, según los censos del Gobierno de La Rioja, 13.268 vacunos, 35.092 ovinos, 2.326 cabras, y varios miles de equinos. Consume biomasa vegetal en régimen de pastoreo en casi total libertad con poca intervención humana y con mínimos consumos de energía fósil e insumos externos. El vacuno, orientado a la cría de terneros que se venden a los 3-5 meses de nacer, es la especie más representativa, mientras que en el pasado lo fue el ovino trashumante (Calvo Palacios, 1977; Lasanta y Errea, 2001). El manejo del ganado es muy parecido en todas las especies. La mayor parte del año permanece libre en el monte. Tan sólo en invierno, o en los momentos de partos, recibe un complemento de pienso y paja, suministrado directamente en el campo (Fig. 3) o en el pesebre, en una cantidad dependiente del tiempo, de su estado fisiológico y de su etapa reproductiva.

La raza vacuna tradicional era autóctona (la *camerana*) de capa negra, del tronco de las vacas negras serranas, caracterizadas por su elevada rusticidad y adaptación al medio. Desde los años setenta del pasado siglo se introdujeron sementales de aptitud cárnica de razas foráneas: *Pardo-alpina, Charolesa, Limousina, Hereford, Pirenaica, Simmental…*, buscando mejores rendimientos en las canales. Por ello, las vacas son ahora mayoritariamente cruce de varias razas (Fig. 4). Respecto al ovino, en los valles orientales domina la oveja autóctona: la *Chamarita*, de pequeño tamaño, elevada rusticidad y buena reproductora, mientras que en los valles occidentales es frecuente ver ovejas de cruces muy diversos.

Figura 3. Vacuno comiendo paja en la pista de Hornillos a Valdeosera (Camero Viejo). En la estación fría el vacuno suele recibir un complemento de alimento, unas veces junto a las naves y otras en el campo, pero en muy raras ocasiones se estabula. El ovino, por el contrario, suele estabularse unos días (aunque no todos los ganaderos lo hacen) en la época de cría.

Figura 4. Rebaño de vacuno en Ajamil (Camero Viejo). La cabaña vacuna actual procede de mezclas de distintas razas. En la foto se adivinan rasgos de Camerana, Pardo-alpina, Limousin, Charolesa y Pirenaica. Al fondo una ladera de matorrales parcialmente desbrozada y bosques de Quercus pyrenaica.

3. Toma de información y métodos

3.1. Evolución de la superficie desbrozada y de los incendios registrados

En la Consejería de Agricultura, Ganadería, Mundo Rural y Medio Ambiente (Gobierno de La Rioja) se tomó información sobre la superficie desbrozada anual (desde 1986 a 2022) del área de estudio, y sobre incendios (número de siniestros y superficie quemada cada año) en La Rioja desde 1968 a 2023, periodo del que se dispone de información. Lamentablemente, no tenemos información a escala municipal, por lo que no conocemos con exactitud la evolución de los fuegos forestales en la Sierra. Es una laguna importante, pero consideramos que la información para La Rioja es tan clara que permite asumir algunas conclusiones sobre el efecto del PSC y el pastoreo en el control de incendios.

3.2. Almacenamiento de carbono orgánico en el suelo

Para conocer el almacenamiento de carbono se tomaron muestras de suelos en ocho LULC: (i) matorrales (M), tanto de *C. laurifolius* como de *G. scorpius*, que representan el proceso de revegetación natural tras el abandono de tierras sin pastoreo del ganado; (ii) pastos de mediana edad (PMD), con unos 15 años desde su desbroce; (iii) pastos de desbroce antiguo (PAD), con más de 25 años desde su desbroce; (iv) pastos de control (CP), es decir áreas que han sido pastoreadas durante siglos y que, por lo tanto, pueden considerarse pastos naturales; representarían la etapa final de áreas desbrozadas y pastoreadas periódicamente; (v) repoblaciones forestales sin gestionar (RPN); (vi) repoblaciones forestales gestionadas (RPG), en las que se efectúa algún aclareo y pasta el ganado; (vii) bosques de rebollos (*Q. pyrenaica*) sin gestionar (BN), por lo que cuentan con sotobosque de matorral que dificulta el pastoreo y (viii) dehesas de rebollos (D) en las que pasta el ganado. En cada LULC se tomaron muestras en al menos 2 sitios elegidos al azar; en cada uno de éstos se extrajeron muestras de tres puntos, que se combinaron para dar lugar a muestras compuestas (268 en total), hasta 40 cm de profundidad. La densidad aparente se estimó con muestras inalteradas de 100 cm^3 y mediante el uso de ecuaciones de pedotransferencia.

Los análisis del suelo se realizaron en los laboratorios del Instituto Pirenaico de Ecología (IPE-CSIC). La densidad aparente (DA) se estimó mediante el secado en estufa de las muestras inalteradas a 105°C durante 24 horas. La materia orgánica (MO) del suelo se midió mediante el método de pérdida por ignición (a 375°C); el carbono total (C) se determinó mediante combustión en seco en el analizador elemental Vario Max; el carbono orgánico del suelo (Corg) se calculó a partir de la extracción sobre el carbono total del carbono inorgánico, estimado a partir de la obtención del contenido de carbonatos en los suelos calcáreos; los stocks de carbono orgánico del suelo (SOC) se calcularon ponderando cada valor de Corg con su respectiva profundidad (10 cm) y DA, y se expresaron en Mg ha^{-1}.

4. Resultados

4.1. Desbroce de matorrales para reducir el combustible y crear un paisaje en mosaico

Entre 1986 y 2022 se desbrozaron 39.680,3 ha (Fig. 5), lo que representa el 30,2% de la superficie de matorrales que había a finales del siglo XX (Lasanta Martínez y Errea, 2001), o el 15,8% de la superficie total del área de estudio. Con seguridad la proporción calculada es algo menor porque algunas actuaciones tienen lugar en áreas ya desbrozadas, pero que se han vuelto a cubrir de matorrales porque el pastoreo no es capaz de detener su avance. En cualquier caso, se trata de una actuación paisajística muy importante que se realiza cada año (en toda la serie solo tres años no han tenido desbroces: 1992, 2007 y 2015, por falta de financiación), con una superficie variable (valores extremos de 387,8 ha en 1994 y 2.386,3 ha en 2002; ver Fig. 5) en función de las solicitudes recibidas por parte de los ayuntamientos y del dinero disponible.

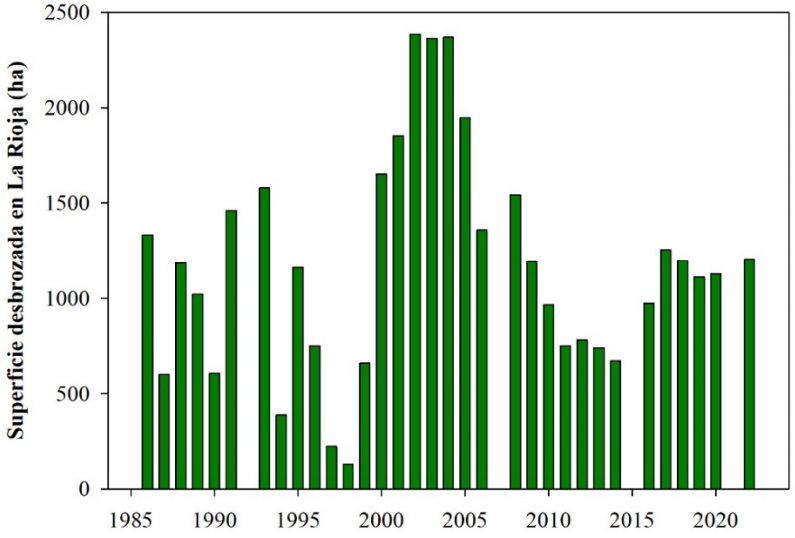

Figura 5. Evolución de la superficie desbrozada en La Rioja (1986-2022).

Los desbroces se realizan en áreas seleccionadas. El PSC establece que como máximo en cada municipio se pueden desbrozar 2 hectáreas por cada Unidad Ganadera Mayor (UGM) en cinco años, para garantizar que el ganado acude a pastar a las áreas desbrozadas y asegurar el retraso de la matorralización. Se realizan en laderas de menos del 30% de pendiente, distribuidas por varios lugares del término municipal a distintas altitudes para dilatar el periodo de pastoreo, y en zonas accesibles con tractor para evitar la apertura de nuevas pistas. La mayor parte de los desbroces se realizan en antiguos campos de cultivo, que se abandonaron desde los años sesenta del pasado siglo, cubiertos de matorrales

de *G. scorpius*, *S. rosmarinus, B. sempervirens, Crataegus monogyna, Prunus spinosa*… en suelos alcalinos, y *C. laurifolius* en suelos silíceos.

El PSC persigue eliminar combustible y transformar zonas de matorral en pastos atractivos para el ganado. Combina el desbroce mecánico (Fig. 6a) con el pastoreo posterior del ganado (Fig. 6b) para ralentizar el rebrote de matorrales. Los efectos más importantes son los siguientes:

(i) La eliminación de combustible, ya que la parte aérea de los matorrales es eliminada y triturada (Fig. 7), mientras que se dejan las raíces en el suelo.

(ii) La creación de un paisaje en mosaico, donde alternan pastos, pequeños bosquetes, matorrales y bosques (Fig. 8). Por otro lado, como máximo se pueden desbrozar 10 ha en la misma unidad de tratamiento, dejando al menos 2 ha sin desbrozar entre las unidades.

(iii) El incremento de la superficie pastoral, creando áreas atractivas para diferentes especies ganaderas (Fig. 9). Así el ovino y el vacuno prefieren pastos herbáceos, mientras que el caprino y el equino incluyen en su dieta brotes tiernos de matorrales y arbustos. En este sentido, el PSC establece que se deben dejar sin desbrozar los antiguos márgenes de los campos para favorecer el pastoreo de yeguas y cabras, y se mantengan como corredores ecológicos. También estipula que entre las áreas desbrozadas y los bosques debe quedar una franja de matorrales creando diferentes ecotonos, que contribuyen a mejorar la biodiversidad.

Figura 6. A) Se utilizan tractores con aperos de cuchillas o cadenas para cortar los matorrales. Las raíces se quedan en el suelo. B) Pastoreo de cerdos en Jalón de Cameros. El vacuno y ovino son las especies más abundantes, con presencia frecuente de equinos y menos de caprinos. No obstante, en ocasiones se pueden ver también cerdos.

Figura 7. A) Al fondo desbroces en la antigua aldea de Dehesillas (valle del Jubera). Parte de los matorrales se han cortado para eliminar combustible. Dentro de los nuevos pastos permanecen arbustos aislados que dan sombra al ganado y sirven de posaderos para la avifauna. B) Manchas de pastos tras el desbroce de matorrales desde la pista de Torremuña (Camero Viejo). Estas manchas actúan como cortafuegos en el caso de producirse un incendio. C) Eliminación de matorrales en antiguos campos abandonados en Santa Marina (valle del Jubera). Se observan restos de los matorrales sobre el suelo. En la actualidad los tallos se trituran para favorecer la incorporación de materia orgánica al suelo.

Figura 8. Paisaje en mosaico en el sector alto de una ladera de Jalón de Cameros. Los pastos se han regenerado a partir del desbroce de matorrales. Se ve la alternancia entre pequeños bosques y áreas de matorral, formando un paisaje fragmentado con manchas de escasa extensión. Los antiguos límites de los campos permanecen cubiertos con matorrales para el pastoreo del caprino y equino, así como para favorecer los desplazamientos y alimentación de la fauna.

Figura 9. A) Caprino y ovino pastando en el valle del Leza. El caprino prefiere matorrales y arbustos, mientras el ovino aprovecha herbáceas. B) Equino en San Vicente de Robres (valle del Jubera). El equino no se estabula nunca, pastando en libertad incluso con el suelo cubierto de nieve. En su dieta incluye ramas de matorral.

4.2. Disminución de la superficie quemada

Entre 1968 y 2023 se registraron 4.002 siniestros y se quemaron 28.377,13 ha, de las que 20.139,1 ha (un promedio de 1060 ha/año) se quemaron entre 1968 y 1986, y 8.238,05 ha (un promedio de 222,65 ha/año) entre 1987 y 2023 (Tabla 1). Si el periodo de estudio lo partimos por décadas (Fig. 10) se observa el fuerte incremento registrado de la superficie quemada entre 1978 y 1986, respecto a la década precedente. De hecho, entre 1968 y 1977 ardieron 208 ha/año y entre 1978 y 1986 1.806 ha/año. A partir de 1987 se reduce considerablemente la superficie quemada; durante la primera década (1987-1996) se quemaron 421,5 ha/año, disminuyendo posteriormente, de manera que a partir de 1997 el promedio anual fluctúa entre 144 y 155 ha/año. Un hecho a destacar es que las líneas de evolución del número de incendios y de superficie quemada son parecidas, al igual que lo son entre sí las del número de conatos y de siniestros (Fig. 10). Ello incide en algo muy lógico: son los incendios los principales causantes de la superficie quemada. Por otro lado, la disminución de los incendios tiene lugar antes que la de los conatos. Los primeros disminuyen a partir de 1987, coincidiendo con la puesta en marcha del PSC, mientras que los segundos hay que esperar a 2016 para ver una tendencia clara. De hecho, antes del PSC los conatos suponían el 20,8% de los siniestros y después el 60,8%.

La Figura 11 muestra la superficie quemada y desbrozada. En el primer año de la serie se quemaron 708,4 ha, reduciéndose en los años posteriores. A partir de 1978 se produce un incremento espectacular, pasando de 40,9 ha en 1977 a 1.765,4 ha en 1978. Durante 9 años aumenta el número de incendios y siniestros, respecto a los años precedentes (ver también la Tabla 1), alcanzando un punto álgido en 1981 con 111 siniestros (14 conatos y 97 incendios), que quemaron 3.233,9 ha. 1985 fue el peor año, ya que se registraron 94 siniestros (10 conatos y 84 incendios) con 3.836,2 ha quemadas.

Tabla 1. Evolución de los siniestros y superficie quemada en La Rioja (1968-2023).

Año	Nº de conatos	Nº de incendios	Nº de siniestros	Sup. quemada (ha)
1968	3	16	19	708,4
1969	7	7	14	41,8
1970	7	13	20	76,7
1971	6	19	25	222,6
1972	3	4	7	81,2
1973	1	16	17	279,1
1974	5	8	13	27,2
1975	2	15	17	480,2
1976	5	20	25	121,4
1977	5	6	11	40,9
1978	4	39	43	1765,4
1979	5	33	38	1644,5
1980	10	65	75	1237,5
1981	14	97	111	3233,9
1982	9	55	64	1704,7
1983	10	35	45	765,3
1984	10	49	59	1062,7
1985	10	84	94	3836,2
1986	19	42	61	2809,4
1987	12	15	27	159,5
1988	10	42	52	477,2
1989	24	118	142	1531,9
1990	32	35	67	289,8
1991	27	33	60	355,8
1992	48	44	92	109,3
1993	36	27	63	224,7

1994	46	62	108	497,4
1995	86	91	177	468,1
1996	45	33	78	103,6
1997	73	20	93	60,38
1998	79	47	126	181,42
1999	66	36	102	172,28
2000	137	60	197	225,32
2001	75	48	123	318,98
2002	83	41	124	165,02
2003	44	20	64	110,01
2004	40	7	47	35,69
2005	72	33	105	174,14
2006	61	12	73	49,9
2007	73	20	93	69,3
2008	95	15	110	71,53
2009	89	29	118	336,68
2010	89	25	114	281,84
2011	58	24	82	62,63
2012	77	28	105	108,95
2013	25	6	31	27,65
2014	74	21	95	111,94
2015	38	20	58	281,74
2016	35	12	47	92,28
2017	64	17	81	249,09
2018	27	8	35	55,17
2019	75	13	88	55,09
2020	6	40	46	23,91
2021	53	24	77	454,11
2022	68	21	89	195,46
2023			55	53,22

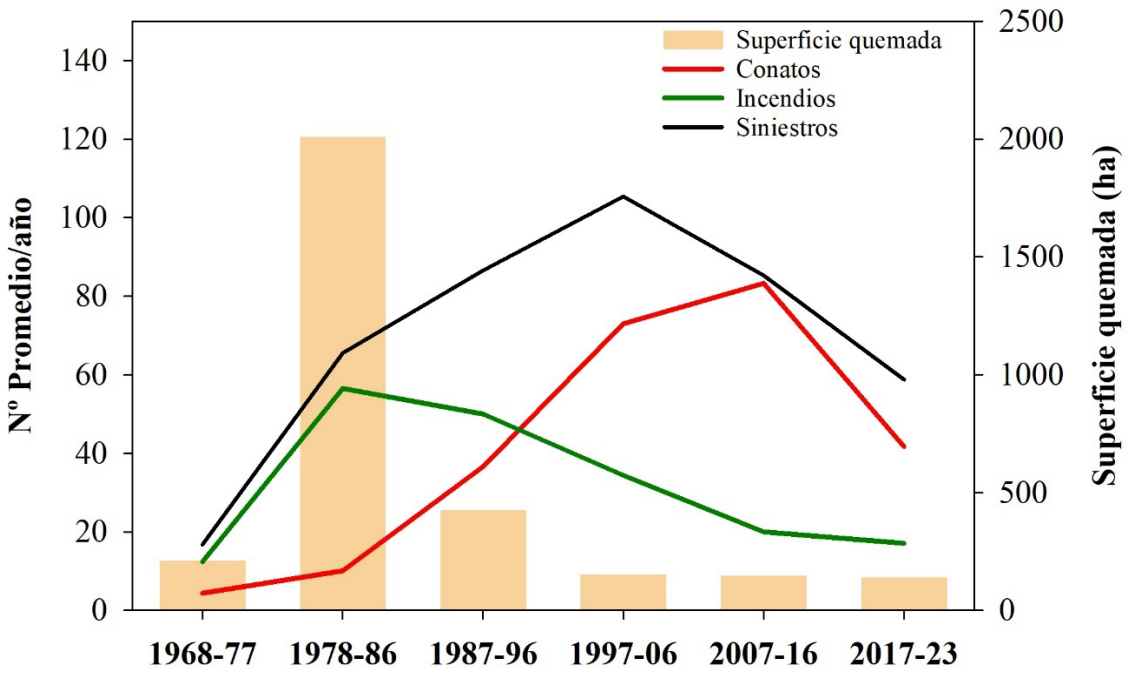

Figura 10. Evolución de número de conatos, incendios, siniestros y superficie quemada (1968-2013).

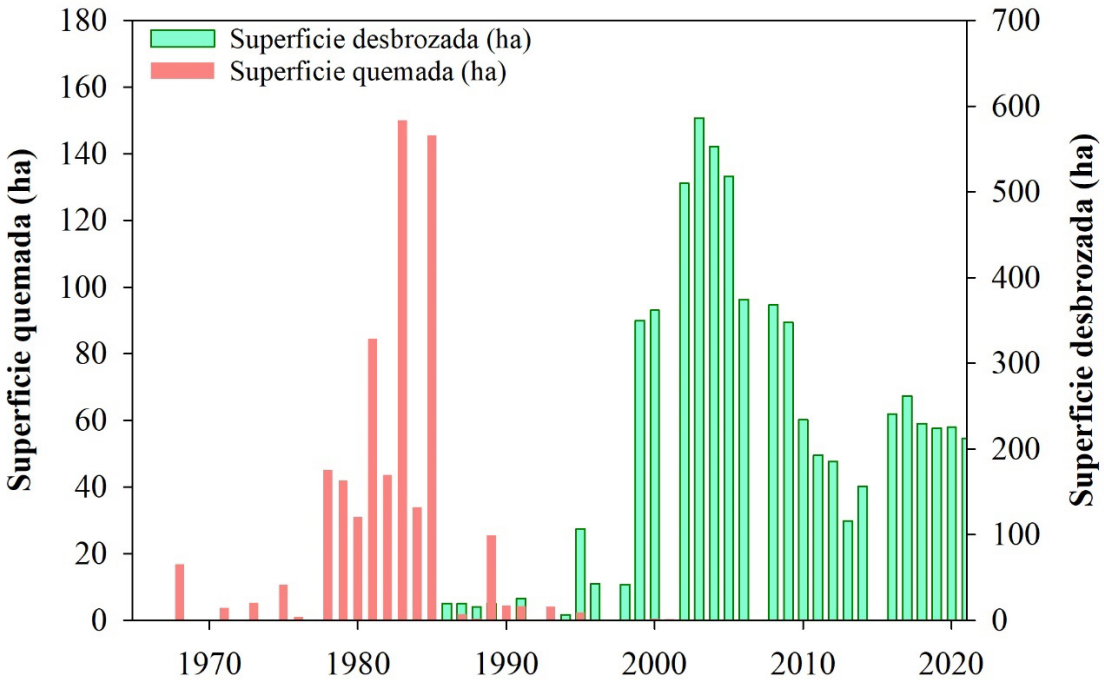

Figure 11. Desbroce de matorrales e incendios forestales en La Rioja.

En la misma figura se puede observar también que la puesta en marcha del PSC coincide con la reducción de la superficie quemada. Desde 1987 disminuye la superficie quemada, si bien hay años que rompen la tendencia, como 1989 (1.531,9 ha). Es significativo que en una docena de años no se quemaron ni 100 ha/año (1997, 2004, 2006, 2007, 2008, 2011, 2013, 2016, 2018, 2019, 2020 y 2023). En la gráfica se observa también un repunte en los años 2021 (454 ha) y 2022 (195,4 ha). En ambos años, la mayor superficie quemada tuvo lugar en Yerga (más de 400 ha en 2021 y 104 ha en 2022), fuera del área de estudio y de los municipios donde se realizan desbroces.

4.3. Almacenamiento de carbono orgánico en el suelo en diferentes LULC

La Fig. 12 muestra el SOC en diferentes pastos y en matorral. El pasto natural (115,7 Mg/ha) y el matorral (116,1 Mg/ha) presentan valores similares, inferiores en ambos casos a los pastos regenerados tras el desbroce, alcanzando el valor más alto en desbroces antiguos (142,9 Mg/ha). Una diferencia importante es que en los primeros 10 cm el valor se incrementa M<PMD<PAD<CP, mientras que en los dos estratos inferiores (entre 20 y 40 cm) se produce una brusca caída en CP respecto al resto de LULC.

En la misma figura se aprecia que los bosques presentan valores más altos de SOC que el matorral y los pastos, con la excepción de PAD (142,9 Mg/ha) cuyos valores son superiores a D (137,8 Mg/ha). Las repoblaciones aportan valores superiores a los bosques naturales, alcanzando RPG el valor más alto (213,3 Mg/ha), seguido por RPN (187,6 Mg/ha), BN (162,4 Mg/ha), y el más bajo D (137,8 Mg/ha). Otro hecho a destacar es que las repoblaciones presentan valores más elevados que los bosques naturales en todo el perfil del suelo.

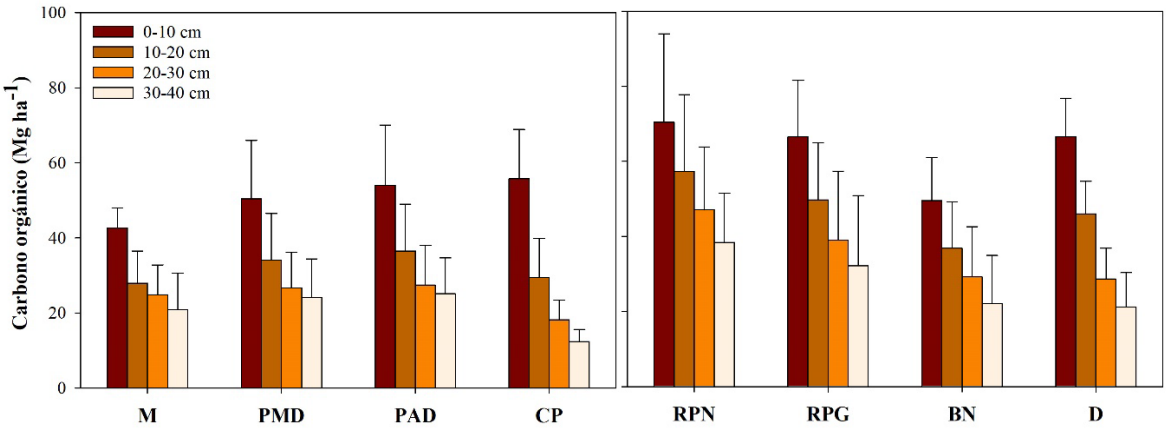

Figura 12. Acumulación de carbono orgánico en las diferentes profundidades del suelo. Nótese: M: matorrales; PMD: pastos de mediana edad; PAD: pastos de desbroce antiguo; CP: Pastos control; RPN: Repoblaciones forestales sin gestionar; RPG: Repoblaciones forestales gestionadas; BN: Bosques de rebollos sin gestionar; D: Dehesa de rebollos.

5. Discusión

En la media montaña mediterránea se mantienen sistemas ganaderos extensivos que cumplen un papel importante en la economía agraria y en la sostenibilidad del medio rural (Bernués Jal, 2007; Lasanta *et al.,* 2019). De manera simultánea aportan servicios ecosistémicos a las áreas adyacentes, como mayores volúmenes de escorrentía, sin incrementar significativamente las tasas de erosión, conservación de la biodiversidad o el mantenimiento de paisajes culturales muy atractivos para el turismo (Rodríguez Ortega *et al.,* 2014; Keesstra *et al.,* 2028; Nadal-Romero *et al.,* 2018, Lasanta *et al.,* 2024), lo que puede constituir una fuente complementaria de ingresos y la fijación de población en áreas muy despobladas como la media montaña mediterránea (Sluiter, 2005; Benjamin *et al.,* 2007; Sayadi *et al.,* 2007). Por otro lado, a escala global, el pastoreo es considerado como una actividad clave para la economía verde, la vida y el bienestar de millones de personas. Los beneficios del pastoreo son reconocidos por organismos internacionales como la Organización de las Naciones Unidas para la Alimentación, ONUAA, más conocida como FAO, y el Programa de las Naciones Unidas para el Medio Ambiente (PNUMA) (Herrera, 2020).

En los resultados de este trabajo se ha comprobado que el binomio desbroce de matorrales – pastoreo del ganado implica la creación de un paisaje en mosaico con mayor fragmentación de las unidades paisajísticas. En un estudio realizado en la montaña riojana (Lasanta *et al.,* 2016) se comprobó que la regeneración de pastizales tras el desbroce de matorrales duplicaba el número de manchas y reducía su tamaño a la mitad, además de incrementar el índice de diversidad y disminuir el de dominancia. La regeneración de pastizales entre matorrales y bosques reduce la homogeneización del paisaje (grandes manchas con escasa diversidad de usos y cubiertas del suelo), que es el resultado habitual del abandono de tierras en las montañas europeas durante su historia reciente (MacDonald *et al.,* 2000; Mottet *et al.,* 2006; Bracchetti *et al.,* 2012, García-Ruiz y Lana-Renault, 2011). Por el contrario, el desbroce de matorrales origina un paisaje en mosaico con formaciones arbóreas, matorrales y pastos que se combinan en el territorio. Se crean contactos frecuentes entre distintos ecotonos, que contribuyen a incrementar la presencia de insectos, aves, reptiles y pequeños mamíferos que buscan alimentación y refugio. Lo mismo ocurre con los árboles aislados y pequeñas manchas de bosque, que son considerados como "estructuras clave" para alcanzar altos valores de biodiversidad (Fischer *et al.,* 2010; Lindenmayer, 2017).

El pastoreo del ganado es esencial para mantener el paisaje en mosaico. Sin el pastoreo el PSC sería muy poco eficaz, ya que en pocos años las áreas desbrozadas se cubrirían nuevamente de

matorrales (Lasanta-Martínez, 2005). El pastoreo reduce la biomasa vegetal y ralentiza el proceso de sucesión vegetal que llevaría nuevamente a la matorralización (Casasús *et al.,* 2007; Ruiz-Mirazo *et al.,* 2009; Álvarez-Martínez *et al.,* 2016).

El número de incendios y la superficie quemada han disminuido en las últimas décadas en La Rioja al igual que ha ocurrido en otras áreas mediterráneas, como consecuencia de la mejora de los sistemas de detección y de los medios técnicos utilizados en la extinción (Rodrigues *et al.,* 2016; Turco *et al.,* 2016; Urbieta *et al.,* 2019). Sin embargo, la disminución de la superficie quemada es mucho mayor en La Rioja que en el conjunto de España y en otras zonas mediterráneas, porque a las causas señaladas se suma el efecto de las tareas de prevención realizadas en La Rioja que incluyen la eliminación de biomasa vegetal, la fragmentación del paisaje y el pastoreo (Lasanta *et al.,* 2018, 2022).

La fragmentación del paisaje y el pastoreo del ganado influyen de dos maneras en la disminución del número de incendios y de la superficie quemada: (i) reduce la biomasa vegetal y el material combustible. Lasanta *et al.* (2024) señalan que las áreas en las que se sustituye el matorral por pastos pasan del modelo 6 de Rothermel (1983), con una carga de combustible muy inflamable de 10-15 Mg/ha, al modelo 1 (carga de 1 Mg/ha). Eliminar combustible en zonas de monte mediterráneo es una buena estrategia para disminuir incendios, porque el clima durante los meses secos genera alto potencial de ignición, por lo que es muy fácil que se generen fuegos si hay abundante biomasa vegetal (Fonseca *et al.,* 2017). (ii) En el caso de producirse un fuego es más fácil extinguirlo en un paisaje en mosaico que en un paisaje homogéneo. Es muy conocido que la continuidad espacial de la vegetación inflamable aumenta considerablemente el riesgo de incendio y dificulta su extinción, mientras que la diversidad de materiales combustibles dificulta la propagación y continuidad del incendio facilitando su intervención (Vega-García y Chuvieco, 2006; Viedma *et al.,* 2009; Moreira *et al.,* 2011). Por otro lado, las áreas de pasto, intercaladas entre matorrales y bosques, actúan como cortafuegos muy eficaces para controlar el avance de los fuegos (Lasanta *et al.,* 2022). En este trabajo se ha señalado que el número de incendios ha disminuido antes y en mayor proporción que el número de conatos, lo que se debe a la mejora de los medios de detección y extinción, a lo que contribuye –sin duda- el paisaje en mosaico.

Junto a las dos razones señaladas hay una tercera muy importante para justificar la disminución de la superficie quemada: la erradicación de los fuegos pastorales en la Sierra riojana. La quema de matorrales para regenerar pastos forma parte de la cultura mediterránea (García-Ruiz *et al.,* 2020a), realizándose todavía en algunas montañas (Ruiz-Mirazo *et al.,* 2011; San-Miguel-Ayanz *et al.,* 2013). En el área de estudio, la mayor parte de los incendios previos al PSC eran ocasionados por fuegos pastorales (Gaviria y Baigorri,1982). Con la aplicación del PSC ya no tiene sentido para los ganaderos regenerar pastos a partir de la quema de matorrales porque la Administración se los proporciona de manera gratuita. Además, se arriesgarían a un grave delito medioambiental (Lasanta *et al.,* 2022). Por otro lado, hay que tener en cuenta que la mayoría de los incendios que se registran en la actualidad tienen lugar lejos de la Sierra, estando muy ligados a tareas agrícolas. En este sentido, Lasanta *et al.* (2024) señalan que en uno de los siete valles de la sierra riojana (el del Leza) se quemaron un promedio de 34,1 ha/año en el periodo 1968-1985, y tan sólo 1,2 ha/año entre 1986 y 2022. En este segundo periodo en 31 de los 37 años no hubo ni un solo incendio.

La combinación de eliminación de matorrales y pastoreo aporta resultados muy positivos para controlar los fuegos forestales como se ha analizado en este trabajo. No obstante, hay que ser conscientes de que el fuego es una amenaza constante, que puede ocurrir en cualquier momento y en cualquier lugar, por lo que hay que seguir invirtiendo en políticas de prevención y extinción.

En el presente estudio se ha comprobado también que la regeneración de pastos tras el desbroce de matorrales y el pastoreo posterior son medidas positivas para la calidad del suelo y el almacenamiento de carbono orgánico: PMD y PAD incrementan un 16% y un 23% el SOC, respecto a M. Sin embargo, CP presenta valores similares a M. Estos resultados sugieren que el desbroce de matorrales es positivo para el SOC, posiblemente por dos razones: (i) la incorporación de materia orgánica al suelo por la trituración de los matorrales y (ii) por la convivencia de herbáceas (gramíneas y leguminosas,

fundamentalmente) y raíces de matorral. Las primeras parecen acumular carbono en los primeros centímetros del suelo, mientras que las raíces parecen favorecer la descomposición de materia orgánica y la acumulación del carbono a capas más profundas. El hecho de que CP no posea raíces de matorrales podría explicar que los valores de SOC no se incrementen respecto a M. No obstante, algunos estudios realizados en la misma área de estudio ponen de relieve que CP tiene SOC más altos que M, especialmente en suelos alcalinos (Lasanta *et al.,* 2024), lo que exige profundizar más en esta cuestión.

También se ha constatado la importancia de los bosques en relación con el almacenamiento de SOC, y la consecuente mejora de la calidad de los suelos (Chiti *et al*., 2012). En general, las repoblaciones forestales, han sido la práctica de gestión más utilizada tras el abandono de campos de cultivo en la montaña mediterránea. La mayoría de la literatura científica concluye que las repoblaciones forestales pueden acumular un valor significativamente más alto de carbono orgánico en el suelo en comparación con otros usos; sin embargo, todavía existe una alta variabilidad de resultados, dependiendo de los usos de suelo anteriores, la topografía y climatología, así como las diferentes especies utilizadas en estas prácticas. En general los valores son muy elevados en las capas superficiales debido al gran aporte de materia orgánica. Sin embargo, la alta acumulación de materia orgánica no tiene tanta relevancia como lo es el tipo de materia orgánica de difícil digestión y descomposición para los organismos del suelo, pudiendo permanecer en estado inestable y no avanzar en su evolución hasta convertirse en carbono recalcitrante o mineralizado. Trabajos previos en la zona de estudio confirman estos resultados, con porcentajes de material lábil superiores al 30% (Cortijos-López *et al.,* 2024). También hay que destacar la importancia de la gestión forestal, cuyas cortas y talas dan lugar a subproductos (ramas y raíces) que se dejan en el lugar, incorporando en su descomposición materia orgánica al suelo, y la ganadería que favorece el crecimiento de especies adaptadas al pastoreo con abundantes raíces finas, además de aportar excrementos.

5.1. Paisajes ganaderos como estrategia para mitigar el cambio climático

Los paisajes culturales de la montaña mediterránea, muy vinculados al aprovechamiento ganadero y agrícola durante siglos (a veces milenios) (Alcolea *et al.,* 2017; García-Ruiz *et al.*, 2015, 2020a) se han visto afectados profundamente por el abandono de tierras a lo largo del siglo XX (MacDonald *et al.,* 2000; Lasanta *et al.,* 2021). La principal consecuencia visible es que los antiguos campos de cultivo y muchas laderas de pastos se han transformado en cubiertas de matorrales y bosques (García-Ruiz y Lana-Renault, 2011; Gartzia *et al.,* 2014; Sanjuán *et al.,* 2018), que han provocado una homogeneización del paisaje con la pérdida de muchos rasgos culturales (Peña-Angulo *et al.,* 2019; Errea *et al.,* 2023).

En este contexto de abandono de tierras, algunos autores opinan que el resilvestramiento o renaturalización (*rewilding*) de áreas marginales tiene algunos beneficios ambientales y socioeconómicos (Pereira y Navarro, 2015; Tree, 2018; Palau, 2020). El *rewilding* podría definirse como la recuperación natural de espacios forestales tras el abandono de tierras sin intervención humana, es decir disminuyendo el control humano sobre los paisajes, lo que eliminaría a largo plazo los rasgos de los paisajes culturales (García-Ruiz *et al.,* 2020 b). Implicaría la disminución a corto plazo y desaparición a medio-largo plazo de la ganadería extensiva. Ello implicaría la matorralización de los pastos y la acumulación de biomasa forestal, lo que incrementaría el riesgo de incendios forestales. Estos últimos emiten a la atmósfera, de forma repentina, el carbono almacenado durante mucho tiempo en suelos y árboles, además de otros GEIs como el metano, contribuyendo al calentamiento global (Herrera, 2020). En España, por ejemplo, los incendios forestales emiten una media anual de 1,5 millones de toneladas de CO_2, habiendo años en que se duplica dicha cantidad (ZEO, 2016).

Los partidarios del *rewilding* argumentan que la desaparición de la ganadería extensiva favorecería la expansión de ungulados silvestres y otro tipo de fauna que cumplirían la misma función que la ganadería extensiva. Para ellos lo importante es que haya herbivoría, lo que se puede conseguir con

animales salvajes o domésticos, ya que ambos mantienen paisajes en mosaico con pastos intercalados entre otras cubiertas, que aportan alto valor y diversidad (Palau, 2020). Sin embargo, es dudoso que el resultado sea similar, ya que en la actualidad los herbívoros salvajes conviven con el ganado doméstico, ejerciendo labores complementarias (García-González *et al.,* 1990). Por otro lado, los pastores dirigen, al menos en parte, los patrones del pastoreo, planificando el consumo del pasto e indirectamente el paisaje resultante. Hay que tener en cuenta, además, que los rumiantes salvajes aprovechan de forma más irregular el pasto que la ganadería extensiva (Herrera, 2010). En este sentido, Aldezábal *et al.* (2002) insisten en que los herbívoros salvajes ejercen una labor interesante, pero que la conservación de los pastos está vinculada al mantenimiento del pastoreo, es decir a la herbivoría ejercida por los animales domésticos. Un resultado de este trabajo es que se registran altos valores de SOC en pastos mejorados a partir del desbroce de matorrales y pastoreados a continuación, en comparación con las primeras fases de revegetación. Un efecto adicional del pastoreo es que contribuyen a la fertilización del suelo y potencian la vida microbiana, lo que favorece un buen crecimiento de las plantas y la acumulación de carbono en el ecosistema (Herrera, 2020). Algunos estudios demuestran que el suelo acumula más carbono con pastoreo equilibrado que en ausencia de pastoreo o cuando se produce sobrepastoreo, ya que conlleva la degradación del suelo (Chen *et al.,* 2015). En este sentido, Manzano y White (2019) señalan que los suelos de los pastizales de California serían capaces de secuestrar más carbono a lo largo del siglo XXI que los bosques que los sustituirían en el caso de que el pastoreo cesara. Este resultado lo justifican, en gran parte, por la reducción de las emisiones ligada a la disminución de incendios.

Los sistemas pastorales tienen gran capacidad para mitigar el CC porque los pastos almacenan grandes cantidades de carbono en el suelo, constituyendo uno de sus mayores sumideros a largo plazo (Puche *et al.,* 2019), similar a los suelos de los bosques según algunos autores (Berninger *et al.,* 2015; Nadal-Romero *et al.,* 2021) o sólo ligeramente inferior según Guo y Gifford (2002). Los pastos constituyen un excelente almacén de carbono orgánico por varias razones: (i) por contener muchas raíces finas, con abundante materia orgánica de fácil y constante descomposición, mientras que los matorrales tienen raíces más gruesas de descomposición más lenta y difícil (García-Pausas *et al.,* 2017); (ii) por los excrementos que aporta el ganado, siempre en cantidades mayores que en áreas de matorral que suelen pastarse poco o nada. Además, las áreas cubiertas por matorrales tienen menos biomasa subterránea al faltar algunas herbáceas que necesitan ser pastadas para sobrevivir, por lo que incluyen entre sus estrategias de supervivencia la producción de un sistema radicular muy denso de raíces (García-Pausas *et al.,* 2011); y (iii) por la abundancia de gramíneas con alta densidad de pequeñas raíces en la biomasa subterránea, lo que mejora la estabilidad de los agregados y contribuye a estabilizar el SOC en el suelo (Guidi *et al.,* 2014). Además, hay que tener en cuenta que los pastos tienen mayor proporción de carbono orgánico recalcitrante que matorrales y bosques de coníferas, lo que sugiere que los pastos estabilizan el SOC mejor que las otras dos cubiertas (Nadal-Romero *et al.,* en revisión).

Este estudio enfatiza la relevancia de los pastos, pero también pone de manifiesto la necesidad de paisajes en mosaico donde las áreas renaturalizadas se alternen con otras de aprovechamiento agrícola y ganadero, siempre con la correcta gestión del territorio.

Conclusiones

En la media montaña mediterránea se mantienen sistemas ganaderos extensivos que juegan un papel importante en la sostenibilidad del medio rural y en la gestión y conservación del paisaje. El abandono de tierras a lo largo del siglo XX ha impulsado la expansión generalizada de matorrales y bosques. Con ello se han modificado los rasgos y funciones ecosistémicas de los paisajes tradicionales. Ello tiene implicaciones negativas como la homogeneización y banalización del paisaje y el incremento de los fuegos forestales.

Se confirma nuestra hipótesis de que una intervención moderada en áreas selectivas, mediante desbroce de matorrales y pastoreo del ganado, resulta positiva para (i) la reducción del material

combustible, (ii) la formación de un paisaje en mosaico, (iii) la disminución de los incendios forestales y la superficie quemada, y (iv) la mejora del SOC en áreas desbrozadas y pastoreadas respecto a los matorrales. Sin embargo, no se llega a conclusiones claras respecto al SOC en bosques y pastos naturales.

Los resultados de este trabajo ponen de relieve que el desbroce de matorrales y el pastoreo son buenas estrategias para reducir la superficie quemada e incrementar el SOC en la media montaña mediterránea, contribuyendo a mitigar el cambio climático. La media montaña mediterránea está poco poblada, pero todavía permanece una población que quiere seguir viviendo de los recursos locales, teniendo los pastos un potencial importante para el desarrollo de la ganadería extensiva. Las políticas públicas deben apoyar de manera decidida a la ganadería extensiva y el pastoreo del ganado, para mitigar el cambio climático, la conservación de paisajes culturales de gran valor en la montaña mediterránea, el suministro de servicios ecosistémicos a la sociedad y la fijación de población.

Agradecimientos

Proyecto MOUNTWATER (TED2021-131982B-I00 MCIN/AEI/10.13039/ 501100011033) financiado por el MICCN y NextGeneration EU/PRTR. El grupo de investigación "Procesos Geoambientales y Cambio Global" está financiado por el Gobierno de Aragón y el Fondo Social Europeo (E02_23R). Los evaluadores anónimos, con sus sugerencias y comentarios, han mejorado el trabajo.

Referencias

Aboagye, I.A., Beauchemin, K.A., 2019. Potential of Molecular weight and structure of Tannins to reduce methane emissions from rumiants: A Review. *Animals* 9 (11), 865. https://doi.org/10.3390/ani9110856

Aguilera, E., Díaz-Gaona, C., Reyes-Palomo, C., García-Laureano, R., Sánchez-Rodríguez, M., Rodríguez-Esteve, V., 2018. *Producción ecológica mediterránea y cambio climático: Estado del conocimiento.* Cátedra de Ganadería Ecológica Ecovalia-Clemente Mata. Universidad de Córdoba.

Alcolea, M., Domingo, R., Piqué, R., Montes, L., 2017. Landscape and firewood at Espantalobos Mesolithic site (Huesca, Spain). First results. *Quaternary International* 457, 198-210. https://doi.org/10.1016/j.quaint.2016.10.007

Aldezábal, A., García-González, R., Gómez, D., Fillat, F., 2002. El papel de los herbívoros en los ecosistemas de pastos. *Ecosistemas* 11(3), www.aeet.org/ecosistemas/investigacion6.htm

Álvarez-Martínez, J., Gómez-Villar, A., Lasanta, T., 2016. The use of goats grazing to restore pastures invaded by shrubs and avoid desertification: a preliminary case study in the Spanish Cantabrian mountains. *Land Degradation & Development* 27, 3-13. https://doi.org/10.1002/ldr.2230

Arizaleta, J.A., Fernández Aldana, R., Lopo, L., 1990. Los matorrales de La Rioja. *Zubía* 8, 83-127.

Arnáez, J., Lana-Renault, N., Lasanta, T., Ruiz-Flaño, P., Castroviejo, J., 2015. Effects of farming terraces on hydrological and geomorphological processes. A review. *Catena* 128, 122-134. https://doi.org/10.1016/j.catena.2015.01.021

Benjamin, K., Bouchard, A., Domon, G., 2007. Abandoned farmlands as components of rural landscapes: an analysis of perceptions and representations. *Landscape and Urban Planning* 83, 228-244. https://doi.org/10.1016/j.landurbplan.2007.04.009

Berninger, F., Susiluoto, S., Gianelle, D., Balzarolo, M., 2015. Management and site effects on carbon balances of European mountain meadows and rangelands. *Boreal Environment Research* 20(6), 748-760.

Bernués Jal, A., 2007. Ganadería de montaña en un contexto global: evolución, condicionantes y oportunidades. *Pastos* 37(2), 133-175.

Bernués, A., Rodríguez-Ortega, T., Ripoll-Bosch, R., Alfnes, F., 2014. Socio-cultural and economic valuation of ecosystem services provided by Mediterranean mountain agroecosystems. *PloS One* 9(7), e102479. https://doi.org/10.1371/journal.pone.0102479

Bracchetti, L., Carotenuto, L., Catorci, A. 2012. Land cover changes in a remote area of central Apennines (Italy) and management directions. *Landscape and Urban Planning* 104, 157-170. https://doi.org/10.1016/j.landurbplan.2011.09.005

Calvo Palacios, J.L., 1977. *Los Cameros. De región homogénea a espacio-plan*. Instituto de Estudios Riojanos, Logroño, 2 vols.

Casasús, I., Bernués, A., Sanz, A., Villalba, D., Riedel, J.L., Revilla, R., 2007. Vegetation dynamics in Mediterranean forest pastures as affected by beef cattle grazing. *Agriculture, Ecosystems & Environment* 121(4), 365-370. https://doi.org/10.1016/j.agee.2006.11.012

Chen, W., Huang, D., Liu, N., Zhang, Y., Badgery, W.B., Wang, X., Shen, Y., 2015. Improved grazing management may increase soil carbon sequestration in temperate steppe. *Scientific Reports* 5, 10892. https://doi.org/10.1038/srep10892

Chiti, T., Díaz-Pinés, E., Rubio, A., 2012. A soil organic carbon stocks of conifers, broadleaf and evergreen broadleaf forest of Spain. *Biology and Fertility Soils* 48, 817-826. https://doi.org/10.1007/s00374-012-0676-3

Cuadrat, J.M., Vicente-Serrano, S.M., 2008. Características espaciales del clima en La Rioja modelizadas a partir de Sistemas de Información Geográfica y técnicas de regresión espacial. *Zubía. Monográfico* 20, 119-142.

Errea, M.P., Cortijos-López, M., Llena, M., Nadal-Romero, E., Zabalza-Martínez, J., Lasanta, T., 2023. From the local landscape organization to land abandonment: an analysis of landscape changes (1956-2017) in the Aísa Valley (Spanish Pyrenees). *Landscape Ecology* 38, 3443-3462. https://doi.org/10.1007/s10980-023-01675-1

Food and Agriculture Organization, FAO, 2017. *The estate of Food and Agriculture 2017: Leveranging Food Systems for inclusive Rural Transformation.* FAO, Rome, 28 pp. Disponible en: http://www.fao,org/3/a-i7658e.pdf

Fernández Aldana, R., 2015. *Mapa de los bosques de La Rioja*. Gobierno de La Rioja: 207 pp. + mapa 1: 150.000

Fernández Rebollo, P., Carbonero Muñoz, M.D., García Moreno, A., 2015. Contribución de la ganadería extensiva al mantenimiento de las funciones de los ecosistemas forestales. *Cuadernos de la Sociedad Española de Ciencia Forestal* 39, 147-162.

Fischer, J., Stott, J., Law, B.S., 2010. The disproportionate value of scattered trees. *Biological Conservation* 143, 1564-1567. https://doi.0rg/10.1016/j.biocon.2010.03.030

Fonseca, F., de Figuereido, T., Nogueira, C., Queirós, A., 2017. Effect of prescribed fire on soil properties and soil erosion in a Mediterranean mountain area. *Geoderma* 307, 172-180. https://doi.org/10.1016/j.geoderma.2017.06.018

García-González, R., Hidalgo, R., Montserrat, C., 1990. Patterns of livestock use in time and space use by livestock in a summer range of Western Pyrenees. *Mountain Research and Development* 10(3), 241-255. https://doi.org/10.2307/3673604

García-Pausas, J., Casals, P., Romanyà, J., Vallecillo, S., Sebastià, M.T., 2011. Seasonal patterns of belowground biomass and productivity in mountain grasslands in the Pyrenees. *Plant Soil* 340, 315-326. https://doi.org/10.1007/s11104.010-0601-1

García-Pausas, J., Romanyà, J., Montané, F., Rios, A.I., Taull, M., Rovira, P., Casals, P. 2017. Are soil carbon stocks in mountain grasslands comprised by land-use changes? In. J. Catalán *et al.,* (Eds.). *High Mountain Conservation in a Changing World*. *Advances in Global Research*, 62. https://doi.org/10.1007/978-3-319-55982-7_9

García-Ruiz, J.M., Lana-Renault, N., 2011. Hydrological and erosive consequences of farmland abandonment in Europe, with special reference to the Mediterranean region-A review. *Agriculture, Ecosystems & Environment* 140 (3-4), 317-338. https://doi.org/10.1016/j.agee.2011.01.003

García-Ruiz, J.M., López-Moreno, J.I., Vicente-Serrano, S.M., Lasanta, T., Beguería, S. 2011. Mediterranean water resources in a Global Change scenario. *Earth-Science Reviews* 105(3-4), 121-139. https://doi.org/10.1016/j.earscirev.2011.01.006

García-Ruiz, J.M., López-Moreno, J.I., Lasanta, T., Vicente-Serrano, S., González-Sampériz, P., Valero-Garcés, B.L., Sanjuán, Y., Beguería, S., Nadal-Romero, E., Lana-Renault, N., Gómez-Villar, A., 2015. Efectos geoecológicos del cambio global en el Pirineo Central español: una revisión a distintas escalas espaciales y temporales. *Pirineos* 170, e012. https://doi.org/10.3989/pirineos.2015.170005

García-Ruiz, J.M., Tomás-Faci, G., Diarte-Blanco, P., Montes, L., Domingo, R., Sebastián, M., Lasanta, T., González-Sampériz, P., López-Moreno, J.I., Arnáez, J., Beguería, S., 2020a. Trashumance and long-term deforestation in the subalpine belt of the Central Spanish Pyrenees. An interdisciplinary approach. *Catena* 195, 104744. https://doi.org.101016/j.catena.2020.104744

García-Ruiz, J.M., Lasanta, T., Nadal-Romero, E., Lana-Renault, N., Álvarez-Farizo, B., 2020b. Rewilding and restoring cultural landscapes in Mediterranean mountains: Opportunities and challenges. *Land Use Policy* 99, 104744. https://doi.org/10.1016/j.landusepol.2020.104850

Gartzia, M., Alados, C.L., Pérez-Cabello, F., 2014. Assessment of the effects of biophysical and anthropogenic factors on woody plant encroachment in dense and sparse mountain grasslands base on remote sensing data. *Progress in Physical Geography* 38, 201-217. https://doi.org/10.1177/0309133314524429

Gerber, P.J., Henderson, B., Makkar, H.P., 2013. Mitigación de las emisiones de gases de efecto invernadero en la producción ganadera. Una revisión de las opciones técnicas para la reducción de las emisiones de gases diferentes al CO_2. *FAO Producción y Sanidad Animal* 177. Roma, 201 pp.

Gil-García, M.J., Tomás-Las Heras, R., Núñez Olivera, E., Martínez Abaigar, J., 1996. Acción humana sobre el medio natural en la Sierra de Cameros a partir del análisis polínico. *Zubía. Monográfico* 8, 29-41.

Gómez Urdáñez, J.L. 1986. Subsistencia y descapitalización en el Camero Viejo al final del Antiguo Régimen. *Cuadernos de Investigación Histórica Brocar* 12, 103-140.

González, M. 2012. *Alimentos kilométricos. Las emisiones de CO_2 por la Importación de Alimentos al Estado Español.* Amigos de la Tierra. https://www.tierra.org/wp-content/uploads/2016/01/informe_alimentoskm.pdf

Guidi, C., Versterdal, L., Gianelle, D., Rodeghiero, M., 2014. Changes in soil organic carbon and nitrogen following forest expansion on grassland in the Southern Alps. *Forest Ecology and Management* 328, 103-116, https://doi.org/10.1016/j.foreco.2014.05.025

Guo, L.B., Gifford, R.M., 2002. Soil carbon stocks and land use change: a meta-analysis. *Global Change Biology* 8(4), 345-360. https://doi.org/10.1046/j.1354-1013.2002.00486.x

Herrera, P.M. (ed.), 2020. Ganadería y cambio climático: un acercamiento en profundidad. *Cuaderno Entretantos, 6*. Fundación Entretantos y Plataforma por la Ganadería Extensiva y el Pastoralismo.

Hoffmann, I., 2010. Climate change and the characterization, breeding and conservation of animal genetic resources. *Animal Genetics* 41(1), 32-46. https://doi.org/10.1111/j.1365-2052.2010.02043.x

IPCC, 2020. *Climate Change and Land Special Report*. WMO /UNEP. https://www.ipcc.ch/srccl/

Keesstra, S., Nunes, J., Novara, A., Finger, D., Avelar, D., Kalantari, Z., Cerdà, A., 2018. The superior effect of nature based solutions in land management for enhancing ecosystems services. *Science of the Total Environment* 610-611, 997-1009. https://doi.org/10.1016/j.scitotenv.2017.08.077

Lasanta, T., 2009. La ganadería en Cameros: entre la adaptación a los recursos y la dependencia del exterior. En: T. Lasanta y J. Arnáez (Eds.), *Gestión, usos del suelo y paisaje en Cameros. Universidad de La Rioja* – Instituto de Estudios Riojanos, pp. 191-222, Logroño.

Lasanta, T., Ruiz-Flaño, P., 1990. Especialización productiva y desarticulación espacial en la gestión reciente del territorio en las montañas de Europa occidental. En: J.M. García-Ruiz (Ed.)*, Geoecología de las áreas de montaña.* Geoforma Ediciones, pp. 267-295, Logroño

Lasanta, T., Arnáez, J., Eds. 2009. *Gestión, usos del suelo y paisaje en Cameros (Sistema Ibérico, La Rioja).* Universidad de La Rioja – Instituto de Estudios Riojanos, 373 pp., Logroño.

Lasanta, T., Errea, M.P., Bouzebboudja, M.R., Medrano, L.M., 2013. *Pastoreo y desbroce de matorrales en Cameros Viejo*. Instituto de Estudios Riojanos. Colección Ciencias de la Tierra, 30, 186 pp., Logroño.

Lasanta, T., Nadal-Romero, E., Errea, P., Arnáez, J., 2016. The effects of landscape conservation measures in changing landscape patterns: A case study in Mediterranean mountains. *Land Degradation & Development* 27, 373-386. https://doi.org/10.1002/ldr.2359

Lasanta, T., Khorchani, M., Pérez-Cabello, F., Errea, P., Sáenz-Blanco, R., Nadal-Romero, E., 2018. Clearing shrubland and extensive livestock farming: Active prevention to control wildfires in the Mediterranean mountains. *Journal of Environmental Management* 227, 256-266. https://doi.org/10.1016/j.envman.2018.08.104

Lasanta, T., Nadal-Romero, E., García-Ruiz, J.M., 2019. Clearing shrubland as a strategy to encourage extensive livestock farming in the Mediterranean mountains. *Cuadernos de Investigación Geográfica* 45(2), 487-513. http://doi.org/10.18172/cig.3616.

Lasanta, T. Nadal-Romero, E., Khorchani, M., Romero-Díaz, M.A. 2021. Una revisión sobre las tierras abandonadas en España: de los paisajes locales a las estrategias de gestión. *Cuadernos de Investigación Geográfica* 47(2), 477-521. http://doi.org/10.18172/cig.4755

Lasanta, T., Cortijos-López, M., Errea, M.P., Khorchani, M., Nadal-Romero, E., 2022. An environmental management experience to control forest fires in the mid-mountain area: shrub clearing to generate mosaic landscapes. *Land Use Policy* 118, 106147, https://doi.org/10.1016/j.landusepol.2022.106147

Lasanta, T., Cortijos-López, M., Errea, M.P., Llena, M., Sánchez-Navarrete, P., Zabalza, J., Nadal-Romero, E., 2024. Shrub clearing and extensive livestock as strategy for enhancing ecosystem services in degraded Mediterranean midmountain areas. *Science of the Total Environment* 906, 167668. https://doi.org/10.1016/j.scitotenv.2023.167668

Lasanta Martínez, T., 2005. Gestion des champs abandonnés pour le dévelopment de l'élevage extensif dans les Pyrénées espagnoles. *Sud-Ouest Européén* 19, 109-117.

Lasanta Martínez, T., Errea Abad, M.P., 2001. *Despoblación y marginación en la Sierra Riojana.* Instituto de Estudios Riojanos. Colección de Ciencias Sociales, 9, 181 pp., Logroño.

Lindenmayer, D.B., 2017. Conserving large old trees as small natural features. *Biological Conservation* 211, 51-59. https://doi.org/10.1016/j.biocon.2016.11.012

López de Calle, C., Tudanca, J.M., 2014. Contemplando Cameros desde la arqueología: actitudes y planteamientos metodológicos en la interpretación del paisaje. *Berceo* 167, 121-175.

MacDonald, D., Crabtree, J.R., Wiesinger, G., Dax, T., Stamou, N., Fleury, P., Gutiérrez-Lazpita, J., Gibon, A., 2000. Agricultural abandonment in mountain areas of Europe: Environmental consequences and policy response. *Journal of Environmental Management* 59(1), 47-69. https://doi.org/10.1006/jema.1999.0335

Manzano, P., White, S.R., 2019. Intensifying pastoralism may not reduce greenhouse gas emissions: wildlife-dominated landscape scenarios as a baseline in life-cycle analysis. *Climate Research* 77(2), 91-97. https://doi.org/10.3354/cr01555

Moreira, F., Viedma, O., Arianoutsou, M., Curt, T., Koutsias, N., Rigolot, E., Bilgili, E., 2011. Landscape-wildfire interactions in southern Europe: implications for landscape management. *Journal of Environmental Management* 91(10), 2389-2402. https://doi.org/10.1016/j.envman.2011.06.028

Moreno Fernández, J.R., 1994. *El monte público en La Rioja durante los siglos XVIII y XIX: aproximación a la desarticulación del régimen comunal*. Gobierno de La Rioja, 295 pp., Logroño

Mottet, A., Ladet, S., Coque, N., Gibon, A., 2006. Agricultural land-use change and its drivers in mountain landscapes: a case study in the Pyrenees. *Agriculture, Ecosystems & Environment* 114, 296-310. https://doi.org/10.1002/ldr.2542

Nadal-Romero, E., Cortijos-López, M., Llena, M., Cammeraat, E., Lasanta, T., en revisión. Farmland and pasture abandonment in Mediterranean mountains: implications on soil organic carbon dynamics through density fractionation. *Geoderma Regional.*

Nadal-Romero, E., Lasanta, T., Cerdà, A., 2018. Integrating extensive livestock and soil conservation policies in Mediterranean mountain areas for recovery of abandoned lands in the Central Spanish Pyrenees. A long-term research assessment. *Land Degradation & Development* 29, 263-273. https://doi.org/10.1002/ldr.2542

Nadal-Romero, E., Rubio, P., Kremyda, V., Absalah, S., Cammeraat, E., Jansen, B., Lasanta, T., 2021. Effects of agricultural land abandonment on soil organic carbon stocks and composition of soil organic matter in the Central Spanish Pyrenees. *Catena* 205, 105441. https://doi.org/10.1016/j.catena.2021.105441

Nogués-Bravo, D., Araujo, M.B., Lasanta, T., López-Moreno, J.I., 2008. Climate change in Mediterranean mountains during the 21st century. *Ambio. A Journal of the Human Environment* 37(4), 280-285. https://doi.org/10.1579/0044-7447(2008)37[280:CCIMMD]2.0.CO;2

Ortigosa, L., 1990. Las repoblaciones forestales como estrategia pública de intervención en regiones de montaña. En: J.M. García-Ruiz (Ed.), *Geoecología de las áreas de montaña.* Geoforma Ediciones, pp. 297-311, Logroño.

Ortigosa, L., 1991. *Las repoblaciones forestales en La Rioja: resultados y efectos geomorfológicos*. Geoforma Ediciones, 149 pp., Logroño.

Palau, J., 2020. *Rewilding Iberia. Explorando el potencial de la renaturalización en España*. Lyns, 388 pp., Barcelona.

Pascual Sánchez, D., Pla Ferrer, E., 2024. *Layman's report*. LIFE MIDMACC: Mid-mountain adaptation to climate change. LIFE CCA/ES/001099 – 2019-2024. www.life-midmacc.eu

Peña-Angulo, D., Khorchani, M., Errea, P., Lasanta, L., Martínez-Arnáiz, M., Nadal-Romero, E., 2019. Factors explaining the diversity of land cover in abandoned fields in a Mediterranean mountain. *Catena* 181, 104064. https://doi.org/10.1016/j.catena.2019.05.010

PEPAC, 2023. *Plan Estratégico de la Política Agraria Común (PAC) 2023-2027*. https://www.mapa.gob.es/pac-2023-2027/

Pereira, H.M., Navarro, L.M. (Eds.), 2015. *Rewilding European Landscapes*. Springer Open. Heidelberg. https://doi.org/10.1007/978-3-319-12039-3

Puche, N., Senapati, N., Flechard, C.R., Klumpp, K., Kirschbaum, M.U.F., Chabbi, A., 2019. Modelling carbon and water fluxes of managed grasslands: Comparing flux variability and net carbon budgets between grazed and mowed systems. *Agronomy* 9(4), 183. https://doi.org/10.3390/agronomy9040183

Rodrigues, M., Jiménez, A., De la Riva, J., 2016. Analysis of recent spatial-temporal evolution of human driving factors of wildfires in Spain. *Natural Hazards* 84, 2409-2070. https://doi.org/10.1007/s11069-016-2533-4

Rodríguez-Ortega, T., Oteros-Rozas, E., Ripoll-Bosch, R., Tichit, M., Martín-López, B., Bernués, A., 2014. Applying the ecosystem services framework to pasture-based livestock farming systems in Europe. *Animal* 8, 1361-1372. https://doi.org/10.1017/S1751731114000421

Rojas-Downing, M.M., Nejadhashemi, A.P., Harrigan, T., Woznicki, S.A., 2017. Climate change and livestock: Impacts, adaptation, and mitigation. *Climate Risk Management* 16, 145-163. https://doi.org/10.1016/j.crm.2017.02.001

Rothermel, R.C., 1983. *How to predict the spread and intensity of forest range fires*. U.S. Forest Service, Ogden, U.T.

Rubio, A., Roig, S., 2017. *Impactos, vulnerabilidad y adaptación al cambio climático en los sistemas extensivos de producción ganadera en España*. Oficina Española de Cambio Climático. Ministerio de Agricultura y Pesca, Alimentación y Medio Ambiente, Madrid. https://www.mineco.gob.es/es/cambio-climático/publicaciones/publicaciones/informeganaderíaextensivatcm30-435573.pdf

Ruiz-Mirazo, J., Robles, A.B., González-Rebollar, J.L., 2009. Pastoralism in natural parks of Andalucia (Spain): a tool for fire prevention and the naturalization of ecosistems. In: F. Pacheco, F., P. Morand-Fehr (Eds.). *Changes in Sheep and Goat Farming Systems at the Beginning of the 2st Century*. CIHEAM-IAMZ, pp. 141-144, Zaragoza.

Ruiz-Mirazo, J., Robles, A.B., González-Rebollar, J.L., 2011. Two-year evaluation of fuelbreaks grazed by livestock in the wildfire prevention program in Andalusia (Spain). *Agriculture, Ecosystems & Environment* 14, 13-22. https://doi.org/10.1016/j.agee.2011.02.002

Sabio Alcutén, A., 1997. *Los montes públicos en Huesca (1859-1930).* Instituto de Estudios Altoaragoneses. Colección de Estudios Altoaragoneses, nº 43, 313 pp., Huesca.

Sanjuán, Y., Arnáez, J., Beguería, S., Lana-Renault, N., Lasanta, T., Gómez-Villar, A., Álvarez-Martínez, J., Coba-Pérez, P., García-Ruiz, J.M., 2018. Woody plant encroachment following grazing abandonment in the subalpine belt: a case study in Northern Spain. *Regional Environmental Change* 18, 1103-1115. https://doi.org/10.1007/s10113-017-1245-y

San-Miguel-Ayanz, J., Moreno, J.M., Camia, A., 2013. Analysis of large fires in European Mediterranean landscapes: lessons learned and perspectives. *Forest Ecology and Management* 290, 11-22. https://doi.org/10.1016/j.foreco.2012.10.050

Sayadi, S., González-Roa, M.C., Calatrava-Requena, J., 2009. Public preferences for landscape features: The case of agricultural landscapes in mountainous Mediterranean areas. *Land Use Policy* 26, 334-344. https://doi.org/10.1016/j.landusepol.2008.04.003

Sluiter, R., 2005. Mediterranean land cover change: Modelling and monitoring natural vegetation using GIS and remote sensing. *Nederlandse Geografische Studies* 333, 17-144.

Tang, S., Zhang, Y., Zhai, X., Wilkes, A., Wang, C., Wang, K., 2018. Effect of grazing on methane uptake from Eurasian steppe of China. *BMC Ecology* 18(1), 11. https://doi.org/10.1186/s12898-018-0168-x

Tree, I., 2018. *Wilding. The return of nature to a British farm*. Picador, Londres.

Turco, M., Bedia, J., Di Liberto, F., Fiorucci, P., von Hardenberg, J., Koutsias, N., Llasat, M-C, Xystrakis, F., Provenzale, A., 2016. Decresing fires in Mediterranean Europe. *PloS One* 11, e0150663. http://doi.org/10.1371/journal.pone.0150663,2016

Urbieta, L.R., Franquesa, M., Viedma, O., Moreno, L.M., 2019. Fire activity and burned forest lands decreased during the last three decades in Spain. *Annals of Forest Science* 76, 90. https://doi.org/10.1007/s13595-019-0874-3

Vega-García, C., Chuvieco, E., 2006. Applying local measures of spatial heterogeneity to Landsat-TM images for predicting wildfire occurrence in Mediterranean landscapes. *Landscape Ecology* 21, 515-605. https://doi.org/10.1007/s10980-005-4119-5

Viedma, O., Angeler, D.G., Moreno, J.M., 2009. Landscape structural features control fire size in a Mediterranean forested area of central Spain. *International Journal of Wildland Fire* 18(5), 575-583. https://doi.org/10.1071/WF08030

Zero Emissions Objetive, ZEO, 2016. Incendios forestales y cambio climático: el pez que se muerde la cola.

Zhu, Y., Merbold, L., Leitner, S., Xia, L., Pelster, D.E., Díaz-Pines, E., Abwanda, S., Mutuo, P., Butterbach-Bahl, K., 2020. Influence of soil properties on N_2O and CO_2 emissions from excreta deposited on tropical pastures in Kenya. *Soil Biology and Biochemistry*, 140, 107636. https://doi.org/10.1016/j.soilbio.2019.107636

Administración / Administration

Universidad de La Rioja
Servicio de Publicaciones
Piscinas, 1, 26006 LOGROÑO (España)
Tel.: (+34) 941299187 Fax: (+34) 941299193
Correo-e: publicaciones@unirioja.es

Edición electrónica / E-Journal

EISSN: 1697-9540
http://publicaciones.unirioja.es/revistas/cig
cig@unirioja.es

Indización y Calidad / Indexation and Quality Analysis

Bases de Datos y Recursos para el análisis de la calidad de las revistas científicas /
Databases and Resources for the analysis of the Scientific Journal's Quality:

CARHUS Plus+ 2018
CIRC (EC3 Metrics)
Dialnet Métricas (Fundación Dialnet)
DOAJ (Directory of Open Access Journals)
ERIH Plus (European Science Fundation)
ESCI, Emerging Sources Citation Index (Web of Science™ , Clarivate Analytics)
Fuente Académica Plus (EBSCO)
Latindex (Catálogo)
MIAR (Matriz de Información para el Análisis de Revistas)
Periodicals Index Online (ProQuest)
SCIMAGO Journal & Country Rank (SJR)
Scopus (Elsevier)
Sello de Calidad FECYT

Cuadernos de Investigación Geográfica / *Geographical Research Letters*

A scientific journal of Physical Geography

CUADERNOS DE INVESTIGACIÓN GEOGRÁFICA
GEOGRAPHICAL RESEARCH LETTERS
TOMO 50 (2), Año 2024

UNIVERSIDAD DE LA RIOJA